Modified Design of a Precision Planter

For a Robotic Assistant Farmer

A Thesis Submitted to the College of

Graduate Studies and Research

In Partial Fulfillment of the Requirements

For the Degree of Master of Science

In the Department of Mechanical Engineering

University of Saskatchewan

Saskatoon

By

Reza Aminzadeh

PERMISSION TO USE

In presenting this thesis/dissertation in partial fulfillment of the requirements for a Postgraduate degree from the University of Saskatchewan, I agree that the Libraries of this University may make it freely available for inspection. I further agree that permission for copying of this thesis/dissertation in any manner, in whole or in part, for scholarly purposes may be granted by the professor or professors who supervised my thesis/dissertation work or, in their absence, by the Head of the Department or the Dean of the College in which my thesis work was done. It is understood that any copying or publication or use of this thesis/dissertation or parts thereof for financial gain shall not be allowed without my written permission. It is also understood that due recognition shall be given to me and to the University of Saskatchewan in any scholarly use which may be made of any material in my thesis/dissertation.

Requests for permission to copy or to make other uses of materials in this thesis/dissertation in whole or part should be addressed to:

Head of the Department of Mechanical Engineering

3B48 Engineering Building, 57 Campus Drive, Saskatoon, SK

Saskatoon SK S7N 5A9

OR

Dean

College of Graduate Studies and Research

University of Saskatchewan

107 Administration Place

Saskatoon, Saskatchewan S7N 5A2, Canada

Abstract

Modified design of a planter to be attached to a mobile robot, was the main objective of this project. This research project was part of a larger project, called "Developing robotics assisted technology for farming".

The main motivation for this research project is the fact that mobile robot, is an electric powered vehicle with limited power and pulling force. Thus, a customized planter with a customized connection mechanism should be designed. Besides, it should require less draft force compared to existing planters so that it can be pulled by the mobile robot. The developed planter should have the same efficiency as the existing planters in seeding.

To find the forces between soil engagement tool (disc coulter) and soil, experiments were designed and performed in the Linear Soil Bin at University of Saskatchewan. Disc and tilt angle of a disc coulter was changed and draft, vertical and side forces applied to it were measured to find the disc and tilt angle combinations that results in minimum draft force. Experiments showed that 7° disc angle and 25° tilt angle provides the least draft force compared to other disc angle and tilt angle combinations. Then, using the knowledge obtained from literature and the soil bin experiments, a planter was designed conceptually and in detail, based on the existing CNH planter. For further analyses computer modeling was performed. The whole planter was modeled in 3D, using SolidWorks. Stress analysis was performed in ANSYS Workbench to calculate safety factor of the designed parts. Two prototypes were fabricated and were attached to the mobile robot for field tests. Tests were performed in indoor settings to measure the total draft force required to pull developed planters. Draft force was very close to the value that was calculated in design stage. Results showed that an average of 460 N pulling force is required to

pull one row planter for 50 mm depth of cut, which can be compared to n existing CNH corn planter that requires a pulling force of between 900 N to 1300 N. Seed drop accuracy and function of the developed planters in opening and closing a packed soil in presence of residue, were also observed in outdoor tests.

Acknowledgment

I want to thank my supervisor Prof. Reza Fotouhi who guided me through the work and supported me both in my research and my personal life. I am also grateful for the help of my advisory committee for excellence of this research. I want to appreciate the time and financial support that Mr. Jim Henry and CNH industries dedicated to this research.

I also want to thank my colleagues, Mr. Ahad Armin, Mr. Carlos Mondragon, Mr. Ashkan Oghabi and Mr. Farzam Ayatizadeh, who helped me with my experiments and analysis. Also the help of department assistants, Mr. Douglas Bitner and Mr. Louis Ruth are greatly appreciated for helping me to setup the experiment setups and tests.

Dedication

This thesis is dedicated to my mom and dad,

who sacrificed their dreams to make mines come true.

&

My lovely sister, Neda, and my best friends, Farnoosh and Sina,

which being away from them was the hardest thing I have ever experienced.

Table of contents

Permission to use i

Abstract ii

Acknowledgment iv

Dedication v

Table of contents vi

List of Tables ix

List of Figures x

Chapter 1- Introduction 1

1-1-Robotic farming 1

1-2-Seeders and Planters 2

1-2-1- Soil engaging component: 4

1-2-2- Depth Control system 5

1-2-3- Seed metering system 6

1-2-4- Packing system 6

1-2-5- Shock absorber system 6

1-2-6- Lift and transportation linkage and mechanism 7

1-3-Motivation of study and problem statement 8

1-4-Objective 9

1-5-Methodology 10

1-6-Outline of the thesis 10

1-7-Literature review 11

Chapter 2- Experiments in the Soil Bin: Disc-Soil Interaction 19

2-1-Introduction 19

2-2- Test setup: 23

2-3- Test Parameters: 26

2-4- Test procedure: 27

2-5- Test results and discussion: 29

2-5-1- Draft force: 30

5-2- Vertical Force: 33
2-5-3- Lateral Force: 36
2-6- Summary: 38
Chapter 3- Design 39
3-1- Design process 39
3-2- Conceptual design 40
3-2-1-Furrow Opener Assembly 44
3-2-2-Packing Assembly 47
3-2-3-Seeding Assembly 48
3-2-4-Connection Assembly 53
3-3-Detail Design and Analysis: 55
3-3-1-Static force analysis: 55
3-3-2- Optimization of the packing pressure and spring force: 60
3-3-3- Spring Design: 65
3-4-Summary 75
Chapter 4- Stress Analysis Using Finite Element Method 76
4-1- Introduction 76
4-2- Planter parts stress analysis using ANSYS Workbench 77
4-2-1- Depth control link 77
4-2-2- Disc Holder 84
4-2-3- Seed drop tube 88
4-2-4- Spring connection 89
4-2-5- Press wheel link 93
4-2-6- vertical pull bar 96
4-2-7- Horizontal pull bar 101
4-3- Summary 105
Chapter 5-Prototyping, test-rig and verification 106
5-1- Fabrication of the prototype 106
5-2- Tests 107
5-2-1- Outdoor tests: 109
5-2-2- Indoor tests 112
5-3-Summary 122
Chapter 6- Conclusion and Future Work 124

6-1-Summary and Conclusion 124
6-2-Contributions 127
6-3-Future works 128
References: **131**
APPENDIX A- Pictures of Developed Planter **135**
APPENDIX B- Stress Analysis of the Disc Holder with Different Mesh Sizes **138**
APPENDIX C- Matlab Code and Simulink Model for Low Pass Filter **145**
Appendix D- Comparison and Validation of the Experimental Soil Bin Results with Analytical Analysis **146**
APPENDIX E- Detailed Drawings of the Designed Parts **149**

List of Tables

Table 2- 1- Constant parameters of the experiments 27

Table 2- 2- Variable parameters of the experiments 27

Table 2- 3- Compaction Level of the soil in the soil bin 28

Table 2- 4- Experimental results 30

Table 3- 1- Dimensions of the gauge wheel and press wheel 59

Table 3- 2- Initial values for optimization problem 63

Table 3- 3- Properties of HD spring wire, for d>3 mm[21] 69

Table 3- 4- Dimensions and properties of the main spring 71

Table 3- 5- Strength properties of the extension spring wire for d=6 mm.[21] 74

Table 3- 6- Dimensions and properties of the press wheel spring 74

Table 4- 1- Components of external forces in the coordinate system parallel to faces of depth control link 79

Table 4- 2- Reaction forces at cylindrical supports A and B 83

Table 4- 3- Reaction forces and moments for disc holder 88

Table 4- 4- reactions of supports B and D of spring connection 92

Table 5- 1- Average, minimum and maximum of the tests 120

Table B- 1-Number of nodes, element sizes and maximum real stress for different stress analyzes of disc holder with different mesh sizes 139

Table D- 1- Experimental and analytical comparison for forces on disc plough for 7º disc angle and 25º tilt angle 147

List of Figures

Figure1- 1- Grizzly mobile robot uses Laser scanner, GPS, IMU and other sensors for navigation and control. 2

Figure1- 2- A seeder/fertilizer unit: 1) Shock absorber/depth control cylinder, 2) Fertilizer tube, 3) Fertilizer knife, 4) Seed knife, 5) Seed tube, 6) Press wheel. 3

Figure1- 3- Different types of tine type furrow openers 4

Figure1- 4- Disc coulter cutting through the soil and residue 5

Figure1- 5- A complete planter and its parts: 1) Disc Coulter, 2) Gauge wheel, 3) Soil covering disc, 4) Press wheel, 5) Seed hopper, 6) Shock absorber spring, 7) Parallelogram linkage. 7

Figure1- 6- A Folded planter, ready for transport 8

Figure 2- 1- Schematic of a disc coulter, showing disc angle (ɣ) and tilt angle (β) 21

Figure 2- 2- A furrow created by a disc coulter with a disc angle of 14º 22

Figure 2- 3- Soil bin, College of Engineering, University of Saskatchewan 23

Figure 2- 4- Sheep foot and smooth roller to pack the soil 24

Figure 2- 5- Load Cells, position and orientation: 1) Side force, 2) Draft forces, 3) Vertical force 25

Figure 2- 6- Disc coulter and adjustable connection link to set disc angle 26

Figure 2- 7- Using wedges to set tilt angle 26

Figure 2- 8- Draft force on the disc coulter for different disc angles, tilt angle=0 31

Figure 2- 9- Draft force on the disc coulter for different disc angles, tilt angle=15 31

Figure 2- 10- Draft force on the disc coulter for different disc angles, tilt angle=20 31

Figure 2- 11- Draft force on the disc coulter for different disc angles, tilt angle=25 32

Figure 2- 12- Comparative chart of Draft force for different disc and tilt angles 33

Figure 2- 13- Vertical force on the disc coulter for different disc angles, tilt angle=0 34

Figure 2- 14- Vertical force on the disc coulter for different disc angles, tilt angle=15 35

Figure 2- 15- Vertical force on the disc coulter for different disc angles, tilt angle=20 35

Figure 2- 16- Vertical force on the disc coulter for different disc angles, tilt angle=25 35

Figure 2- 17- Lateral force on the disc coulter for different disc angles, tilt angle=0 36

Figure 2- 18- Lateral force on the disc coulter for different disc angles, tilt angle=15 37

Figure 2- 19- Lateral force on the disc coulter for different disc angles, tilt angle=20 37

Figure 2- 20- Lateral force on the disc coulter for different disc angles, tilt angle=25 37

Figure 3- 1- Engineering design process [21] 39

Figure 3- 2- Existing planter and its components, 1)Disc Coulter, 2)Gauge wheel, 3)Soil covering disc, 4)Press wheel, 5)Seed hopper, 6)Down force spring, 7)Parallelogram linkage 41

Figure 3- 3- Sketches of the design of two planters, utilizing disc coulter 42

Figure 3- 4- SolidWorks model of the new designed planter 43

Figure 3- 5-Furrow opener assembly parts, 1) Disc holder, 2) Disc, 3) Gauge wheel, 4) Depth control link 44

Figure 3- 6- A 460 mm diameter disc coulter, d_1=50 mm into the soil, (a) Side view, (b) Top view which shows the width of the furrow opened by the disc. 45

Figure 3- 7- Disc holder, part 1 in Figure 3-5 46

Figure 3- 8-Packing assembly parts, 5) Press wheel, 6) Press wheel links, 7) Spring connection, 8) Extension spring 47

Figure 3- 9- Parts that are involved in seed placement, 5) Press wheel, 12) Sprocket 1 and its connection link, 10) Chain loop 1, 9) Sprocket 2 and sprocket 3 and their connection shaft, 11)

Chain loop 2, 13) Seed hopper, 14) Pneumatic precision seed metering device, 16) Seed drop tube, 15) Runner type opener 49

Figure 3- 10- Singulator disc and the seeds stick to it because of vacuum pressure 51

Figure 3- 11- Connection assembly parts, 17) main spring, 18) Vertical pull bar, 19) horizontal pull bar 53

Figure 3- 12- Parts of connection mechanism, 18) vertical pull bar, 19) horizontal pull bar and 20) lifting mechanism (hand wrench) 54

Figure 3- 13- Forces for lifting condition of the planter 55

Figure 3- 14- Schematic side view of the planter, showing external forces in x and y directions 56

Figure 3- 15- Schematic view of the press wheel and its linkage (See Figure 3-9 for its location) 61

Figure 3- 16- Position and orientation of the springs 67

Figure 3- 17- Free body diagram of the parallelogram link and the spring 68

Figure 3- 18- Parameters of the extension spring 72

Figure 4- 1- Developed planer (parts in green are the ones that stress analysis is performed on them) 77

Figure 4- 2- Meshing of the Depth control link 78

Figure 4- 3-Geometry and supports of depth control link 80

Figure 4- 4- Equivalent (Von Mises) stress contour for depth control link 81

Figure 4- 5- Total Deformation contour for depth control link 82

Figure 4- 6- Depth control link and Schematic forces and supports in 2D for hand calculation.. 83

Figure 4- 7- Meshing for disc holder 86

Figure 4- 8- Geometry, forces and support of the disc holder part 87

Figure 4- 9- Equivalent (Von Mises) Stress contour for disc holder 88

Figure 4- 10- Spring connection location 89

Figure 4- 11- Meshing for spring connection 90

Figure 4- 12- Geometry, loads and supports of spring connection.. 91

Figure 4- 13- Maximum principal stress contour for spring connection 92

Figure 4- 14- Meshing for press wheel link... 94

Figure 4- 15- Geometry, external loads and supports for press wheel link 95

Figure 4- 16- Equivalent (Von Mises) stress contour for press wheel link 96

Figure 4- 17- (a) vertical and horizontal pull bar in seeding configuration, (b) vertical and horizontal pull bar in transportation configuration 97

Figure 4- 18- meshing for vertical pull bar 98

Figure 4- 19-Forces for lift configuration of the planter.. 99

Figure 4- 20- Geometry, external loads and supports for vertical pull bar in (a) pulling configuration, and (b) lifting configuration 100

Figure 4- 21- Equivalent (Von mises) stress for vertical pull bar, in (a) pulling condition and (b) lifting condition.. 101

Figure 4- 22- Meshing for horizontal pull bar 102

Figure 4- 23- Geometry, external loads and supports for horizontal pull bar, in (a) pulling condition, and (b) lifting condition 103

Figure 4- 24- Equivalent (Von Mises) stress for horizontal pull bar in (a) pulling condition and, (b) lifting condition 105

Figure 5- 1- Parts that are designed or modified are shown in blue 106

Figure 5- 2- a) The assembled new planter, b) Existing CNH planter 108

Figure 5- 3- Location of the outdoor tests, north of engineering building 110

Figure 5- 4- The set of two planters, attached to the wheeled mobile robot in transport position 110

Figure 5- 5- The furrow opened by the planter 111

Figure 5- 6- The closed furrows by press wheels 112

Figure 5- 7- Load cells attached between the mobile robot and planter, 1) Grizzly mobile robot, 2) Hitch (pin removed), 3) Load cell, 4) Planters set, 5) Hand winch....................................... 113

Figure 5- 8- Mobile robot pulling the planters set inside the soil bin.. 114

Figure 5- 9- calibration setup 115

Figure 5- 10- Calibration graph for Load cell, V = 0.0505m - 0.0004 115

Figure 5- 11-Measured draft force for 2 inch depth of disc in the soil...................................... 117

Figure 5- 12- Measured draft force for 3 inch depth of disc in the soil..................................... 118

Figure 5- 13- Raw and filtered data (measured draft force), for 2 inch disc depth 119

Figure 5- 14- Raw and filtered data (measured draft force), for 3 inch disc depth 119

Figure 5- 15- Space between seeds dropped by planter.. 120

Figure A- 1- Side view of the developed planter 135

Figure A- 2- Disc coulter, Gauge wheel, Disc holder and depth control link 136

Figure A- 3- Power transmission from the press wheel to the singulator disc 137

Figure A- 4- Horizontal pull bar, Vertical pull bar and hand wrench used for lifting the planter 137

Figure B- 1- Sphere of influence tool in ANSYS Workbench for mesh refinement................. 138

Figure B- 2- Analysis 1, a) Meshing, b) Stress contour.. 140

Figure B- 3- Analysis 2, a) Meshing, b) Stress contour.. 141

Figure B- 4- Analysis 3, a) Meshing, b) Stress contour 142

Figure B- 5- Analysis 4, a) Meshing, b) Stress contour 143

Figure B- 6- Analysis 5, a) Meshing, b) Stress contour 144

Figure C- 1-Simulink model for low pass filter with cut off frequency of 2 Hz 145

Figure D- 1- Disc plough and the external forces 146

Chapter 1- Introduction

1-1-Robotic farming

Agriculture and farming is considered one of the most exhaustive works which requires a lot of effort to perform seeding, planting, weeding, spraying and harvesting.

Robotics technology has helped us to improve the quality of our lives in different aspects. But still implementation of robots in the field of agriculture, especially farm activities, is a challenge for scientists and engineers. Robots can help us plant accurately, water accurately and also control weeds and pests more accurately. These all mean, higher quality products, cheaper food and less labor.

This research is part of a larger project, named "Developing robotics assisted technology for farming". In the overall project, a new robotic technology will be developed to help farmers in weed control and planting for certain types of crops. This research can be broken down into a few sub-projects: 1) Navigation of wheeled robot in a semi-structured farm setting, 2) Designing tools (robotic arms) for robotic assisted farming (weeding, seeding, and planting); this goal includes design and construction of ground engagement tools, and 3) Implementation of robotic assisted farming (i.e. navigation when the robot arm is engaged with the ground). The contribution of this project in the overall project is to design a seeding mechanism, with optimum manner which will result in minimum required force from the mobile robot while it performs seeding with accuracy.

The mobile robot that is being used for this research is an 850-kg autonomous guided vehicle (AGV) named Grizzly (Figure 1-1). Its dimensions are 1.8x1.3 m and its height is 1.0 m.

It can go as fast as 4.4 m/s and in its high performance condition, it can pull up to 7500 N on its drawbar.

Figure1- 1- Grizzly mobile robot uses Laser scanner, GPS, IMU and other sensors for navigation and control.

Equipment installed on the mobile robot for navigation and position control are DGPS (Differential Global Positioning System), central IMU (Inertia Measurement Unit) and a tilting laser scanner unit. Navigation of the robot is controlled by DGPS. With the differential correction signal receiving from the base GPS via radio, its positioning will be as accurate as 20 mm. The central IMU gives the orientation of the mobile robot. The laser scanner unit with its 180º view and also its tilt unit can cover the whole area in front of the robot, to detect any obstacle in front of the robot.

1-2-Seeders and Planters

A seeder (and by extension a planter) is a mechanical system which can be attached to a tractor to place the seeds into the soil and cover it for germination. A planter is an accurate seeding mechanism which utilizes precision seed metering system to singularize the seeds for planting. On the other hand, a seeder uses mass flow seed metering system; so it does not have the accuracy of a planter. Each of these systems has its own pros and cons. A seeder mechanism is shown in Figure 1-2.A complete seeding mechanism consists of the following components [2]:

- Soil engaging components
- Depth control components
- Seed metering components
- Soil packing components
- Shock absorbing components
- Lift and transportation linkage and mechanism

To be able to design and develop a planter, a good knowledge of the components of planters and their function is required. A short description for each group of components and their different types is provided below.

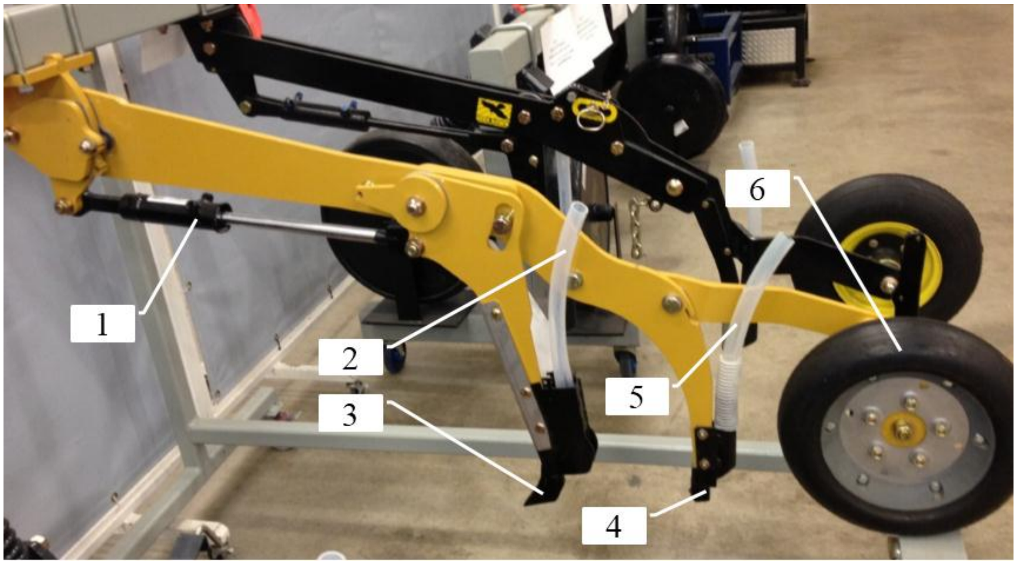

Figure1- 2- A seeder/fertilizer unit: 1) Shock absorber/depth control cylinder, 2) Fertilizer tube, 3) Fertilizer knife, 4) Seed knife, 5) Seed tube, 6) Press wheel.

1-2-1- Soil engaging component:

Soil engagement component is the tool in a seeder or a planter that is in contact with the soil to dig a furrow to place the seed. Two major classes of furrow openers are tine (hoe, shank or knife) type and disc coulter type. Each of these types requires their specific mechanism and has its own features. Different types of tine furrow openers are shown in figure 1-3.

Figure1- 3- Different types of tine type furrow openers

Disc type furrow openers or disc coulters are available as single or double or even triple disc configurations. They open a furrow by cutting and pushing the soil to the sides. Disc Coulters are more accurate; they need less draft force and make fewer disturbances in the soil. They are more effective in the fields with large amount of residue. But they have shorter life due to its small thickness and its axial rotation compared to tine type furrow openers.

No-till farming is the trending method of farming since 1970s. No-till or zero-tillage farming is a method of cultivation without disturbing the soil through tillage. Using this method, farmers conserve water and soil material (nutrients) and also reduce erosion. It also reduces labor required for farming which will result in fewer carbon dioxide emission into the atmosphere.[1] Having this in mind, it can be said that disc coulters are more favorable for planting; because they are more efficient in residue handling and they cause less disturbance in the soil compared to other types of furrow openers. Figure 1-4 shows a disc coulter which is cutting through the soil and residue.

Figure1- 4- Disc coulter cutting through the soil and residue

http://salesmanual.deere.com

1-2-2- Depth Control system

Farm equipment engineers usually use two types of mechanisms to control the depth of the furrow; parallelogram system and trailing arm system. Parallelogram system, is more accurate, easier to control and more rigid with higher strength, but is more complex and expensive, needs more space and it is heavier. On the other hand, trialing arm system is simpler, cheaper and lighter but it does not provide enough accuracy in depth control and down force control. Seeder mechanism in Figure 1-2 is an example of trailing arm system and Figure 1-5 shows a parallelogram mechanism.

The seeding mechanisms which utilize a disc opener usually use a gauge wheel and is very accurate in depth control. The gauge wheel is usually installed on the side of the disc, and its height can be changed and set by the farmer to get the proper depth. The gauge wheel in a planter is shown in Figure 1-5.

1-2-3- Seed metering system

A planter has a precise seed metering system; this is the major difference between a planter and a seeder. Generally seed metering systems are categorized into two main groups, mass flow seed metering system and precision seed metering system. A planter utilizes a precision seed metering system while a seeder usually comes with a mass flow seed metering system. Precision seed metering systems technically are used to singularize seeds and deliver them at a pre-specified spacing to the soil, one by one. A mass flow seed metering system controls the output rate of the seed to make sure the seed is fed to the ground with the proper rate. Figure 1-5 shows a planter mechanism which utilizes disc coulter to dig a furrow and vacuum (pneumatic disc) for precision seed metering system. Other types of precision seed metering systems are finger type, pressure drum, mechanical plate type and belt type.

1-2-4- Packing system

Packing is the process of putting soil back into the furrow after the seed is placed in the soil. With proper packing the seed is in complete contact with the soil to grow and cannot be blown away by the wind, etc. Packing can be done using a press-wheel (packer-wheel).

1-2-5- Shock absorber system

In a farm, there are always rocks in the soil that causes heavy loads (shock loads to be applied to the soil engagement tool). To avoid this shock load, a shock absorbing system should be designed for the seeding mechanism. This can be spring system, pneumatic or hydraulic shock absorber. See Figure 1-2 for a pneumatic shock absorber and Figure 1-5 for a spring shock absorber. This system gives the ability to the seeding mechanism to go up and down as it goes through the field.

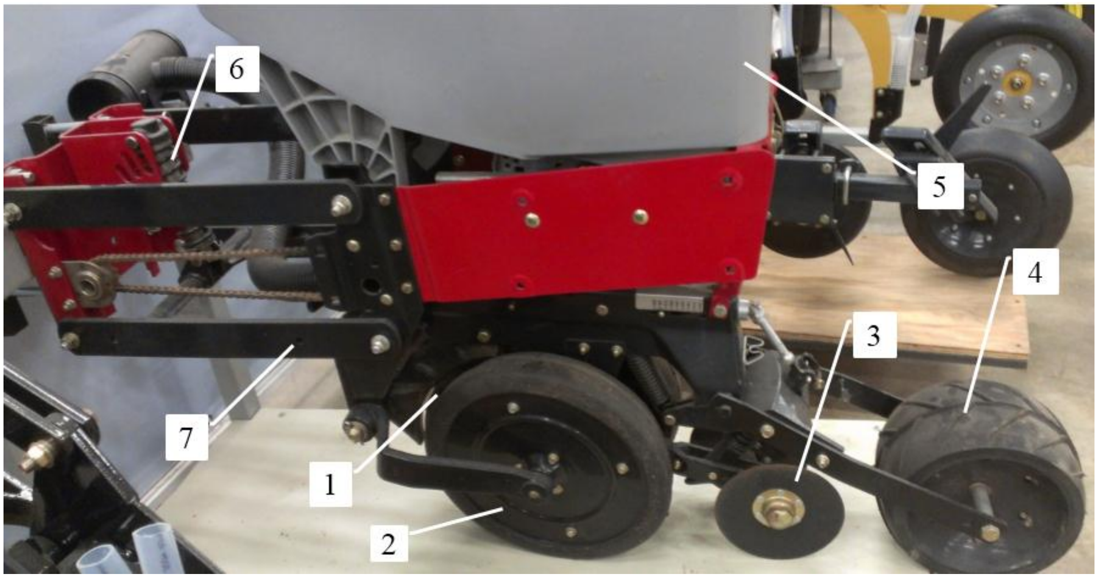

Figure1- 5- A complete planter and its parts: 1) Disc Coulter, 2) Gauge wheel, 3) Soil covering disc, 4) Press wheel, 5) Seed hopper, 6) Shock absorber spring, 7) Parallelogram linkage.

1-2-6- Lift and transportation linkage and mechanism

Planters consist of a series of row planters which can go up to 30 rows. A system of linkage is needed to attach all these row planters together and then attach to the tractor using a hitch. When performing precision seeding, as the planter reaches the border of the farm, it has to lift up the planters off the ground to make a turn. To do so, they utilize a hydraulic system. Also to transport the planters on the roads, they need a mechanism to fold the planter to make it as narrow as possible fit in the road, see figure 1-6. Hydraulic systems are used to do all the lifting and folding of the planters.

Figure1- 6- A Folded planter, ready for transport

http://www.caseih.com/en_us/products/plantingseeding/pages/1200-planters.aspx

1-3-Motivation of study and problem statement

The need for a customized planter to be attached to a wheeled mobile robot for Robotic Assisted Farming project, has been seen. The implement attached to the robot can affect its performance in navigation. So an implement (planter) was designed to be attached to the mobile robot to perform seeding during autonomous farming. With design and development of such a customized planter comes a series of challenges, depicted below.

1. Mobile robot is an electric powered machine with limited pulling force compared to regular tractors used for faming activities. This planter must be designed in optimum manner, so that it needs minimum drag force, and consumes minimum power. Besides, commercial planters come in a series of row planters; but in this case only one or two row planters are needed.
2. Due to power limitations, which mentioned above, not more than two row planters can be attached to the mobile robot. So a customized attachment mechanism is needed in order to attach two row planters to the mobile robot.

3. In regular planters, hydraulic power is used for lifting mechanism, fans and vacuum pumps. Hydraulic systems are heavy and not suitable for an electric powered robot. So another substitution for this source of power should be designed to lift the planter and run the vacuum system.
4. The pneumatic precision seed metering system needs power to rotate the singulator disc with a speed proportional to the forward speed of the planter. In commercial planters, all row planters are attached together, and the power is transmitted from a drive wheel to a common shaft and then to each singulator using chain and sprocket. In the developed planter, a new method is used and the power is transmitted from press wheel (packer wheel) to the singulator disc.

Beside the challenges mentioned above, other efforts have been done to increase the quality of seeding, such as optimization of the packing force and normal force on gauge wheel and disc to improve seed germination.

1-4-Objective

The main objective of this research is ***to design a customized planter to retrofit to the Grizzly mobile robot for precision farming.*** This objective can be broken down into the following sub-objectives:

1) To obtain an background knowledge about seeders, planters, their components and the forces applied to them.
2) To study the effect of disc angle and tilt angle on the forces applied to disc coulters.
3) To design a planter conceptually and then in detail.
4) To analyze the designed planter for strength.
5) To fabricate and test the designed planter for evaluation.

1-5-Methodology

This project was done in different steps that led to prototyping and testing of a new planter. These steps are as follows:

1) A thorough study was performed on different types of seeders and planters, their components to get more familiar with these equipments. Also a thorough literature survey about soil-tool interaction (Disc Coulters) and design of the seeders and planters was done.
2) To find more about disc-soil interaction and to find the optimum disc angle and tilt angle that results in minimum draft force, a series of experiments was designed and performed in the soil bin.
3) Conceptual design was completed and the first draft of the designed planter was created.
4) Detail design, including static analysis, optimization of press wheel force was performed.
5) Finite Element Method (ANSYS Workbench) was used for stress analysis to verify the strength of designed parts under working loads and their safety factors were calculated.
6) Parts for the designed planter was fabricated, assembled and prepared for tests.
7) Tests were designed for the developed planter, to study its performance in different working conditions. The results of the tests, especially the draft force, were compared with analytical hand calculations.

1-6-Outline of the thesis

This thesis consists of 5 chapters and 4 appendices.

Current chapter, is an introduction to the field of design of seeders and planters. It also offers a literature survey in this field.

Chapter 2 describes the details of the experiments that were performed in the soil bin to study effects of disc and tilt angle on soil- disc interaction.

Chapter 3 is the detail of the design process that includes conceptual design, static analysis and optimization of the packer wheel force, etc.

Chapter 4 is the stress analysis of the designed parts to verify about their strength under external loads. The parts that passed the stress analysis successfully are sent to a shop for fabrication.

Chapter 5 gives details of the prototype and discusses tests that were performed and show performance of the prototype. These tests show that the objectives of this research have been achieved successfully.

Chapter 6 brings a summary and conclusion of this research. Also the suggestions for improvements and future work are discussed in this chapter.

At the end of the thesis a list of the references that were used in this thesis is provided. Appendices include the pictures of the developed planter, details of the stress analysis of the disc holder with different mesh sizes, Matlab code used for data filtering, and finally the parts drawings.

1-7-Literature review

Although many works have been done in the field of design of seeders and planters, but not many of them has been published. Because most of them were done by agriculture machinery companies, which prefer not to publish the details of their work. But some research works have been done to study the interaction between soil and different tools. The literature survey provided here consists of two main categories. The first category covers the works that are done in soil-tool interaction, and the second category gathers up a compilation of research in design and development of seeders and planters. At the end of this section a brief conclusion discusses how these research works are different from what is being offered in this thesis and also how these works have helped with the progress of this research.

Murray et al. [2] gathered thorough, complete and detailed information about seeders and planters and their components. In this book, the authors introduced all the parts that commercial planters have in different categories and discuss their usage and performance. They talk about different seeders and planters and categorize their components into 7 groups: 1)soil and residue cutting devices, 2)Row preparation devices, 3)Furrow opening devices, 4)Seed firming devices, 5)Seed covering devices, 6)Row specific seedbed firming devices and 7)Non-row specific seedbed firming/leveling devices.

Another study was performed by Upadhyaya et al. [3] about "Advances in soil dynamics" and their work was published in a book with the same name. In this book they provide a compilation of the works that have been done by others in last 35 years in this field. Their study covers theoretical works that have been done in soil dynamics, soil-tire traction dynamics, soil-tillage tool interaction dynamics and discrete element modeling of the soil machine interaction. In chapter 3, they discuss different tillage tools and their interaction with soil. In this chapter they mention that the draft force is dependent to 5 different factors: 1) Soil state properties, 2) Operational parameters, 3)Tool Geometry, 4)Tool shape, 5) Tool arrangement.

Osman et al. [4] performed some experiments in light clay soil, to study the effect of tilt angle (15, 20 and 25 degrees) on the parameters of ploughing and soil. The author's main concern was the properties of the soil when the tilt angle of the ploughing discs are set to maximum. Because farmers set this angle to maximum to get fewer depth and consequently fewer energy consumption on their tractors. The disc that is used for ploughing is mostly a concave disc that is mounted on the frame with a disc angle, between 42 to 45 degrees. So they performed a series of experiment in a farm in Sudan with light clay soil to study change of ploughing parameters such as wheel slippage and effective field capacity, as tilt angle changes. At the same time the change in soil parameters were studied.

Altuntas et al. [5] used different furrow openers and working speeds to study the effect of these parameters on soil properties, draft force and percentage of emergence of tuber seedlings. They used hoe, shoe and shovel type furrow openers and three different working speeds to plant potato for their experiments. The outcome of their experiments is presented in the form of graph and tables. They showed that the soil penetration resistance is reduced and the draft force is increased in higher speeds. The lowest draft force with high percentage of emergence was obtained using shovel furrow opener. Also in one of the graphs presented in the paper, the average value for draft force for these three types of furrow openers is 20 to 25 N.

A PhD research has been done about prediction of soil-disc forces at Department of agriculture engineering, University of Newcastle, in 1989 by Alam [6]. He developed a mathematical model for the interaction of soil and concave disc plough implements. He also developed a simple experimental setup to evaluate his theoretical model. He used a 3-axis dynamometer to measure soil-disc forces for a specific soil and one specific disc geometry. Generally his experimental results confirm his predicted values and also literature for disc forces.

Kushwaha et al. [7] performed experiments in a soil bin to evaluate the performance of disc coulter for no-till condition, for different amount of residue and different disc sizes. Authors performed experiments on 3 disk diameters, 360 mm (2 mm thick), 460 mm (4 mm thick), 600 mm (4.5 mm thick) for the depth of 50 mm to 70 mm. Tests were done at the average speed of 6.4 Km/h. Their experiments showed that draft and vertical forces are increased by increasing the disc size as well as plowing depth. The straw cutting performance of the 460 mm coulter was 100% for all penetration depths and all straw densities. Also it was observed that increasing the disc size doesn't increase the draft force significantly.

Tice et al. [8] did a thorough review of available mathematical models that predict acting forces on disc coulters. The authors compared 12 different mathematical models and evaluated them experimentally. The experiments were performed for different disc thicknesses and different wedge slopes. Different graphs are plotted to compare the results of the experiment and the mathematical models. Results showed that among all 12 mathematical models, only one model agrees the most with experimental results. They also concluded that the sliding friction between soil and disc on the side surface of the disc has a significant contribution to the draft force and mathematical models should include the side friction.

Tice et al. [9] also did some work on the effect of disc thickness, wedge slope and depth of cut on working parameters of the disc coulters. The authors performed experiments on 10 different discs with different thickness and wedge slopes. It was observed that the minimum draft and vertical force were obtained for thinnest disc with sharpest wedge. They also studied the effect of these parameters on speed ratio, the ratio between the rotational velocity of the disc and linear speed of the disc. Experiments showed that the greatest speed ratio was obtained for thicker discs. Larger speed ratio showed more effectiveness on residue cutting.

In [10], Hann et al. studied the effects of varying the speed ratio, disc angle and tilt angle settings on the performance of a driven concave disc. The relative speeds ratio (ratio between forward speed and the rotational speed of the disc) range is from -3 (backward) to 6 (forward).

Their experiments showed that driving the disc forward caused a significant reduction in draught force but didn't have a significant effect on side force. Also for all driving speeds and all tilt and disc angles, having a driven disc will result in higher total power required and the free-wheeling disc represented the most efficient speed ratio.

Afiffy et al. [11] designed and performed experiments in soil bin to study the effect of disc angle and tilt angle on the properties of soil and furrow and also the soil-disc forces. Two discs with two disc diameters and different disc and tilt angles are used on soils with the three different levels of compaction. Draft force, vertical force and side force are measured and the soil strength of the furrow wall is studied. Also patterns for the furrow shape are obtained. Separate graphs and figures are provided to show the effect of disc and tilt angle, level of soil compaction and depth of cut on draft force, vertical force, side force and strength of the furrow wall. Results showed that the minimum draft force for 460 mm diameter disc was obtained with the compound angle of 5 and 25 degrees, e.g. 5º disc angle and 25º tilt angle. For the 460 mm disc diameter, the maximum strength for furrow wall was obtained with 7.5º disc angle and 20º tilt angle.

Effect of disc angle, tilt angle, soil water content and forward speed on draft force required for a disc plough has been studied by Shirin et al. [12]. The authors used a 700-mm diameter concave disc and performed experiments on soils with average moisture of 23.3%, 29.4% and 33.4%. The tests were run in 3 different speeds of 3 km/h, 4 km/h and 5 km/h and 3 different tilt angles of 17º, 20º and 23º. The results showed that increasing the soil moisture and tilt angle will decrease the draft force. Also it was observed that the minimum draft force is obtained in 45º disc angle.

Fink et al. [13] designed and developed a no-till drill with single disc furrow opener to plant soybeans. They used pneumatic down pressure system to provide down force on the disc and press wheel and keep this force constant for a range of vertical displacement. Different types of press wheels with different vertical forces were used to find out about their efficiency. The results showed that the V-shaped press wheel with 207 KPa down pressure provided highest soybean emergence among others.

Chen et al. [14] investigated the effect of press wheel and gauge wheel and fertilizer banding attachment on the performance of drill planter under field and laboratory conditions. They showed that when the press wheel and/or gauge wheel were not used, plant population was reduced and crop emergence was delayed both in normal and dry soil. But in a very wet seeding condition it resulted in better emergence and plant population. Also it was observed that seeding depth is less uniform when press and gauge wheels are not used.

Karayel et al. [15] studied the effect of down force on the performance of precision planters. They used different down forces with single and double disc furrow openers to perform their tests. They determined spacing uniformity, sowing depth, emergence mean time and percentage to find out about the effect of down force. Their results showed that for precision seeding, the down force on the planter should not be smaller than 880 N. Down forces of 1150 N and 1400 N showed the highest uniformity for sowing depth and percentage of emergence.

Another study on the effect of different press wheels and down force on crop emergence and yield was conducted by Johnston et al. [16]. They used combination of different openers and press wheels with different down forces on press wheel, and determined the emergence and yield that was obtained for wheat, canola and field peas. Their study showed that a 333 N down force on packer wheel provided the best results for emergence and yield for all combinations of openers and packer wheels. Higher packing force tend to reduce the emergence of some crops such as canola.

Cochran et al. [17] studied the vertical force on different furrow openers and depth control devices. They performed tests in soil bin on 3 different furrow openers, a runner type, a chisel type and a double disc furrow opener. They also did the same study for 3 different depth control devices, a gauge wheel, a sliding gauge device and a depth band. For all of these tools, the resistance to penetration was measured. They also used these data to develop mathematical model and formulation to relate vertical force to depth of cut and projected vertical bearing area.

Gratton et al. [18] developed a mathematical model to optimize the change of down force on the press wheel. The down force on the press wheel will change due to vertical displacements on the field. They solved the optimization problem for both trailing arm linkage and parallelogram linkage. The independent variables for optimization problem are linkage dimensions, spring constant and opener's assembly weight. Their model proved to provide less change in down force compared to pneumatic and hydraulic down force systems. They also designed and developed the mechanism to compare the theoretical and experimental results.

The effect of change in disc angle, tilt angle and forward speed on performance of disc plow has been studied by El-shazley et al. [19]. The author coupled a hydraulic dynamometer between tractor and implement to measure interaction forces. The graphs of soil bulk density, penetration resistance, kinematic parameter, draft force, draught power and crop yield is provided with respect to change in disc angle, tilt angle and forward speed. The lowest draft force was obtained at 45º disc angle.

In this thesis the whole process of the design and development of a modified planter is presented. The main objective of this research work is to reduce the total draft force which is required to pull the planter, so it can be pulled by a mobile robot. A literature survey was performed in the field of soil-disc interaction. Then experiments were performed in the soil bin to study the effect of disc angle and tilt angle on the reaction forces of the disc coulter. Conceptual design and detail design was performed. A new method to transfer power to run the singulator disc is suggested and the change in the downward force of the press wheel is minimized. The modified planter is fabricated and indoor and outdoor tests were performed to verify its performance.

Generally it can be said that, not many work has been done on disc coulters as furrow openers. Most of the studies include concave disc behavior when they are being used as ploughing device. The closest work to the soil bin experiments was done by Afify et al. [11]. Their work includes a limited number of disc angle and tilt angle combinations and does not cover a wide range of angles. Also, not many work has been published about design and development of planters. The information obtained from this literature survey, helped a lot in design process. Interaction of the runner type opener, and optimum down force on the gauge wheel, disc and press wheel for the highest germination is obtained from the literature. Detail of this process is presented in chapter 3.

Chapter 2- Experiments in the Soil Bin: Disc-Soil Interaction

2-1-Introduction

No-till farming, as mentioned in chapter 1, is a method of faming which is a trend among farmers now. In no-till method, the seed is planted into the ground without soil preparation and tillage. So, it will preserve soil moisture and nutrients, and saves the energy that is used for tillage. No-till or reduced tillage method can save up to half of the fuel consumption [20]. The only problem that farmers are facing when practicing no-till farming, is the residue which is remained on the soil from the last cultivation. Although the residue preserves the seeds from being blown away by the wind, but cutting through them to make the furrow is the main issue for planter designers.

With the hoe drills, the crop residue gets piled up by the tool and blocks the way of the machine [7]. Among all different types of furrow openers, experience and experiments have shown that disc coulters have the best residue handling [7]. With the sharp edge, they cut through the soil and residue and open the furrow. It causes fewer disturbances in the soil, which is one of the goals of no-till farming; because fewer disturbances in the soil mean less moisture loss and less nutrient loss. That is why disc coulter is chosen for further studies and is used for the design of the planter.

Disc coulters have different parameters that will affect their performance and also their interaction with soil. Disc diameter, disc thickness, edge angle, disc angle, tilt angle and also depth of the cut are the parameters that can change the forces acting on the disc when cutting through the soil.Edge angle is the slope of the edge of the disc that defines its sharpness. Although it seems to be a negligible parameter among other parameters of the soil, it plays an important role in residue cutting ability of the disc. Also it can change the draft force required to pull the disc [9].

As it is shown in Figure 2-1, disc angle is the angle of rotation of the disc around vertical axis. It is the angle that horizontal axis of the disc makes with the direction of motion. And the tilt angle is the angle of the disc with the vertical plane, or the angle created by rotation of the disc around disc’s horizontal axis.

Having a disc angle of greater than zero, in a planter that uses disc coulter, is inevitable. Because the disc should open a furrow, wide enough that a seed can fit in (See Figure 2-2). But the tilt angle is optional. We call it a compound angle when a disc coulter is orientated using both disc and tilt angles. The effect of these angles and their combination had to be studied, to find the best combination that result in minimum draft force (the horizontal reaction force to the disc motion).

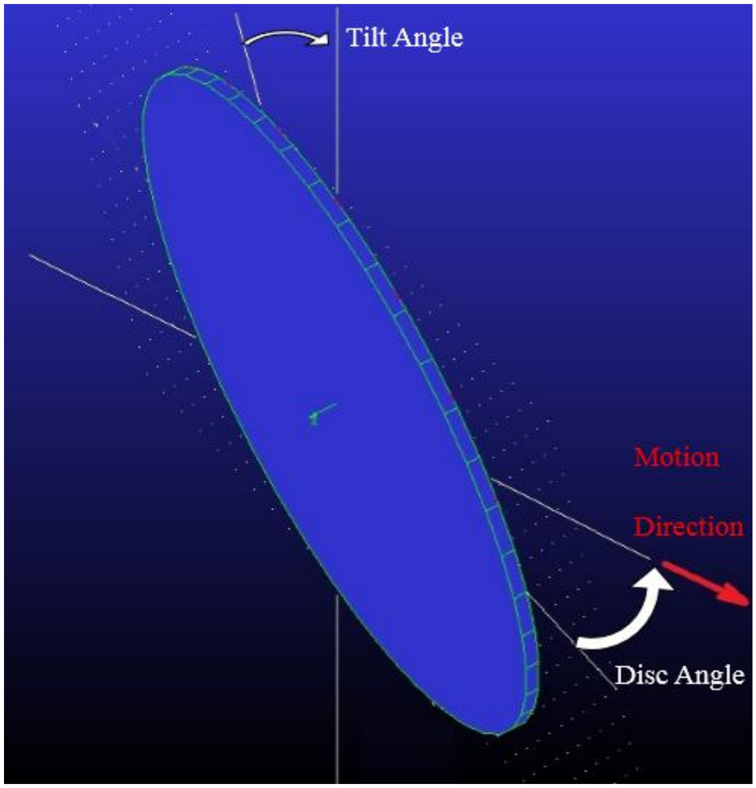

Figure 2- 1- Schematic of a disc coulter, showing disc angle (ɣ) and tilt angle (β)

So to study the effect of disc and tilt angles on the forces applied to disc from the soil, a set of experiments was designed and performed in the soil bin, facility of the College of Engineering, University of Saskatchewan.

Most of the previous research works that are done in this field, to study the effect of disc and tilt angles on the disc forces, are for the period that concave discs were used instead of plane discs [10, 12]. Concave discs were more popular for ploughing until almost 20 years ago when no-till farming started to grow around the world. The only similar study was performed by Afify [11] at University of Saskatchewan. They studied the soil-disc interaction for a limited number of disc and tilt angles.

Figure 2- 2- A furrow created by a disc coulter with a disc angle of 14º

Other parameters of the disc that affect the forces of the disc have been studied before. In all these research works, disc tool is used as a coulter, which means zero disc and tilt angle.

Obviously with increasing the depth of cut (the depth that disc goes into the soil) the reaction forces will increase, due to more friction and more interaction between soil and disc on the sides of the disc [7, 8, 9]. The effect of disc diameter and its thickness on disc's performance in residue handling and its draft force are also studied extensively in [9, 11]. A 460 mm diameter disc with 4 mm thickness and 0.12 edge slop has chosen for further study, because it has proven to be more effective in residue handling [7], and produces less draft force compared to thicker discs [8, 9].

2-2- Test setup:

Soil bin at the College of Engineering, University of Saskatchewan (Figure 2-3), is used to measure forces acting on different soil engagement tools. The bin is 1.8 m wide and 12 m long with an effective length of 9 m. The middle (about 5.7 m) of the soil bin is designated for force measurements using data logger. Soil engagement tools must be attached to a carriage that can move along the soil bin. Forces acting on the tool are measured using load cells in horizontal, vertical and lateral directions. The soil used in the bin is Saskatchewan soil, which is silty clay loam, 47% sand, 24% silt, and 29% clay and has about 0.3 m depth.

Figure 2- 3- Soil bin, College of Engineering, University of Saskatchewan

Carriage is a cubic structure which is used to prepare soil, as well as running attached tool for measuring forces. It moves along the soil bin on two rails on the sides of soil bin, on four steel wheels. An 11.2 kW electric motor with an electromagnetic clutch provides the power via a drive chain to move the carriage.

Figure 2- 4- Sheep foot and smooth roller to pack the soil

To prepare the soil, soil preparation tools must be attached to the carriage. After spraying water on the soil to increase the water content of the soil to a desired level, roto-tiller loosens the soil. Then to pack the soil, sheep foot and smooth roller are used (Figure 2-4). A connection mechanism is installed on the carriage to connect the tillage tool and it can be moved in the lateral direction; so it gives the ability to use the whole width of the soil bin. A control panel is used to control the speed, to start, stop and control the direction of the motion of the carriage. Six load cells are used to measure the forces applied to tillage tool in the vertical, horizontal and lateral directions. Three load cells to measure vertical force (2 in front and 1 in the back), 2 load cells to measure horizontal force (draft force) and 1 load cell for measuring lateral force (side force). The position and orientation of load cells are shown in Figure 2-5. In this picture one of the load cells for vertical force, which is located at the back, is not shown. The equipment were calibrated by another member of our team (Ahad Armin) for his experiments. The draft force reported here, is the summation of the two forces measured by the horizontal load cells. These two load cells can also provide moment in the horizontal plane, if needed.

An adjustable link is used to attach the disc to the carriage. Utilizing this link we can set the disc angle of the coulter disc (Figure 2-6). To set the tilt angle, wedges with different angles are used in between the bolting plate. In Figure 2-7 it is shown how a 25º angle wedge is used in test setup to create the tilt angle.

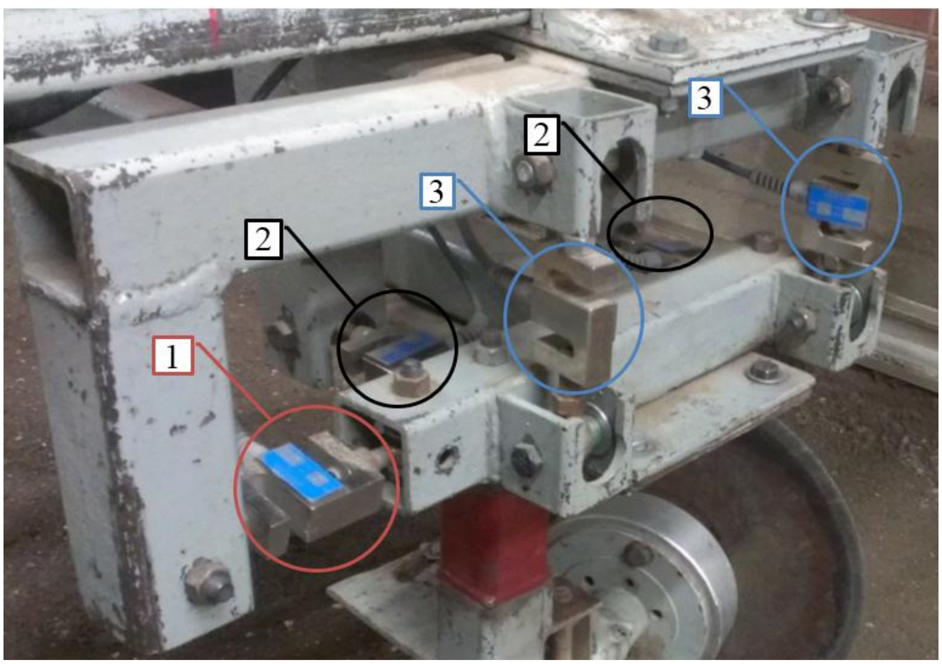

Figure 2- 5- Load Cells, position and orientation: 1) Side force, 2) Draft forces, 3) Vertical force

Figure 2- 6- Disc coulter and adjustable connection link to set disc angle

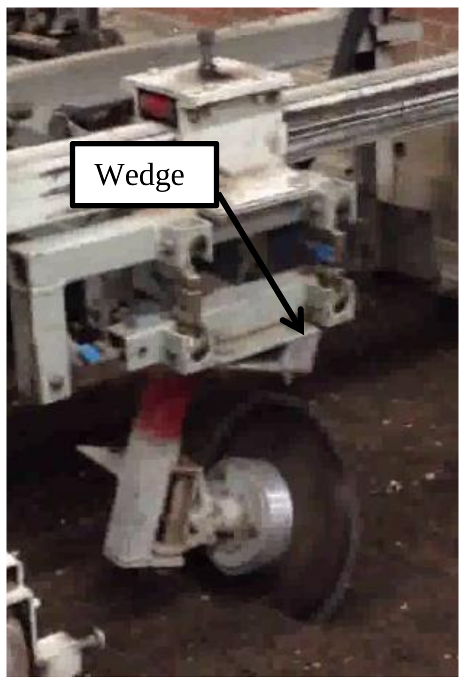

Figure 2- 7- Using wedges to set tilt angle

2-3- Test Parameters:

We can split all the parameters in the series of experiments into two main group, constant parameters and variable parameters. Table 2-1 shows the parameters that were kept constant during all the experiments. Table 2-2 shows the variables of the experiments and their range of change.

Table 2- 1- Constant parameters of the experiments

Constant parameter name	Value	Unit
Soil moisture(water content)	13%	NA
Carriage Speed	6	Km/hr
Cutting depth	50	mm
Packing Level	Medium	NA
Disc size	460	mm
Disc Thickness	4	mm

Table 2- 2- Variable parameters of the experiments

Variable name	Range (Degrees)	Step (Degrees)
Disc angle (ɣ)	0-28	7
Tilt angle (β)	15-25	5

2-4- Test procedure:

Before doing any tests, the soil was prepared. The process of soil preparation usually takes about 3 hours. First, water was sprayed on the soil to increase the water content of the soil to a desired level. The common soil water content used for corn planting is about 13%. So, it was tried to keep the soil moisture about the same level. The water penetrates into the soil after about 1.5-2 hours. After that the roto-tiller was used to loosen and mix the soil. Two passes of roto-tiller would be enough to thoroughly mix and loosen the soil. Then to pack the sub-surface soil, sheep foot drum was used. The drum can be attached to the carriage and as indicated in table 2-3, 4 passes of sheep foot would be enough for medium packing. After that, the smooth heavy drum was attached to the carriage to do the final flattening and surface packing of the soil. Again, as shown in Table 2-3, 4 passes will result in medium packing level.

When the soil bin was ready, the disc coulter was attached to the carriage with the proper disc angle and tilt angle. Then the disc was lowered till it touches the leveled soil. This point will be depth zero. From this point the disc was lowered for another 50 mm, as the cutting depth is 50 mm. Then the carriage speed was set to 6 km/hr. Then start button was pressed, the carriage moved forward and as soon as it touches first trigger switch, which starts recording data, until it touches the end switch. Before it reaches to the end of soil bin, the stop button was pressed to stop the carriage.

Table 2- 3- Compaction Level of the soil in the soil bin

Compaction Level	Number of passes for packing drums
Low Compaction	2
Medium Compaction	4
High Compaction	6

Each test was repeated 4 times to confirm the results and have sufficient repeatability of data.

After each soil preparation, 3 samples of the soil were collected to measure the soil moisture content. The samples were weighed and placed in the oven for 24 hours to dry. The difference between the weight of the samples before and after drying indicated the percentage of the water content of the soil.

2-5- Test results and discussion:

Experiments were performed with zero tilt angle and several disc angles. The same thing was done with tilt angle of 15, 20 and 25 degrees. For each combination of disc and tilt angles, test was repeated 4 times. Table 2-4 shows the average readings of the load cells for each direction and the results for all experiments and compound angles. Since there are more than one load cell in the horizontal (draft) and vertical direction, the amount indicated in Table 2-4 are the summation of all the load cells in each direction.

Table 2- 4- Experimental results: Forces are average of 4 different tests for each set of angles

Tilt Angle (Degrees)	Disc Angle (Degrees)	Vertical Force (N)	Lateral Force (N)	Draft (N)
0	0	110	2.00	72.0
	7	123	215	108
	14	118	231	148
	21	132	555	176
	28	135	1180	230
15	0	102	25.0	83.0
	7	65.0	265	122
	14	52.0	432	143
	21	54.0	760	151
	28	60.0	534	176
20	0	93.0	24.0	85.0
	7	110	193	116
	14	93.0	810	132
	21	90.0	630	143
	28	102	432	148
25	0	89.0	32.0	102
	7	84.0	760	97.0
	14	112	537	106
	21	110	440	130
	28	97.0	463	121

2-5-1- Draft force:

For the purpose of the design of the planter and energy consumption, we can tell that draft force is the most important parameter during the motion of disc. Figure 2-8, 2-9, 2-10 and 2-11 show the draft force of the disc with the tilt angle of 0, 15, 20 and 25 degrees, respectively, for different disc angles. Also Figure 2-12 shows all of them together for a comparative analysis.

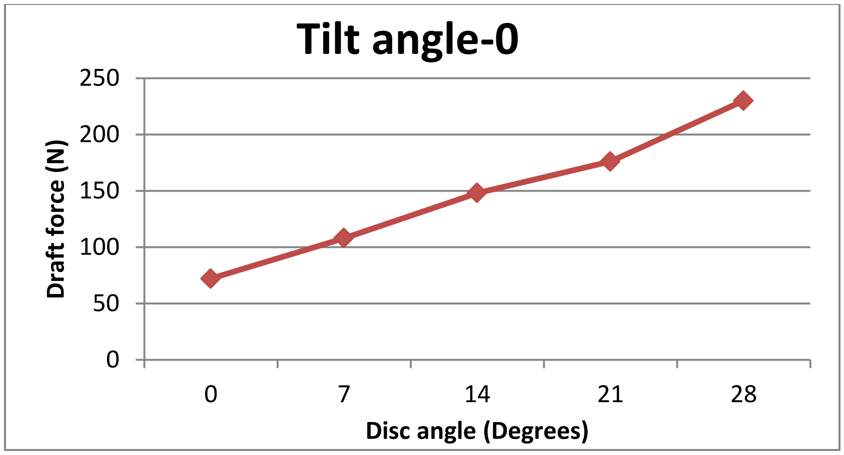

Figure 2- 8- Draft force on the disc coulter for different disc angles, tilt angle=0

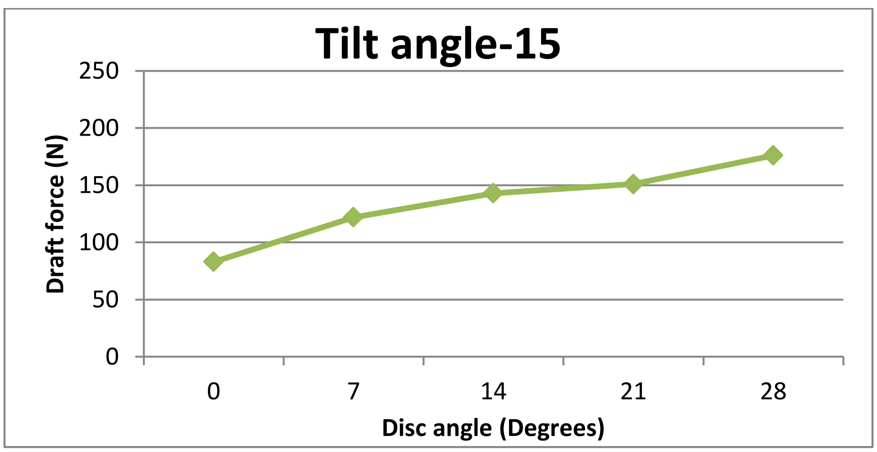

Figure 2- 9- Draft force on the disc coulter for different disc angles, tilt angle=15

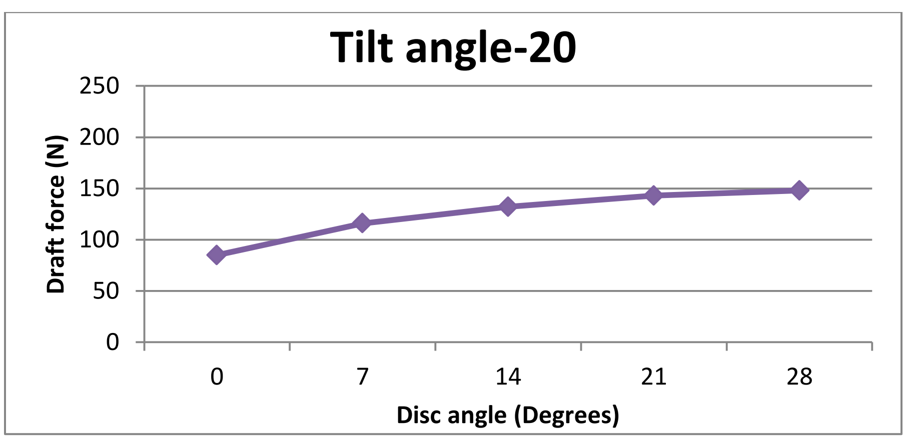

Figure 2- 10- Draft force on the disc coulter for different disc angles, tilt angle=20

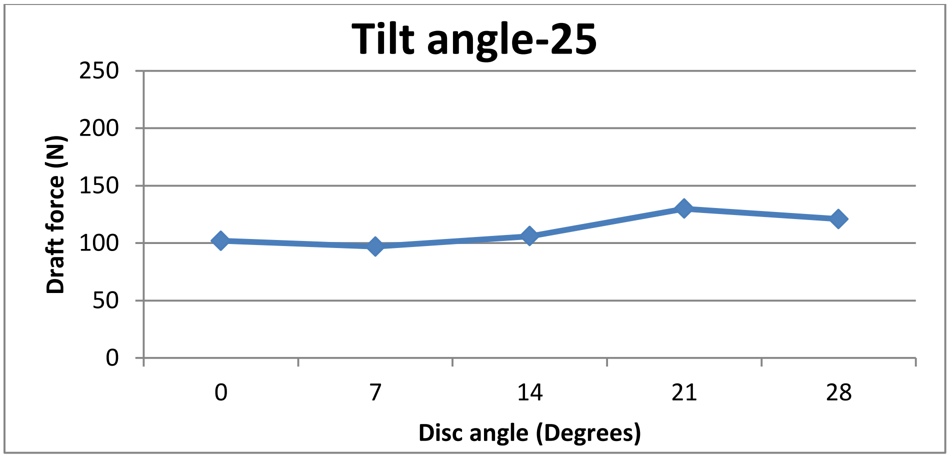

Figure 2- 11- Draft force on the disc coulter for different disc angles, tilt angle=25

We can simply see the effect of disc and tilt angle on the draft force from the graphs. First of all, when tilt angle is zero (Figure 2-8), increasing the disc angle increases the draft force. That can simply be explained; as the disc angle increases, the mirrored face of the disc on the plane perpendicular to the direction of motion increases. It is actually similar to the phenomenon of motion of a body inside a fluid. Bodies with larger face experience larger drag force. However, when tilt angle is not zero, the pattern changes. A single angle disc (tilt angle zero) opens a furrow by pushing and pressing the soil to the sides. On the other hand, a compound angle disc lifts up the soil and displaces it to the sides to open the furrow. It can be said that a using a tilt angle can help to keep the draft force from increasing intensively, when increasing the disc angle.

Generally, larger disc angle means larger draft force. But, as mentioned before, having a disc angle is inevitable; because disc angle is the parameter that is responsible for the width of the furrow. So to keep the draft as low as possible, we have to choose the smallest disc angle possible. We can see from Table 2-4 and also Figure 2-12 that the lowest draft force with a non-zero disc angle was obtained with a compound angle of 7º disc angle and 25º tilt angle.

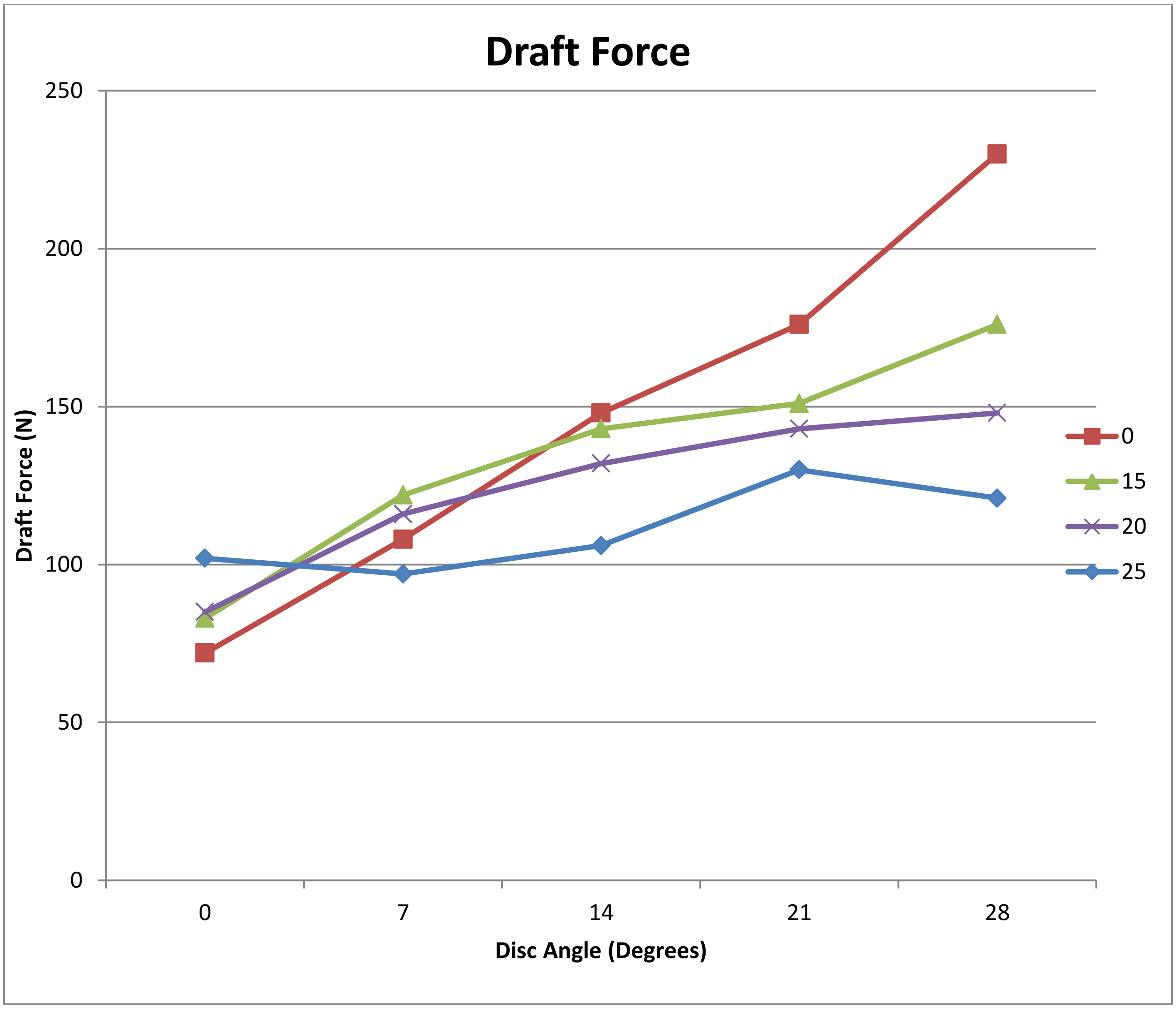

Figure 2- 12- Comparative chart of Draft force for different disc and tilt angles

5-2- Vertical Force:

The vertical force shows how much force we need to keep the disc into the soil, when pushing it forward. The zero of the load cells was set when the disc was attached to the carriage and not in touch with soil. So the weight of the disc does not affect the vertical load.

Figure 2-13, 2-14, 2-15 and 2-16 show the vertical force for different disc angles with 0º, 15º, 20º and 25º tilt angles, respectively. Generally speaking, a pattern or trend cannot be found for the results for vertical forces. The only noticeable fact is that the vertical force reduces when we have a compound angle. As mentioned before, a compound angle disc ($\gamma \neq 0$, $\beta \neq 0$) displaces the soil particles upward and to the sides to open the furrow. The reason for less vertical force can be the added weight of the soil particles as they pile up on top of the disc.

Since the vertical force is not a criterion for the selection, further study and analysis is carried out. These data were used at the design section, when we have chosen a specific disc and tilt angle. So, as experimental results showed, the minimum draft force was obtained with 7º disc angle and 25º tilt angle. The vertical force for corresponding angles is 84 N.

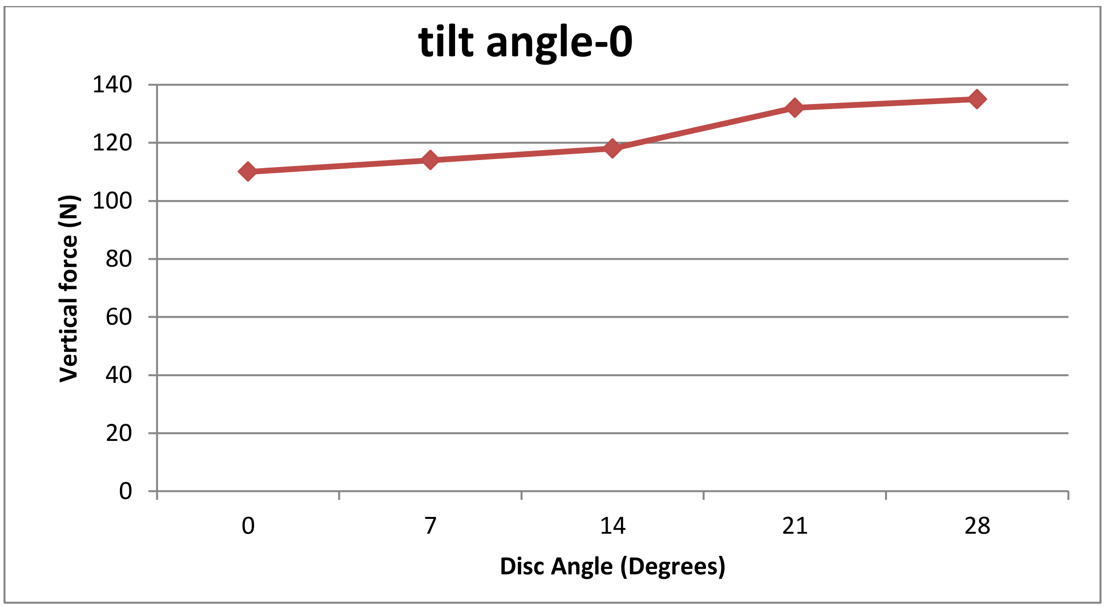

Figure 2- 13- Vertical force on the disc coulter for different disc angles, tilt angle=0

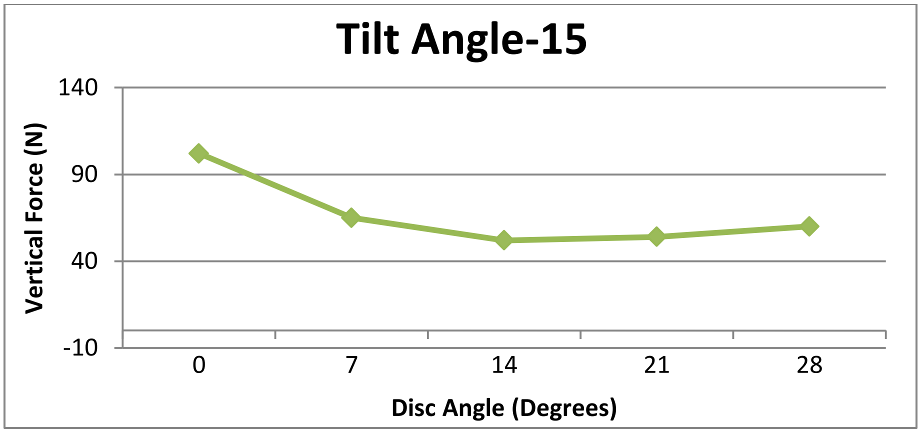

Figure 2- 14- Vertical force on the disc coulter for different disc angles, tilt angle=15

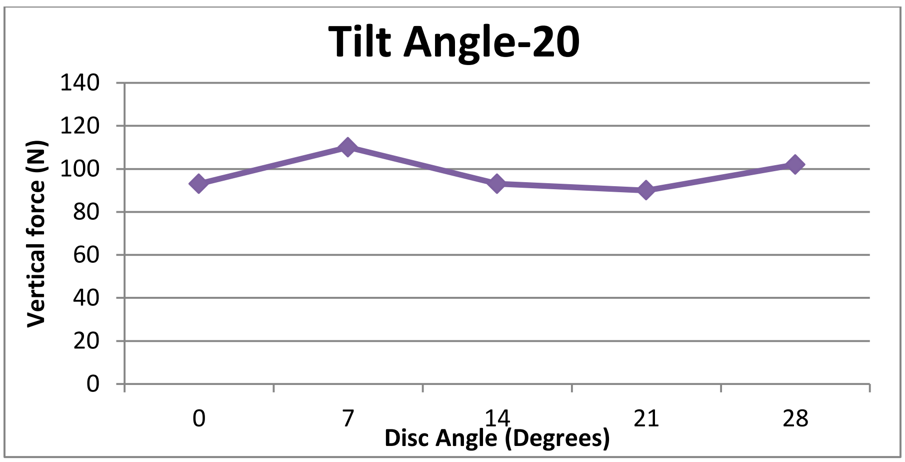

Figure 2- 15- Vertical force on the disc coulter for different disc angles, tilt angle=20

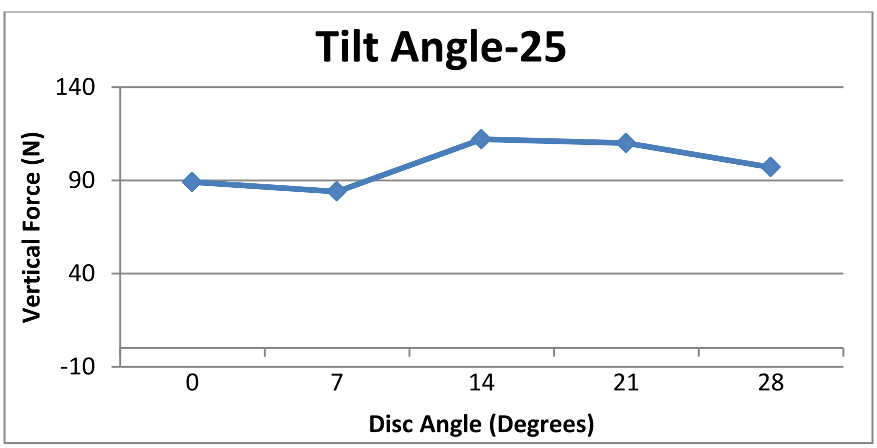

Figure 2- 16- Vertical force on the disc coulter for different disc angles, tilt angle=25

2-5-3- Lateral Force:

Unlike vertical force, lateral or side forces seem to be more predictable. Obviously increasing the disc angle will increase the lateral force; because with a non-zero disc angle, the system becomes asymmetrical, which results in a higher lateral force in some angles. But when we use tilt angle to form a compound angle, it may help to reduce the lateral force. This effect can be seen in Figure 2-18, 2-19 and 2-20 compared with 2-17. The reason for the reduction in the lateral force in the presence of tilt angle can be explained the same as the draft force. A compound angle disc instead of pushing and pressing the soil to the side, it lifts up the soil and displaces it to the side. This will result in lower lateral force as well as lower draft force at some angle combinations.

As it mentioned for vertical force, these data are used in the design section, when we have chosen a specific disc and tilt angle. Thus, for the 7º disc angle and 25º tilt angle, lateral force which is equal to 760 N.

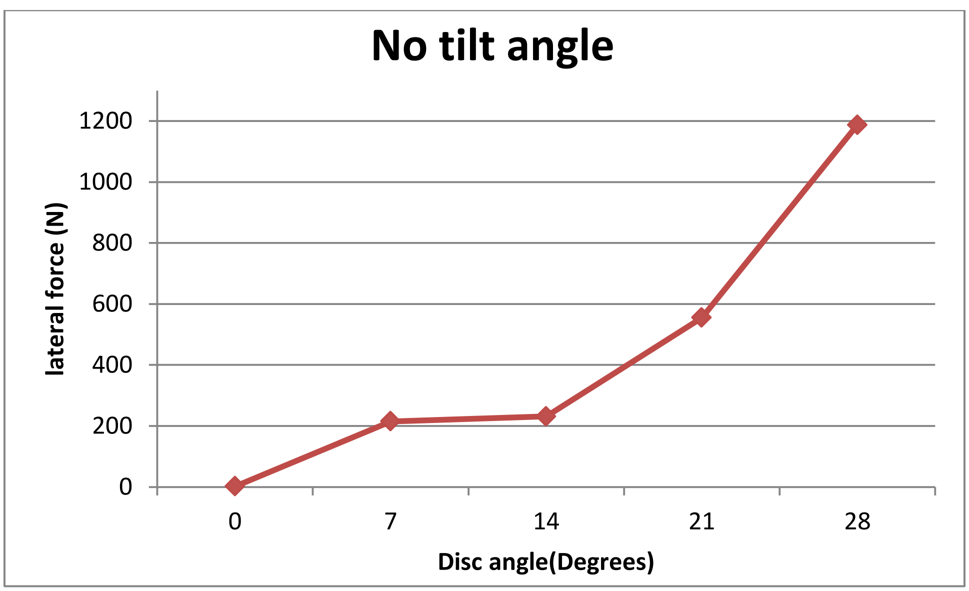

Figure 2- 17- Lateral force on the disc coulter for different disc angles, tilt angle=0

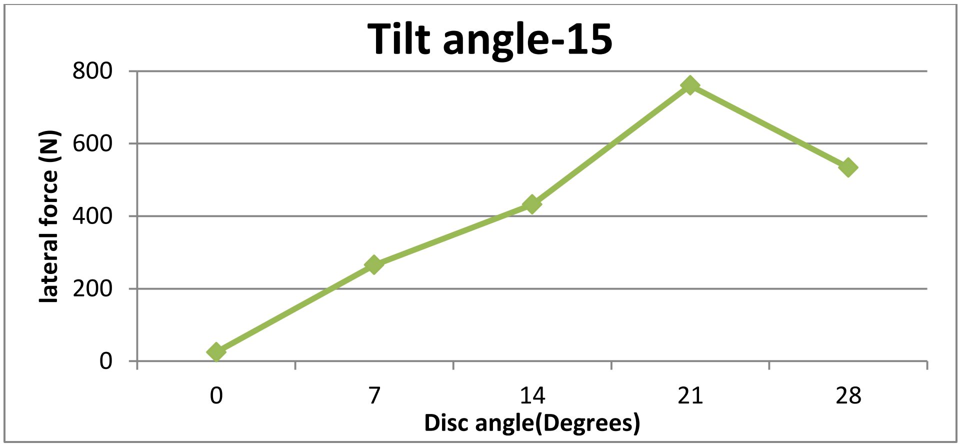

Figure 2- 18- Lateral force on the disc coulter for different disc angles, tilt angle=15

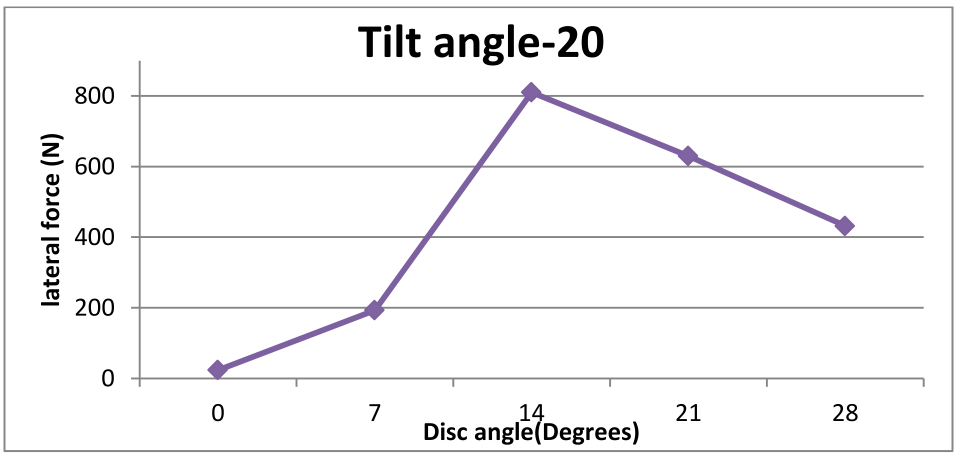

Figure 2- 19- Lateral force on the disc coulter for different disc angles, tilt angle=20

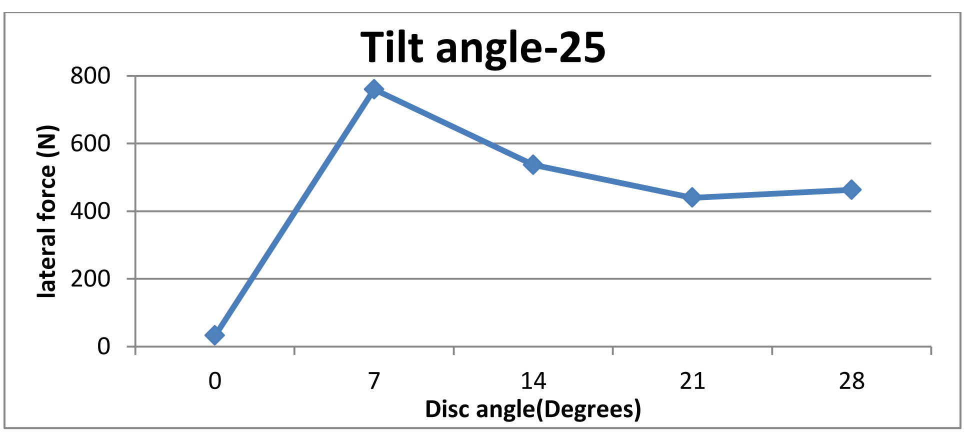

Figure 2- 20- Lateral force on the disc coulter for different disc angles, tilt angle=25

2-6- Summary:

A series of experiments is performed to study the effect of disc and tilt angles on the forces applied on the disc from the soil, when disc moved through the soil with uniform speed. The experiments were done in the soil bin, facility of College of Engineering, University of Saskatchewan. The goal of these tests was to find the best combination of disc angle and tilt angle which leads to minimum draft force. The disc used in tests had a 460 mm diameter and depth of cut was set to 50 mm. Force in 3 direction of draft, vertical and lateral are measured by load cells. The results of the experiments showed that the compound angle of 7º disc angle and 25º tilt angle gives the lowest draft force, which is 97 N. Although single angle disc, or zero disc angle gives lower draft force, but as mentioned earlier in this chapter, disc angle cannot be zero for the purpose of seeding. The corresponding vertical and lateral force for 7º disc angle and 25º tilt angle are 84 N and 760 N, respectively. Results for the angles that are in common with the work of Afify et al. [11] are close to each other and are validated by their results. Besides, results obtained in experiments are also compared and validated by the analytical work done by fellow research group member, Yun Zhang. The details of it is provided in appendix D. The results obtained in this chapter are used in the design process, static analysis and stress analysis of the developed planter, which is discussed in detail in chapter 3 and 4.

Chapter 3- Design

3-1- Design process

The objective of this research is to design and develop a customized planter to attach to the wheeled mobile robot with the limitations and challenges that mentioned in chapter 1. So we can say that this masters research project, is actually an engineering design practice, which took all the steps needed that an engineering design process requires.

“To design is either to formulate a plan for the satisfaction of a specified need or to solve a problem” [21]. In this case, design is being used to satisfy a specific need: a customized planter that our mobile robot can pull. Engineering design process or mechanical engineering design process is a series of steps that each designer have to go through, to reach to the solution of the problem or to satisfy the need. Figure 3-1 shows the steps or phases of a general engineering design process.

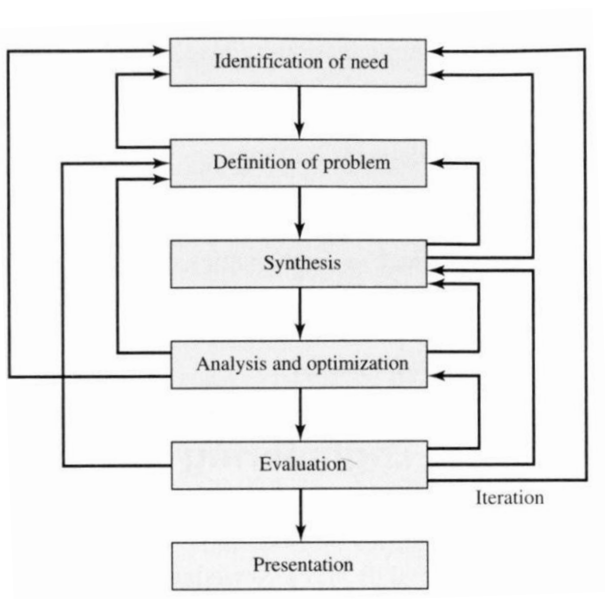

Figure 3- 1- Engineering design process [21]

A brief summary of the design procedure of the customized planter is mentioned below: The need of a customized planter for the mobile robot was brought up by the main project- Robotic assisted farming. A thorough study about design of planters and their components and tool-soil interaction is performed. More data and information was collected by performing experiments on soil-disc interaction in the soil bin. Conceptual design was performed and between a few ideas, one was selected for analysis and detailing. Design was reviewed and revised after different analyses, and the new design was analyzed again to satisfy all the design criteria. Finalized design was sent to machine shop in order to fabricate the prototype. Fabricated parts were assembled and attached to the mobile robot to perform autonomous planting. Satisfactory results were obtained in tests and evaluation phase, which shows the success of the design process.

3-2- Conceptual design

The conceptual design phase started with the selection of the parts that were preferred to be used in the planter. Taking a look at an existing planter, figure 3-2, we can see different parts and components.

CNH-Saskatoon partially supported this research, and they donated two planters to us to be used for prototype. Some of parts of this planter were used, and other parts were modified for our new planter. Coupled seed hopper and precision seed metering system is one of the parts that was used without any change from the donated planter. No research or analyses were performed on this part; because design of the seed hopper and singulation system was not part of the objectives of this research. So the seed hopper and its frame were kept without any change and they were added to new designed parts.

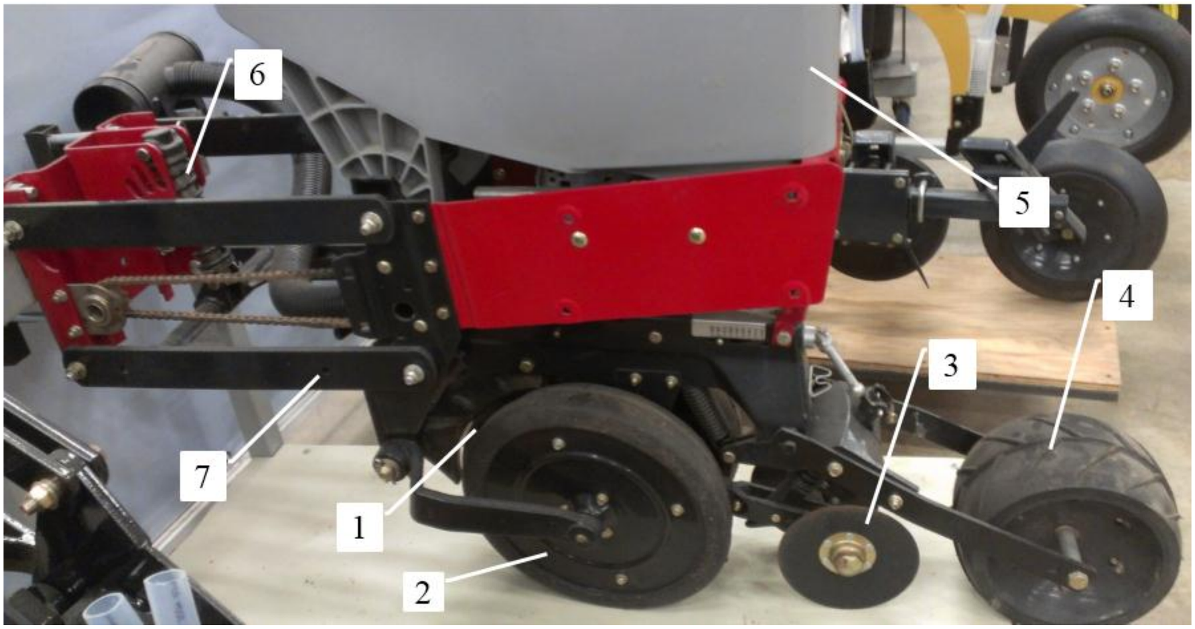

Figure 3- 2- Existing planter and its components, 1)Disc Coulter, 2)Gauge wheel, 3)Soil covering disc, 4)Press wheel, 5)Seed hopper, 6)Down force spring, 7)Parallelogram linkage

With these in mind, few design ideas were suggested. Figure 3-3 shows a couple of sketches for conceptual design that were done by hand. In the first sketches and conceptual design step, the main objective was to keep the planter easy to pull, small so that can be connected to the robot, easy to build, inexpensive and as light as possible so it does not require huge power. When the decision has been made on the general idea, a first sketch of 3D model was generated in SolidWorks. Figure 3-4 shows the 3D model of the modified planter. In this figure, the parts that are shown in grey, are the parts that are used from the existing planter without any change, and the blue parts are the developed and new parts that further analysis has been performed on them.

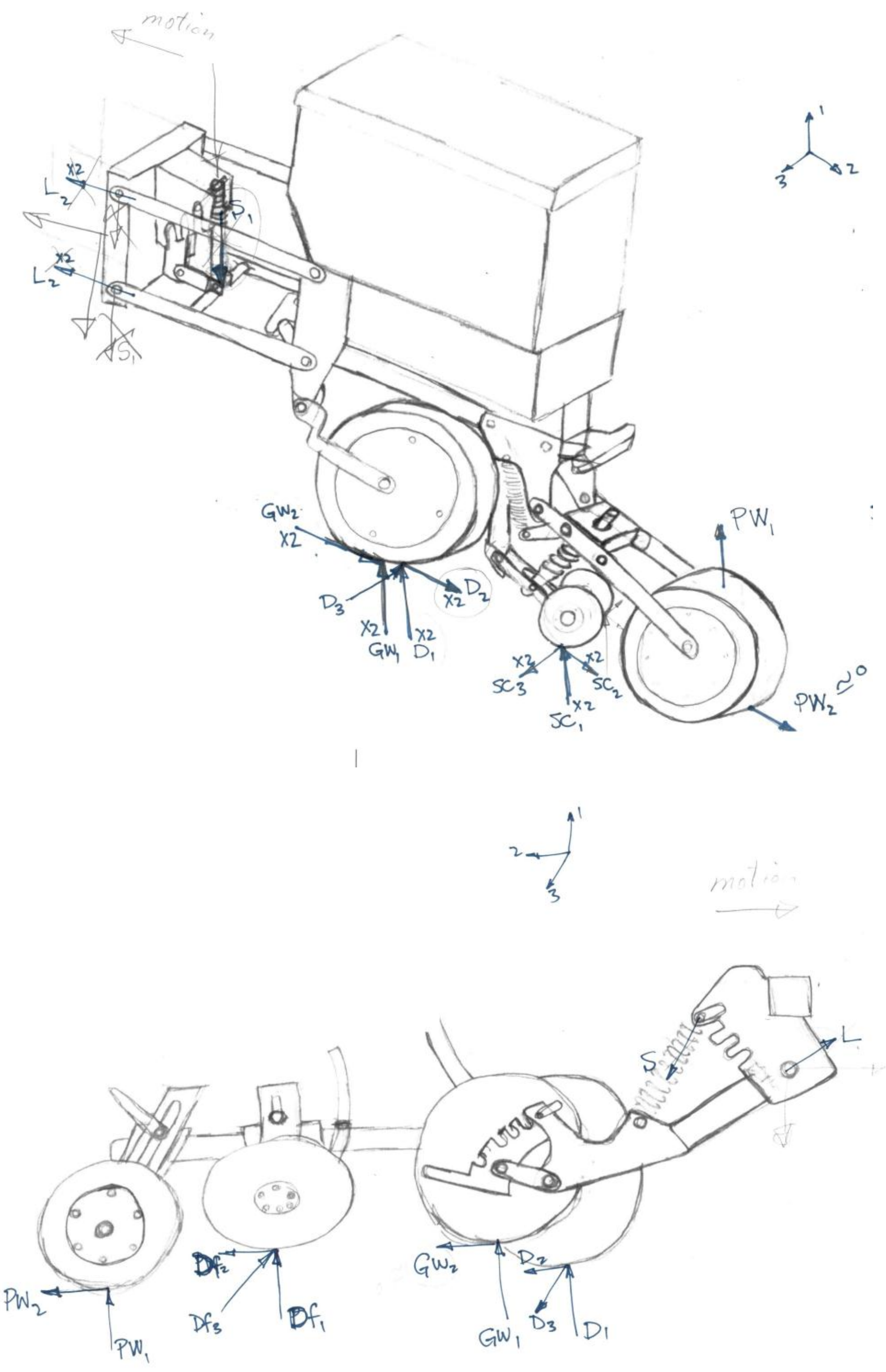

Figure 3- 3- Sketches of the design of two planters, utilizing disc coulter

Generally it can be said that, most of the research and analysis has performed on the parts that are in contact with the soil and their attachments (Figure 3-4). These parts can be categorized in groups for easier further analysis,

- Furrow opener assembly: Disc, gauge wheel, disc holder and depth control link
- Packing assembly: Press wheel, Press wheel links, Spring connection and extension spring
- Seeding assembly: Seed drop tube, runner type opener, power transmission and vacuum system
- Connection assembly: Main spring, vertical connection bar, horizontal connection bar and lifting mechanism.

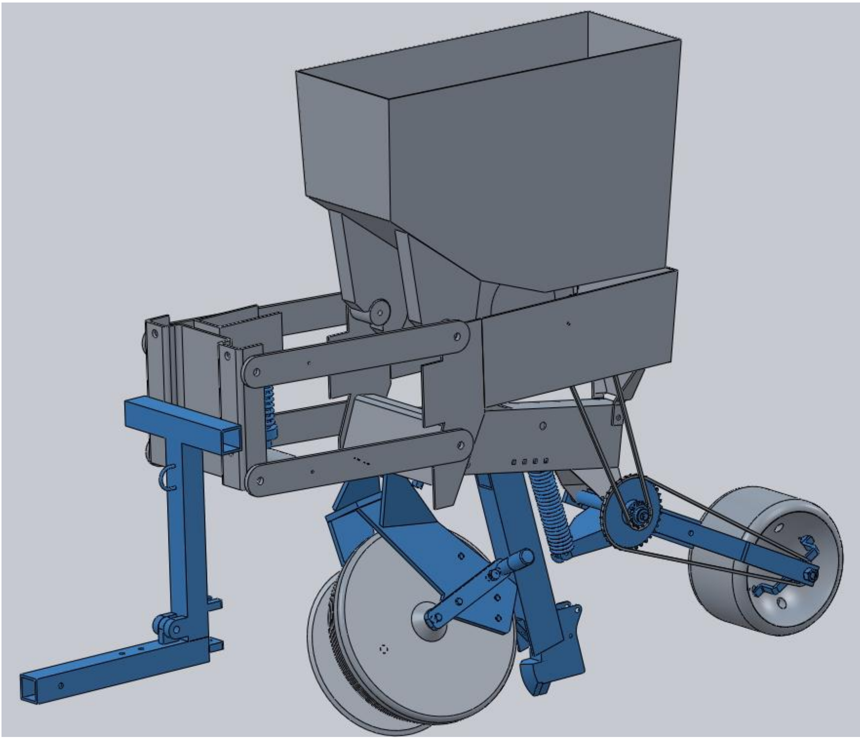

Figure 3- 4- SolidWorks model of the new designed planter

Details of each of these groups and their parts that are studied for design purpose come in order.

3-2-1-Furrow Opener Assembly

The parts for this group are shown in figure 3-5.

Starting with the soil engagement tool, the existing planter has double discs with compound angle and installed at a staggered position. The disc angle and tilt angles of these discs are ɣ=5º and β=7º, respectively.

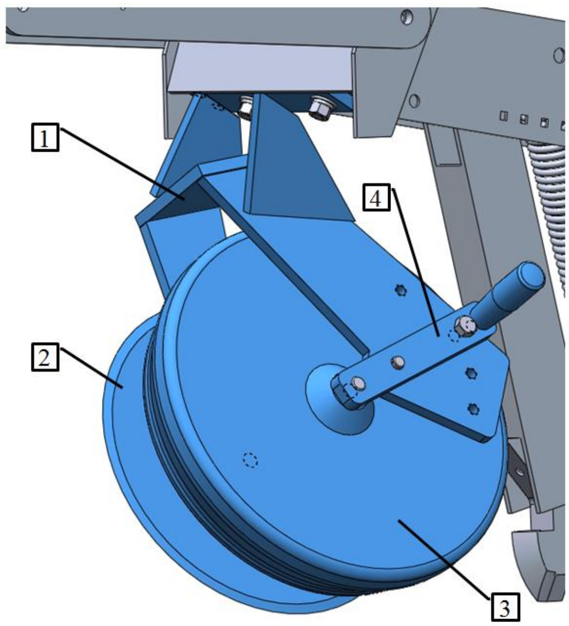

Figure 3- 5-Furrow opener assembly parts, 1) Disc holder, 2) Disc, 3) Gauge wheel, 4) Depth control link

As the plan was to reduce the draft force, one of the discs was removed and a single disc furrow opener was used. In addition to that, using the results of the soil bin experiments (chapter 2), a new compound angle was used: ɣ=7º disc angle, and β=25º tilt angle. We double check the width of the furrow that opens by the disc coulter. As mentioned before, the furrow must be wide enough that provides a proper bed for placement of the seed. The disc used for calculations, is the same disc used in chapter 2 for experiments. So it has a D=460 mm diameter. Figure 3-6(a) shows the disc, d_1=50 mm into the soil. The contact line AC can be seen in top view Figure 3-6(b). So if the depth of cut is d_1, the width of the furrow, d_2, can be calculated, as follows,

$$AC = 2 \times \sqrt{OA^2 - OB^2} = 2 \times \sqrt{230^2 - 180^2} = 286.4\, mm \qquad \text{(Eq. 3-1)}$$

$$d_2 = AC \times Sin7 = 286.35 \times Sin7 = 34.9\, mm \qquad \text{(Eq. 3-2)}$$

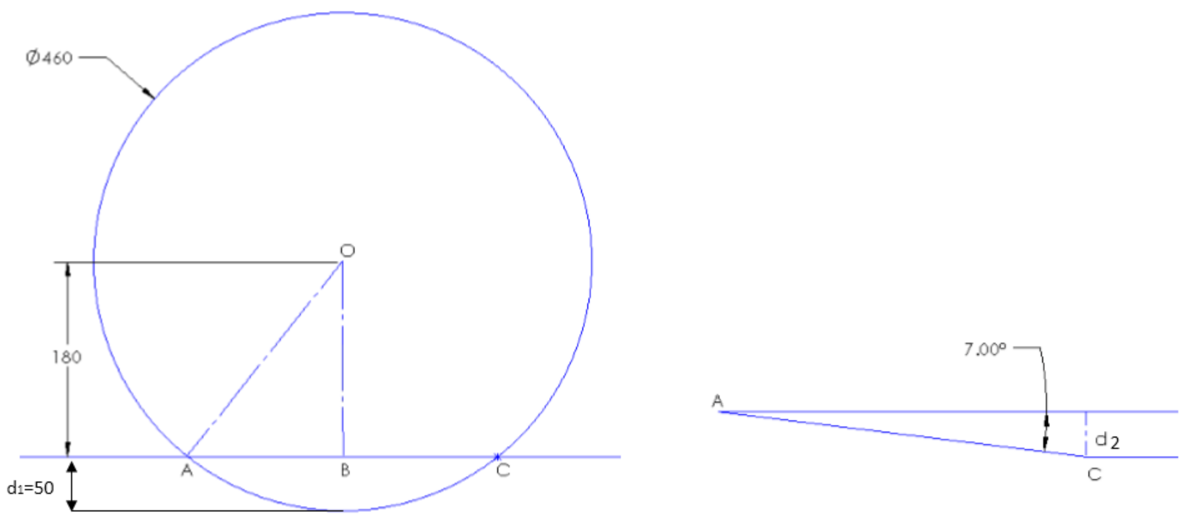

(a) (b)

Figure 3- 6- A 460 mm diameter disc coulter, d_1=50 mm into the soil, (a) Side view, (b) Top view which shows the width of the furrow opened by the disc.

Eq. 3-2 shows that the width of the furrow for 460 mm diameter disc with a 7º disc angle and d_1=50 mm depth of cut, will be around d_2=35 mm. The largest corn seeds are not larger than 15 mm. Thus, the furrow is wide enough to embrace the seed.

Technically one gauge wheel is needed for one disc coulter to control the depth and help with better residue handling. The existing planter uses two gauge wheels because the furrow opener in this type of planter is a double disc furrow opener. But since in the developed planter only one disc coulter is used, just one gauge wheel is needed. This means less draft force because of less contact with the soil.

To attach the disc coulter with the mentioned angles and its gauge wheel to the frame, a new part was designed to align and keep the disc in position. The part that does the similar job in existing planter is a casted, expensive and heavy part that is replaced by a new part, called disc holder in the developed planter (See Figure 3-5). This part can be bolted to the body of the planter and the disc and depth control link can be attached to it with bolts.

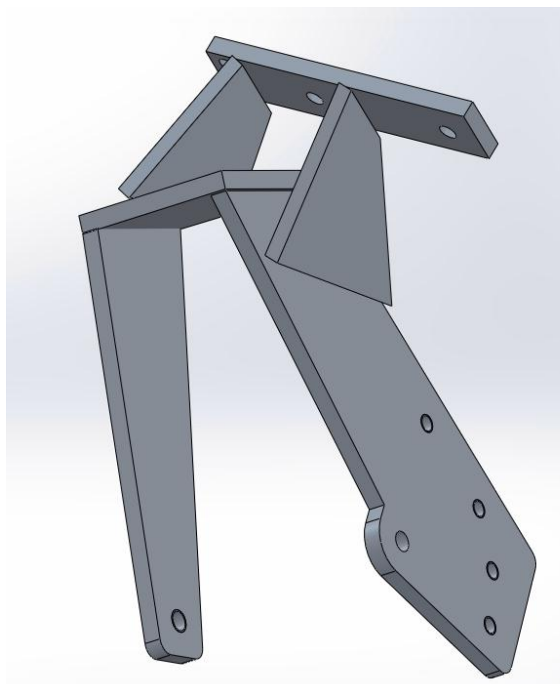

Figure 3- 7- Disc holder, part 1 in Figure 3-5

Disc holder is made of 6 different plates that can be welded together. This kind of design makes its fabrication very easy and relatively inexpensive. Although for mass production casting is preferred. The disc holder, not only holds the disc in the proper disc angle and tilt angle, but also supports the gauge wheel and helps to adjust the depth of the furrow by utilizing depth control link. It gives enough space to the gauge wheel to move up and down, parallel to disc, to set the depth of cut to specific values. The tapped holes on the disc holder gives the options of 0, 25, 50 and 75 mm for depth of cut to the operator. Disc holder can be seen in Figure 3-7.

3-2-2-Packing Assembly

Packing assembly includes press wheel, press wheel links, spring connection, and extension spring, shown in Figure 3-8 and Figure 3-4. The extension spring provides the down force for the press wheel. This force is transferred from the spring to the spring connection and from the spring connection to the press wheel links. Press wheel links hold the shaft of the press wheel, and push it down on the soil, to close the furrow and pack the soil over the seed. Figure 3-8 shows these parts.

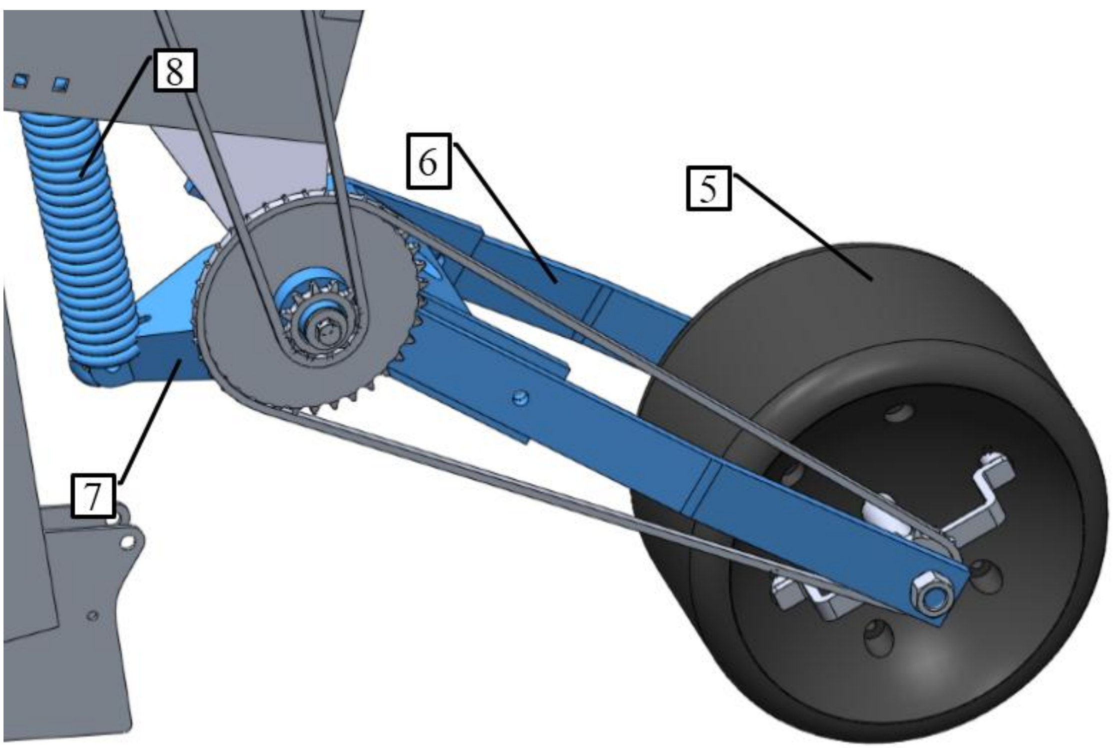

Figure 3- 8-Packing assembly parts, 5) Press wheel, 6) Press wheel links, 7) Spring connection, 8) Extension spring

One of the main analyses that was performed on this group of parts, is the optimization of the change in the packing down force. An optimization problem has been solved to minimize the change in the down force of the press wheel, when it moves up and down through the field. The detail of the analysis is presented in section 3-3-2, after the static analysis on the whole planter is performed.

3-2-3-Seeding Assembly

The journey of a seed to be placed into the soil starts from the seed hopper. It enters the precision seed metering system and sticks to the singulator disc because of the vacuum pressure. Then it is released from the singulator disc and enters the seed drop tube. It drops along the seed drop tube, due to gravity, and reaches to the soil right behind the runner shaped opener. Runner type soil opener helps to keep the soil open, right before the seed drops into to furrow. Another job of the runner type opener is to pack the bottom part of the furrow which provides a better environment for seed placement and germination. Figure 3-9 shows all the parts that are involved in seeding.

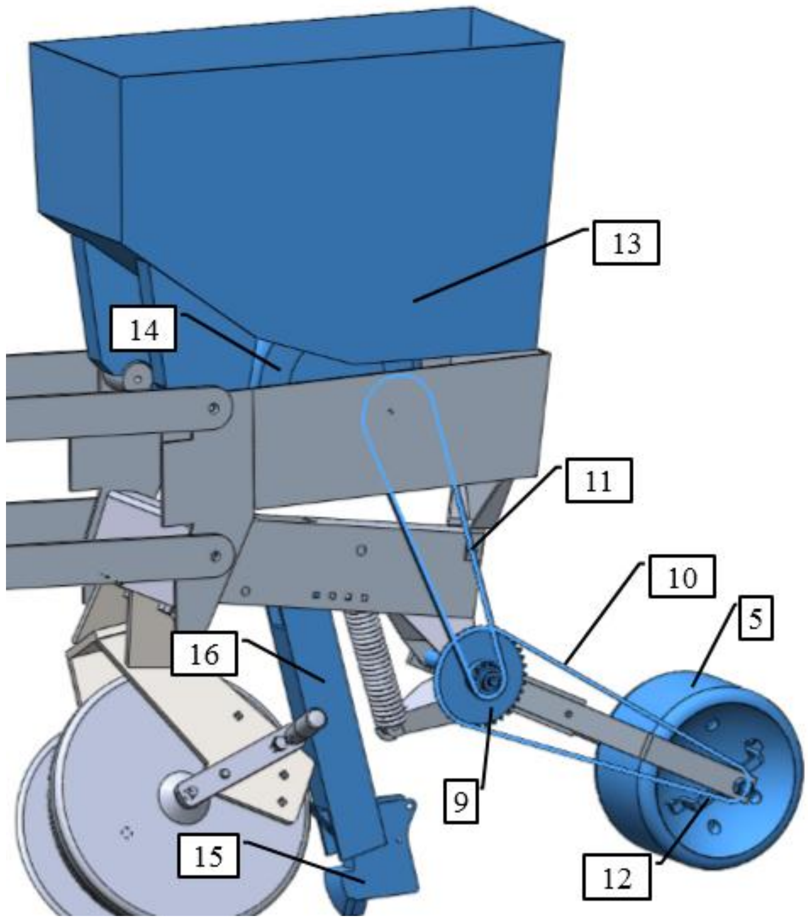

Figure 3- 9- Parts that are involved in seed placement, 5) Press wheel, 12) Sprocket 1 and its connection link, 10) Chain loop 1, 9) Sprocket 2 and sprocket 3 and their connection shaft, 11) Chain loop 2, 13) Seed hopper, 14) Pneumatic precision seed metering device, 16) Seed drop tube, 15) Runner type opener

As mentioned in chapter 1, one of the challenges of this modified design is to rotate the singulator disc. In the existing planters, a drive wheel transmits power to a common shaft as it moves on the ground. Then the shaft distributes the power between row planters, and then via sprocket and chain the power is transmitted to the singulator disc. Since only two row planters must be attached to the mobile robot, this mechanism is not used here. Different ideas were discussed. One of the ideas was to use an electric motor and gearbox to rotate the singulator disc. The RPM of the motor must be proportionally set to the speed of the robot, in order to keep the distance between the seeds equal. The complexity and high cost of this idea was the reason to reject it. Finally the decision was made to transmit power from each press wheel to its singulator disc. It is a novel idea that has never been used in any planter before. Since the press wheel is pushed on the soil by the extension spring, it usually doesn't slip. Besides, the rotational velocity of the press wheel is always proportional to the forward speed of the planter. So to find the conversion factor, to convert forward speed of the planter to the RPM of the seed disc, we can have,

$$\mathrm{N}_h \times n_s = \frac{V\left(\frac{Inch}{s}\right)}{l_d\ (Inch)} \times 60 \qquad \text{(Eq. 3-3)}$$

In which N_h is the number of holes on the singulator disc, n_s is the rotational speed of the singulator disc, V is the forward speed of the planter and l_d is the desired space between two seeds, as they are placed into the soil. Figure 3-10 shows how the seeds line up on a singulator disc. After rearranging and unit conversion of Eq. 3-3,

$$n_s = V(mph) \times \frac{1}{l_d\ (Inch)} \times \frac{1}{\mathrm{N}_h} \times 1056 \qquad \text{(Eq. 3-4)}$$

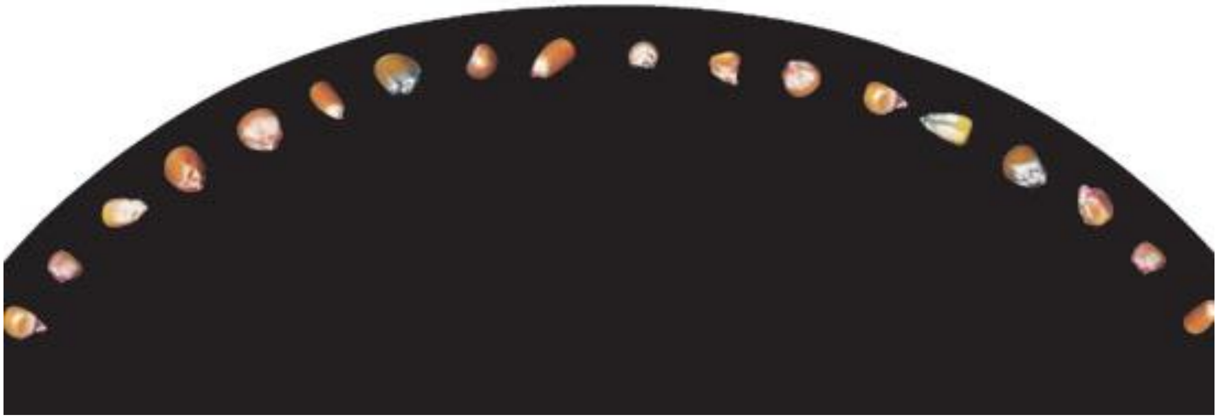

Figure 3- 10- Singulator disc and the seeds stick to it because of vacuum pressure

http://www.caseih.com/en_us/products/plantingseeding/pages/1200-planters.aspx

For corn planters, seed discs are available in 24 holes and 48 holes. The mobile robot can go from 0.1 up to 10 mph. Common forward speed for corn planting is 5 mph and spacing of 127 mm for best corn seed germination. Putting these data into Eq. 3-4, and for 24 hole singulator disc,

$$n_s = V(mph) \times \frac{1}{l_d\ (Inch)} \times \frac{1}{N_h} \times 1056 = 5 \times \frac{1}{5} \times \frac{1}{24} \times 1056 = 44\ rpm \qquad \text{(Eq. 3-5)}$$

For 48 hole singulator disc,

$$n_s = 5 \times \frac{1}{5} \times \frac{1}{48} \times 1056 = 22\ rpm \qquad \text{(Eq. 3-6)}$$

It is recommended that that RPM of the singulator disc falls between 12-60 rpm [21]. So, 48 hole singulator disc was chosen, because even with higher forward speeds, its RPM still will remain in recommended zone.

So, using a packer wheel with a diameter of 280 mm (11 inches),

$$n_w = \frac{V(mph)}{R(inch)} \times 63360 \frac{inch}{mile} \times \frac{1}{60} \frac{hr}{min} \times \frac{1}{2\pi} \frac{cycle}{rad} = \frac{5}{5.5} \times 63360 \times \frac{1}{120\pi} = 152.8\ rpm \qquad \text{(Eq. 3-7)}$$

The ratio between wheel rotational velocity, n_w, and singulator disc rotational velocity, n_s, will be 152.8/22= 6.95. This rpm conversion can be created using sprockets and chain. But one step conversion results in huge diameter difference between driver and driven sprockets, which neither is possible, nor is recommended. Thus, it was decided to do this conversion in two steps, we chose ratio 13 to 36 and ratio 12 to 30 teeth sprockets.

n_1= 36/13= 2.77

n_2= 30/12= 2.5 (Eq. 3-8)

To check, n1× n2= 2.77×2.67= 6.93

This satisfies the ratio that was needed. So Sprocket 1 was chosen to has 13 teeth, sprocket 2 has 36 teeth, sprocket 3 has 12 teeth and sprocket 4 has 30 teeth. Sprocket 1 is attached to the press wheel and is driven by press wheel and Sprocket 4 is attached to the singulator disc and rotates the disc. This system can be seen in Figure 3-9.

A vacuum pump provides vacuum pressure for the pneumatic precision seed metering system. For corn planting a vacuum pressure between 18-20 inch H_2O is needed [22]. Less vacuum will result in seed misses, which means one seed will be missed along the series of the seeds that are planted. Higher vacuum may cause an increase in doubles, which means more than one seed will be sucked into one hole and consequently, more than one seed will be planted in one spot. Thus, a proper vacuum pressure must be provided for the pneumatic seed metering system and the singulator disc. In existing planters, huge vacuum fans are used to provide vacuum pressure for all the row planters in use. In our case, since only two row planters are used, a shop vacuum was used to provide vacuum pressure. Different shop vacuums with different powers were tested to find the proper power for this purpose. The shop vacuum used for final tests of the planter, is a 5hp shop vacuum by RIDGID.

3-2-4-Connection Assembly

As mentioned earlier, a mechanism is needed to connect the planter to the robot, push the planter downward when in use, and lift it off the ground when in transportation. Connection assembly consists of the main spring, vertical pull bar, horizontal pull bar and lifting mechanism. These parts are shown in figure 3-11. The job of the main spring is to push the planter on the soil and provide enough down force on the planter and gauge wheel.

Another part that had to be designed was the attachment link that connects row planters to the mobile robot. This mechanism also should have the ability to lift up the row planters from the ground for transportation and making turns.

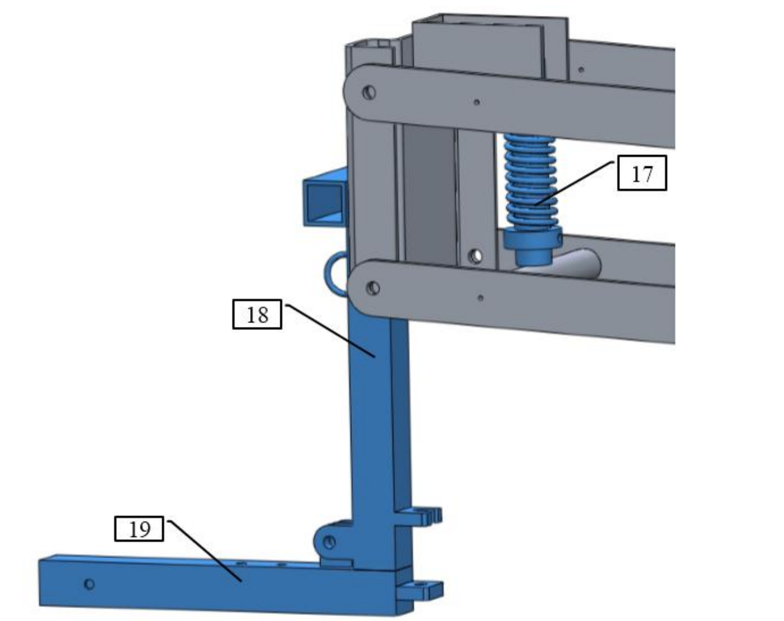

Figure 3- 11- Connection assembly parts, 17) main spring, 18) Vertical pull bar, 19) horizontal pull bar

In the existing row planters, hydraulic cylinders lift up a series of row planters off the ground for transportation. As mentioned in chapter 1, hydraulic power is not available for this purpose from mobile robot. For the lift mechanism different ideas were examined. Using a power screw, worm gear or even a hand-operated wrench were among the ideas that were discussed. Hand-operated wrench was chosen for this system because of its simplicity, lower cost and easy maintenance (See Figure 3-12).

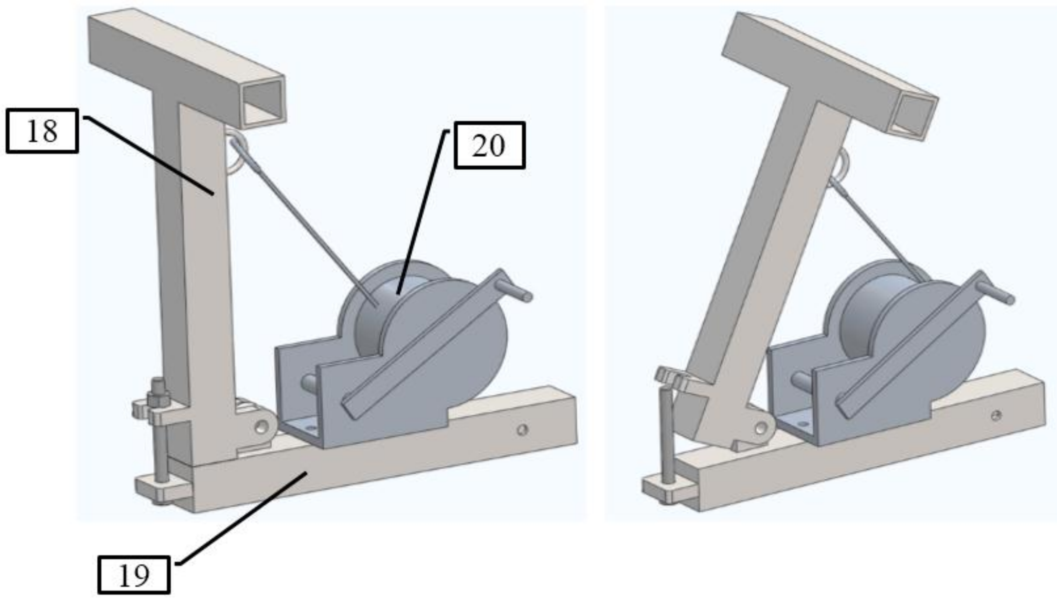

Figure 3- 12- Parts of connection mechanism, 18) vertical pull bar, 19) horizontal pull bar and 20) lifting mechanism (hand wrench)

Figure 3-13 can be used to calculate the force that is needed to lift up the planter. The weight of the planter and its center of mass is estimated by SolidWorks. This weight is estimated to be about 980 N, including the weight of the seed inside the seed hopper. Using moment equilibrium equation about the joint that vertical pull bar rotates (point O), the tension in cable can be found.

$$TSin33 \times 421 = W \times 738.7$$

$$T = 980 \times \frac{738.7}{421Sin33} = 3157\ N \qquad \text{(Eq. 3-9)}$$

So, a hand wrench was chosen that can lift up to 5340 N (equals to 1200 lbf.). This gives a safety factor of 1.7 for the lift mechanism.

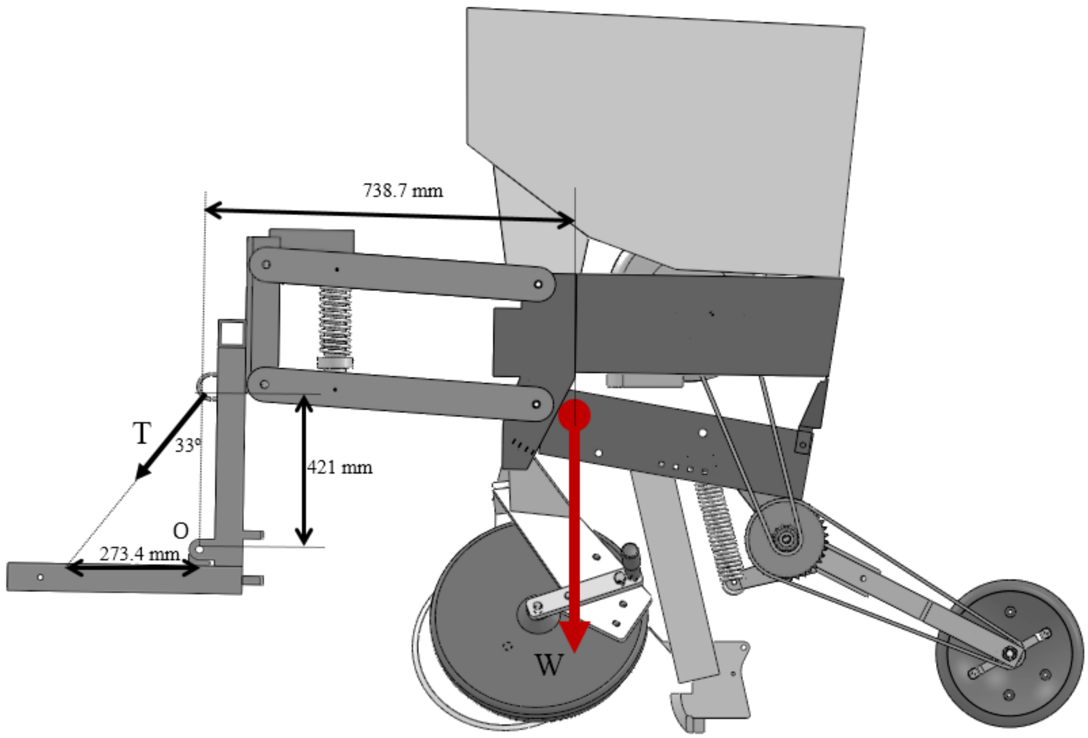

Figure 3- 13- Forces for lifting condition of the planter

3-3-Detail Design and Analysis:

Different analyses have been performed on the modified planter to verify its strength and performance. Static analysis, hand calculations, optimization and stress analysis were performed on the designed planter before fabrication of the prototype.

3-3-1-Static force analysis:

To perform a static analysis, all external forces that are applied to the planter must be first defined. Figure 3-14 shows a schematic figure of the planter and the external forces. Forces in the side direction are not shown in this picture. All the forces can be categorized into three groups: 1) Soil interaction forces, 2) gravitational forces, 3) forces from the mobile robot.

Soil interaction forces are applied to the planter at each point of contact. Disc coulter, gauge wheel, seed delivery shoe and press wheel are the parts that are interacting with the soil.

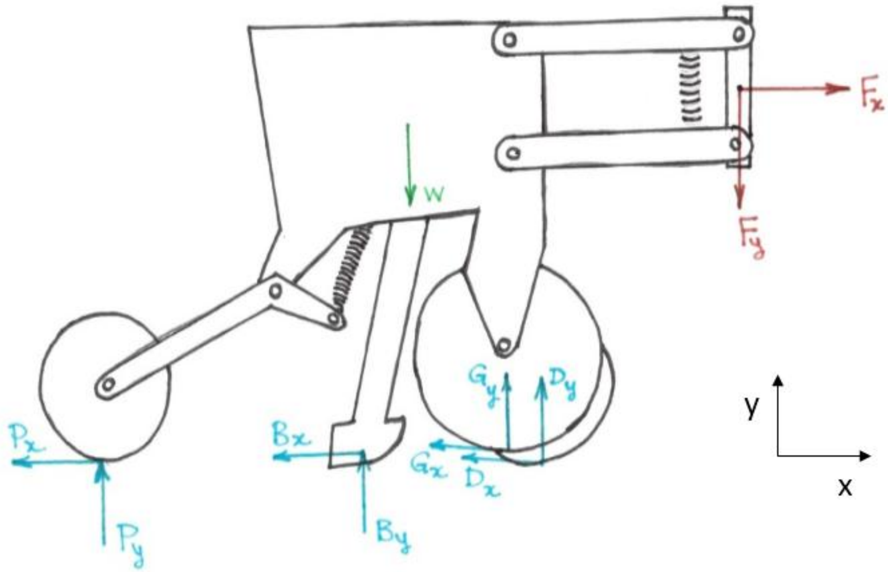

Figure 3- 14- Schematic side view of the planter, showing external forces in x and y directions

If we assume that the planter is moving with constant velocity, which means semi-static condition, the following equilibrium equation in the X direction can be written,

$$F_x = D_x + G_x + B_x + P_x \tag{Eq. 3-10}$$

And in the y direction,

$$F_y = D_y + G_y + B_y + P_y - W \tag{Eq. 3-11}$$

In which:

F_x is the pulling force applied from the mobile robot, which is also known as the total draft force for the whole planter. D_x, G_x, B_x and P_x are the frictional forces applied to disc, gauge wheel, seed delivery shoe and press wheel, respectively. Frictional force for the gauge wheel and press wheel are a combination of slipping friction and rolling friction.

F_y is the vertical force from the mobile robot that push the planter downward and keep the disc into the soil. D_y, G_y, B_y and P_y are normal reaction forces applied to disc, gauge wheel, seed delivery shoe and press wheel, respectively. W is the weight of the whole planter. The following analysis was done to find the total draft force, F_x, and the vertical force, F_y. Some of these forces are known or found by the experiments, in chapter 2, and some of them are found from the literature.

Experiment on the soil- disc interaction presented in chapter 2, showed that for the disc orientation that was chosen (γ=7º, β=25º), D_x = 97 N and D_y = 84 N.

Studies showed that for the best emergence and highest yield results, the packer wheel and the gauge wheel down force must have a specific amount and should be kept constant. Research works on the down force on the disc coulter and gauge wheel showed that, it should not be smaller than 880 N, and suggested a down force of approximately 1200 N [15]. Some other works suggested 940 N or higher for best emergence results [13]. Also for the press wheel down force, experiments and reported works have indicated that 333 N provides adequate emergence and grain yield [16]. Using the data obtained from the literature, P_y = 333 N and G_y = 1200 N were chosen. There are some works done on the forces acting on the runner type tillage tools. A research done in 1974 showed that the vertical force on a runner type furrow opener, for 50 mm cutting depth is about 2 lbf, or 8.9 N [17].

The unknown parameters in Eq. 3-10 are W and F_y. With the 3D model and also available existing planters, we can have an estimation of the weight. The weight of the planter is approximately 980 N, including the weight of the seeds inside the seed hopper. So one can write,

$$F_y = D_y + G_y + B_y + P_y - W = 84 + 1200 + 9 + 333 - 980 = 646\ N \quad \text{(Eq. 3-12)}$$

A summary of the forces in y direction and their values can be found in Table 3-1.

Table 3- 1- Vertical forces applied to the modified planter

Force source	Symbol	Value (N)
Disc vertical force	D_y	84
Gauge wheel normal force	G_y	1200
Runner vertical force	B_y	9
Press wheel normal force	P_y	333
Weight	W	980
Total vertical force	F_y	646

Now that all the forces in the Y direction are known, it is easier to find the forces in the X direction; because G_x and P_x are frictional forces which are dependent on the normal forces. The motion resistance for a rigid wheel depends on the normal vertical force, wheel size and soil properties as it moves on the soil and compacts the soil [23].

$$G_x = \frac{G_y^2}{5.7cb_G D_G} \quad \text{(Eq. 3-13)}$$

$$P_x = \frac{P_y^2}{5.7cb_P D_P} \quad \text{(Eq. 3-14)}$$

In Eq. 3-13 and 3-14, c is the cohesion of the soil, b_G and D_G are the gauge wheel width and diameter and b_P and D_P are the press wheel width and diameter, respectively. All units are in SI system. So for the Saskatchewan soil, with 13% water content, the cohesion is 25 kPa [26].

The available commercial gauge wheel and press wheel are used, which their dimensions can be found in table 3-2.

Table 3- 2- Dimensions of the gauge wheel and press wheel

	Width (m)	Diameter (m)
Gauge Wheel	0.08	0.41
Press Wheel	0.17	0.29

Now G_x and P_x can be easily calculated.

$$G_x = \frac{G_y^2}{5.7cb_GD_G} = \frac{1200^2}{5.7\times25000\times0.08\times0.41} = 308\ N \qquad \text{(Eq. 3-15)}$$

$$P_x = \frac{P_y^2}{5.7cb_PD_P} = \frac{333^2}{5.7\times25000\times0.17\times0.29} = 16\ N \qquad \text{(Eq. 3-16)}$$

Also for the shoe type furrow opener or the seed delivery shoe, researches show that for the similar soil conditions and forward speed of 4.5 Km/hr and 6 cm cutting depth, the average draft force is 25 N.[5]

So the total amount of draft force, needed for the planter can be calculated as,

$$F_x = D_x + G_x + B_x + P_x = 97 + 308 + 25 + 16 = 446\ N \qquad \text{(Eq. 3-17)}$$

A summary of the forces in y direction and their values can be found in Table 3-3.

Although the vertical force and the draft force which is needed for the planter have been calculated, but these values can change easily as the planter moves along the farm field; because soil and its properties and its interaction with the tool is very changing. Having that in mind, a safety factor of 2 for the stress analysis and design is used to cover this unpredictability.

Table 3- 3- Horizontal forces applied to the modified planter

Force source	symbol	Value (N)
Disc draft force	D_x	97
Gauge wheel friction	G_x	308
Runner draft force	B_x	25
Press wheel friction	P_x	16
Total draft force	F_x	446

3-3-2- Optimization of the packing pressure and spring force:

In the design of the planters different methods are used to provide down force, and create the flexibility to absorb shocks. Springs are the most commonly used method, but other methods such as hydraulic or pneumatic cylinders are used in different designs. Springs are simple, inexpensive, and they do not need any maintenance or supporting components.

For the best results of germination and highest yield the packing force must be kept constant. But the farm field that the planter travels on is not flat; so the planter and the press wheel experiences bumps and holes that cause change in the packing force. With a proper design the change in the packing force can be minimized. A schematic figure of the press wheel and its linkage is shown in figure 3-15. In this figure point O is assumed to be fixed and the press wheel link can rotate about it. External forces and dimensions are shown in parametric form.

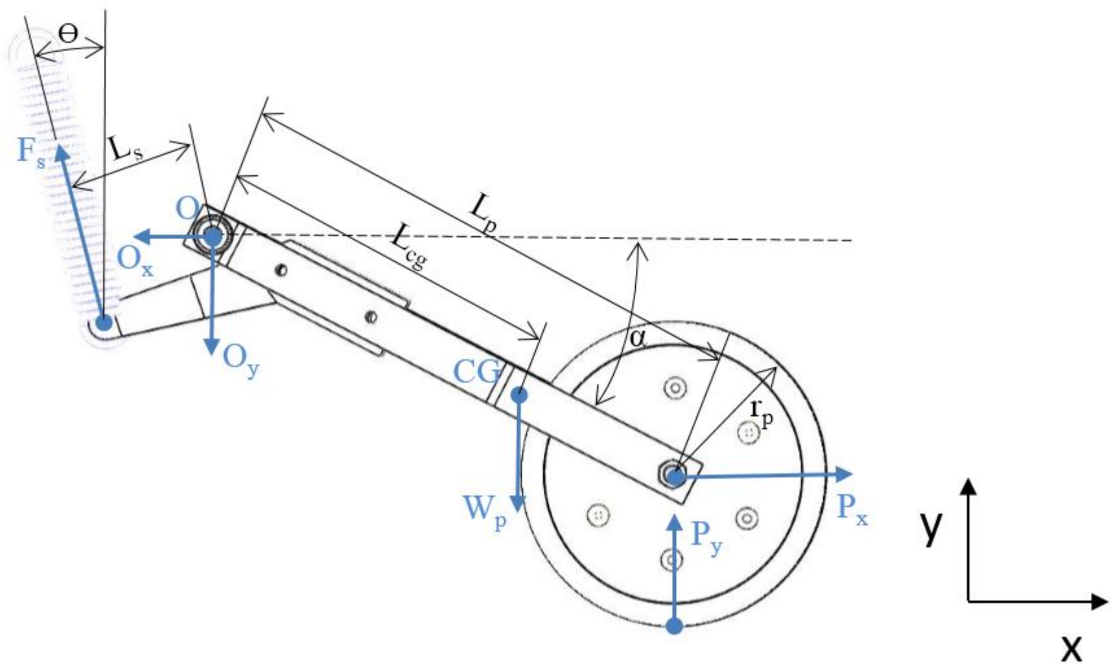

Figure 3- 15- Schematic view of the press wheel and its linkage (See Figure 3-9 for its location)

F_s is the force of the spring that provides the down force, O_x and O_y are the reaction forces on point O, W_p is the weight of the linkage and the wheel combined, and P_y and P_x are the soil reaction forces on the wheel. The angle Θ is the angle that F_s makes with the vertical direction and α is the angle that press wheel link makes with horizontal direction. L_p, L_{cg} and L_s are the distances of point O to the center of the wheel, CG and F_s, respectively. The parameter r_p is the radius of the press wheel.

The equations of the static equilibrium show the relationship between these parameters. In the X direction:

$$P_x - O_x - F_s Sin\theta = 0 \qquad \text{(Eq. 3-18)}$$

and in the Y direction,

$$P_y - W_p - O_y + F_s Cos\theta = 0 \qquad \text{(Eq. 3-19)}$$

And the moment equilibrium equation about point O,

$$P_y L_p Cos\alpha + P_x L_p Sin\alpha - W_p L_{cg} Cos\alpha - F_s L_s = 0 \qquad \text{(Eq. 3-20)}$$

Eq. 3-20 can be rearranged to find P_y,

$$P_y = \frac{W_p L_{cg} Cos\alpha + F_s L_s - P_x L_p Sin\alpha}{L_p Cos\alpha} = W_p \frac{L_{cg}}{L_p} + F_s \frac{L_s}{L_p} \frac{1}{Cos\alpha} - P_x tan\alpha \qquad \text{(Eq. 3-21)}$$

And also it is known that, for the spring force it can be written that,

$$F_s = k(S - S_0) \qquad \text{(Eq. 3-22)}$$

in which k is the spring constant, S is the current length of the spring and S_0 is the solid length of the spring. Using Eq. 3-14 to calculate P_x we can say,

$$P_y = W_p \frac{L_{cg}}{L_p} + k(S - S_0) \frac{L_s}{L_p} \frac{1}{Cos\alpha} - \frac{P_y^2}{5.7 c b_P D_P} tan\alpha \qquad \text{(Eq. 3-23)}$$

Thus, taking the derivative of Eq. 3-23 with respect to α,

$$\frac{dP_y}{d\alpha} = k \frac{L_s}{L_p} \left[(S - S_0) \frac{Sin\alpha}{Cos^2\alpha} + \frac{dS}{d\alpha} \frac{1}{Cos\alpha} \right] - \frac{2}{5.7 c b_P D_P} P_y \frac{dP_y}{d\alpha} tan\alpha + \frac{P_y^2}{5.7 c b_P D_P} (1 + tan^2\alpha) \qquad \text{(Eq. 3-24)}$$

So, rearranging Eq. 3-24 to find $\frac{dP_y}{d\alpha}$, the objective function will be,

$$F(L_s, L_p, k, \alpha) = \frac{dP_y}{d\alpha} = \frac{k \frac{L_s}{L_p} \left[(S - S_0) \frac{Sin\alpha}{Cos^2\alpha} + \frac{dS}{d\alpha} \frac{1}{Cos\alpha} \right] + \frac{P_y^2}{5.7 c b_P D_P} (1 + tan^2\alpha)}{1 + \frac{2}{5.7 c b_P D_P} P_y tan\alpha} \qquad \text{(Eq. 3-25)}$$

So the objective of the optimization is to minimize F as our objective function which will result in the minimum change in the normal force on the press wheel.

Other parameters, such as S, S_0, P_y, $\frac{dS}{d\alpha}$, c, b_p and D_p are either in hand or can be easily calculated.

P_y was set to 333 N and c, b_p and Dp are 25 KPa, 0.17 m and 0.29 m, respectively. Considering the initial values for L_s, L_p, L_{cg} and α in table 3-4, Eq. 3-19 can be used to find F_s.

Table 3- 4- Initial values for optimization problem

Parameters	Initial value
L_s	125 mm
L_p	450 mm
L_{cg}	290 mm
α	26º
W_p	142.6 N
P_y	333 N
c	25KPa
b_p	170 mm
D_p	290 mm

The weight is calculated by Solid works, based on the initial dimensions and also material properties chosen for the linkage and the wheel. Using Eq. 3-20,

$$F_s = \frac{P_y L_p Cos\alpha + P_x L_p Sin\alpha - W_p L_{cg} Cos\alpha}{L_s} = \frac{333\times 0.45\times cos26 + 16\times 0.45\times \sin 26 - 142.6\times 0.29\times cos26}{0.125} = 805.4\ N \quad \text{(Eq. 3-26)}$$

Also making the assumption that the changes of α is small it can be written as,

$$ds = L_s d\alpha \quad \text{(Eq. 3-27)}$$

Or,

$$\frac{ds}{d\alpha} = L_s \quad \text{(Eq. 3-28)}$$

Constraints for this optimization problem are defined by physical or mechanical limitations. L_s and L_p cannot be too long or too short. And there are some restrictions for the range of change of α. The spring used for the down force cannot be too loose or too tough. Assuming a range of motion of 100 mm for the press wheel in the vertical direction (which is actually chosen with a safety factor of 2) will result in a length change of 27.7 mm for the spring-based on the initial dimensions of the packing system. A spring with very high spring constant will result in very high extra forces on the press wheel. At the same time, a spring with a very low spring constant cannot provide enough down pressure on the press wheel. So based on the dimensions of the planter and order of the magnitude of the applied forces, the constraints can be defined as,

$100 \text{ mm} < L_s < 200 \text{ mm}$ (Cons-1)

$450 \text{ mm} < L_p < 650 \text{ mm}$ (Cons-2)

$13 \text{ N/mm} < k < 30 \text{ N/mm}$ (Cons-3)

$0^{o} < \alpha < 60^{o}$ (Cons-4)

The objective function, F, is a function of L_s, L_p, k and α. It can be told that F is a linear function with respect to L_s and k and is inversely related to L_p. So to reduce the complexity of the problem, it can be said that to minimize the objective function, L_s and k needs to be decreased and L_p must be increased. Using minimum L_s and k and maximum L_p that constraints allow, the objective function to be simplified to a single parameter problem. So rewriting Eq. 3-25 with the calculated parameters,

$$F(\alpha) = \frac{k\frac{L_S}{L_P}((S-S_0)\frac{Sin\alpha}{Cos^2\alpha}+\frac{dS}{d\alpha}\frac{1}{Cos\alpha})+\frac{P_y^2}{5.7cb_PD_P}(1+tan^2\alpha)}{1+\frac{2}{5.7cb_PD_P}P_y tan\alpha} = \frac{223.7sin\alpha+520.8cos\alpha+16}{1+0.1sin\alpha cos\alpha} \quad \text{(Eq. 3-28)}$$

So to find the minimum of F, the derivative of Eq. 3-28 can be taken, and make it equal to zero.

$$\frac{dF}{d\alpha} = \frac{(223.7cos\alpha-520.8sin\alpha)(1+0.1sin\alpha cos\alpha)-0.1cos2\alpha(223.7sin\alpha+520.8cos\alpha+16)}{(1+0.1sin\alpha cos\alpha)^2} = 0 \quad \text{(Eq. 3-29)}$$

Solving this equation using Matlab, we get,

$\alpha_{min} = 18.71^o$

F_{min} = 564 N/rad = 9.8 N/Degree

9.8 N/Degree change in the normal force of the press wheel means less than %29 change in the down force when the press wheel has its maximum displacement.

Now the results of the optimization can be used, to replace the initial values and recalculate the parameters. Then the optimization can be done again, and the same process again and again to get the best results.

With the iterations, α_{min} approaches 19.6º and the value for F_{min} remains almost the same.

Obviously, if L_s and k could be reduced or increased values for L_p could be chosen, smaller F could be obtained; but dimensional and mechanical constraints could not be satisfied.

3-3-3- Spring Design:

There are two springs used in the design of the planter. They provide down force, to push planter downward, to keep the disc into the soil and push the press wheel down to pack the soil.

Although a dead weight can provide the down force for the planter and its press wheel, but it means higher inertia for the system. Higher inertia for the system will result in higher power consumption and also out-of-control movements and huge dynamic loads when encountering external forces. Springs will increase system stability. On the other hand, springs help the planter to be flexible. It can go easily up and down on the field and be flexible when it hits a rock.

Based on the dimensions and forces, two proper springs were designed for the planter. Figure 3-16 shows the position and orientation of the main spring and the press wheel spring. The main spring which is installed on the front of the planter provides the down force on the disc and gauge wheel. One end of this spring is attached to a fixed plate, which is attached to the robot. The other end pushes the parallelogram linkage downward to provide the down force. The second spring provides the down force for the press wheel. It is an extension spring. The feature of the extension springs that makes it a good choice for this purpose is the preload. Extension springs have the ability to be fabricated with the pre-tension or pre-stress. This can help to have smaller spring constant with higher forces.

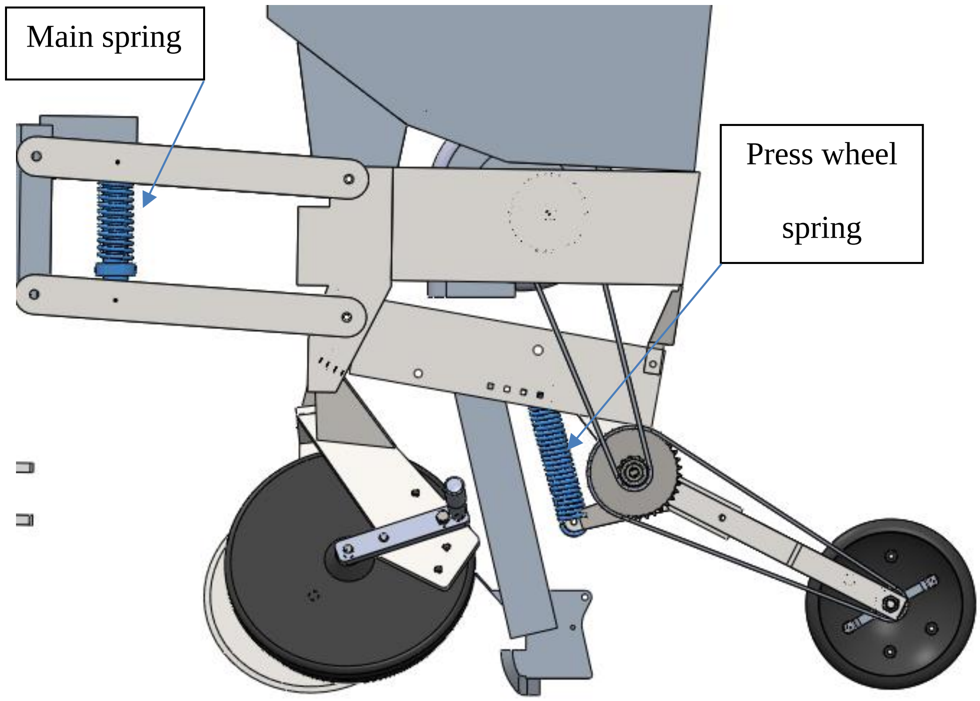

Figure 3- 16- Position and orientation of the springs

A) Main spring design:

The free body diagram of the parallelogram linkage is shown in Figure 3-17 with the dimensions. Some lines are removed to make this figure simpler for analysis. Using this free body diagram, the spring force can be found.

$$F_y L_2 = F_{sm} L_1 \tag{Eq. 3-31}$$

$$F_{sm} = \frac{F_y L_2}{L_1} = 726 \times \frac{500}{370} = 981\ N \tag{Eq. 3-32}$$

This load is applied to the link shown in figure 3-17 all the time in static and steady working condition.

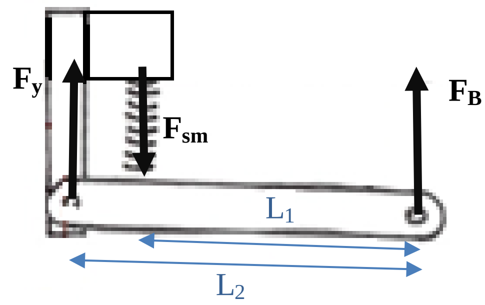

Figure 3- 17- Free body diagram of the parallelogram link and the spring

Assuming ±100 mm displacement for the planter (on point B) as it goes on the farm field will result in ±27 mm displacement on the spring (on point sm). In the static condition the spring displacement from its free length is 27 mm. So it can be said that,

$$F_{sm} = k\Delta l \qquad \text{(Eq. 3-33)}$$

$$\mathrm{k} = \frac{981}{0.027} = 36333\ N/m$$

In which k is the spring constant and Δl is the displacement of the spring from its free length. Also in the steady working condition, the length of the spring should be S=150 mm. So with 27 mm displacement, the free length of the spring should be 150+27=177 mm.

The spring index, C, can be defined as,

$$\mathrm{C} = \frac{D_s}{d_s} \qquad \text{(Eq. 3-34)}$$

in which D_s is the mean coil diameter of the spring and d_s is the diameter of the wire of the spring. It is recommended that spring index be between 4 and 12 [21]. Thus, C=6 was chosen and d_s changes from 5mm to 10 mm, a wire diameter can be found that matches the dimensions and also gives a safety factor of more than one.

There are different types of wires used to make springs. Hot Drawn (HD) wires are commonly used. For HD wire, the following properties are given in Table 3-5.

Table 3- 5- Properties of HD spring wire, for d_s>3 mm[21]

Name	Parameter	Value
Shear Modulus of Elasticity	G	78.6 GPa
Modulus of Elasticity	E	196.5 GPa
Wire ultimate tensile strength constant	A	1783 MPa.mm^m
Wire ultimate tensile strength constant	M	0.190

In table 3-3, G is the Shear module of elasticity, E is the module of elasticity. The Ultimate tensile strength, S_{ut}, and Yield shear strength, S_{sy}, are defined as follows [21],

$$S_{ut} = \frac{A}{d^m} \qquad \text{(Eq. 3-35)}$$

$$S_{sy} = 0.45 S_{ut}$$

Choosing d_s=8.5 mm and C=5.5, which result in D_s=46.75 mm,

$$S_{ut} = \frac{A}{d^m} = \frac{1783}{8.5^{0.19}} = 1187.3\ MPa \qquad \text{(Eq. 3-36)}$$

$$S_{sy} = 0.45 S_{ut} = 594\ MPa$$

To find other parameters of the spring Eq. 3-36 can be used.

$$N_a = \frac{\mathrm{G}d^4}{8kD^3} = \frac{78.6 \times (8.5 \times 10^{-3})^4}{8 \times 37730 \times (46.75 \times 10^{-3})^3} = 13.3 \qquad \text{(Eq. 3-37)}$$

N_a is the number of the active coils of the spring. For the ground and squared ends, the total number of coils and the free length can be found, using Eq. 3-37 and 3-38.

$$N_t = N_a + 2 = 13.3 + 2 = 15.3 \quad \text{(Eq. 3-38)}$$

$$S_0 = pN_a + 2d = 177 \quad \text{(Eq. 3-39)}$$

In Eq. 3-37 and 3-38, N_t is the total number of coils, and p is the pitch of the spring. So Using Eq. 3-38 the pitch can be found too.

$$\mathrm{p} = \frac{S_0 - 2d}{N_a} = \frac{177 - 2 \times 8.5}{13.3} = 12\ mm \quad \text{(Eq. 3-40)}$$

Now to check for safety factor and strength of the spring, the shear stress in the coil needs to be calculated, using Eq. 3-41.

$$\tau = K_B \frac{8FD}{\pi d^3} \quad \text{(Eq. 3-41)}$$

In this equation, K_B is the correction factor and can be calculated using Eq. 3-42.

$$K_B = \frac{4\mathrm{C} + 2}{4\mathrm{C} - 3} = \frac{4 \times 5.5 + 2}{4 \times 5.5 - 3} = 1.26 \quad \text{(Eq. 3-42)}$$

So if an assumption is made that the spring experience its maximum deformation as is expected, the maximum spring force on the spring will be

$$F_{sm} = k\Delta l = 37730.7 \times 0.054 = 2037.5\ N \quad \text{(Eq. 3-43)}$$

The shear stress in the coil will be, τ=497.6 MPa and the safety factor can be calculated as,

$$n_s = \frac{S_{sy}}{\tau} = \frac{594}{497.6} = 1.2 \quad \text{(Eq. 3-44)}$$

which is greater than one.

So the dimensions and properties of the main spring as designed are shown in table 3-6.

Table 3- 6- Dimensions and properties of the main spring

Material	Hard drawn spring wire
D	8.5
D	46.75 mm
C	5.5
P	12 mm
S_0	177 mm
N_t	15.3
End type	Ground and Squared

B) Press wheel spring design

The same process can be used to design the spring that is used for press wheel. The only difference is that an extension spring is being used for press wheel, instead of compression spring. The main difference in the detail design of an extension spring is that the maximum stress always happens at the hook, not in the coil. The other difference is the pre-load or pre-tension that can be made in an extension spring while winding it. Pre-load will change the Eq. 3-33 to,

$$F_s = F_i + k_{ex}\Delta S \qquad \text{(Eq. 3-45)}$$

As it is shown in section 3-3-2, with the optimized settings, the spring force can be recalculated, using Eq. 3-26 to get F_s=837 N.

If the displacement for the wheel is assumed to be ±100 mm in vertical direction, the displacement of the spring can simply be calculated, using the dimensions of figure 3-15. So $\Delta S = \frac{L_s}{L_p} \times 100 = 27.78$ mm.

Assuming a spring index of C=5.5 for the spring, Eq. 3-46 can be used to find the range of preferred torsional stress caused by initial tension [21].

$$\tau_i = \frac{33500}{\exp(0.105C)} \pm 1000\left(4 - \frac{C-3}{6.5}\right) psi \quad \text{(Eq. 3-46)}$$

So 15.2 ksi< τ_i < 22.4 ksi. Then choosing, τ_i= 20 ksi= 137.9 MPa and using Eq. 3-47, to find the initial force in the spring, F_i,

$$\tau_i = \frac{8F_iD_s}{\pi {d_s}^3} \rightarrow F_i = \frac{\pi\tau_i {d_s}^3}{8D_s} \quad \text{(Eq. 3-47)}$$

Choosing a spring wire with 7 mm diameter will result in D_s=Cd= 38.5 mm. Thus, F_i=482.4 N.

Using Eq. 3-45, the spring constant of k_{ex} = 12.8 N/mm can be found.

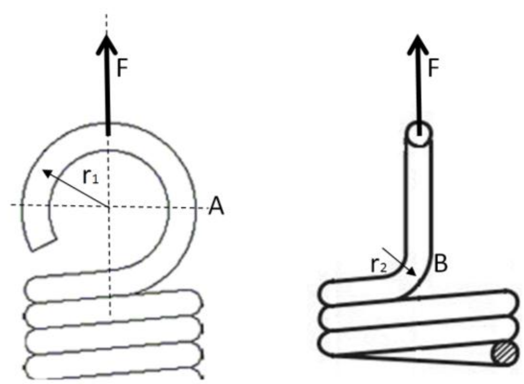

Figure 3- 18- Parameters of the extension spring

As mentioned earlier, the maximum stress usually happens at the hook of the extension spring, at point A or B in figure 3-18. Eq. 3-48 and 3-49 can be used to calculate the stress due to bending and tension at A, and torsional stress at B.

$$\sigma_A = F\left[\frac{K_A 16D}{\pi d^3} + \frac{4}{\pi d^2}\right] \quad \text{(Eq. 3-48)}$$

$$\tau_B = K_B \frac{8FD}{\pi d^3} \quad \text{(Eq. 3-49)}$$

In which K_A and K_B are correction factors that can be found using Eq. 3-50 and 3-51, respectively.

$$K_A = \frac{4C_1^2 - C_1 - 1}{4C_1(C_1 - 1)} \quad , \quad C_1 = \frac{2r_1}{d} \quad \text{(Eq. 3-50)}$$

$$K_B = \frac{4C_2 - 1}{4C_2 - 4} \quad , \quad C_2 = \frac{2r_2}{d} \quad \text{(Eq. 3-51)}$$

And r_1 and r_2 are the radiuses, as shown in Figure 3-18. Assuming $2r_1$=D_s and r_2= 10 mm, Eq. 3-50 and 3-51 can be used to find K_A = 1.16 and K_B=1.4. It is known that maximum displacement for the spring will result in maximum force and stress. Eq. 3-45 can be used to find F_{max}= 1191.6 N. Then K_A and K_B and F_{max} can be replaced into Eq. 3-48 and 3-49, to find

σ_A =818.8 MPa and τ_B =478.1 MPa.

Using the same material that was used for main spring (Hard Drawn spring wire), table 3-3 and Eq. 3-35 can be used to find the properties of the wire. The strength of the spring wire in different modes can be found in Table 3-7.

So, the safety factors of the spring at A and B can be sound.

$$(n_s)_A = \frac{S_y}{\sigma_A} = 1.13 \quad \text{(Eq. 3-52)}$$

$$(n_s)_B = \frac{S_{sy}}{\tau_B} = 1.16 \quad \text{(Eq. 3-53)}$$

Table 3- 7- Strength properties of the extension spring wire for d=6 mm.[21]

Parameter	Equation	Value
S_{ut}	$S_{ut} = \frac{A}{d^m}$	1231.9 MPa
S_{sy}	$S_{sy} = 0.45S_{ut}$	554.4 MPa
S_y	$S_y = 0.75S_{ut}$	923.9 MPa

Using the dimensions of the planter, where the spring must be installed, length and other dimensions of the spring can be found. The extension spring must be installed between two points that are 279.8 mm away from each other in working condition. So the free length of the spring will be 279.8 - 27.8 = 252 mm. Then Eq. 3-54 can be used to find the number of body coils of the spring.

$$L_0 = (2C - 1 + N_b)d \quad \text{(Eq. 3-54)}$$

The number of body coils of the spring is N_b=26.

Finally the dimensions and properties of the extension spring, designed for press wheel can be found in table 3-8.

Table 3- 8- Dimensions and properties of the press wheel spring

Material	Hard drawn spring wire
D	7 mm
D	38.5 mm
C	5.5
L_0	252 mm
F_i	482.4 N
N_b	26
Hook type	Regular circular hook

3-4-Summary

In this chapter, the design process which leads to the developed planter is discussed. All design processes begin with data and information collection. The study of the literature in chapter 1, and the data obtained from the experiments in chapter 2 was used for the design process. Then the conceptual design was performed with some preliminary calculations on different parts that were developed for the planter, such as power transmission for precision seed metering system and lifting mechanism. Then static analysis to find the total draft force and total vertical force of the developed planter was performed. Optimization analysis was performed to minimize the change in the down force of the press wheel, when it moves up and down. Minimization in the change of the down force on the press wheel results in steadier down pressure on the soil and therefore better emergence results. Also spring design process was done to design the springs that provide down force on the gauge wheel and press wheel. Although the safety factor that was found for these springs were slightly higher than 1, but a hidden safety factor was already included in the calculations. This is due to the fact that the maximum vertical displacement that was assumed for the planter is almost twice as its usual value. So another safety factor of two was already inside the calculations.

Chapter 4- Stress Analysis Using Finite Element Method

4-1- Introduction

Finite Element method has been introduced to simplify the problems that involve continuity. FEM gives us an approximate answer to real life problems by discretizing them.

Since the shapes of the parts that are designed for the planter and the loads that are applied to them, are not simple and straight forward, so the calculations to find where the maximum stress happens and also its magnitude cannot be done by hand. Also complexity of the model makes it very difficult to find the interaction between the parts. Thus, to make sure that the designed parts have enough strength and do not fail due to high stresses in them, a stress analysis needed to be performed. Besides that, to validate the FEM results, simple hand calculations are done.(Remove)

The process of modeling and performing stress analysis is done using the following steps, 1) 3D modeling in Solid-Works, 2) Transferring the 3D model to ANSYS, using STEP format, 3) Geometry adjustments (in case of data loss due to file transfer from Solidworks to ANSYS), 4)Meshing, 5)Appling loads and boundary condition, 6) Solving the problem, 7) analysis of the results

Since the shape of the parts and boundary conditions are complicated, ANSYS Workbench is used instead of ANSYS Classic; because ANSYS WB is more convenient in dealing with complex geometries.

4-2- Planter parts stress analysis using ANSYS Workbench

The parts in Figure 4-1 that are marked in green, are the ones that stress analysis is performed on them. These parts are all separately modeled in Solid-Works and are imported into ANSYS Workbench for stress analysis.

The steps from the point that they imported into ANSYS Workbench are presented for each of them. For all the parts presented below, first the analysis is performed using a simple mesh. This preliminary analysis helps to verify where the maximum stress happens. Then for further analysis more efficient meshing can be used, with finer mesh at stress concentration areas.

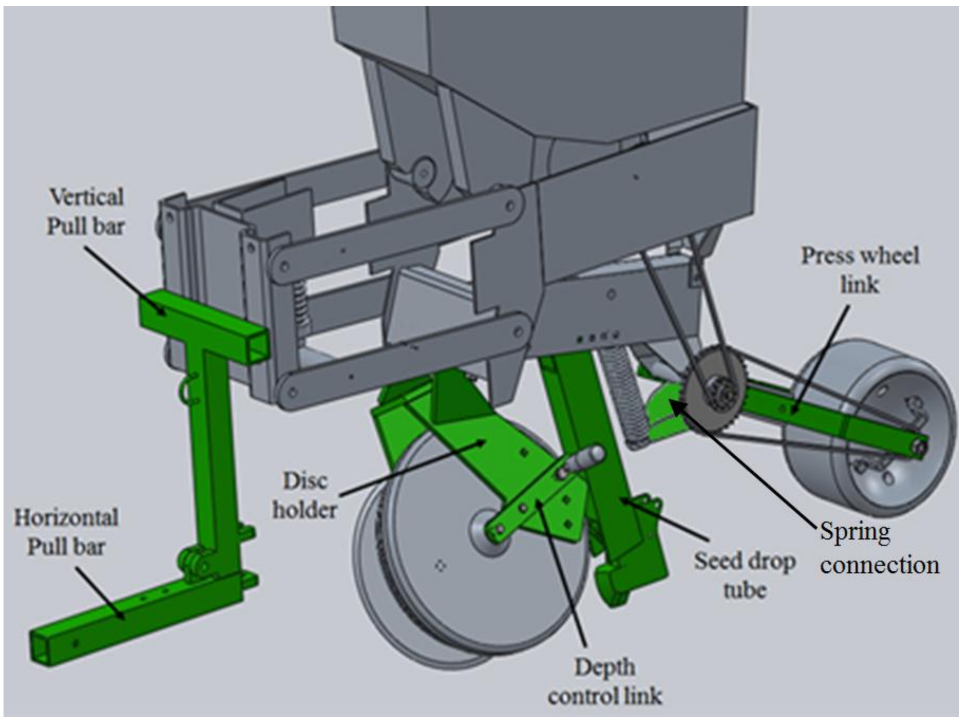

Figure 4- 1- Developed planer (parts in green are the ones that stress analysis is performed on them)

4-2-1- Depth control link

Depth control link is the part that is used to set the depth of the cut in the soil. It is a simple flat part that is hinged on the disc holder in the middle point (point A in Figure 4-3); one end of this part is attached to the gauge wheel and the other end is pinned to the disc holder (point B in Figure 4-2). The hole at the end of the link that is not marked with any letters in Figure 4-3, is the point that a handle is bolted on. The user can remove the pin in point B and use the handle to change the depth of the cut by moving the gauge wheel up or down, when rotating the depth control link about its hinge-point A.

Meshing: Meshing is done using brick (hexahedral) elements. Face sizing is used to set element sizes to 5 mm each. The meshing is shown in figure 4-2. In this figure, it can be seen that the element size is set to 5 mm. The number of nodes with this meshing size is 6025.

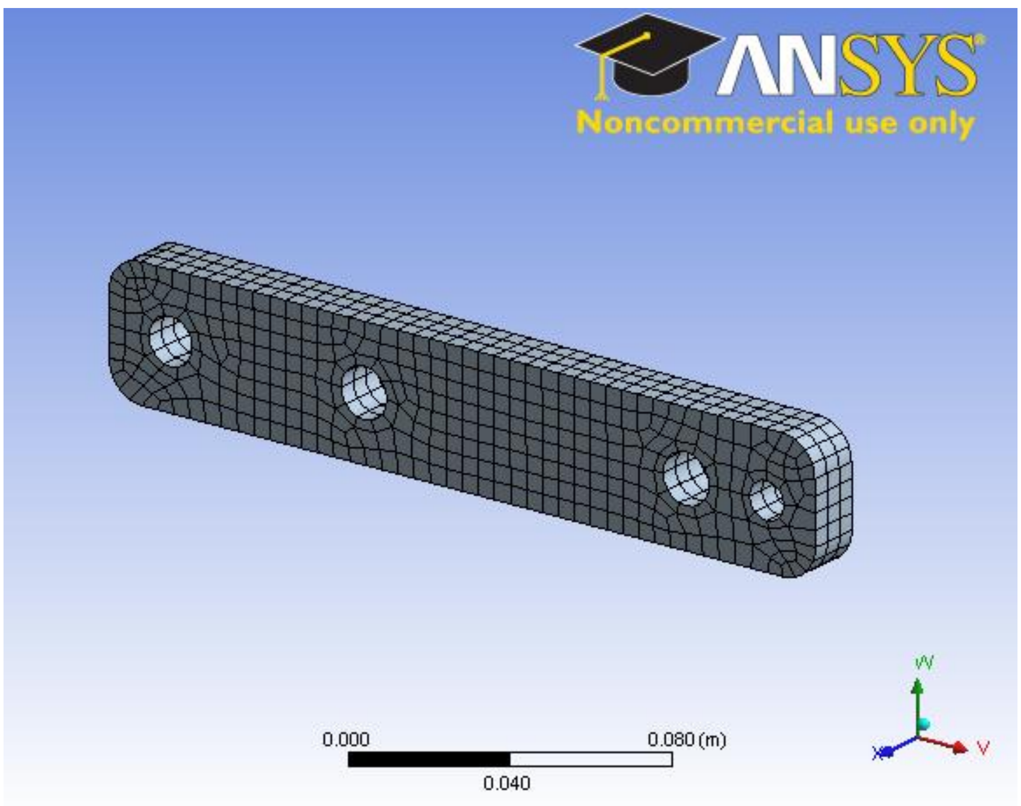

Figure 4- 2- Meshing of the Depth control link

External loads and boundary conditions: The external loads on this part are actually the forces that are applied to gauge wheel when interacting with the soil. The forces calculated in chapter 3, the vertical and horizontal forces on the gauge wheel are G_y=1200 N and G_x=308 N, respectively. These forces are in y and x direction of the ground coordinate system. In other words, they are horizontal and vertical with respect to the ground. But they will have different components with respect to a coordinate system that is parallel to the depth control links faces. Their components in the x, y and z direction of this coordinate system can be calculated, using the geometry of the assembly, trigonometry functions and the disc and tilt angles of the disc. These calculated components can be found in Table 4-1. X, Y and Z components shown in Table 4-1 are parallel to depth control link's sides. These external forces are applied on the surface of the hole, forces C and D, as shown in Figure 4-3.

Table 4- 1- Components of external forces in the coordinate system parallel to faces of depth control link

	Horizontal force	Vertical force
X component	276.6 N	511.1 N
Y component	-131.2 N	1077.8 N
Z component	33.5 N	130.4 N
Total (N)	308 N	1200 N

At point A, which is the hinge, and point B, which is the pin, cylindrical support is defined as boundary condition. Cylindrical support is a type of support that can be used for cylindrical shape that does not bear tangential load, such as bearings. To model pinned or hinge support, radial and axial directions are fixed and tangential DOF is set free to rotate for both cylindrical support A and B.

Remote force can be applied to the part from any point in the space. To define a remote force, the location of force, its direction and which part of the body that the force is applied must be defined. For depth control link, the remote forces are applied in the center of the hole (see Figure 4-3) and to the interior face of the hole.

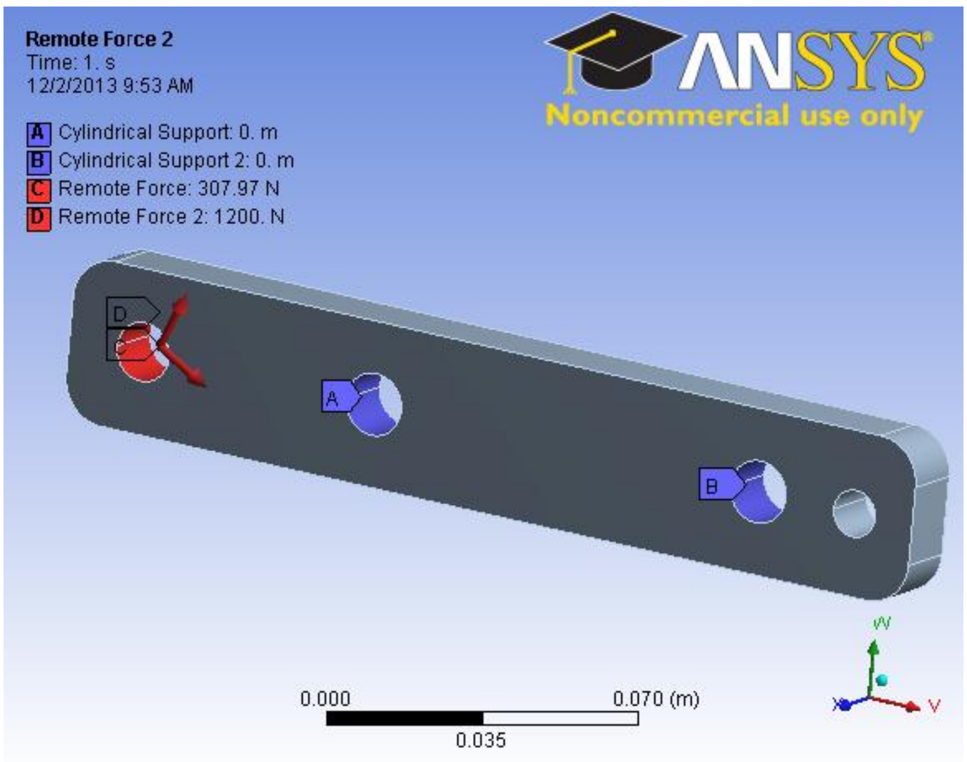

Figure 4- 3-Geometry and supports of depth control link

Solution and results discussion: Now that all the boundary conditions and external forces are defined, we can solve the problem to get equivalent stress (Von Mises) and total deformation. These results are shown in figure 4-4 and 4-5.

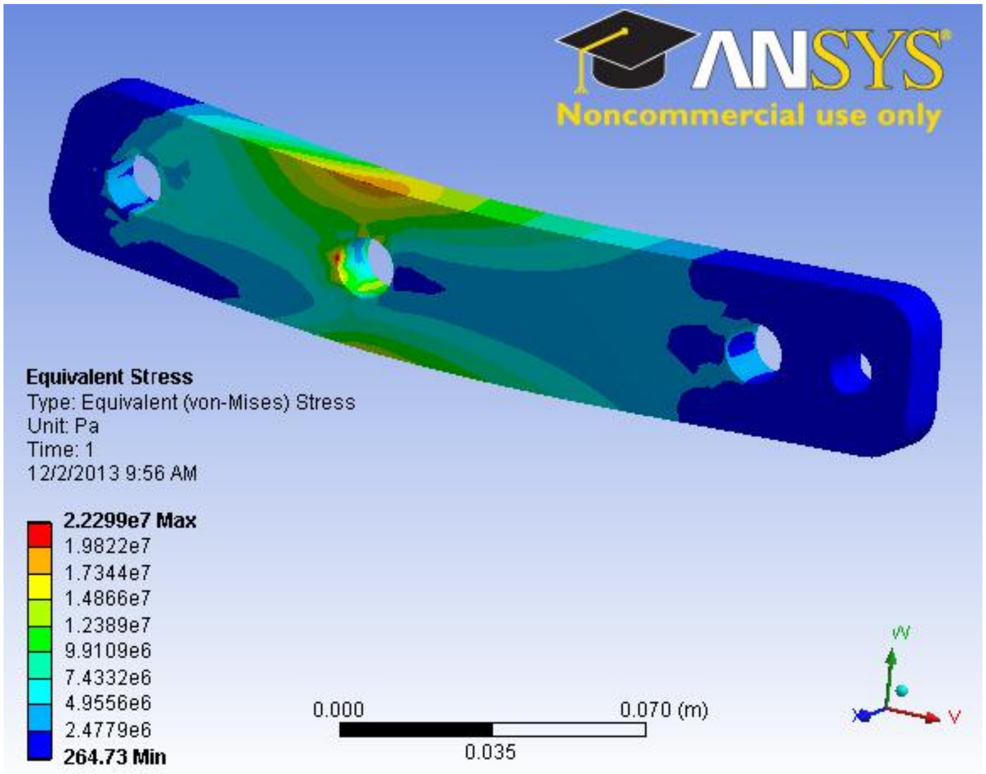

Figure 4- 4- Equivalent (Von Mises) stress contour for depth control link

To analyze the stresses in this part, brick (hexahedral) elements are used. The results of the analysis have been verified by choosing different element sizes and element types. Changing the element size, from 3 mm to 10 mm, showed no significant change in stress distribution and also maximum stress. A smaller size element could not be used, because the number of generated nodes would exceed the number of allowed for the educational license that is available.

As it can be seen in Figure 4-4, the maximum stress is calculated as 22.3 MPa. Since the material selected for this part is structural Steel, it has a yield strength of 250 MPa. Based on the Distortion-Energy theory, this means, for this specific part, a safety factor of more than 10.

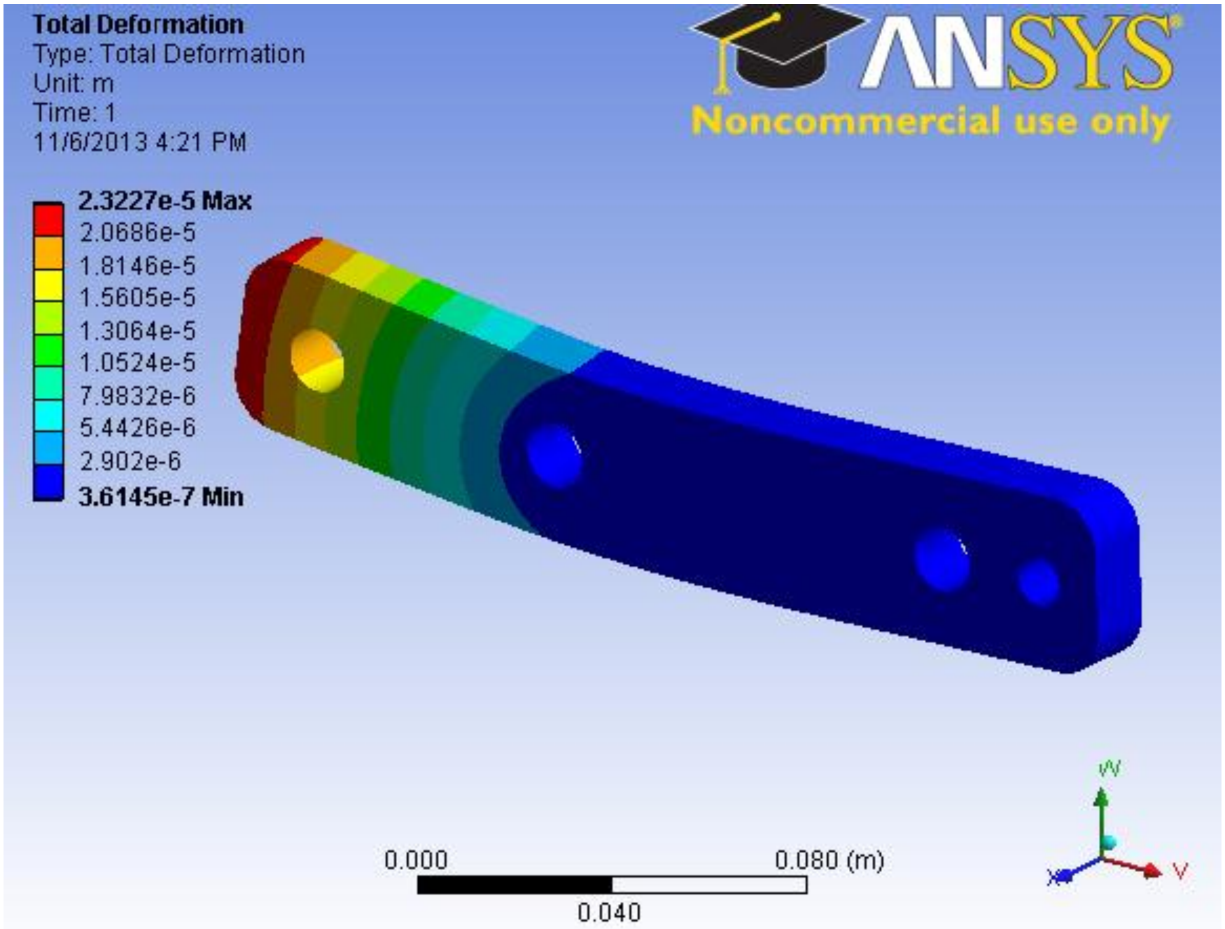

Figure 4- 5- Total Deformation contour for depth control link

Figure 4-5 shows the total deformation on the link. The maximum value for this parameter is 0.023 mm which is very small.

Also the reaction forces at supports are shown in table 4-2.

Table 4- 2- Reaction forces at cylindrical supports A and B

	Support A	Support B
X Axis	-738.8 N	-48.9 N
Y Axis	-1514.6 N	568.0 N
Z Axis	-169.5 N	5.6 N
Total	1693.6 N	570.1 N

To compare the results form FEM with hand-calculations, a simple 2D version of the problem is solved by hand. As it can be seen in Figure 4-6, the magnitudes of the external forces in the x-y plane are 306.1 N and 1192.8 N.

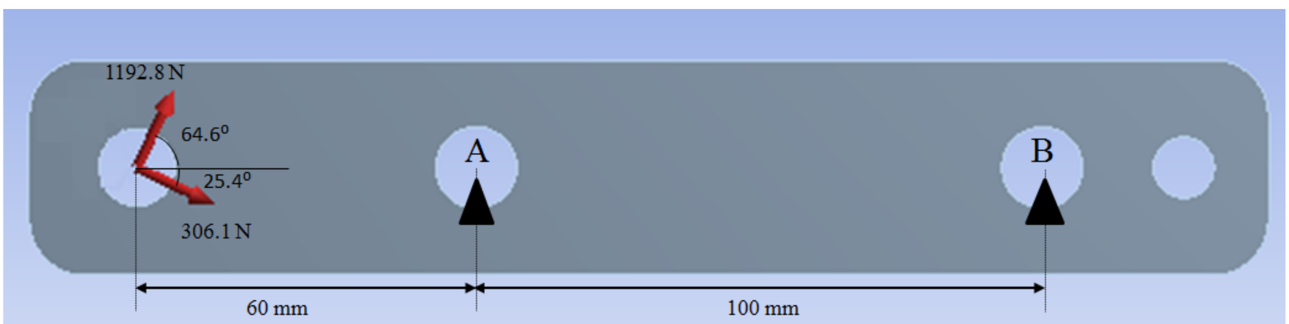

Figure 4- 6- Depth control link and Schematic forces and supports in 2D for hand calculation

Writing the moment about point B,

$$(1192.8Sin(64.6) - 306.1\sin(25.4)) \times 160 - A_y \times 100 = 0 \qquad \text{(Eq. 5-1)}$$

Equation 5-1 will result in $A_y = 1513.9$ N, downward. And subsequently from the equilibrium in the y direction we can conclude that $B_y = 567.7$ N, upward. The values for reaction forces A_y and B_y match the results of the FEM, in y direction.

It can reliably assume that the maximum moment happen at point A. At this point the moment is highest and also the area of cross section is smallest because of the hole. Moment at this point will be $M = 567.7 \times 0.1 = 56.8\ N.m$. The link has a cross section of 15 mm × 38.1 mm and the diameter of the hole is 14.3 mm. So the moment of inertia of the cross section is,

$$I = \frac{1}{12} bh^3 - (\frac{1}{12} bd^3) \quad \text{(Eq. 5-2)}$$

In Equation 5-2, b= 15 mm is the thickness of the link, and h=38.1 mm is the width of the link, and d is the diameter of the hole. This will result in $I = 6.55 \times 10^{-8}\ m^4$.

Considering that modulus of elasticity for structural steel is E=200 GPa, we can use Equation 5-3 to calculate the bending moment in the link, at point A.

$$\sigma_1 = \frac{Mc}{I} = \frac{56.7 \times \frac{0.0381}{2}}{6.55 \times 10^{-8}} = 16.5\ MPa \quad \text{(Eq. 5-3)}$$

At the same time, there is compression stress on the link due to axial forces in the x direction. So, the compression stress can be easily calculated using Eq. 5-4.

$$\sigma_2 = \frac{F}{S} = \frac{1192.8 \cos(64.6) + 306.1 \cos(25.4)}{0.015 \times (0.0381 - 0.0143)} = 2.2\ MPa \quad \text{(Eq. 5-4)}$$

The maximum total stress on the link will be 16.5+2.2= 18.7 MPa, which is close enough to 22.3 MPa that was found from FEM. The main reason for the difference in results is that, the problem is solved in 2D. This means that the stress caused by force element in the Z direction in the link is not considered for simplicity of hand calculations.

4-2-2- Disc Holder

Disc holder is the most complicated part of the planter, because of its irregular shape (Figure 4-7). The sources of forces applied to this part are the depth control link and the disc coulter. All of these forces are known and stress analysis can be performed on it. Since the process of stress analysis is the same that was used for depth control link, the steps will be discussed briefly.

Meshing: The best meshing that was used for this part is shown in Figure 4-7. Since the geometry of the part is complex, tetrahedral element types was chosen by FEM program. The refinement of mesh on the upper corner of the part can be seen in figure 4-7. The element size in this area is set to 3 mm. The rest of the body has an element size of 16 mm. The number of nodes in figure 4-7 is 31561. The element size refinement in the corner of the body was done in order to study the stress concentration in that corner. When there is stress concentration in an area, a mesh convergence study should be performed to find out if the maximum stress result from FEM is “real” or not. If the maximum stress increases with finer mesh, it means there is a singular point in the model, which represents a mathematical singularity, not a real stress value. Instead, the stress at two or three elements away from that singular point remains almost constant during mesh refinement and may be considered as the maximum stress. There are other remedies can also be implement to avoid singularity in a model, such as replacing sharp corners with smooth curves, or use distributed loads instead of concentrated loads. To study this effect and find the best answer and results, different refinements on the area of stress concentration was performed and results were compared. These different meshing and their stress contours are shown in appendix B for comparison.

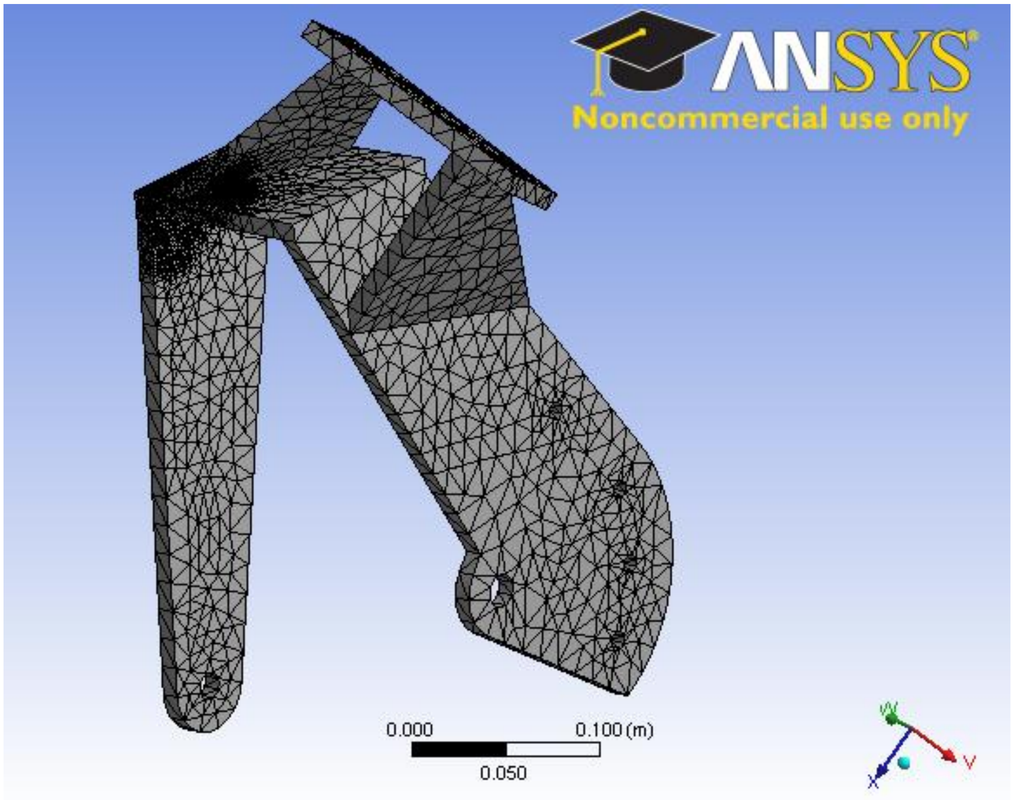

Figure 4- 7- Meshing for disc holder

External loads and boundary condition: Figure 4-8 shows the external loads and the support for disc holder. This part is attached to the chassis by bolts; so face A is assumed to be fixed support. Load B and C are the reaction forces of the depth control link, and they are calculated at previous section. But they are applied in opposite direction and are applied to the center of the holes as remote forces. Forces E, D and F are the disc forces in the horizontal, vertical and lateral direction, respectively. These forces are applied to the point that the disc is in contact with the soil. They will cause moment about the point that the disc is mounted. That is the reason that in figure 4-8 the forces D, E and F are defined as remote force and they are applied away from the point the disc is mounted. The effect of these forces will be applied to the point that the axis of disc is attached.

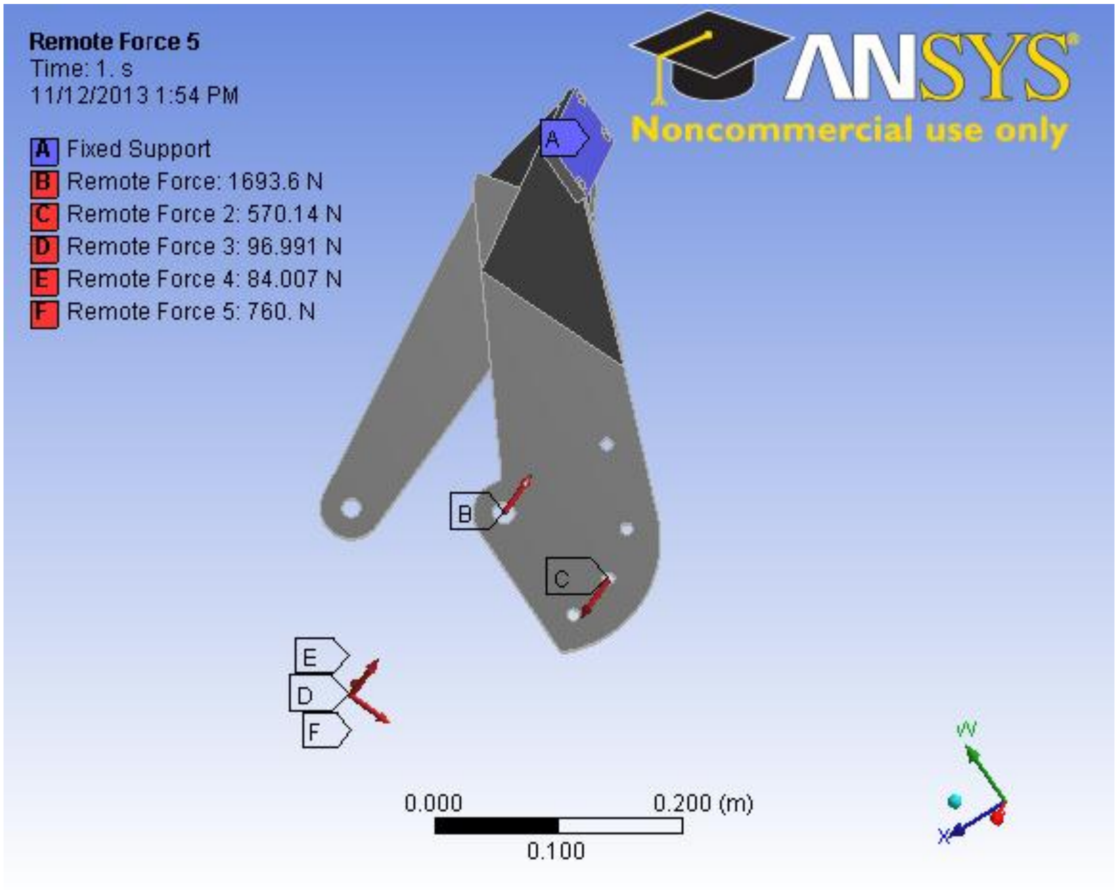

Figure 4- 8- Geometry, forces and support of the disc holder part

Solution and result discussion: The stress contour for disc holder with the meshing shown in figure 4-8, is presented in figure 4-9.

Changing the mesh size to find the real value for maximum equivalent stress showed that it is equal to 180 MPa. Since the material is structural steel, it has a yield strength of 250 MPa. This means a safety factor of 1.4 for this part.

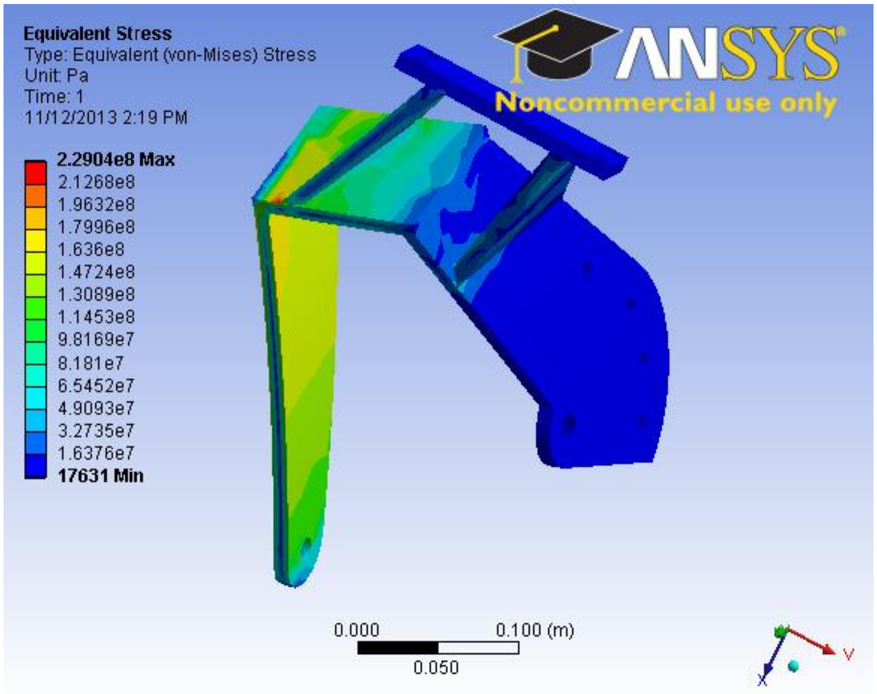

Figure 4- 9- Equivalent (Von Mises) Stress contour for disc holder

The reaction forces and moments on the support for this part can be found in table 4-3.

Table 4- 3- Reaction forces and moments for disc holder

	Support A	
	Force (N)	Moment (N.m)
X	1241.4	-129.77
Y	-300	329.94
Z	1061	261.66
Total	1660.3	440.64

4-2-3- Seed drop tube

The main job of the seed drop tube is to keep the soil open and guide the seed into the furrow. As mentioned in chapter 3, the external loads that are applied to this part are very small. A horizontal force of 25 N and a vertical force of 10 N. The HSS used for this part is a 3 inch by

2 inch rectangular section. Thus, Stress analysis is not needed for this part due to very small forces.

4-2-4- Spring connection

As shown in Figure 4-10, spring connection is used to transfer spring force to the press wheel links.

So at one point there is the spring force and there are 4 points that it is attached to the press wheel links, using bolts.

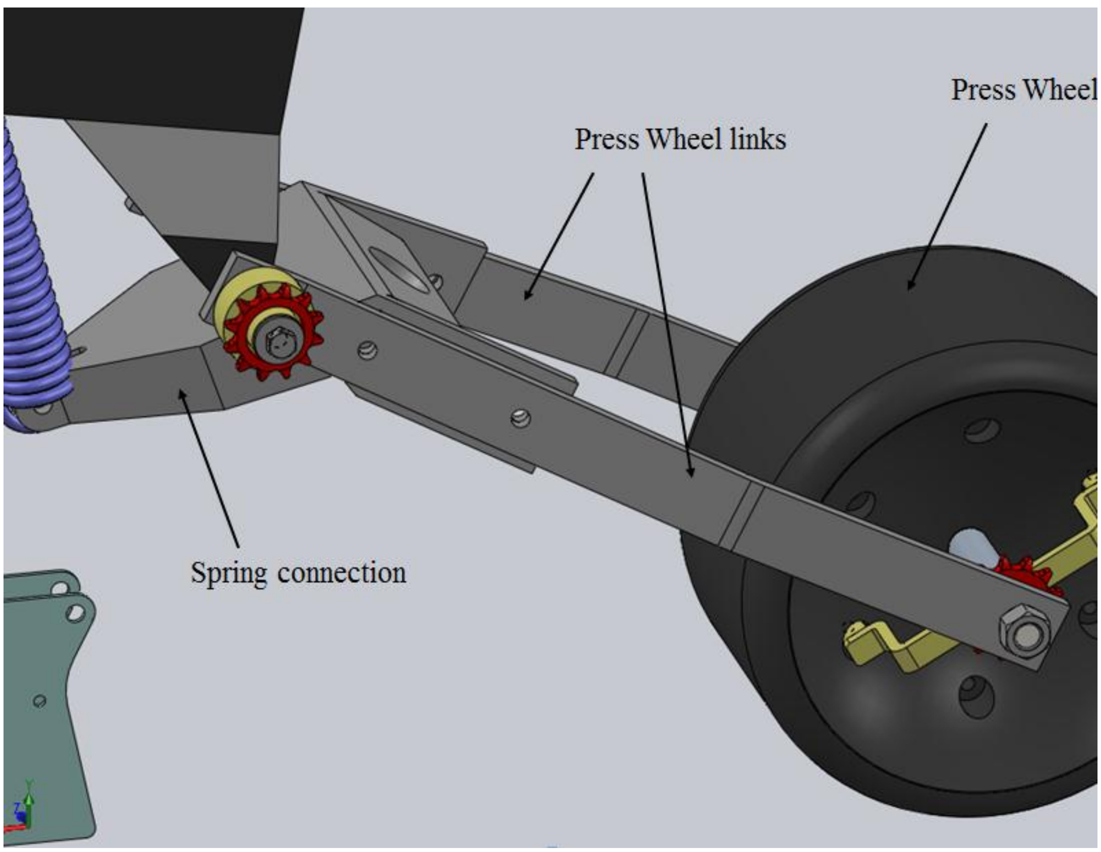

Figure 4- 10- Spring connection location

Meshing: Since this part has a complex geometry, tetrahedral elements are used for meshing. As it can be seen in figure 4-11, finer mesh is used around the holes and the notch on the tip of the part; because stress concentration is expected to happen at these areas. The general element size for the body is 15 mm and in the areas with finer mesh it is 2 mm. The number of nodes are 21079.

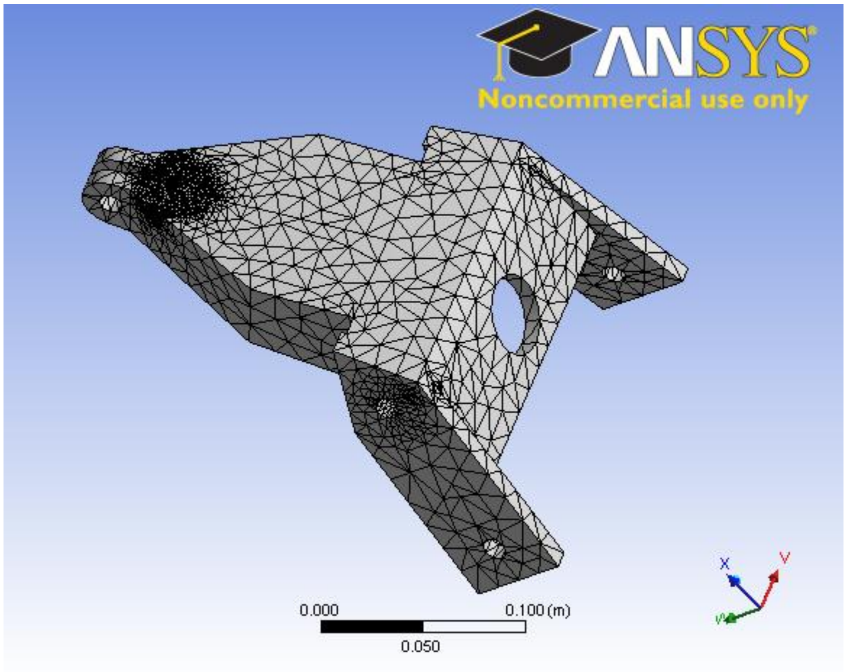

Figure 4- 11- Meshing for spring connection

External loads and boundary condition: Figure 4-12 shows the external loads and boundary condition for spring connection. As calculated at chapter 3, the maximum expected load from the spring will be 1191.6 N. Cylindrical support is used to model the points that the part is being fixed by bolts. So, all its degrees of freedom are fixed at support.

Solution and result discussion: Stress analysis for this part shows that the maximum principal stress happens at holes (Figure 4-13). The real magnitude for the maximum stress is about 42 MPa which happens around the area of stress concentration. As discussed earlier, the value for maximum stress at areas with stress concentration must be studied for mesh convergence. In this case, the maximum stress will increase by decreasing the size of the elements in that area. But the value for the stress close to the singular point remains almost the same; which is the actual value for maximum stress. Maximum principal stress is used for analysis, because this part is made from brittle material. One of the failure criteria for brittle materials is Maximum Normal Stress theory. Since this part is made of cast iron, its ultimate strength will be around S_{ut} = 200 MPa. This will result in a safety factor of 4.76 for this part.

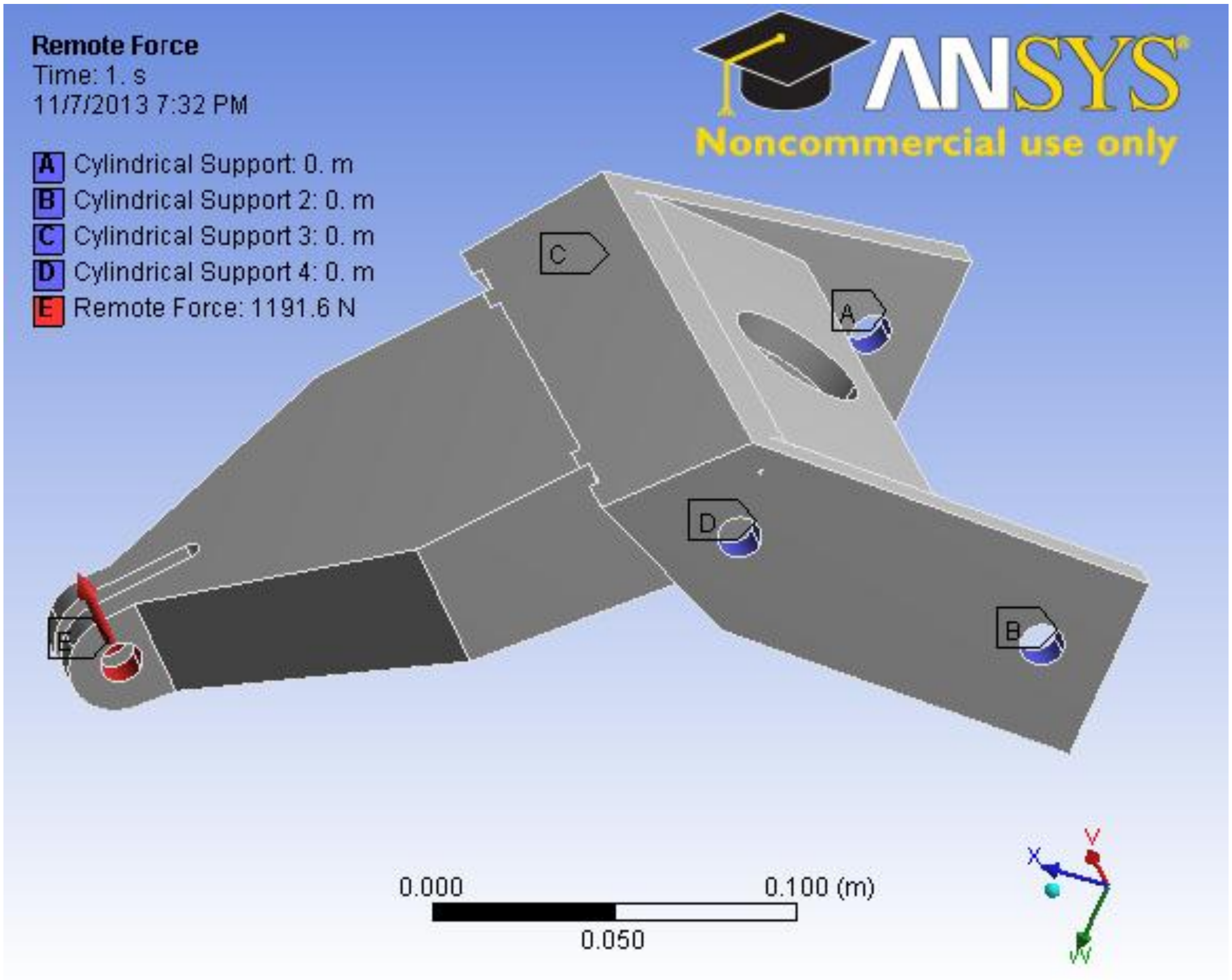

Figure 4- 12- Geometry, loads and supports of spring connection

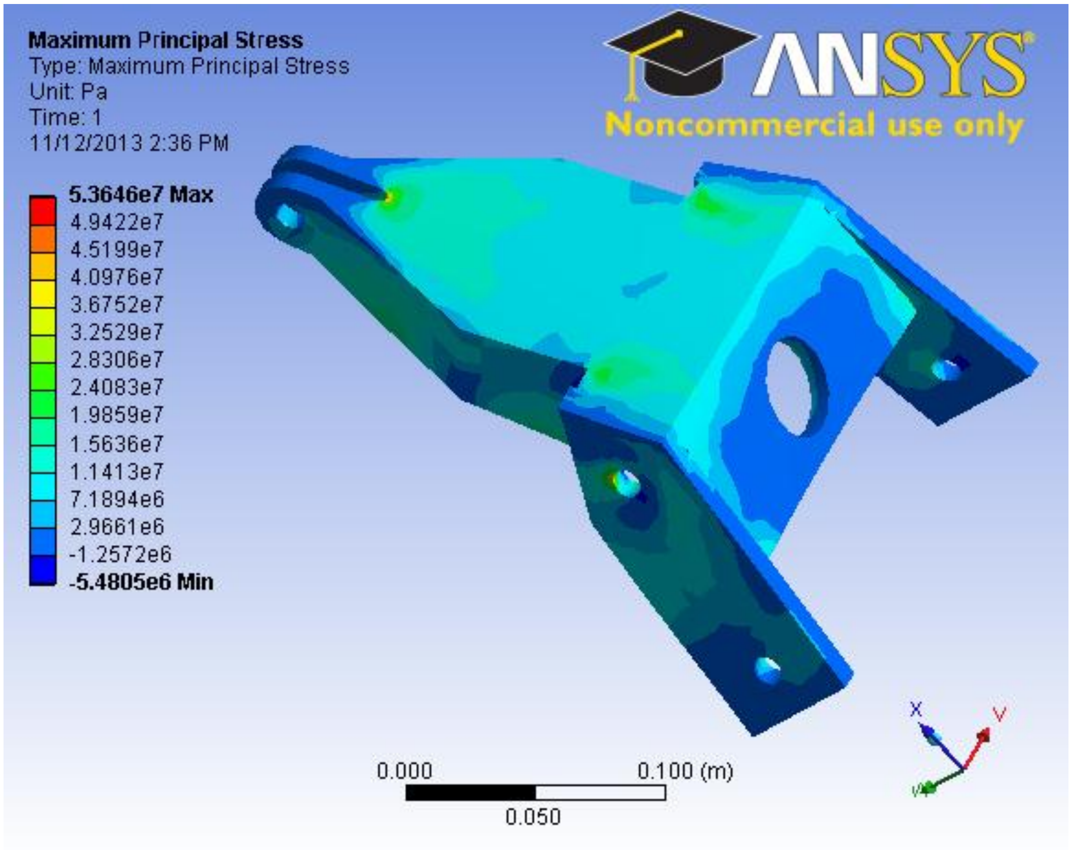

Figure 4- 13- Maximum principal stress contour for spring connection

Another result that was obtained from this analysis is the reaction forces on the supports. These forces are needed for stress analysis of the press wheel links. These forces and moments can be found in table 4-4. Due to symmetry, only reactions of support B and D are shown.

Table 4- 4- reactions of supports B and D of spring connection

	Support D		Support B	
	Force (N)	Moment (N.m)	Force (N)	Moment (N.m)
X	-286.36	-24.98	133.37	6.51
Y	1296.6	-13.46	-887.65	2.45
Z	-632.51	10.3	196.57	-6.9
Total	1470.8	30.19	918.88	9.81

4-2-5- Press wheel link

There are two press wheel links that attach the press wheel to the chassis and also transfer the spring force to the press wheel. Figure 4-15 shows the forces on this part. These forces are applied to the press wheel link form the spring connection part. The link is hinged at one end, point A, and on the other end is fixed only in vertical direction to model the end that is attached to the wheel.

Meshing: Since the stress concentration is happening at one of the holes, finer mesh is used to create the elements in that area. Also to find out about the effect of stress concentration and real value for stress at that point, different meshing sizes and refinements are used and compared. Figure 4-14 shows the mesh used for this part, which has 10 mm element size for the whole part and 3 mm element size for the area with high stresses.

External loads and boundary condition: As mentioned earlier, at point B in figure 4-15, the part is hinged. So, support B is a cylindrical support which is free in tangential direction. Point A is the hole that supports the press wheel shaft. support A is must be fixed only in Z direction (vertical direction). Thus, a zero displacement in Z direction is defined for support A. Forces and moments are applied to this part, form the spring connection. These forces and moments are the reaction force and moments results of the previous analysis, and they are transformed form the coordinate system of the spring connection to the coordinate system of press wheel link.

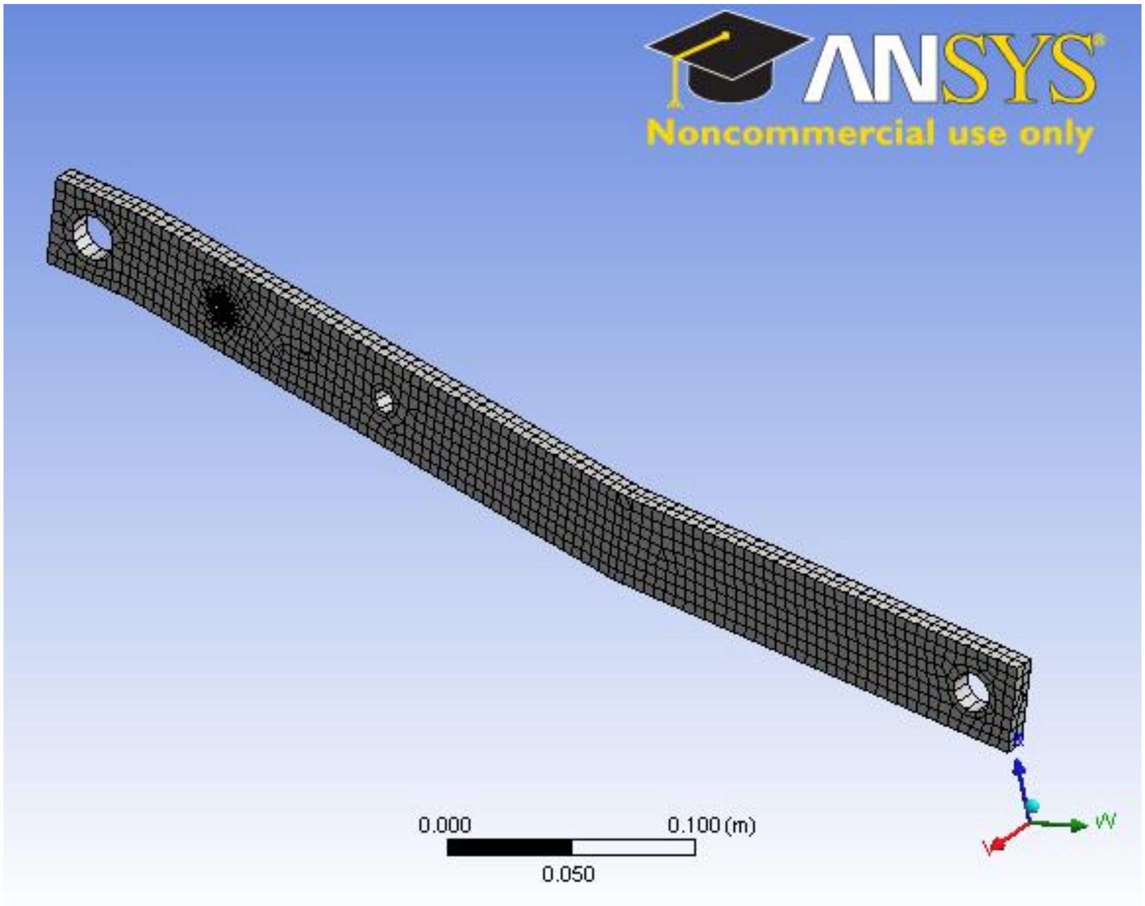

Figure 4- 14- Meshing for press wheel link

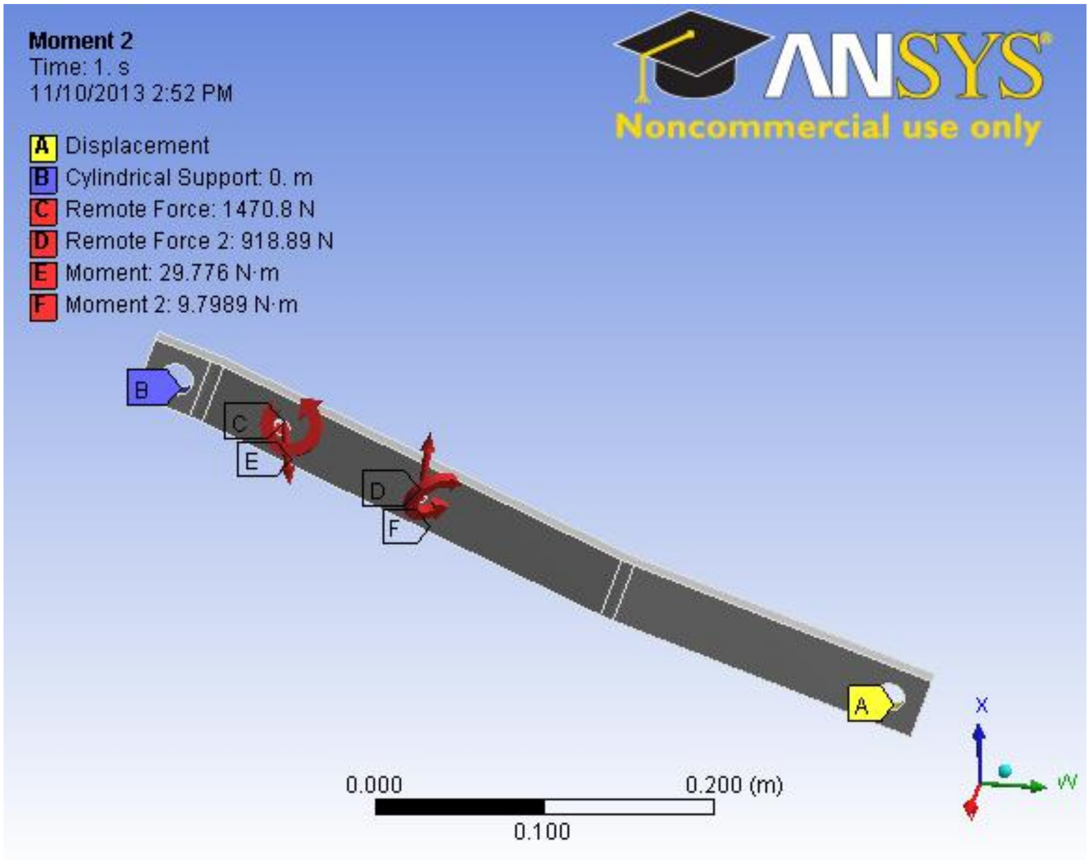

Figure 4- 15- Geometry, external loads and supports for press wheel link

Solution and results discussion: As mentioned before, this problem has been solved using different mesh sizes, to find out about the effect of stress concentration. Analysis showed that the maximum stress is happening at one of the holes, as it is shown in figure 4-16. It has been observed that the maximum stress is about 88 MPa. This part also has been made of structural steel with a yield tensile strength of 250 MPa. This will result in a safety factor of 2.85.

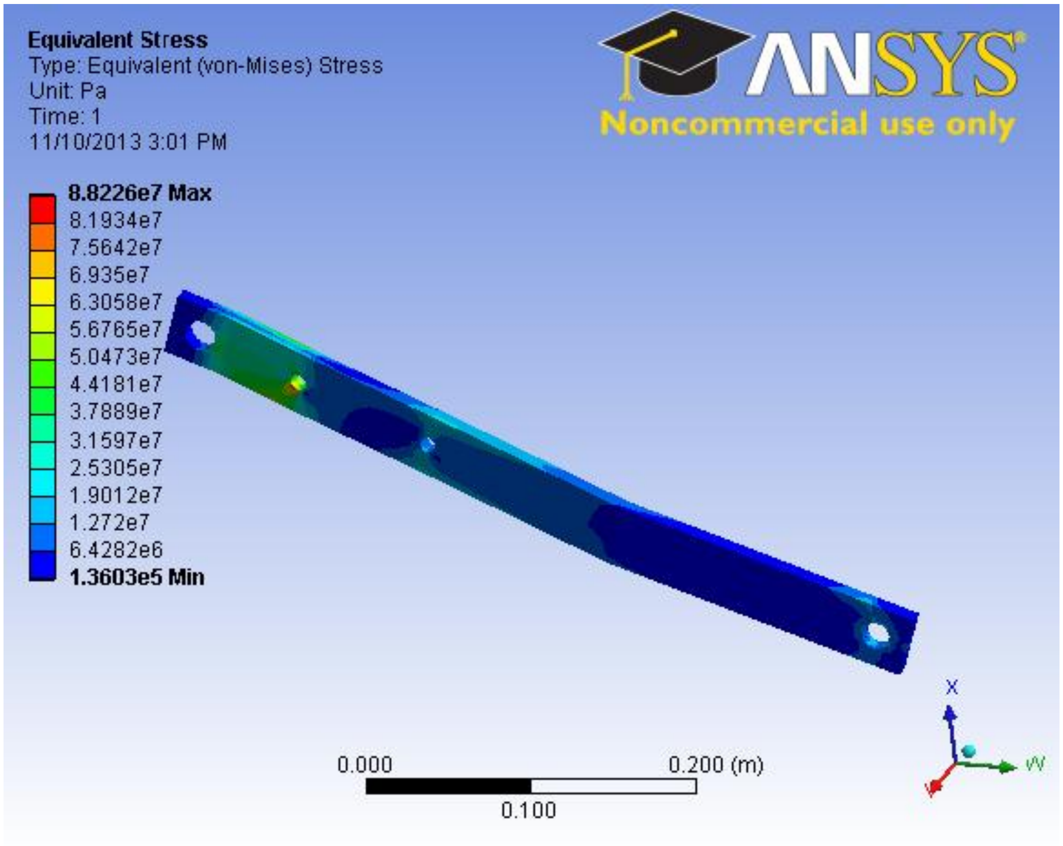

Figure 4- 16- Equivalent (Von Mises) stress contour for press wheel link

4-2-6- vertical pull bar

Vertical and horizontal pull bars are used to attach the planter to the robot and also for transportation, lifts the planter off the ground. Figure 4-17 shows the orientation of these parts for these two functions. Figure 4-17(a) shows the bars and winch in the straight configuration to do the seeding, and figure 4-17(b) shows the bars in the transportation configuration.

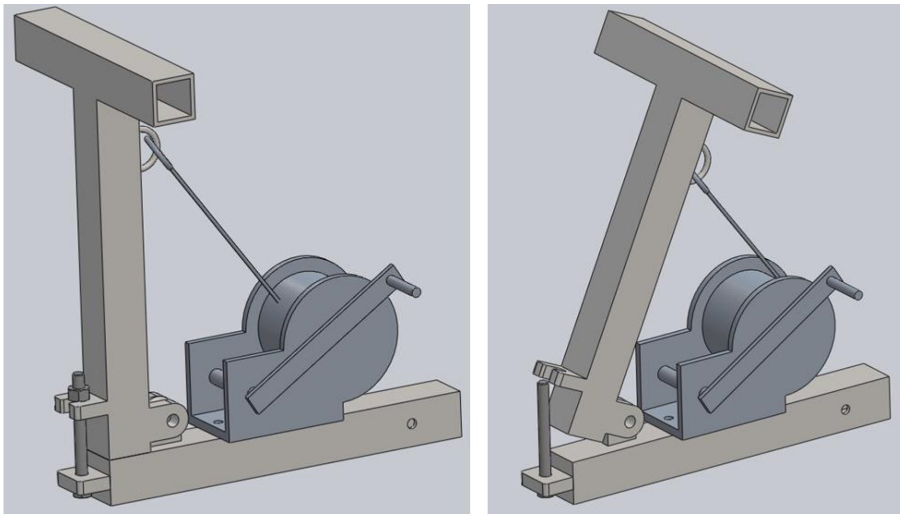

(a) (b)

Figure 4- 17- (a) vertical and horizontal pull bar in seeding configuration, (b) vertical and horizontal pull bar in transportation configuration

Stress analysis has been performed for both of these configurations; because forces and supports are different for each of them.

Meshing: Figure 4-18 shows the meshing for vertical pull bar. Finer mesh has been used for the area that stress concentration is expected. This mesh is used for both analyzes.

External loads and supports: External loads and supports are different for the pulling configuration and lifting configuration.

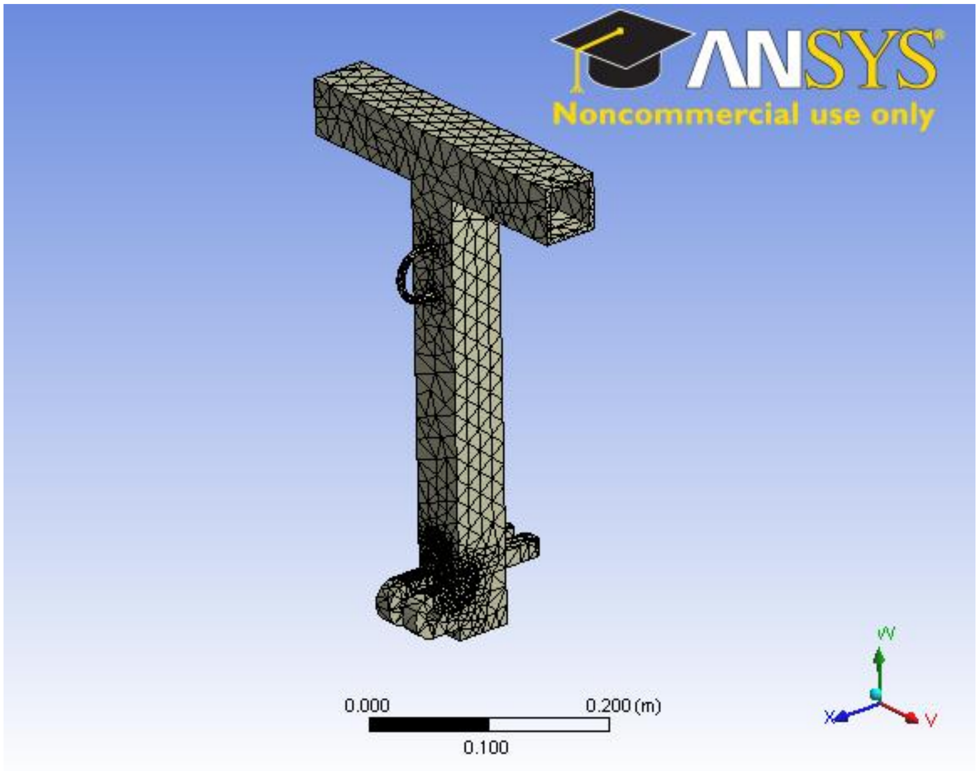

Figure 4- 18- meshing for vertical pull bar

In pulling configuration, the nut on the figure 4-17a is fastened and is keeping the vertical pull bar tight in its place. Also the bottom surface of the vertical pull bar will touch the horizontal pull bar and limits its motion in Y direction. It means that face A is fixed support (fixed by the bolt) and face E is only fixed in vertical directions (Zero displacement support).The external forces are draft force and normal force from the planter, which were calculated in chapter 3. These forces are applied on the upper part of the vertical pull bar, where the planter is attached (Force C and D). These forces are applied to both side of the vertical pull bar, but in Figure 4-20a only one side can be seen. Cylindrical support is used to define the hinge on the bottom at point B. Figure 4-20a shows the forces and supports for vertical pull bar in pulling configuration.

In lifting configuration, the nut is removed and the only support of the bar, is on the pin in point B. The force from the cable and the winch must be high enough to lift the planter off the ground. With calculations done in chapter 3, the tension in the cable was calculated to be T= 3157 N. The weight, W= 980 N, and center of the mass of the planter is calculated by Solid-works. (Figure 4-19) The weight includes the weight of the planter and the seeds inside the hopper.

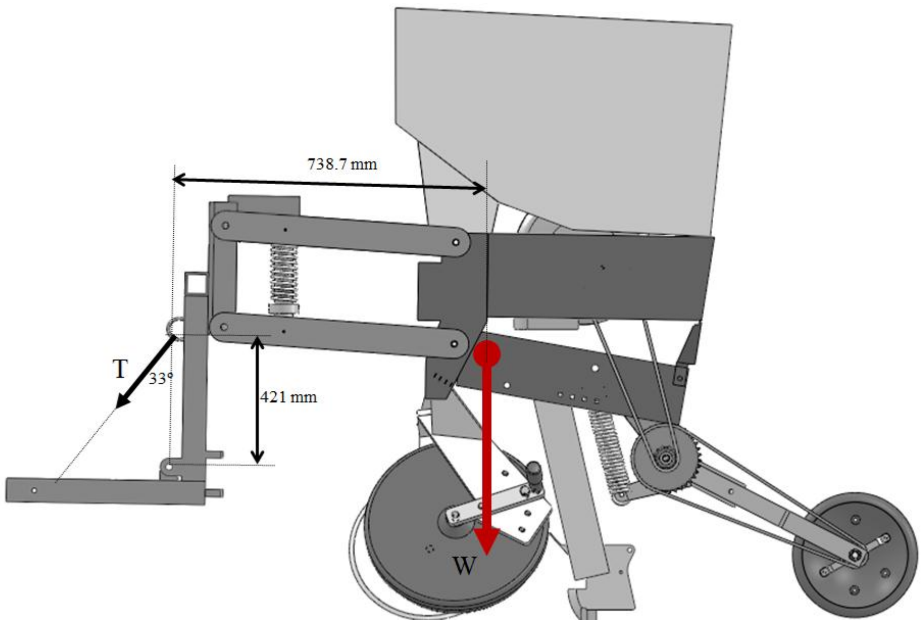

Figure 4- 19-Forces for lift configuration of the planter

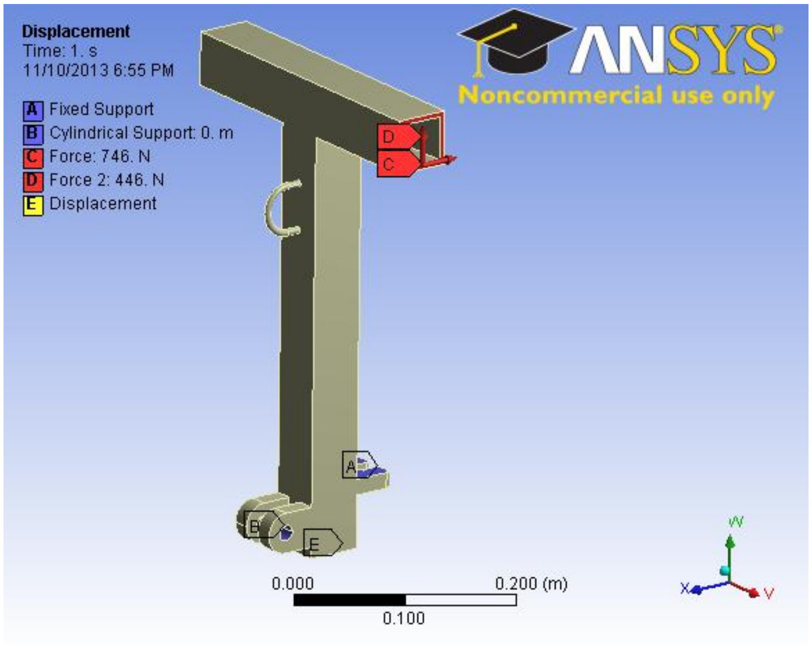

(a)

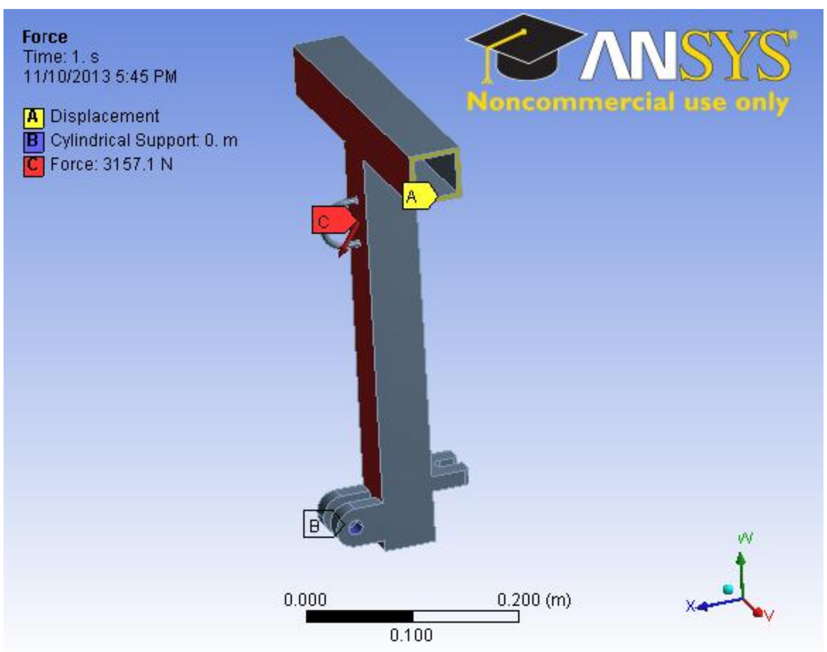

(b)

Figure 4- 20- Geometry, external loads and supports for vertical pull bar in (a) pulling configuration, and (b) lifting configuration

So, to model the vertical pull bar in lifting configuration, a cylindrical support is used for the hinge and the planes that the planter is attached to are fixed in X direction.(Figure 4-20b)

Solution and results discussion: Figure 4-21(a) and 4-21(b) shows the equivalent (Von mises) stress for vertical pull bar in pulling condition and lifting condition, respectively. The method to find the correct value for maximum stress is the same as what discussed before for other parts. The maximum stress in pulling condition is found to be 19 MPa, and in lifting condition 28 MPa. These values result in a safety factor of 13.2 and 8.9, respectively.

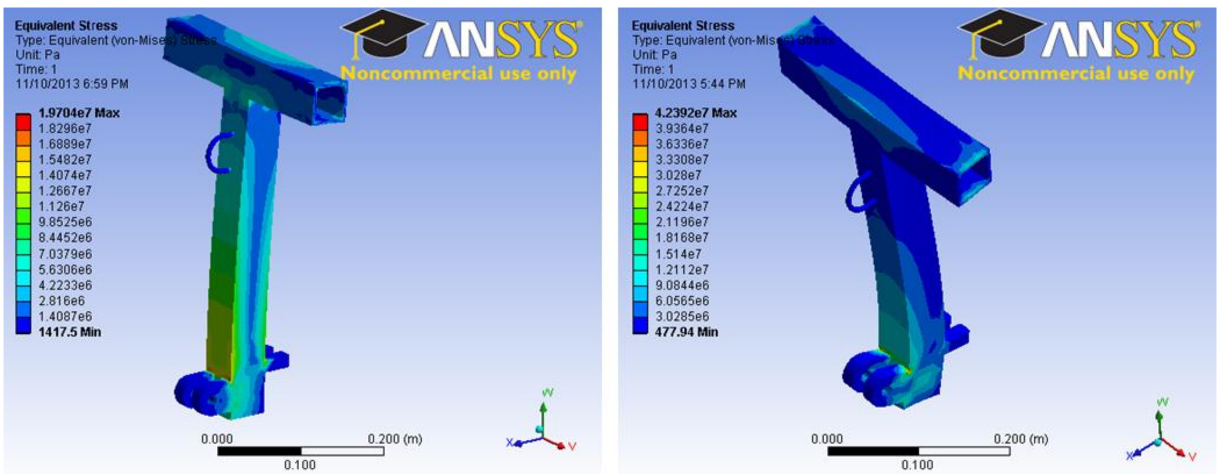

(a) (b)

Figure 4- 21- Equivalent (Von mises) stress for vertical pull bar, in (a) pulling condition and (b) lifting condition

4-2-7- Horizontal pull bar

This part is also analyzed the same as vertical pull bar in two different configurations, pulling and lifting. From the analysis of the vertical pull bar, the reaction forces at supports can be found. These forces are used in analysis of horizontal pull bar.

Meshing: Meshing for this part is shown in figure 4-22 and is used for both configurations. Finer mesh and smaller element sizes are used for regions with stress concentration.

External loads and supports: The first 80 mm of the horizontal pull bar goes inside the hitch that is available at the back of the mobile robot to pull the implement. A pin is used to keep the bar inside the hitch. Reaction forces found from the analysis of vertical pull bar are the external loads on this part.

In pulling condition, external loads are reaction force and moment at points A and E and reaction force at point B in Figure 4-20(a).

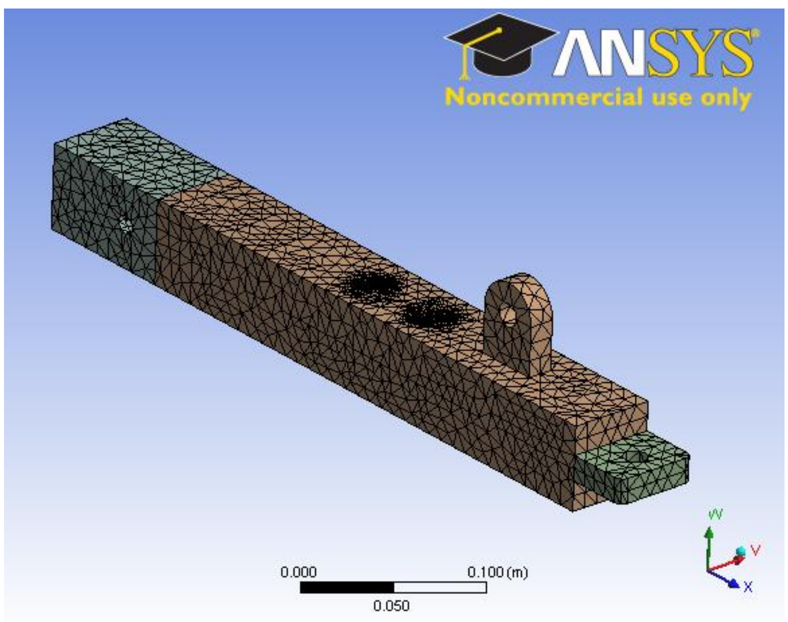

Figure 4- 22- Meshing for horizontal pull bar

In lifting condition, external loads are the reaction force at pin, point B in Figure 4-20(b) and the cable tension. The cable tension is transferred to the horizontal pull bar via the winch and the bolts. Figure 4-23(a) and 4-23(b) shows the external forces and supports for horizontal pull bar in pulling and lifting conditions, respectively.

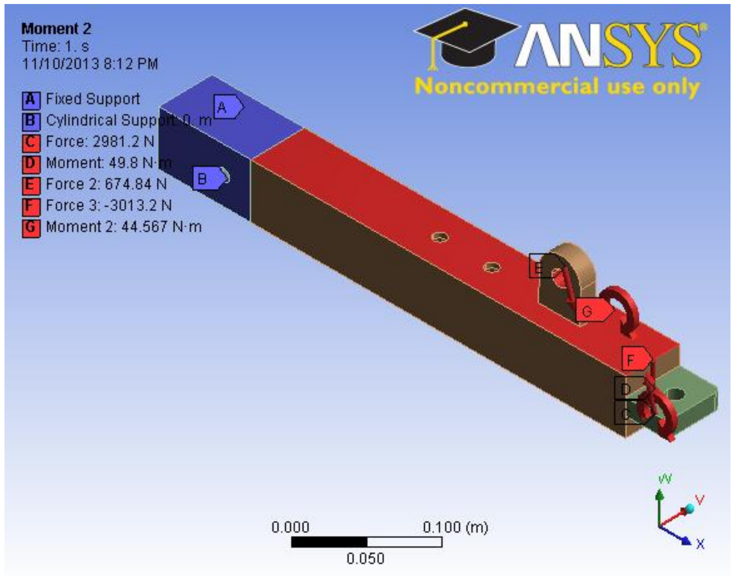

(a)

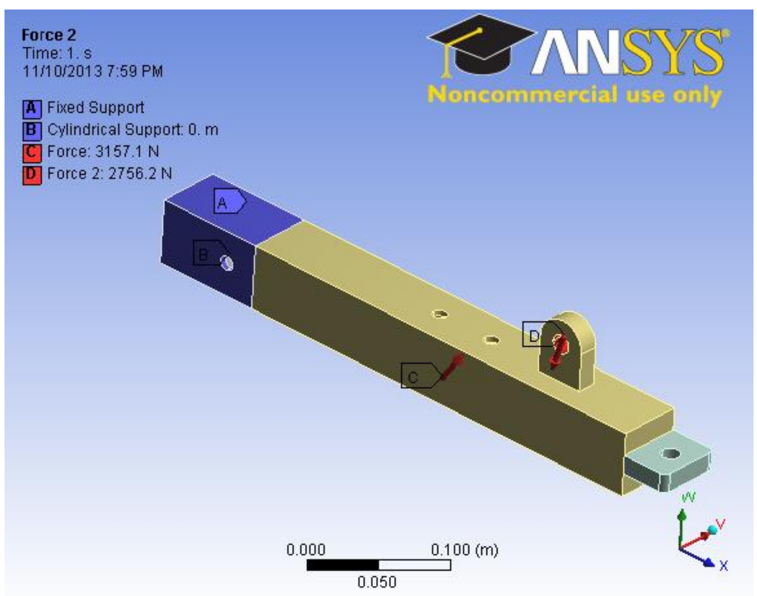

(b)

Figure 4- 23- Geometry, external loads and supports for horizontal pull bar, in (a) pulling condition, and (b) lifting condition

Solution and results discussion: Results for stress analysis of horizontal pull bar in both conditions are shown in Figure 4-24.

In pulling condition, it can be seen that a singularity is happening at the edge of the bar, due to the small area that the force is applied. The reason for that is that the external point force F, in Figure 4-23(a), is applied to the edge. This force is the reaction force of the vertical pull bar on the top surface of the horizontal pull bar. Since the bars are hollow structural steels, the reaction force is applied on the edge. So this stress value may not be real, thus for the rest of the beam it can be said that the maximum stress is about 30 MPa. This means the safety factor for this condition is more than 8.

In lifting condition, the stress concentration happens at the holes that are used to attach the winch. In this case also, finer mesh is used for stress concentration area. Maximum stress can be found to be about 80 MPa. Although the maximum stress is very high, but it is still less than the yield tensile strength of structural steel, which is 250 MPa. This means the safety factor of more than 3 is achieved.

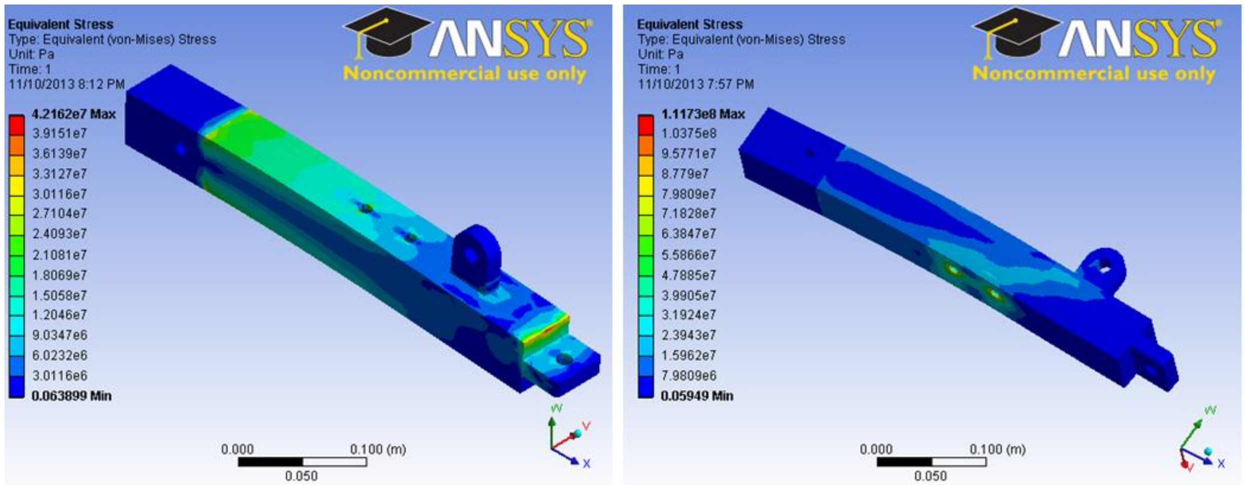

(a) (b)

Figure 4- 24- Equivalent (Von Mises) stress for horizontal pull bar in (a) pulling condition and, (b) lifting condition

4-3- Summary

In this chapter all the new parts that are designed for the developed modified planter are analyzed statically to study their strength to handle the external loads in different working conditions. The stress analysis was performed using Finite Element Analysis. Tetrahedral and hexahedral elements were used depending on the geometry of the part that was analyzed. All the parts were studied for the condition that the implement is in contact with the soil during a simulated seeding operation. Two parts that are involved for lifting the planter off the ground for transportation purposes are also studied for this condition too. Analyzes showed that a safety factor of more than 1.4 is obtained for all parts and in most cases the safety factor is greater than 8. Although the environment of farm and the interaction of the implement with the soil are not very predictable, these parts have enough strength to work in harsher environments with higher loads.

Chapter 5-Prototyping, test-rig and verification

5-1- Fabrication of the prototype

The plan was to fabricate two planters which their disc and tilt angles are mirrored with respect to each other. Using two planters with mirrored angles will cancel out the lateral force on the connection and make the mobile robot to move forward easier. In the industrial similar planters also use the same method to cancel out side forces.

As mentioned in previous chapters, some of the parts are used from the donated existing planters. These parts are either doing nothing specific with respect to seeding and soil interaction (e.g. frame), or the study of their performance was not part of the objectives of this research (e.g. precision seed metering system).

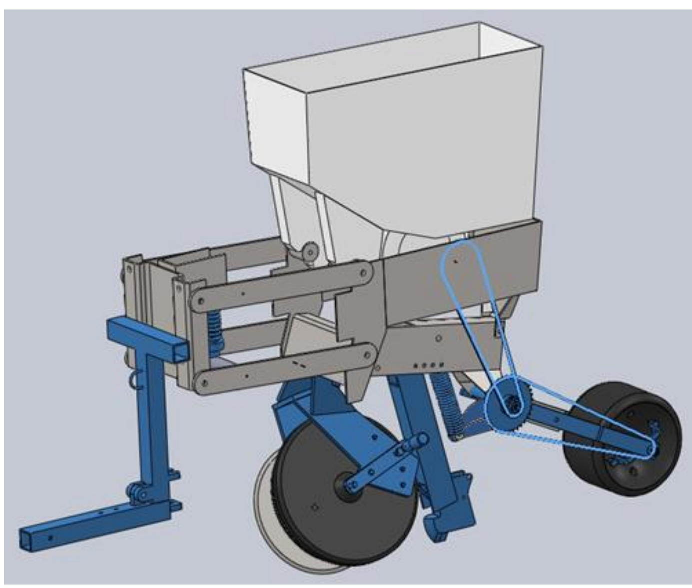

Figure 5- 1- Parts that are designed or modified are shown in blue

Other parts that are completely redesigned by the author, or modified partially, are shown in Figure 5-1 in blue. The drawings for these parts were prepared and sent to a fabrication facility for fabrication. All the drawings are given in appendix D. Some other parts were bought off the shelf, such as ball bearings and sprockets and chains and winch.

After gathering up all the parts together, they were assembled by the author and it is attached to the mobile robot, and tests are performed. Figure 5-2 shows the designed and assembled planters. More pictures of the developed planter can be found in appendix A.

A few of tests are designed for this planter to study its performance and efficiency. The results of these tests are given later in this chapter.

5-2- Tests

Several tests are designed and performed in outdoor and indoor settings, to study the performance of the designed planter. The aspects that are studied in these tests are given below,

- Draft force: Draft force needed to pull the implement when performing seeding was measured. The measured value must be comparable with theoretical value found in chapter 3.
- Opening and closing the furrow: The effectiveness of the planter in opening a furrow and then closing it to cover the seed must be appropriate. The width of the furrow must be wide enough to accommodate a seed and be comparable with existing planter.
- Seed drop accuracy: The distance between seeds must be measured to verify the performance of the new power transmission system, using press wheel.
- Lifting of the planter off the ground for transportation

Among these parameters, the draft force is the most critical one for this research project. Other parameters can help to show that the performance of the new planter is as good as the existing planter.

(a)

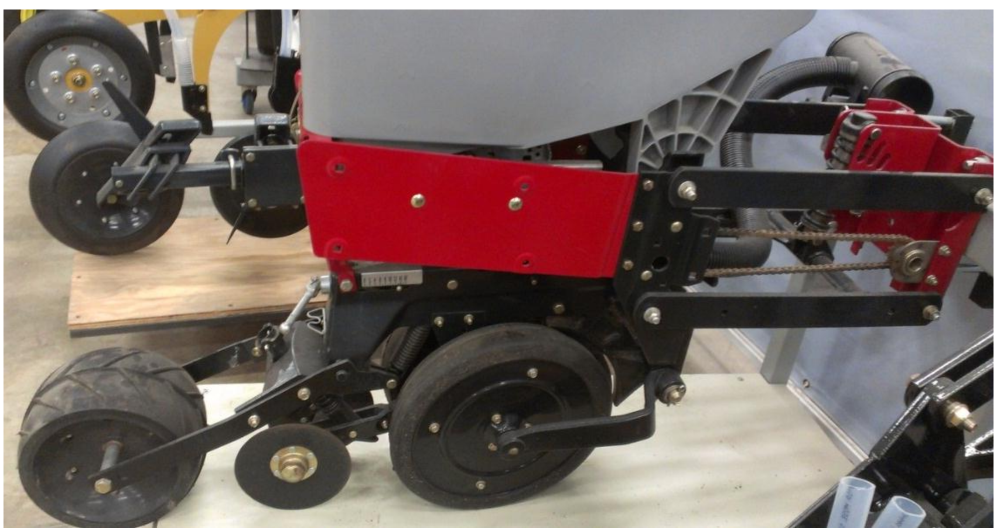

(b)

Figure 5- 2- a) The assembled new planter, b) Existing CNH planter

Two tests are performed in two different test settings, outdoor and indoor. The outdoor test is performed to study the ability of the planter in opening and closing a hard soil in presence of crop residue. Also the depth of the cut and its consistency is studied. Besides that, the lifting mechanism is used to lift the planter off the ground for transportation. The main objective of the indoor test is to measure the draft force. Depth of cut and seed drop accuracy is also studied through the tests.

5-2-1- Outdoor tests:

Outdoor tests were performed on the north-west side of the College of Engineering building, University of Saskatchewan (See Figure 5-3).

The main objective of this test was to observe the performance of the planter and mobile robot in,

- Lifting and transportation
- Cutting the hard soil, opening the furrow and closing the furrow
- Residue handling performance of the planter

The planter was attached to the Grizzly mobile robot, lifted up from the ground, and transported to the test area by the mobile robot (See Figure 5-4). When the robot and planter were in the place to start the test, the planter was set down on the ground, and the depth of cut was set to 50 mm, and then it was pushed into the soil to start the test.

The soil in that area has been used to cultivate grass, and it has become packed and hard over time. Therefore it has a hard soil compared to the common medium packed soil used for corn planting. The water content of the soil was about %15 on the day of the test, 31st of October of 2013. The grass on the soil was used to simulate the residue which is available in farms, when practicing no-till farming. The reason this area was chosen for test was its ease of transportation of the mobile robot and the new planter set.

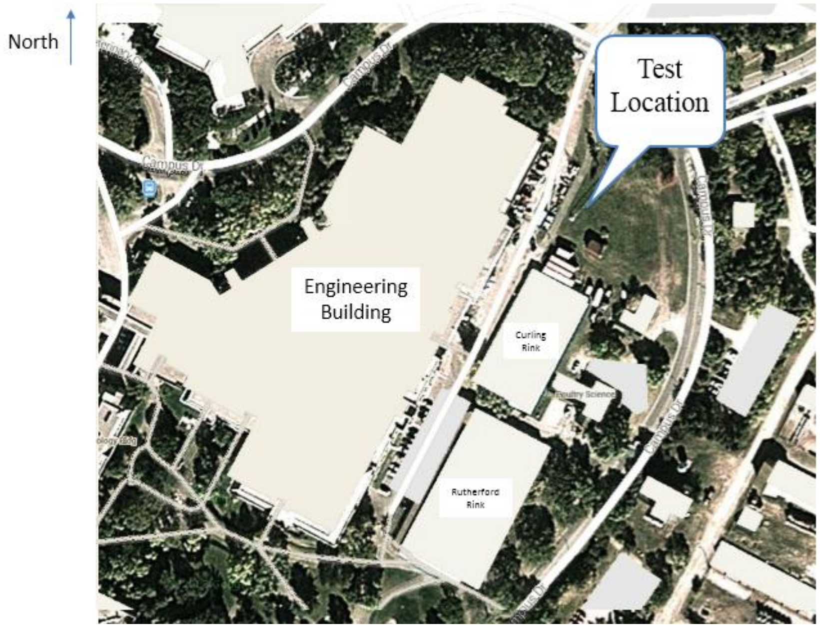

Figure 5- 3- Location of the outdoor tests, north of engineering building

Figure 5- 4- The set of two planters, attached to the wheeled mobile robot in transport position

So when the disc and other parts are engaged with the soil, the robot goes a straight path. The planter opens two furrows and later closes them after seeding. Each furrow is 50 mm deep and two furrows are 380 mm away from each other. Figure 5-5 shows the opened furrow and its width. It can be seen that opened furrow is wider than the width of a corn. It can be estimated easily form the size of the seed drop tube that the width of the furrow is about 40 mm. Although the residue which is available in a farm is more packed than the grass on the test field, but, it can be observed that disc coulter has been successful in cutting through a light amount of residue (grass).

Figure 5-6 shows the line remaining from the closed furrow after was opened by the disc. It can be observed that the disturbance that is caused by this implement is very small. Fewer disturbances in the soil mean less loss of moisture and nutrients of the soil. Also this picture show how complete the press wheel has done its job in covering the soil. If the soil is not covered properly, the seed may not germinate well, or it can even be blown away by wind or can be eaten by small animals and birds.

Figure 5- 5- The furrow opened by the planter

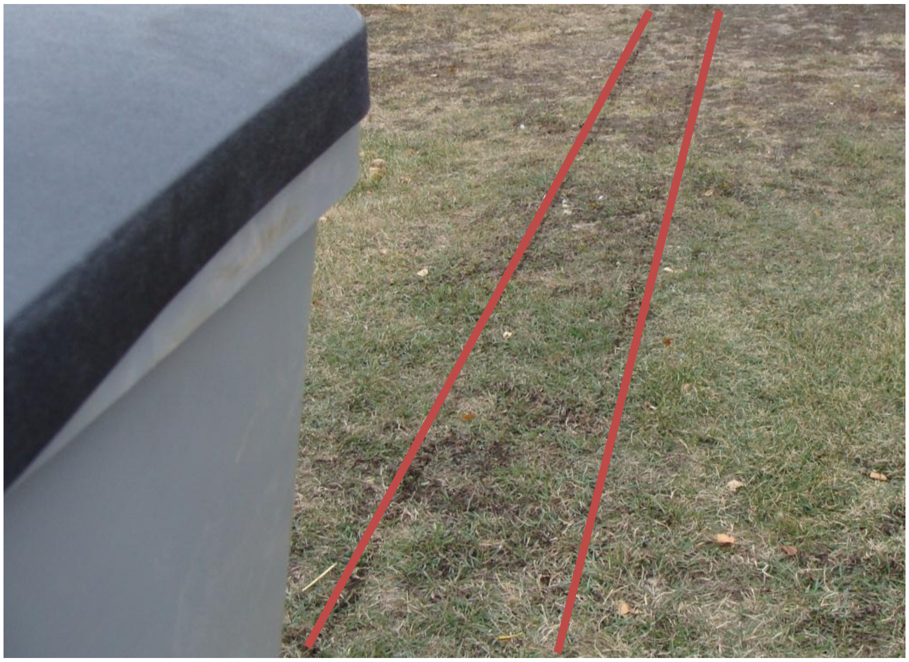

Figure 5- 6- The closed furrows by press wheels

The results that were obtained from this outdoor test were satisfactory and as expected. This was the very first time that designed planter was tested in contact with the soil. In all the steps of the test, from lifting off the ground and transportation to opening the furrow and closing it, its performance was as expected.

5-2-2- Indoor tests

Indoor tests were designed to study the draft force required to pull the implement by the robot. But at the same time the accuracy of seeding has also been studied.

This test was performed in the soil bin, college of Engineering, University of Saskatchewan. All the settings has been prepared to simulate the conditions of a farm land.

Test setup: The planter was attached to the mobile robot and it was pulled while disc was inside the soil. Soil has been prepared, with medium packing (See to chapter 2) and with about 13% soil moisture. The working length of the soil bin for this test was around 5 m. A vacuum was used to provide the negative pressure needed for seed singulator suction. To measure the draft force, two load cells were used. One end of each load cell was attached to the mobile robot and the other end was attached to the planter while pin of the hitch which connects the planter set to the robot was removed (See Figure 5-7).

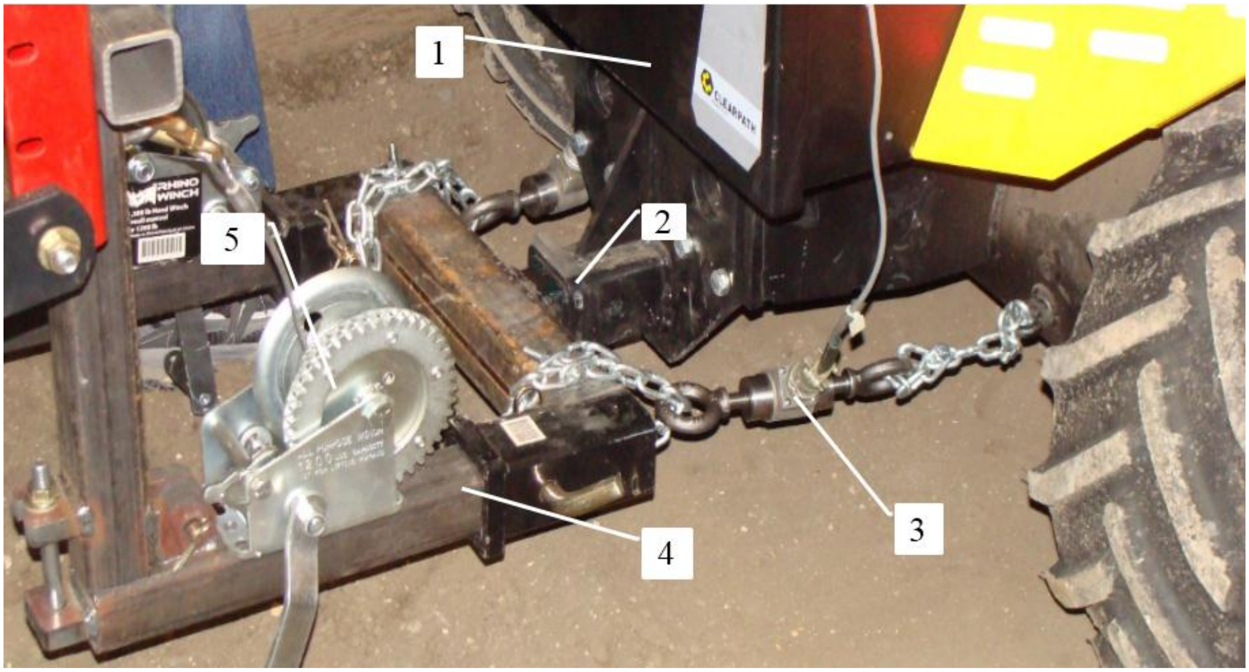

Figure 5- 7- Load cells attached between the mobile robot and planter, 1) Grizzly mobile robot, 2) Hitch (pin removed), 3) Load cell, 4) Planters set, 5) Hand winch

Each of these load cells can carry up to 5000 lb force. To make sure that the load cells are carrying all the load of the pulling force, the connecting pin of the hitch of the robot has been removed and the connection inside the hitch was lubricated to reduce the friction inside the hitch as much as possible. The connection must remain inside the hitch to keep the planter in up-right position and pushed down the disc into the soil. Although the friction inside the hitch will carry some of the pulling force, but it can be calculated and be added to the value that is read by the load cells.

The signal from the load cells are sent to amplifiers and from the amplifiers to the data acquisition and then to a laptop computer to be recorded. The data acquisition software records 10 values per second for each load cell. The power for the vacuum, amplifiers and laptop was provided by a 12V DC battery. The voltage was inverted to 110 V AC, using a 1500 W power invertor so it can provide enough current for all the equipment. The equipment were mounted on top of the mobile robot which pulls the planter set in the soil bin (See Figure 5-8).

Figure 5- 8- Mobile robot pulling the planters set inside the soil bin

Calibration: Load cells were calibrated before attaching to the robot and the planter set. Specific weights were loaded on the load cell and the output voltages were recorded. The gain of the amplifiers were set to have maximum output of 10V for 200Kg mass. Figure 5-9 shows the calibration setup and figure 5-10 shows the data obtained from calibration.

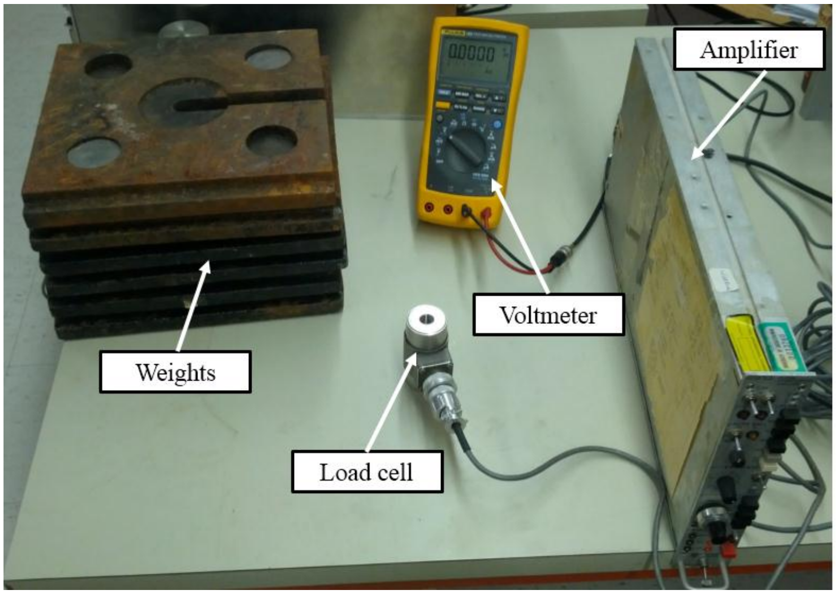

Figure 5- 9- calibration setup

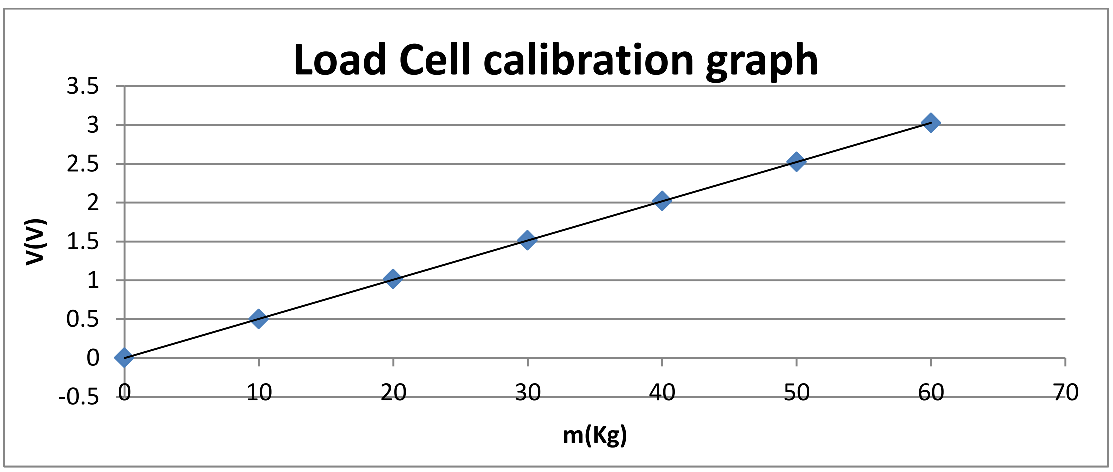

Figure 5- 10- Calibration graph for Load cell, V = 0.0505m - 0.0004

Calibration graph shows that the output of the load cell is completely linear with almost zero intercept.

Procedure: The male and female parts of the hitch were lubricated and the planter set was attached to the mobile robot. Load cells were attached to mobile robot and planter using chains. The depth of cut was set and the planters were lowered down and discs were pushed into the soil. Vacuum tube was attached to the singulators and the vacuum was turned on. Mobile robot moved forward for a very short distance, i.e. about 50 mm, to make sure that the load cells are in tension before the test begined. The software started recording data and then the robot started moving in the soil bin, till it reached the end of its working length. Each test was performed twice.

The first test was done with a 50 mm depth of disc into the soil. The depth for second test was set for 75 mm. The first two tests were performed to study the draft force and also the accuracy of the depth of disc in the soil.

A third test was performed with the shallowest depth, less than 25 mm, only to find out about the precision of the seeding. Because with lower depth, it was easier to recover planted seeds and measure the distance between them.

Test results: The data from the load cells were converted from Volt into Newton. Figure 5-11 shows the forces of load cells (F_{c1} and F_{c2}), friction in the hitch (F_h) and the total draft force that is required from the mobile robot to pull the set of two planters (F_R).The measured forces (summation of the two load cells F_{c1} and F_{c2}) are shown in figures 5-12, 5-13 for 50 mm and 75 mm disc depths, respectively. It can be seen that the fluctuation in the measured forces are high. This was expected, because the soil is not a homogenous material. Although tillage and packing has been used to make the soil structure as homogeneous as possible, but uneven surface of the soil can cause the force to fluctuate. On the other hand, from the design point of view, it can be said that these fluctuation can give the designer a better understanding of what to expect on a farm field. The designer can find out how high the forces can go and how high the safety factors should be set. Beside the nonhomogeneous soil, the environmental noises can cause high frequency fluctuations in the measured results. These noises can be seen in figures 5-12 and 5-

13. The sources of the noises can be the ventilation, the motion of the robot on the soil and other machinery working in the vicinity.

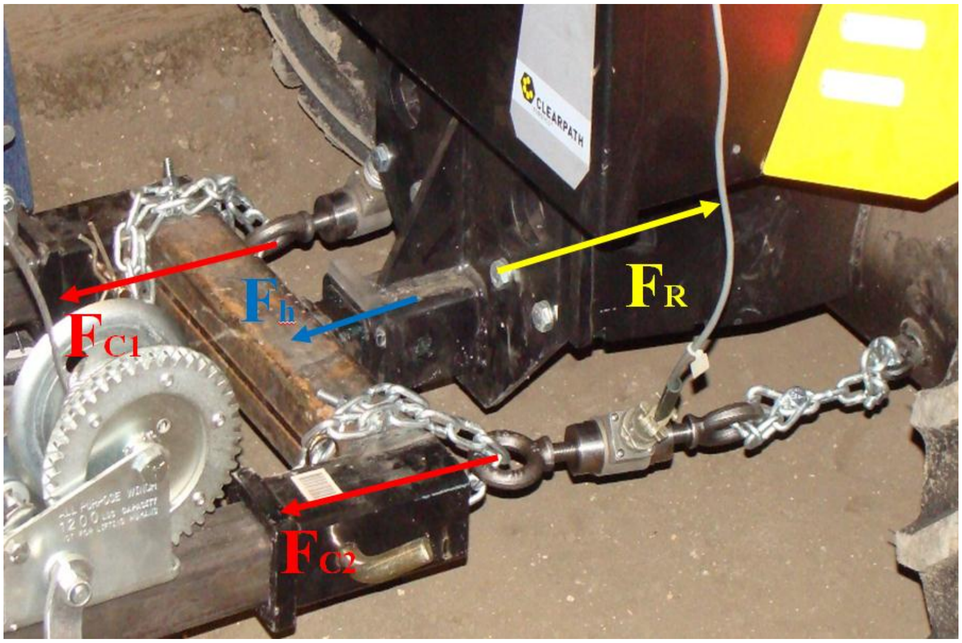

Figure 5- 11- Force balance between robot and set of planters

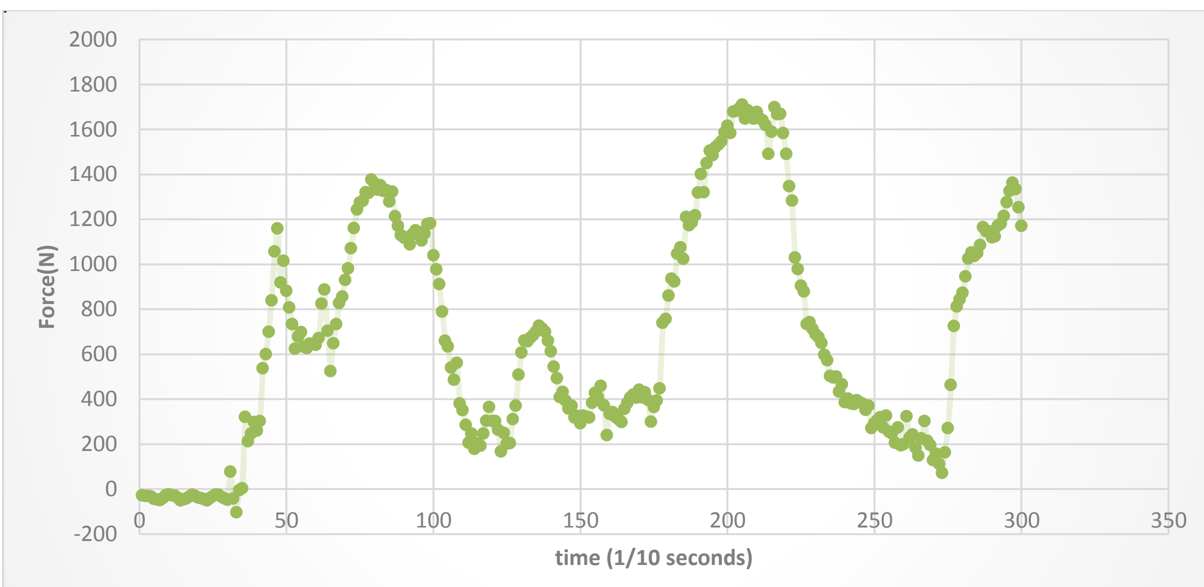

Figure 5- 12-Measured draft force for 50 mm depth of disc in the soil

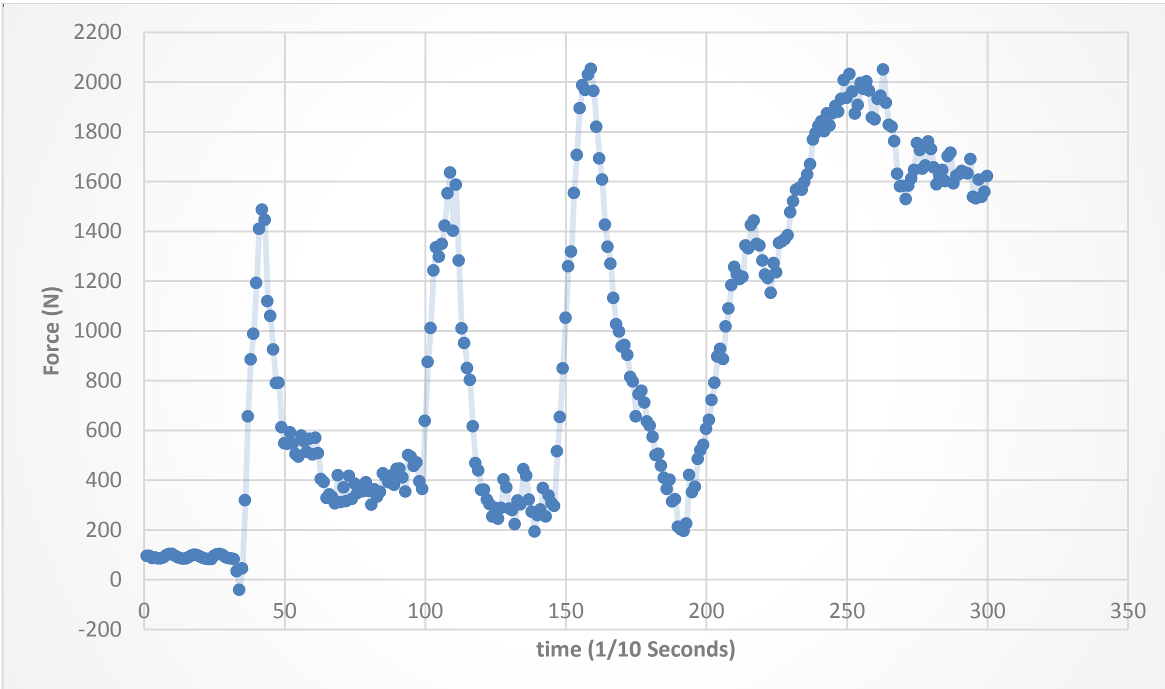

Figure 5- 13- Measured draft force for 75 mm depth of disc in the soil

To remove these noises from the measured data, a low pass filter was used, using Matlab and Simulink. The cut off frequency of the low pass filter was set to 2 Hz. The Matlab code and Simulink model is provided in appendix. Figures 5-13 and 5-14 compare the raw data and filtered data for 50 mm disc depth experiment and 75 mm disc depth experiment, respectively.

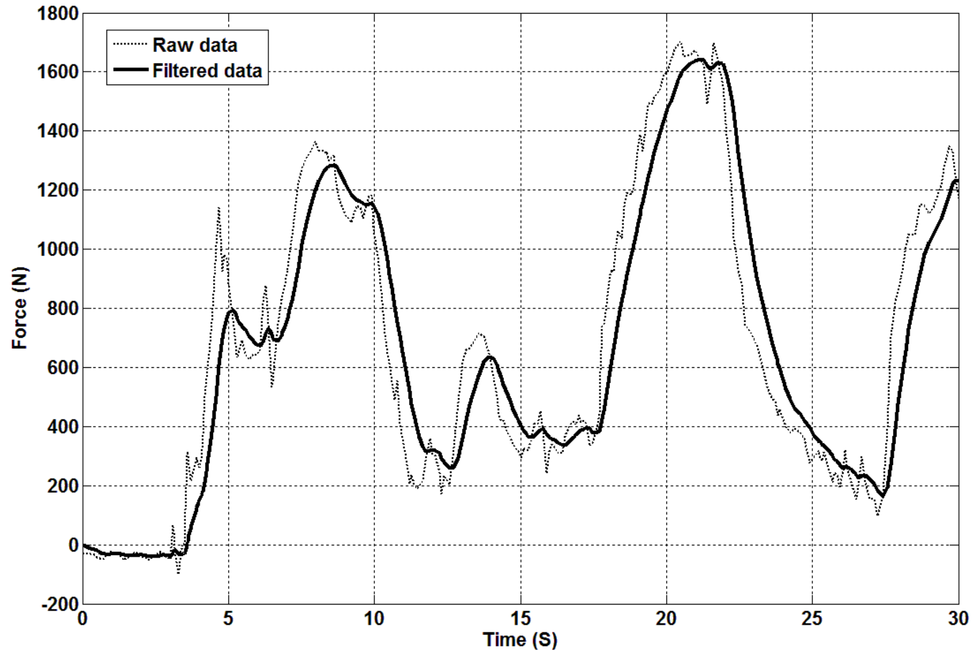

Figure 5- 14- Raw and filtered data (measured draft force), for 50 mm disc depth

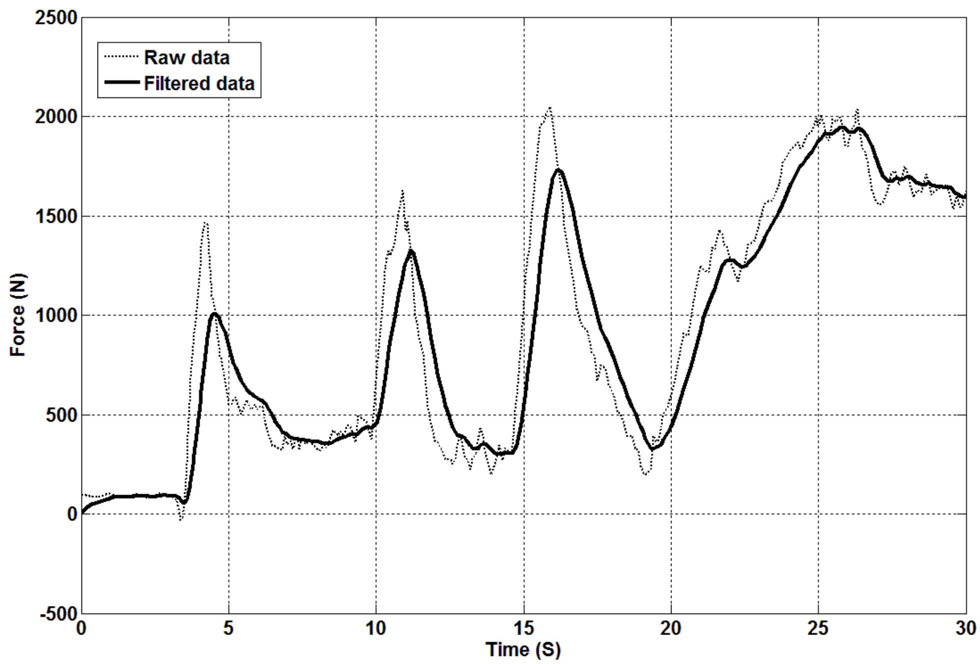

Figure 5- 15- Raw and filtered data (measured draft force), for 75 mm disc depth

For data analysis, the average of useful data, the maximum, and the minimum are reported.

Table 5- 1- Average, minimum and maximum of the tests

	50 mm depth	75 mm depth
Average total force (N)	750	1084
Minimum total force (N)	258	192
Maximum total force (N)	1709	2052

The averages of the forces are calculated as 750 N and 1084 N for 50 mm and 75 mm depth of cut, respectively. Table 5-1 shows the average, minimum and maximum of the data of these two tests.

Seed distances: Figure 5-15 shows the seeds dropped by the planter. It can be observed that the measured distance between the seeds is obtained as expected, which means the power transmission system is working with the proper ratio as designed. The system was designed in chapter 3 to give a seed spacing of 128 mm with a 48 holes singulator disc. But since a 24 holes singulator disc is used instead of 48 holes, the distance between the seeds has been doubled to 260 mm.

Figure 5- 16- Space between seeds dropped by planter

- **Discussion:** The data obtained from load cells in Figures 5-11 and 5-12 has been recorded for a period of 30 seconds. The data also includes the values before the robot starts to move; for analysis these values have been removed.

In chapter 3, the total draft force and vertical force for the planter with 50 mm depth of cut was found to be 446 N and 726 N, respectively. So the total draft force for two planters is expected to be twice as much to be equal to 892 N. It can be seen in table 5-1 that the average force for 50 mm depth is 750 N and compared with the analytical value, is about 142 N smaller.

The major source of error in these experiments is the friction inside the hitch that holds the planter in contact with the mobile robot. As it can be seen in figure 5-7, the planter is attached to the mobile robot, using both hitch tube and load cells. The hitch connection is used to fix the planter in vertical and side axes, and chains provide the pulling force. Although inside of the hitch has been lubricated to reduce the friction inside the connection, nonetheless friction will carry some of the pulling (draft) force. To calculate the friction force, the coefficient of friction and normal force is needed. The vertical force for one planter was calculated to be 726 N (See chapter 3), and for two planters will be equal to 1452 N. The coefficient of friction between steel-steel contact with grease lubrication is around 0.13. This means the friction force in the hitch is about,

$$f = \mu \mathrm{N} = 0.13 \times 1452 = 189\ N \qquad \text{(Eq. 5-1)}$$

Assuming that the total draft force will be the summation of measured draft forces from the load cell and the friction in the hitch tube, the total draft force for pulling the planter set is 750+189= 939 N. The percentage error in the measured draft force can be calculated as follows:

$$Error = \left|\frac{F_{experimental} - F_{analytical}}{F_{analytical}}\right| \times 100 = \left|\frac{939-892}{892}\right| \times 100 = 5.2\% \qquad \text{(Eq. 5-1)}$$

The fact that the behavior of the soil is not very predictable, 5.2% of error is reasonable.

Since always maximum draft force should be used in design, and for choosing factor of safety, it can be concluded that a safety factor of more than 2 is needed for the parts that are affected by the draft force directly. A refine design of the planter is recommended as part of the future work.

Although in the first sight the high safety factors that was obtained in previous chapter seemed to be an over-design, but here it can be concluded that in a farm environment, safety factors as high as 8 can be reasonable. To have heavy duty products with long life, these high safety factors are sometimes necessary.

5-3-Summary

The parts that were designed in chapter 3 and were analyzed in chapter 4, were fabricated and two prototypes of the developed planter has been made. These prototypes were the mirrored version of each other, to cancel out the side force which cause the implement to side track. The parts were assembled together and prepared for tests. The performance of the modified planter was verified in two different tests. The outdoor test was done to study the performance of the planter in lifting and transportation, cutting the hard soil, opening the furrow and closing the furrow and residue handling. This test was mostly an observation experiment and no specific measurements were taken.

Another series of tests were performed in the soil bin. Load cells were attached between the mobile robot and the planter set, and the draft force was measured when the planter set was interacting with the soil with different depths of disc inside the soil during seeding. Besides, the seed drop performance and accuracy of the distance between seeds were measured. The results of the tests were satisfactory. The average draft force obtained from the test with 50 mm depth of cut, for two planters was equal to 750 N. Considering the friction in the mobile robot and planter connection, it resulted in a 5.2% error between the measured and analytical values of the draft forces.

Chapter 6- Conclusion and Future Work

6-1-Summary and Conclusion

The main objective of this research project was to design a customized planter in order to retrofit to a mobile robot with limited towing power. For the design part of this project, the process started with literature survey, to find out about previous work that has been in this area. As expected, no similar work has been reported in the field of design of the seeders and planters. Most of the research in this field is done by the agriculture manufacturers that are not willing to publish their work. Besides, there are some research works done in the field of soil-tool interaction. The data from these researches have been used in the design process. To get more information, a series of lab experiments was performed to study the effect of disc and tilt angles on the forces applied to the disc from the soil. The experiments were done in the soil bin, facility of College of Engineering at the University of Saskatchewan. The goal of these tests was to find the best combination of disc angle and tilt angle which leads to minimum pulling draft force. The disc used in tests had a 460 mm diameter and depth of cut was set to 50 mm. Forces in 3 directions of draft, vertical and side were measured by attached load cells. The results of the experiments showed that the compound angle of 7º disc angle and 25º tilt angle gives the lowest draft force. Although zero disc angle gives lower draft force, but as mentioned in chapter 3, disc angle cannot be zero for the purpose of seeding. The corresponding draft, vertical and lateral force for 7º disc angle and 25º tilt angle were 97 N, 84 N, and 760 N, respectively.

In these tests, the compaction of the soil, soil water content and soil uniformity can affect the results. Also, the depth of cut, the disc diameter and thickness and the forward speed are the parameters that can change the applied forces on disc, particularly, the draft force.

When enough data was collected from literature survey and soil bin experiments, the design of a planter was continued with conceptual design. Different sketches were generated and the final idea was developed in SolidWorks. Some preliminary calculations were also done in conceptual design stage to provide more detail about the new designed planter. Then static analysis to find the total draft force and total vertical force on the developed planter was performed. The analytical hand calculation to find the total draft force on the planter was done by taking use of both theoretical and experimental data. Although agriculture machinery manufacturers do not usually publish the draft force needed to pull one row planter, but with simple power formula equations it can be calculated to be around 1 KN for similar planters [25]. The calculated analytical draft force for the developed planter was found to be 476 N, which is less than half of the draft force needed for commercial planters. Optimization was performed to minimize the change in the down force of the press wheel, when it moves forward. This optimization resulted in 29% in change of the down force with maximum displacement of the press wheel in vertical direction. Using wider range for constraints of this optimization problem can result in smaller change in the downward force on the press wheel. Also spring design process was done to design the springs that provide down force on the gauge and press wheel.

All the new parts that were used in the modified design, were analyzed using computer software, to find out about their strength. The stress analysis was performed using Finite Element software, ANSYS. All the parts were analyzed for the condition that the implement is in contact with the soil during seeding operation. Two parts that are involved for lifting the planter off the ground for transportation were also analyzed for this particular position. Analyzes showed that a safety factor of at least 1.4 is obtained for all parts and in most of cases the safety factor was greater than 8. Although the environment of farm and the interaction of the implement with the soil are not very predictable, these parts have enough strength to work in harsher environments and higher loads.

When the strength of the parts was verified using FEM stress analysis, they were sent to a manufacturing facility for prototyping. The fabricated parts were assembled together and a set of two planters were made. The planter set was made mirrored with respect to each other in order that no side force is transferred to the mobile robot. The performance of the developed planter was further studied in two different tests. The outdoor test was done to study the performance of the planter in lifting and transportation, cutting the hard soil, opening the furrow and closing the furrow and residue handling. This test was solely an observation. The performance of the planter in these tests was satisfactory. The lifting mechanism for transportation was used. The furrow created by the planter was uniform with the expected depth. The disc coulter cut through the grass field without any problems.

Another test was performed in the soil bin to measure the actual total draft force needed to pull the set of developed planters. Load cells were attached between the mobile robot and the planters set, and the draft force was measured when the planter was interacting with soil with different depths of cut and seeding. Besides, the distance between planted seeds was measured and was compared with desired distance. The results of the tests were satisfactory. The average draft force obtained from the indoor test with 50 mm disc depth, for two planters was equal to 750 N. Considering the friction in the hitch between the robot and the planter set resulted in only 5% error between the test result and calculated values. Although the forces recorded from the load cells were fluctuating, but it was expected. Working with more uniform soil, and repeating the tests, the error can be reduced and the results can be validated further.

6-2-Contributions

At the end, it can be said that, the process of the design of a customized planter with smaller draft force was performed successfully. The contributions for this research project are listed below:

1) A customized planter is designed and fabricated that can be attached to Grizzly mobile robot.
2) The developed planter requires less draft force and it can be easily pulled the mobile robot for autonomous farming.
3) Improvements were performed on the planter for higher yield and better germinations. These improvements include the substitution of the down forces with optimized forces for better germination, and also the optimization of the press wheel down force system to get fewer change in the down-ward force.

The differences between the developed planter and the existing CNH planter that are noticeable in Figure 5-2 are listed briefly below.

1) Totall draft force (for the whole planter) of the planter (≈500 N) is lower than CNH planter (≈900-1300 N)[1] due to all the changes that has been done and listed below.
2) Only one disc and one gauge wheel are used in developed planter instead of double disc and double gauge wheel in CNH planter.
3) Different disc and tilt angle for the disc coulter is used here to get smaller draft force.

[1] Reference: Data unofficially provided by CNH Saskatoon.

4) Different depth changing mechanism is used in the developed planter. (See figure 3-5 and 3-7)
5) No seed covering discs are used in developed planter.
6) Transmission power to rotate the singulator disc is taken from the press wheel here.
7) To reduce the change in down force a longer press wheel links is used here.
8) Hand operated lifting mechanism is used in the developed planter here.
9) A connecting linkage to attach the two planters to the mobile robot is designed.

6-3-Future works

There are different aspects of this project that more work can be done on it in the future. Following are several suggestions to improve this planter:

1) **Further experiments in the soil bin:** In the experimental study of the disc properties and soil-disc interaction, more experiments can be performed to study the effect of disc diameter and thickness, its forward speed and depth of cut on the forces. Also soil properties such as soil type and its water content can be studied further. Beside the forces, other properties such as soil disturbance, strength of the wall of the furrow and residue handling of the disc can be measured and studied.
2) **Computer modeling of disc-soil interaction:** Finite element modeling or discrete element modeling can be used to model soil and disc and their interaction. The results of these simulations can be compared with experimental results, obtained in soil bin.
3) **Redesign from scratch:** In the design section, since some parts have been designed were kept from the existing CNH planter; this caused some limitations on the design process. If all the parts were designed from the scratch these problems and limitations can be avoided.

3-a) Also some improvements can be done on the designed parts. A caster wheel can be used at the point that the planter is attached to the mobile robot. This will reduce the load on the hitch, when the planter is lifted up and is in transportation.

3-b) Lifting mechanism can also be improved. Although the designed mechanism is working properly, but in some cases that the robot goes into a small hole or goes on a hill, the planters and their discs may touch the ground. A lifting mechanism which enables high lifting can be more effective.

3-c) The hand wrench that is used for the lifting mechanism can lift up to 1200 lbf (around 5300 N). Although the strength seems to be high enough, but the body of the wrench deformed after several trips. A wrench with higher strength is recommended to be used.

3-d) For the depth control system an improvement can be done for the zero depth setting. Technically, the zero depth of cut was designed to take the disc out of the soil for transportation purposes. Because of the tolerances and small deflections, the disc may still touch the ground in some conditions. So a new setting is suggested that keeps the disc higher than gauge wheel in zero depth configuration.

4) **Disc and tilt angle adjustment:** Another system that can be added to the planter is a mechanism that enables the researcher to change the disc angle and tilt angle. Utilizing such a system can enable the operator to see the effect of disc angle and tilt angle, on the draft force acting on the planters set.

5) **Singulator rotation speed adjustment:** The power transmission system for the precision seed metering system is one of the parts that new design can enhance its performance. The designed system is only designed and set for a specific length between two seeds. A new

design can solve this problem and give the operator the option to choose the seed distance as required.

6) **Tests:** More tests and measurement can be performed using the developed planter. A real seed planting can be performed with the developed planter and study the yield and germination of the seeds and compare the results with available commercial planters. A linkage and connection can be designed in order to attach the planter directly to the carriage of the soil bin. Using this method, all the forces on the whole planter, including vertical and lateral force can be measured. It also gives a longer distance of soil bin for testing.
7) **Vacuum pressure:** More study can be performed on the vacuum pressure for the singulator disc. A proper vacuum system must be used to provide accurate vacuum pressure on the holes of the singulator disc.

References:

1) Beck, D.L., Miller, J.L., Hagny, M.P., 1998, "Successful No-Till on the Central and Northern Plains", ASA Conf., Baltimore, MD.

2) Murray, J.R., Tullberg, J.N., Basnet, B.B., 2006, "Planters and their components: types, attributes, functional requirements, classification and description", ACIAR Monograph No. 121.

3) Updahaya, S.K., Chancellor, W.J., Perumpral, J.V., Wulfson, D., Way, T.R., 2009, "Advances in Soil Dynamics, Volume 3", ASABE

4) Osman, A.N., Xia,L.,Dongxing, Z., 2011, "Effect of tilt angle of disk plough on some soil physical properties, work rate and wheel slippage under light clay soil", Int J Agric & Biol Eng, Vol. 4 No.2

5) Altuntas, E., Ozgoz, E., Taser, O.F., Tekelioglu, O., 2006, "Assessment of different types furrow openers using a full automatic planter", 2006, Asian Journal of Plant Sciences 5(3): 537-542.

6) Alam, M., 1989, "Soil reaction forces on agricultural disc implements", PhD thesis in Agricultural engineering,University of Newcastle.

7) Kushwaha, R.L., Vaishnav, A.S., Zoerb, G.C., 1986, “Soil bin evaluation of disc coulters under no-till crop residue conditions”, ASAE Journal, Vol. 29(1):January-February.

8) Tice, E.M., Hendrick, J.G., 1991, “Disc coulter forces: Evaluation of mathematical models”, ASAE Journal, VOL. 34(6): November-December.

9) Tice, E.M., Hendrick, J.G., 1992, ”Disc coulter operating charactristics”, ASAE Journal, VOL. 35(1): January-February.

10) Hann, M.J., Giessibl, J., 1998, “Force measurements on driven discs”, J. agric. Engng. Res. (1998) 69, 149-157.

11) Afify, M.T., Kushwaha, R.L., Gerein, M.A., 2001, “Effect of combined disc angles on soil forces of coulter discs”, ASAE Meeting Paper No. 01-1059, St. Joseph, Mich.: ASAE.

12) Shirin, A.K.M., Hoki, M., Salokhe, V.M., 1993, “Effects of disc and working parameters on the performance of a disc plough in clay soil”, Agricultural mechanization in Asia, Africa and Latin America, VOL. 24 No.4, 9-12.

13) Fink, J.T., Currence, H.D., 1995, “No-till drill utilizing adjustable seed furrow openers”, Applied Engineering in Agriculture, VOL. 11(6):811-816.

14) Chen, Y., Tessier, S., Irvine, B., 2004, “Drill and crop performances as affected by different drill configurations for no-till seeding”, Soil & Tillage Research 77 (2004) 147–155.

15) Karayel, D., Sarauskis, E., 2011, “Effect of downforce on the performance of no-till disc furrow openers for clay-loam and loamy soils”, Agriculture engineering. Research papers, VOL. 43, no 3, 16-24.

16) Johnston, A.M., Lafond, G.P., May, W.E., Hnatowich, G.L., Hultgreen, G.E., 2003, “Opener, Packer wheel and packing force effects on crop emergence and yield of direct seeded wheat, canola and field peas”, Canadian Journal of plant science. 83:129-139.

17) Cochran, B.J., Porterfield, J.G., Batchelder, D.G., 1974, “Vertical forces on furrow openers and depth control devices”, ASAE paper no. 72-609.

18) Gratton, J., Chen, Y., Tessier, S., 2003, “Design of a spring-loaded downforce system for a no-till seed opener”, Canadian biosystems Engineering, Volume 45:2.29-2.35.

19) El-Shazly, M.A., Morad, M.M., Ali, M.M., Wasfy, K.I., 2008, “Optimization of disc plow performance under Egyptian condition”, Misr J. Ag. Eng., 25(1): 15-37.

20) Reid, J.T., 1978, “A comparison of the energy input of some tillage tools”, ASAE paper No. 78-1039, ASAE St. Joseph, MI 49085.

21) Budynas, R.G., Nisbett, J.K., 2008, “Shigley’s Mechanical Engineering Design”, Eighth Edition, McGraw-Hill.

22) Case IH, “1200 Rigid Trailing Planter”, Operator’s manual, CNH America LLC.

23) Wong, J.Y., 1978, “Theory of ground vehicles”, John Wiley and Sons.

24) Zienkiewicz, O.C., Taylor, R.L., Zhu, J.Z., 2005, “Finite Element Method- Its Basis and Fundamentals”, 6th Edition, Elsevier.

25) Papworth, L., 2006, “Power Requirments for Air Seeders”, Alberta farm machinery research center, Lethbridge, Alberta

26) Bankole, A., Critical State Behaviour Of An Agricultural Soil. Doctoral Thesis at the University of Saskatchewan, Saskatoon, Canada, 1996.

APPENDIX A- Pictures of Developed Planter

In following come pictures of the developed planter.

Figure A- 1- Side view of the developed planter

Figure A- 2- Disc coulter, Gauge wheel, Disc holder and depth control link

Figure A- 3- Power transmission from the press wheel to the singulator disc

Figure A- 4- Horizontal, Vertical pull bars and hand wrench used for lifting the planter

APPENDIX B- Stress Analysis of the Disc Holder with Different Mesh Sizes

As discussed in chapter 4, the maximum stress show in the FEM model may not be valid for most of the cases when there is geometric singularity or concentrated load, or point support. Decreasing the mesh size in the singular area, will increase the maximum stress. But the real maximum stress can be read from two or three elements away from the singular point and the real maximum stress remains almost the same for all the mesh sizes. To check for this, different stress analyses using different mesh sizes were performed on all the parts for the developed planter. The analyses performed for disc holder are presented here for comparison. For all of these meshing methods, an element size was set for the whole body. Besides, mesh refinement was performed around the point that stress concentration happens, utilizing sphere of influence. ANSYS Workbench refines the size of the elements inside the specified circle to the specified size. (Figure B-1)

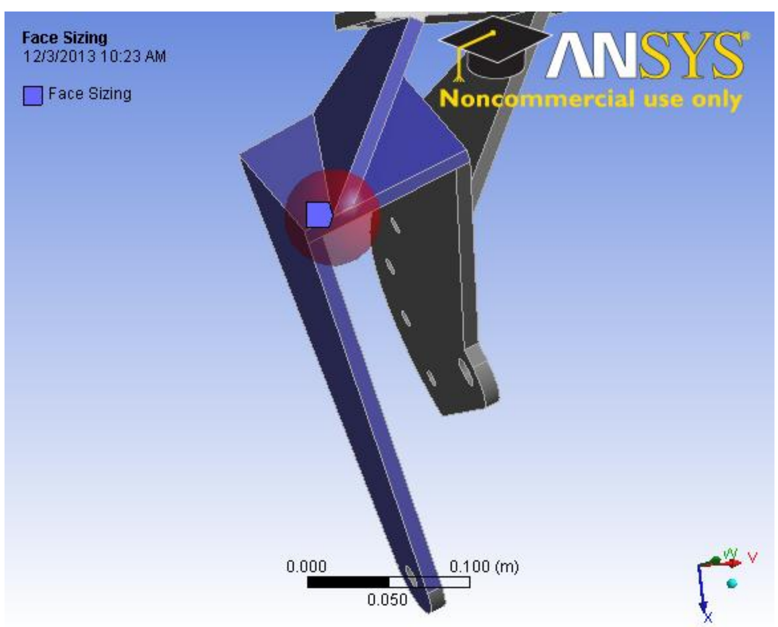

Figure B- 1- Sphere of influence tool in ANSYS Workbench for mesh refinement

Table A-1 lists different mesh sizes and total number of nodes that were used for different analyzes. The Maximum real stress also is shown in this table for comparison. Figures A-2, A-3, A-4, A-5 and A-6 show the corresponding mesh formation shapes and stress contours for the mesh sizes depicted in table A-1.

The license available for the software did not allow going over 32000 nodes for the model. It can be observed from table A-1 and the figures that the real maximum stress remains almost the same for all different meshing methods.

Table B- 1-Number of nodes, element sizes and maximum real stress for different stress analyzes of disc holder with different mesh sizes

	Corresponding Figures	Num. of total nodes	Body element size (mm)	Element size inside of the sphere (mm)	Radius of the sphere of influence (mm)	Maximum real stress (MPa)
1	A-2	29053	7.5	-	-	173
2	A-3	31561	15	3	50	181
3	A-4	28758	15	2	30	183
4	A-5	29053	25	1.5	25	183
5	A-6	29059	30	1	17	182

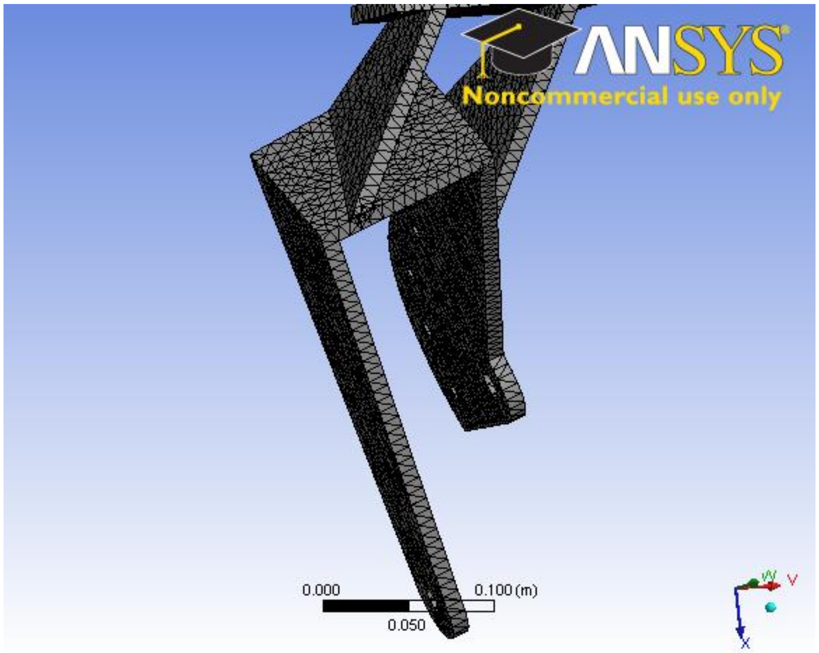

(a)

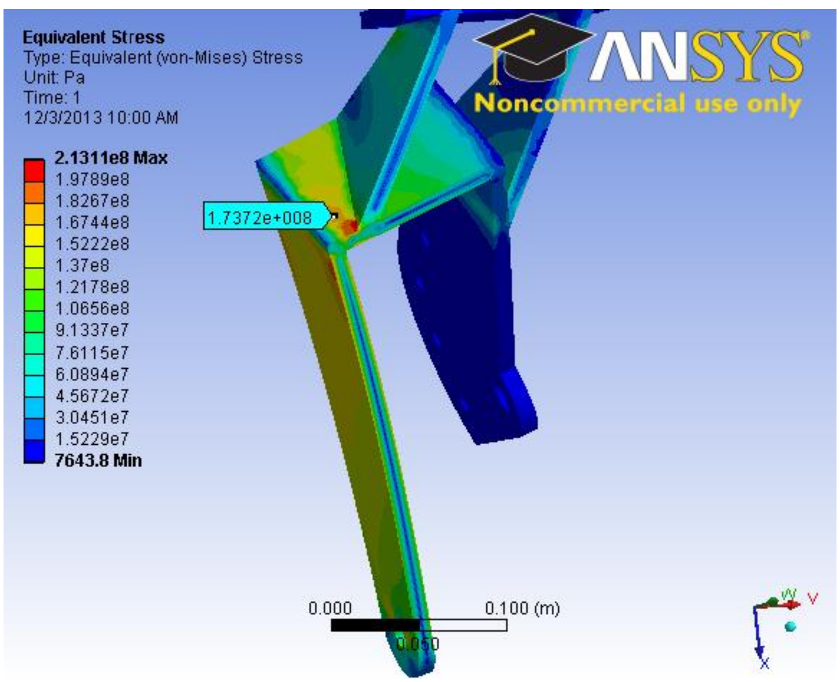

(b)

Figure B- 2- Analysis 1, a) Meshing, b) Stress contour

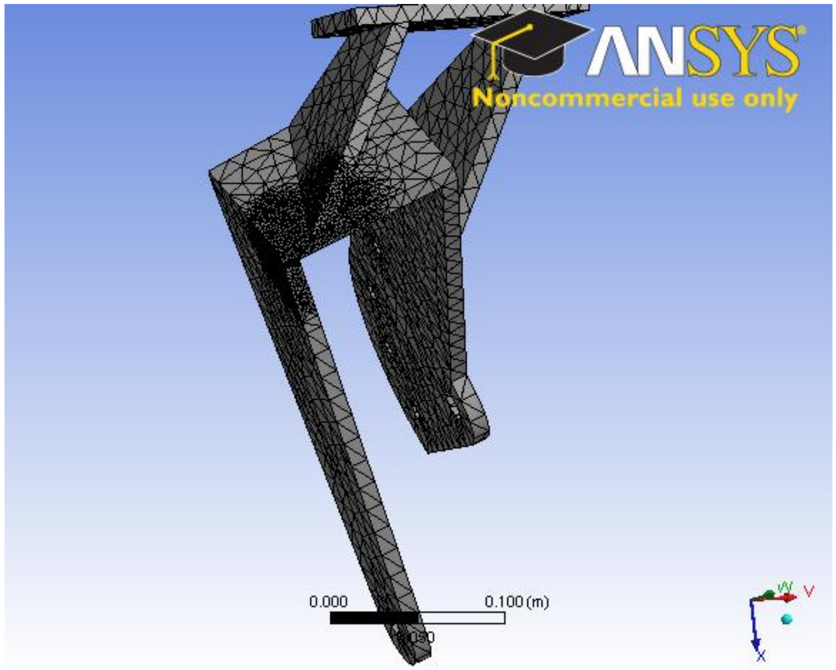

(a)

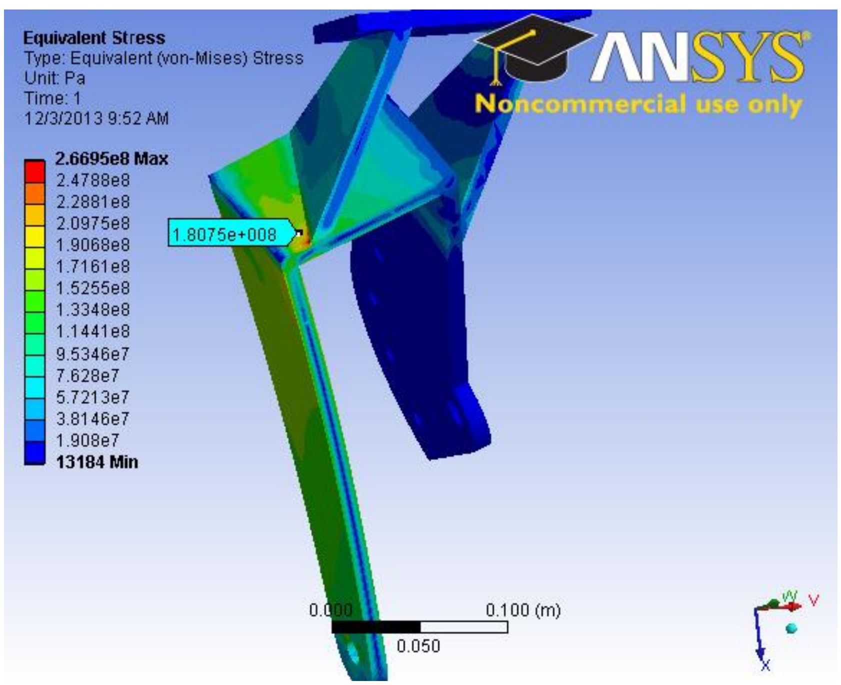

(b)

Figure B- 3- Analysis 2, a) Meshing, b) Stress contour

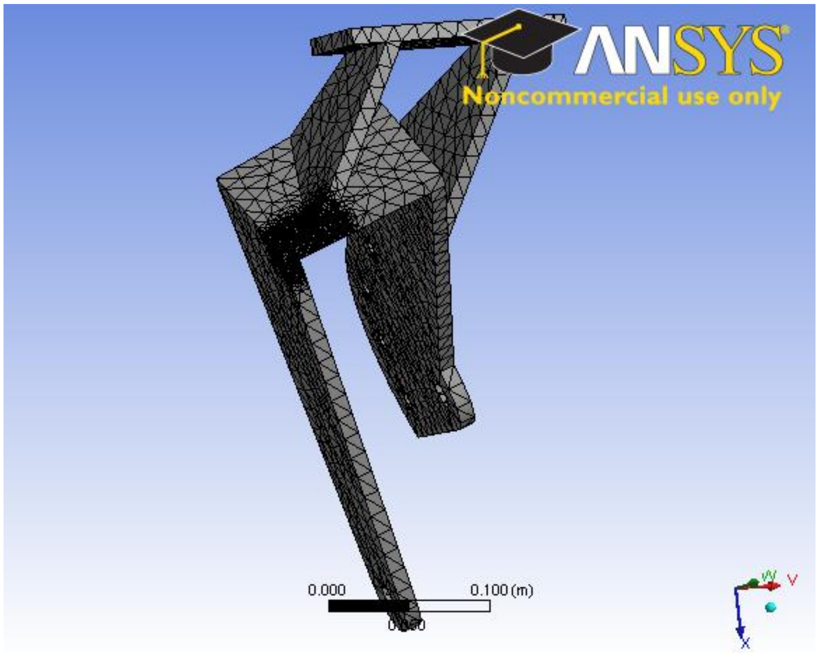

(a)

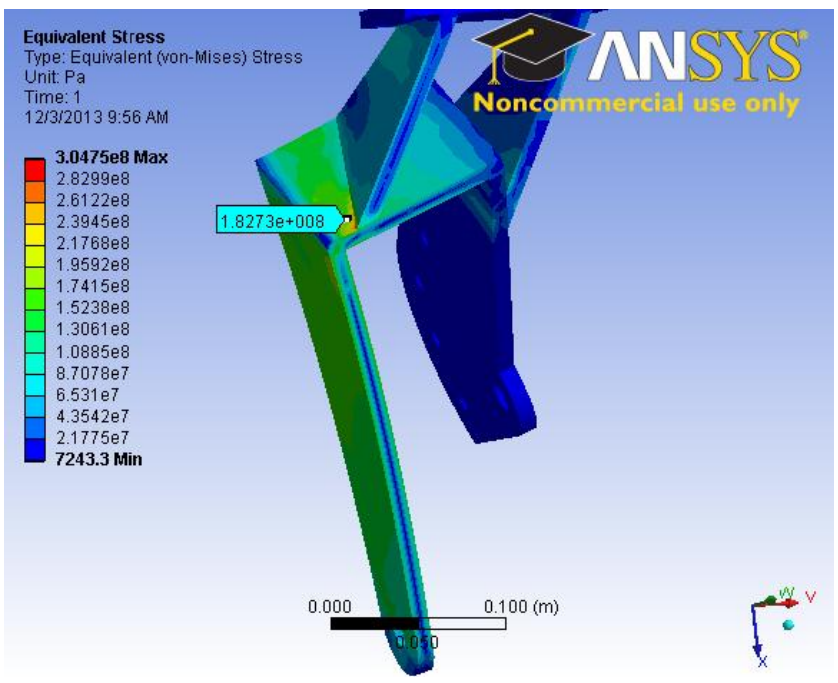

(b)

Figure B- 4- Analysis 3, a) Meshing, b) Stress contour

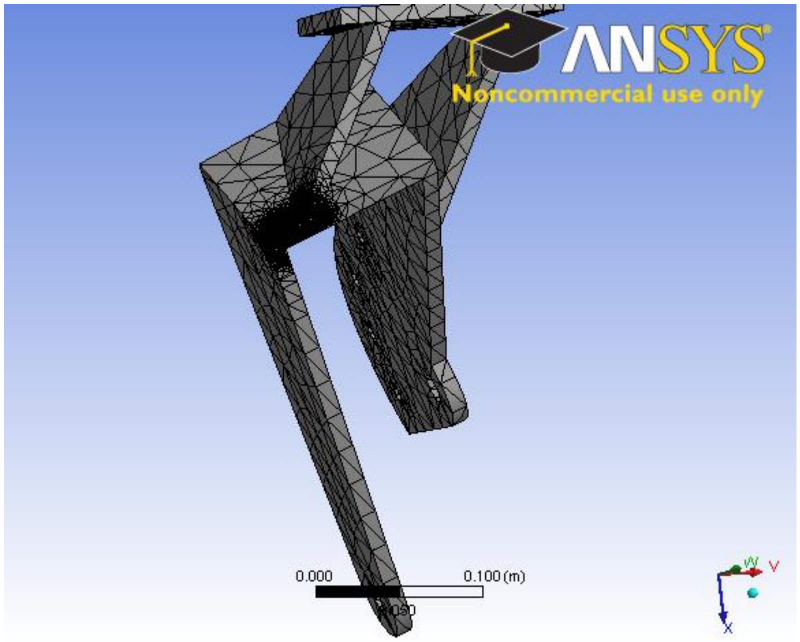

(a)

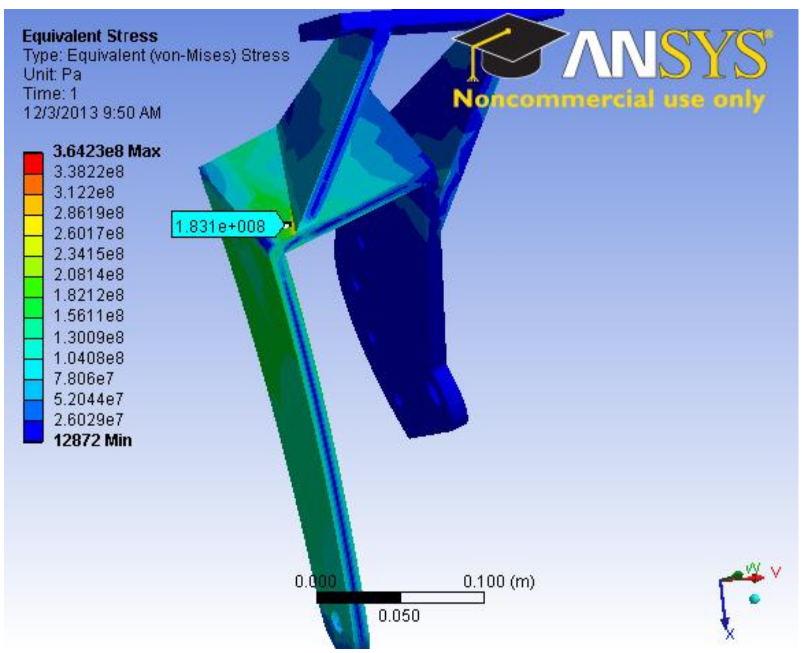

(b)

Figure B- 5- Analysis 4, a) Meshing, b) Stress contour

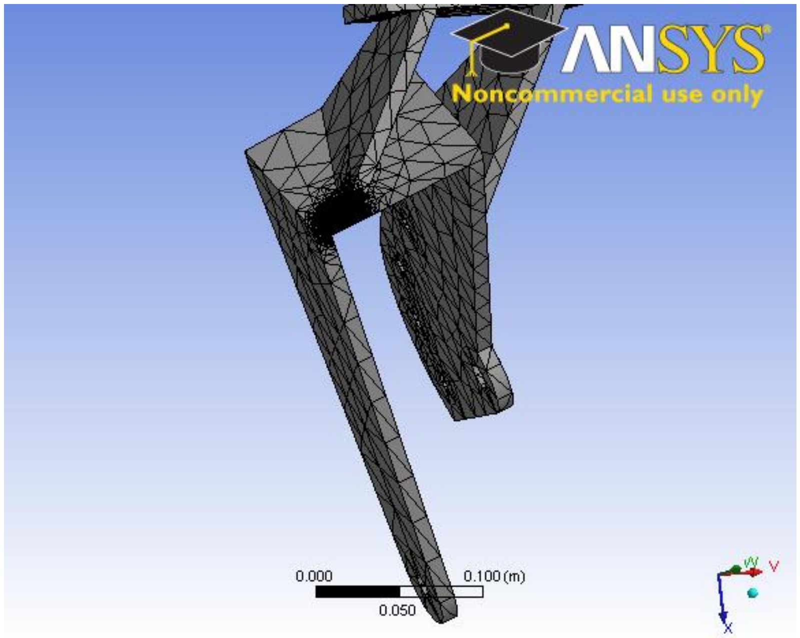

(a)

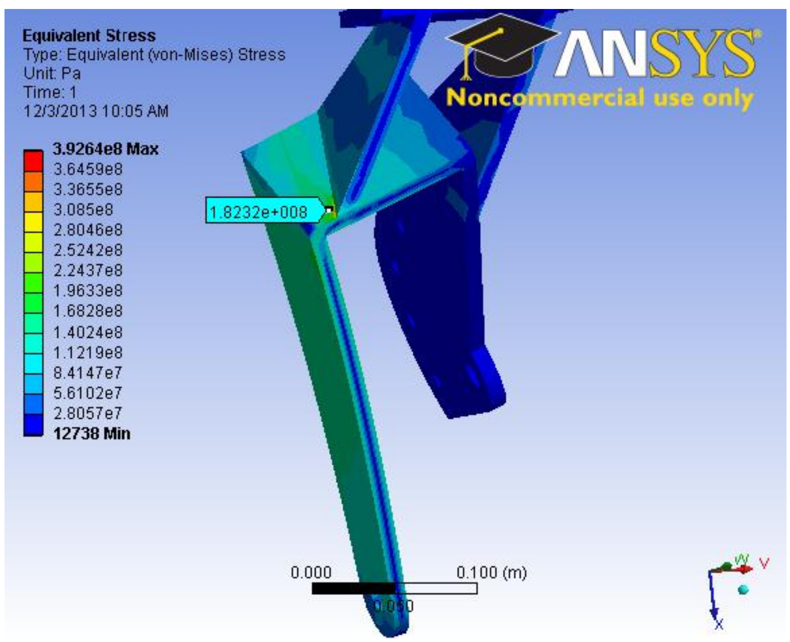

(b)

Figure B- 6- Analysis 5, a) Meshing, b) Stress contour

APPENDIX C- Matlab Code and Simulink Model for Low Pass Filter

A simple Matlab Code was used to import the raw data into Matlab from an Excel file. The imported data is saved as vectors and is used as the input of the Simulink model. The Simulink model applies a simple low pass filter on the raw data and saves the results in a new vector and plots it as output of the filter.

- Matlab Code:

```
clear all
%Read the Excel file
p=xlsread('ExcelFile name');
%copy the time values and force values into separate vector matrices
tt=p(:,6);
FF=-p(:,7);
```

- Simulink Model

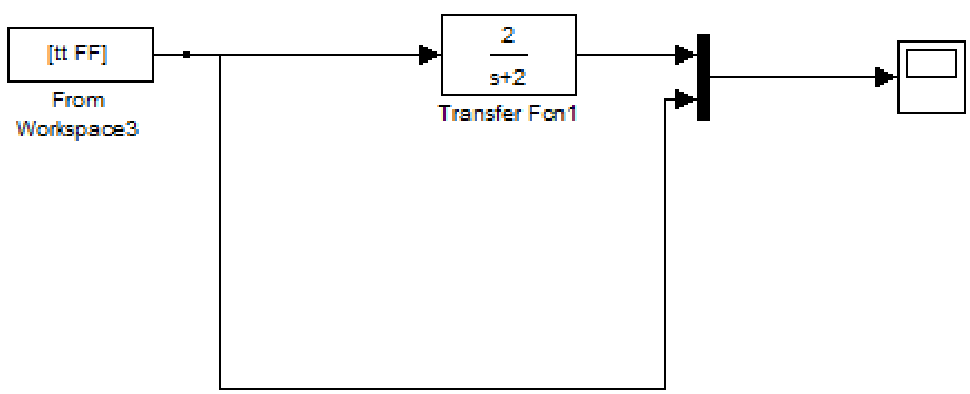

Figure C- 1-Simulink model for low pass filter with cut off frequency of 2 Hz

Appendix D- Comparison and Validation of the Experimental Soil Bin Results with Analytical Analysis

A mathematical model, using static equilibrium, is developed by Yun Zhang, to find draft, side and vertical forces on a plough disc. The force results obtained from the soil bin experiments in chapter 2 for 7º disc angle and 25º tilt angle are compared and validated by this analytical analysis.

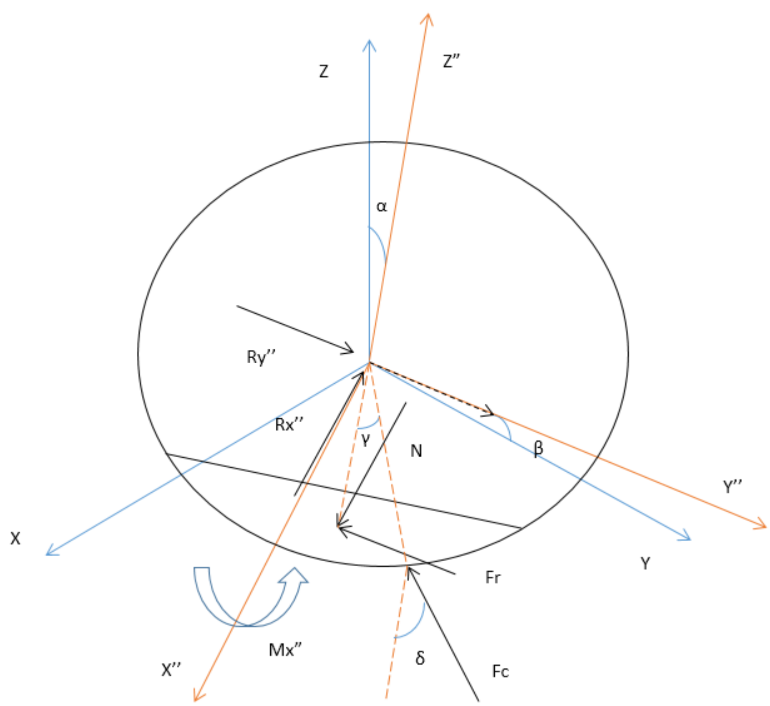

Figure D- 1- Disc plough and the external forces

Figure D-1 shows a disc plough with its local coordinate system (e.g. attached and parallel to the disc), and global coordinate system (e.g. parallel to the direction of motion). The developed analytical model, relates forces applied to the disc plough in its local coordinate system, to the draft, side and vertical forces in the global coordinate system. In Figure D-1, β is the disc angle and α is the tilt angle. Using the static equilibrium equations and transform matrices, it can be written that,

$$\begin{bmatrix} F_x \\ F_y \\ F_z \end{bmatrix} = \begin{bmatrix} Ncos\alpha(cos\beta) - cos\beta(sin\alpha)\left[F_c sind + F_c \dfrac{\rho \sin(\gamma - \delta)}{r_c}\right] + F_c cos\delta(sin\alpha) \\ Nsin\beta + cos\beta\left[F_c sind + F_c \dfrac{\rho \sin(\gamma - \delta)}{r_c}\right] \\ Ncos\beta(sin\alpha) - sin\alpha(sin\beta)\left[F_c sind + F_c \dfrac{\rho \sin(\gamma - \delta)}{r_c}\right] - F_c cos\delta(sin\alpha) \end{bmatrix} \quad (Eq.D - 1)$$

The calculation of F_x, F_y and F_z are based on assumption of F_c (cutting force), N (normal force) and ɣ, δ (F_c angles). Assuming F_c= 457N, N=641N and δ=18º, ɣ=6º, the side force (F_x), draft force (F_y), and vertical force (F_z) can be calculated as,

$$\begin{bmatrix} F_x \\ F_y \\ F_z \end{bmatrix} = \begin{bmatrix} 752N \\ 98N \\ 84N \end{bmatrix}$$

Table D-1 compares the results from the soil bin experiments and analytical calculations.

Table D- 1- Experimental and analytical comparison for forces on disc plough for 7º disc angle and 25º tilt angle

Forces	Analytical (N)	Experimental (N)
Side force (F_x)	752	760
Draft force (F_y)	98	97
Vertical force (F_z)	84	84

Friction force, F_r, can be calculated from two different equations.

$$F_r = \frac{1}{r_c} F_c \rho sin(\delta - \gamma) \qquad (Eq.D - 2)$$

$$F_r = \mu N \qquad (Eq. D-3)$$

Eq. D-2 is derived from the moment equation written in x'' direction. Equation D-3 is the coulomb friction law. To validate the experimental results and to show that the assumptions are valid, F_r can be calculated using Eq. D-2. Then using Eq. D-3, the coefficient of friction can be calculated. If μ obtained from the equation is close to and comparable with coefficient of friction between soil and steel that can be found in literature, the analytical work and also the experimental results are validated.

Thus, using equation D-2 and knowing that F_c= 457N, r_c= 0.18m and the radius of the disc, ρ= 0.23m, then,

$$F_r = 121.4\ N$$

and,

$$\mu = 0.19$$

The coefficient of friction between steel sheet and fine sandy silt (non plastic silt) soil is 0.2[2]. This shows that the assumptions are correct and the experimental results for 7º disc angle and 25º tilt angle are validated.

---

[2] Website of the Fine Civil Engineering Software, http://www.finesoftware.eu/geotechnical-software/help/sheeting-design/table-of-ultimate-friction-factors-for-dissimilar-materials/

APPENDIX E- Detailed Drawings of the Designed Parts

In following come the detailed drawings that were sent to machine shop for fabrication.

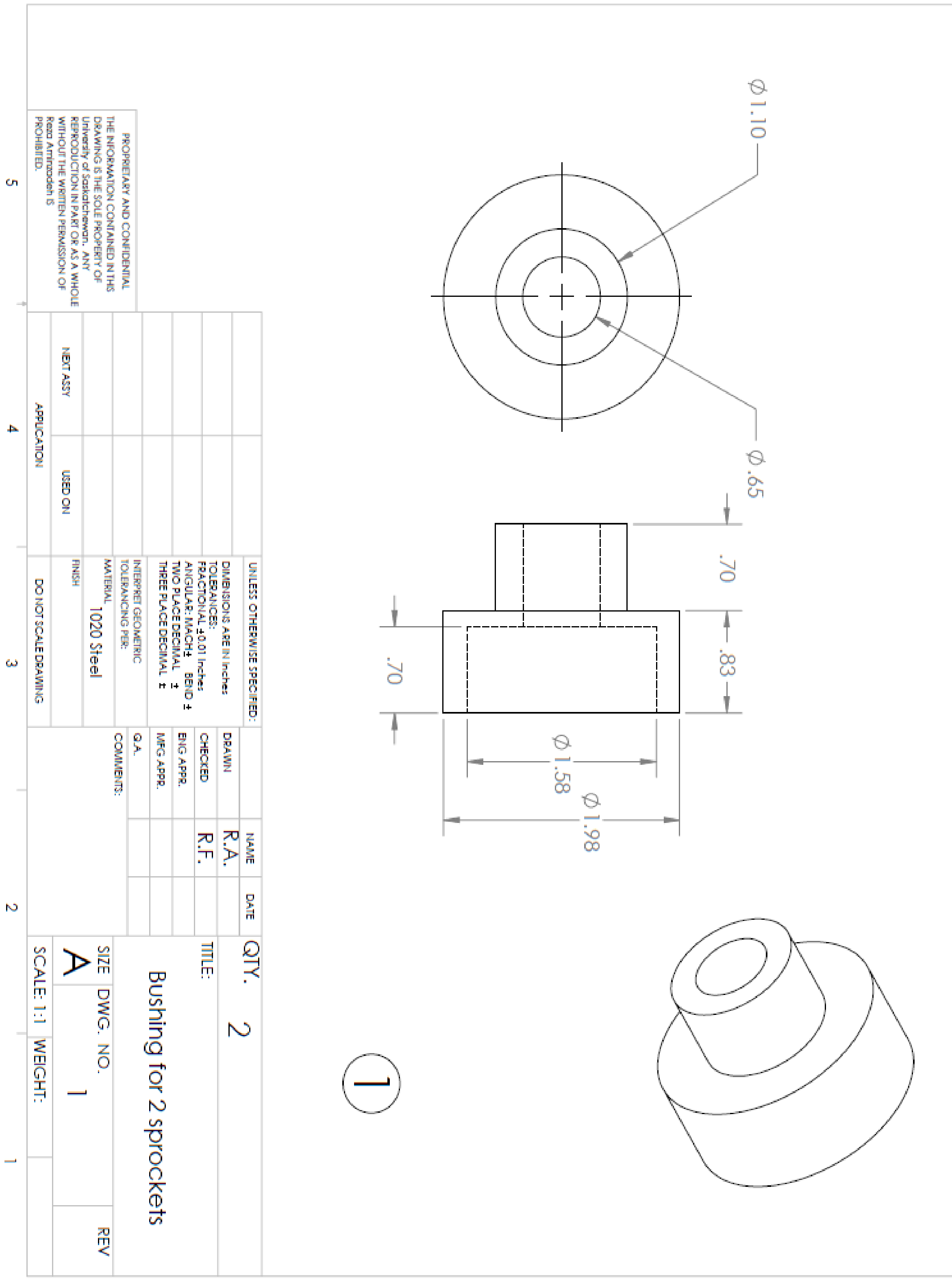

Ø1.10
Ø.65
.70
.83
.70
Ø1.58
Ø1.98
1
UNLESS OTHERWISE SPECIFIED:
DIMENSIONS ARE IN inches
TOLERANCES:
FRACTIONAL ±0.01 inches
ANGULAR: MACH± BEND ±
TWO PLACE DECIMAL ±
THREE PLACE DECIMAL ±
INTERPRET GEOMETRIC TOLERANCING PER:
MATERIAL
1020 Steel
FINISH
DO NOT SCALE DRAWING
NAME
DATE
DRAWN
R.A.
CHECKED
R.F.
ENG APPR.
MFG APPR.
Q.A.
COMMENTS:
QTY.
2
TITLE:
Bushing for 2 sprockets
SIZE
A
DWG. NO.
1
REV
SCALE: 1:1
WEIGHT:
NEXT ASSY
USED ON
APPLICATION
PROPRIETARY AND CONFIDENTIAL
THE INFORMATION CONTAINED IN THIS DRAWING IS THE SOLE PROPERTY OF University of Saskatchewan. ANY REPRODUCTION IN PART OR AS A WHOLE WITHOUT THE WRITTEN PERMISSION OF Reza Aminzadeh IS PROHIBITED.

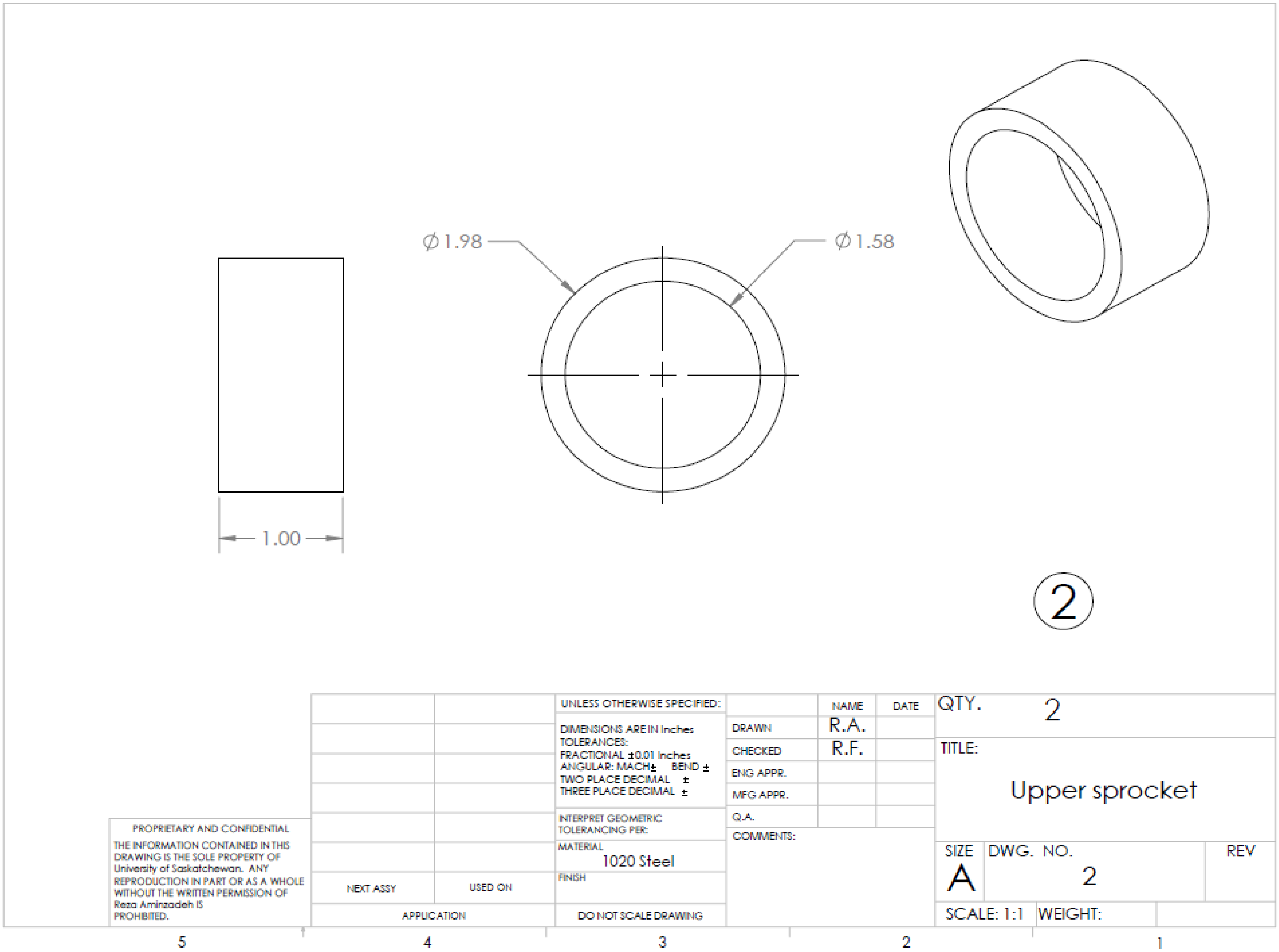
Ø1.98
Ø1.58
1.00
2
PROPRIETARY AND CONFIDENTIAL
THE INFORMATION CONTAINED IN THIS DRAWING IS THE SOLE PROPERTY OF University of Saskatchewan. ANY REPRODUCTION IN PART OR AS A WHOLE WITHOUT THE WRITTEN PERMISSION OF Reza Aminzadeh IS PROHIBITED.
NEXT ASSY
USED ON
APPLICATION
UNLESS OTHERWISE SPECIFIED:
DIMENSIONS ARE IN Inches
TOLERANCES:
FRACTIONAL ±0.01 Inches
ANGULAR: MACH± BEND ±
TWO PLACE DECIMAL ±
THREE PLACE DECIMAL ±
INTERPRET GEOMETRIC TOLERANCING PER:
MATERIAL
1020 Steel
FINISH
DO NOT SCALE DRAWING
NAME
DATE
DRAWN
R.A.
CHECKED
R.F.
ENG APPR.
MFG APPR.
Q.A.
COMMENTS:
QTY.
2
TITLE:
Upper sprocket
SIZE
A
DWG. NO.
2
REV
SCALE: 1:1
WEIGHT:
5
4
3
2
1

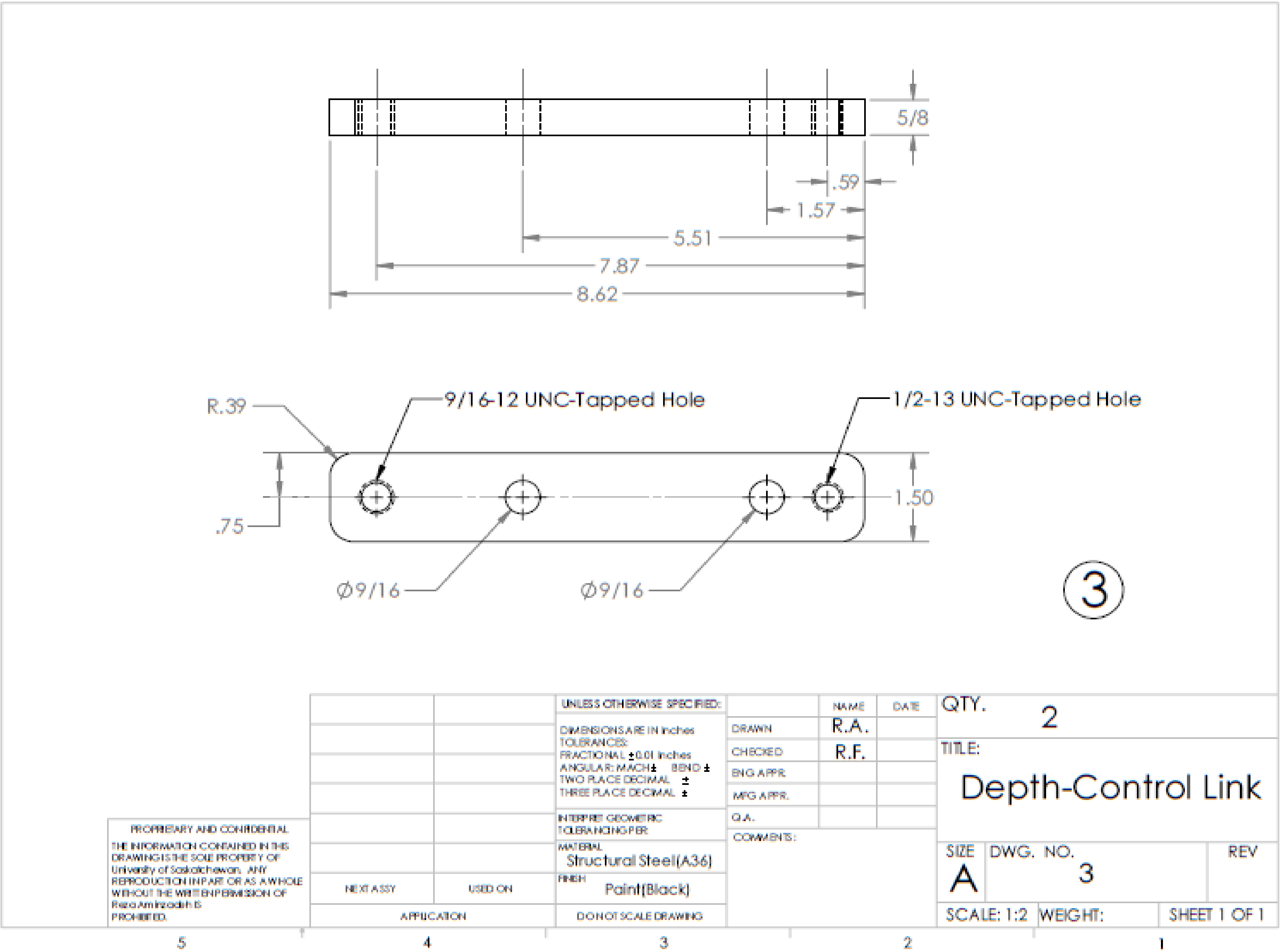
5/8
.59
1.57
5.51
7.87
8.62
R.39
9/16-12 UNC-Tapped Hole
1/2-13 UNC-Tapped Hole
.75
1.50
Ø9/16
Ø9/16
3
PROPRIETARY AND CONFIDENTIAL
THE INFORMATION CONTAINED IN THIS DRAWING IS THE SOLE PROPERTY OF University of Saskatchewan. ANY REPRODUCTION IN PART OR AS A WHOLE WITHOUT THE WRITTEN PERMISSION OF Reza Aminzadeh IS PROHIBITED.
NEXT ASSY
USED ON
APPLICATION
UNLESS OTHERWISE SPECIFIED:
DIMENSIONS ARE IN inches
TOLERANCES:
FRACTIONAL ±0.01 inches
ANGULAR: MACH ± BEND ±
TWO PLACE DECIMAL ±
THREE PLACE DECIMAL ±
INTERPRET GEOMETRIC TOLERANCING PER:
MATERIAL
Structural Steel(A36)
FINISH
Paint(Black)
DO NOT SCALE DRAWING
NAME
DATE
DRAWN
R.A.
CHECKED
R.F.
ENG APPR.
MFG APPR.
Q.A.
COMMENTS:
QTY.
2
TITLE:
Depth-Control Link
SIZE
A
DWG. NO.
3
REV
SCALE: 1:2
WEIGHT:
SHEET 1 OF 1
5
4
3
2
1

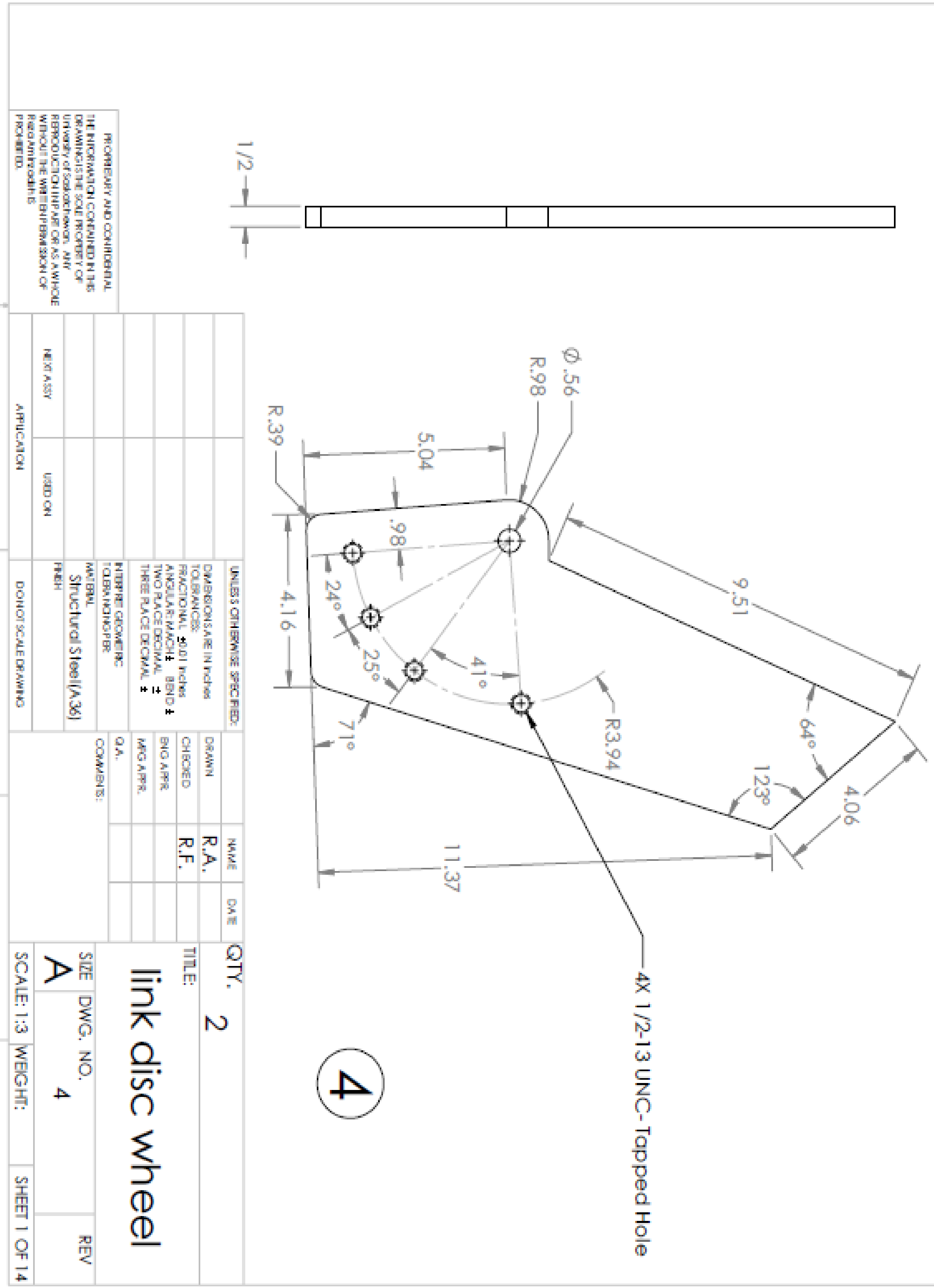

1/2
Ø.56
R.98
R.39
5.04
.98
4.16
24°
25°
41°
71°
R3.94
9.51
64°
123°
4.06
11.37
4X 1/2-13 UNC-Tapped Hole
4
UNLESS OTHERWISE SPECIFIED:
NAME
DATE
DRAWN
R.A.
CHECKED
R.F.
ENG APPR.
MFG APPR.
Q.A.
COMMENTS:
MATERIAL
Structural Steel (A36)
FINISH
NEXT ASSY
USED ON
APPLICATION
DO NOT SCALE DRAWING
QTY.
2
TITLE:
link disc wheel
SIZE
A
DWG. NO.
4
REV
SCALE: 1:3
WEIGHT:
SHEET 1 OF 14
PROPRIETARY AND CONFIDENTIAL

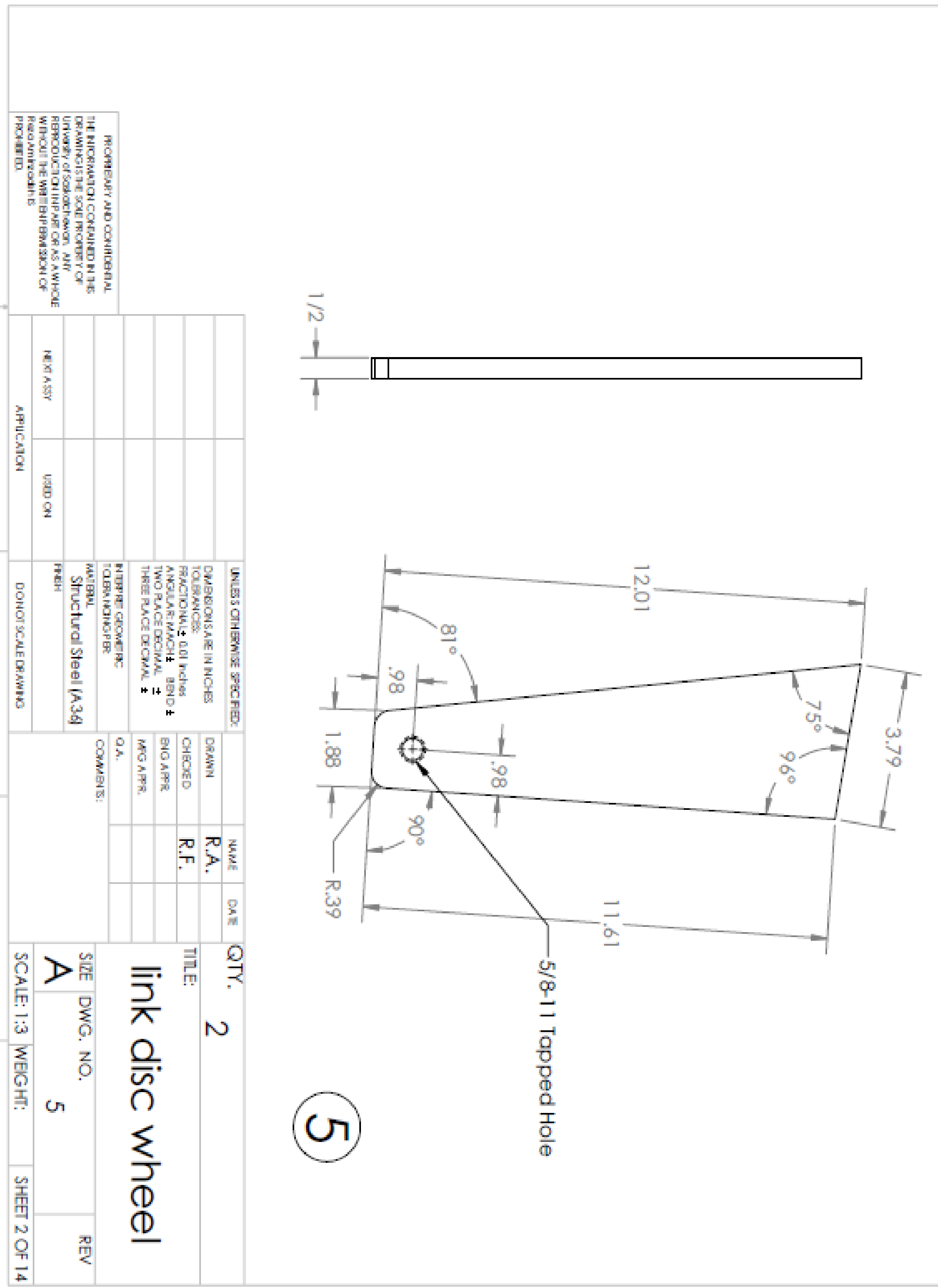

1/2
12.01
81°
.98
1.88
.98
75°
96°
3.79
90°
R.39
11.61
5/8-11 Tapped Hole
5
UNLESS OTHERWISE SPECIFIED:
DIMENSIONS ARE IN INCHES
TOLERANCES:
FRACTIONAL ± 0.01 inches
ANGULAR: MACH ± BEND ±
TWO PLACE DECIMAL ±
THREE PLACE DECIMAL ±
INTERPRET GEOMETRIC TOLERANCING PER:
MATERIAL
Structural Steel (A36)
FINISH
DO NOT SCALE DRAWING
NEXT ASSY
USED ON
APPLICATION
DRAWN
CHECKED
ENG APPR.
MFG APPR.
Q.A.
COMMENTS:
NAME
DATE
R.A.
R.F.
QTY.
2
TITLE:
link disc wheel
SIZE
A
DWG. NO.
5
REV
SCALE: 1:3
WEIGHT:
SHEET 2 OF 14
PROPRIETARY AND CONFIDENTIAL

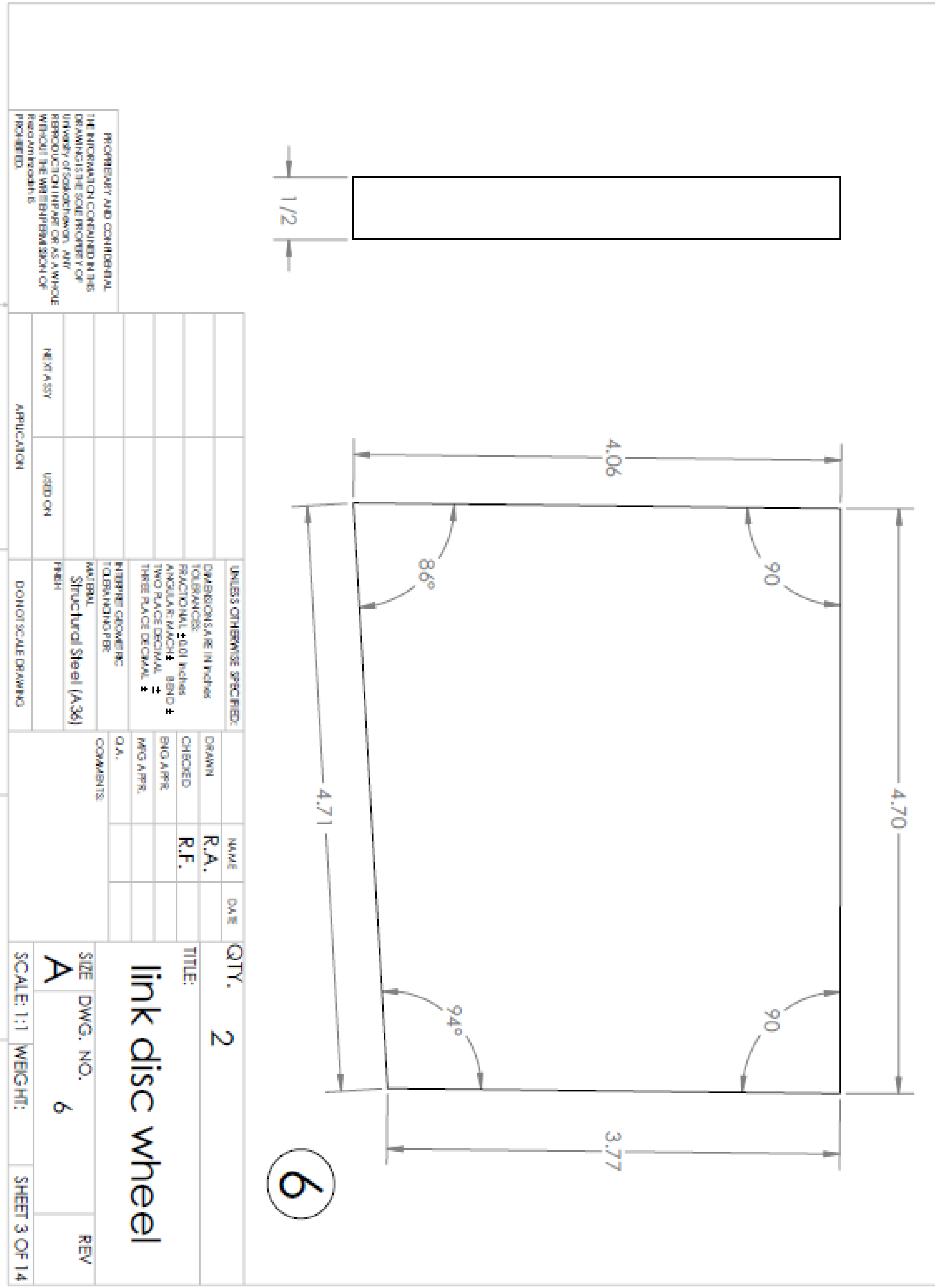

1/2
4.06
4.71
4.70
3.77
86°
90
94°
90
6
UNLESS OTHERWISE SPECIFIED:
MATERIAL
Structural Steel (A36)
DO NOT SCALE DRAWING
APPLICATION
NEXT ASSY
USED ON
DRAWN
CHECKED
ENG APPR.
MFG APPR.
Q.A.
COMMENTS:
NAME
DATE
R.A.
R.F.
QTY.
2
TITLE:
link disc wheel
SIZE
A
DWG. NO.
6
REV
SCALE: 1:1
WEIGHT:
SHEET 3 OF 14

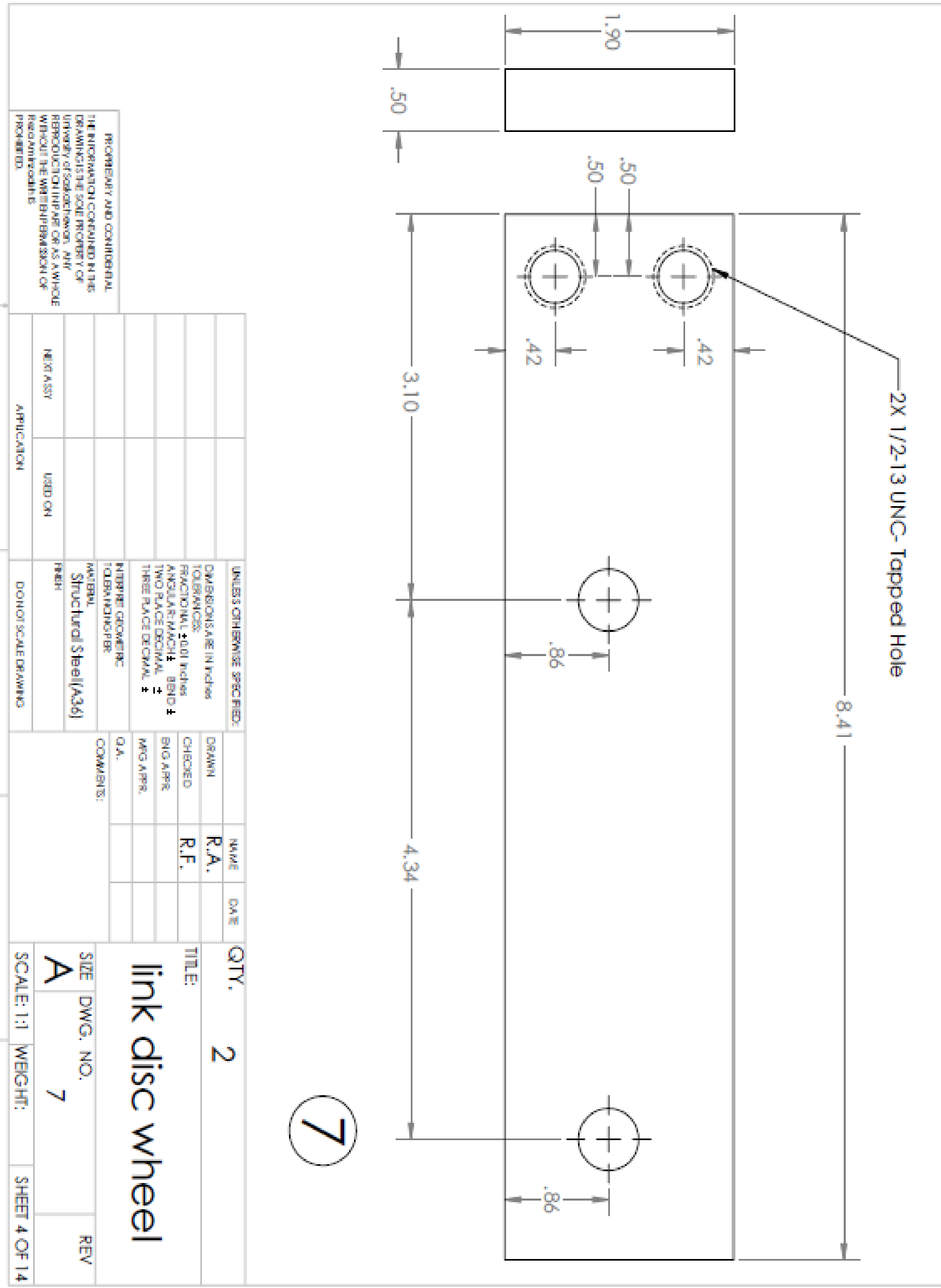
1.90
.50
.50
.50
.42
.42
2X 1/2-13 UNC- Tapped Hole
3.10
8.41
.86
4.34
.86
7
PROPRIETARY AND CONFIDENTIAL
UNLESS OTHERWISE SPECIFIED:
DIMENSIONS ARE IN inches
TOLERANCES:
FRACTIONAL ±0.01 inches
ANGULAR: MACH ± BEND ±
TWO PLACE DECIMAL ±
THREE PLACE DECIMAL ±
INTERPRET GEOMETRIC TOLERANCING PER:
MATERIAL
Structural Steel(A36)
FINISH
NEXT ASSY
USED ON
APPLICATION
DO NOT SCALE DRAWING
NAME
DATE
DRAWN
R.A.
CHECKED
R.F.
ENG APPR.
MFG APPR.
Q.A.
COMMENTS:
QTY.
2
TITLE:
link disc wheel
SIZE
A
DWG. NO.
7
REV
SCALE: 1:1
WEIGHT:
SHEET 4 OF 14

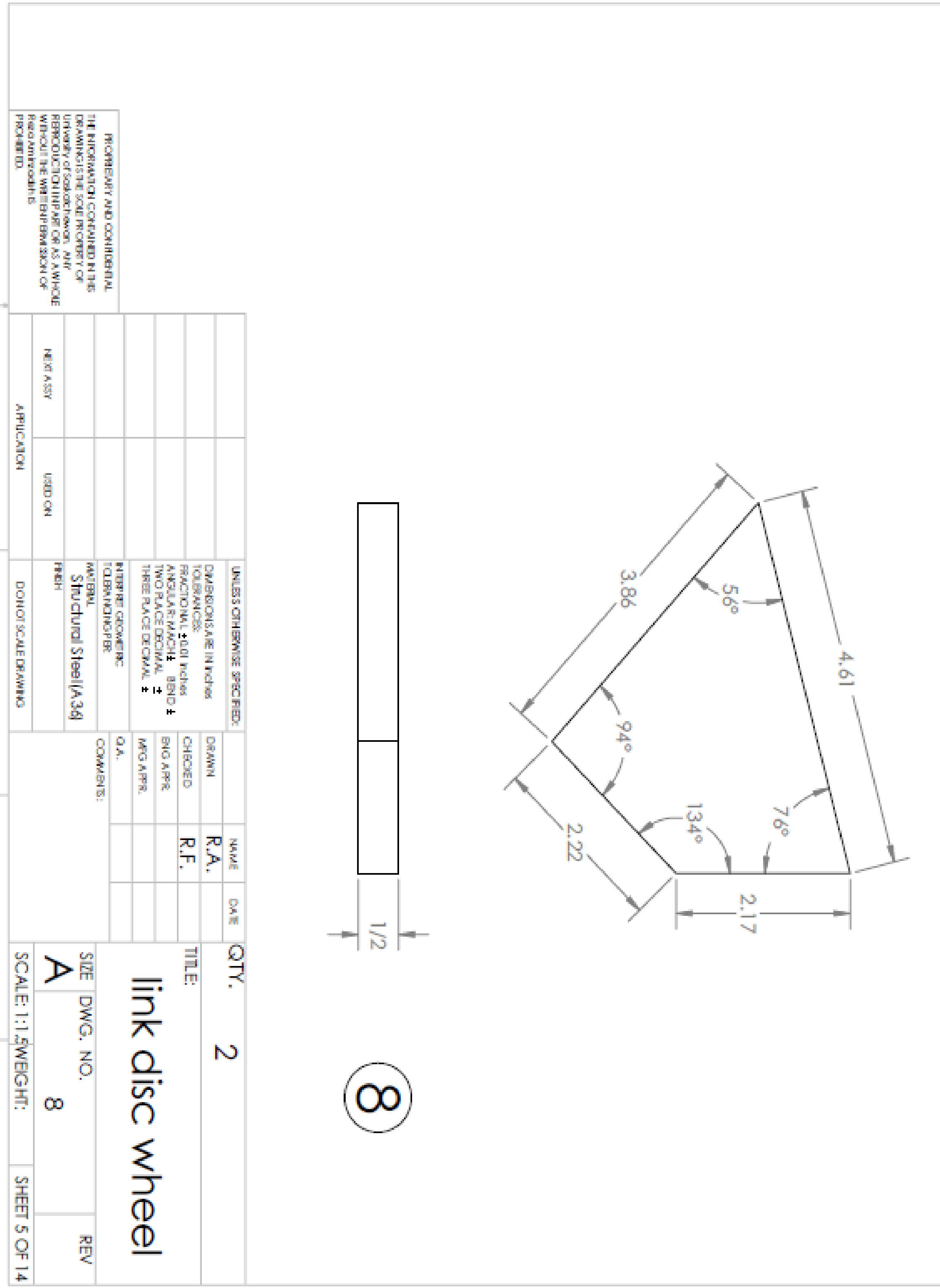
3.86
4.61
2.22
2.17
1/2
56°
94°
134°
76°
8
PROPRIETARY AND CONFIDENTIAL
UNLESS OTHERWISE SPECIFIED:
DIMENSIONS ARE IN inches
MATERIAL
Structural Steel (A36)
FINISH
DO NOT SCALE DRAWING
NEXT ASSY
USED ON
APPLICATION
NAME
DATE
DRAWN
R.A.
CHECKED
R.F.
ENG APPR.
MFG APPR.
Q.A.
COMMENTS:
QTY. 2
TITLE:
link disc wheel
SIZE
A
DWG. NO.
8
REV
SCALE: 1:1.5
WEIGHT:
SHEET 5 OF 14

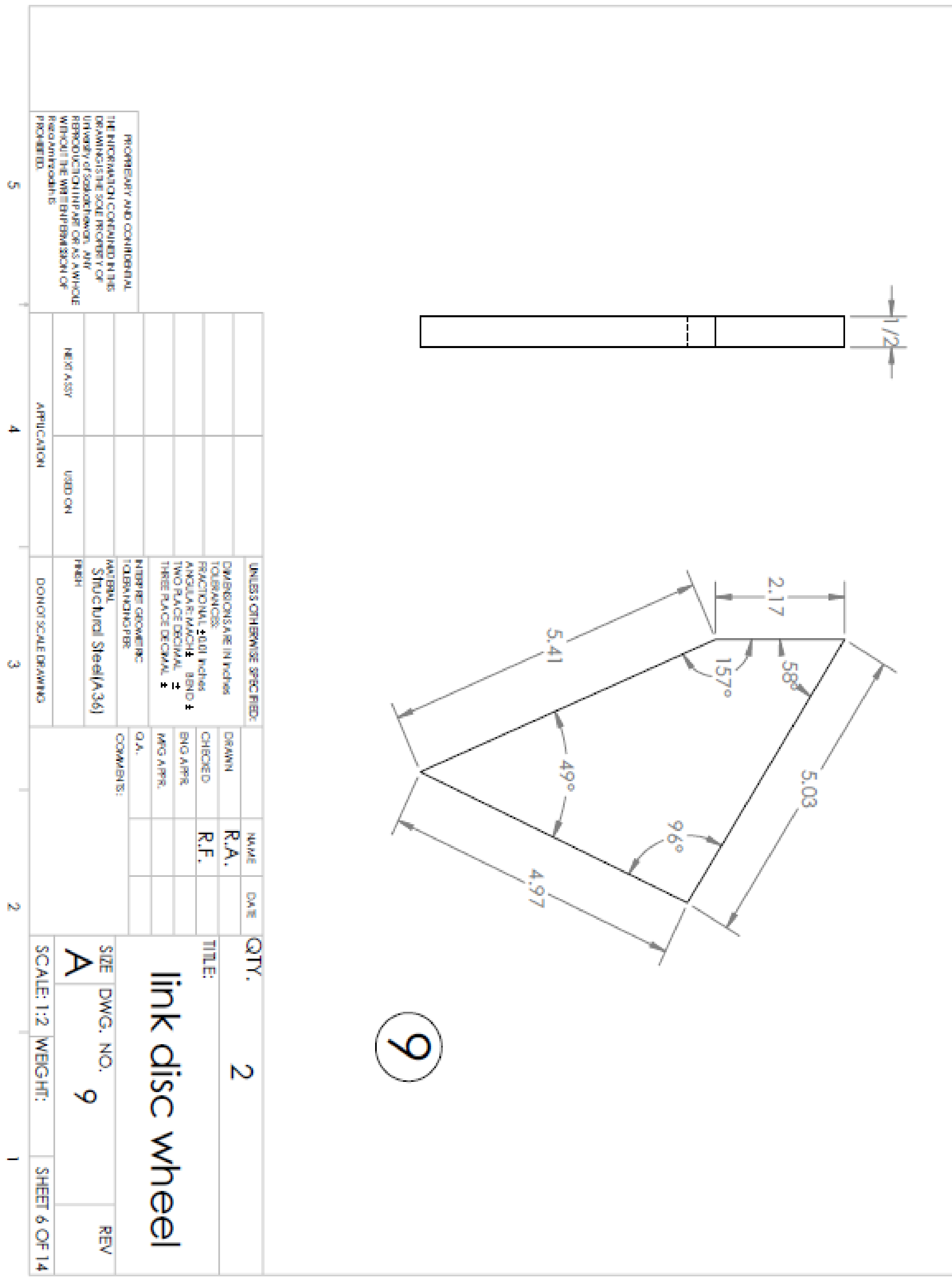
1/2
2.17
5.41
157°
58°
49°
96°
5.03
4.97
9
UNLESS OTHERWISE SPECIFIED:
DIMENSIONS ARE IN inches
TOLERANCES:
FRACTIONAL ±0.01 inches
ANGULAR: MACH ± BEND ±
TWO PLACE DECIMAL ±
THREE PLACE DECIMAL ±
INTERPRET GEOMETRIC TOLERANCING PER:
MATERIAL
Structural Steel(A36)
FINISH
DO NOT SCALE DRAWING
NEXT ASSY
USED ON
APPLICATION
PROPRIETARY AND CONFIDENTIAL
NAME
DATE
DRAWN
R.A.
CHECKED
R.F.
ENG APPR.
MFG APPR.
Q.A.
COMMENTS:
QTY.
2
TITLE:
link disc wheel
SIZE
A
DWG. NO.
9
REV
SCALE: 1:2
WEIGHT:
SHEET 6 OF 14

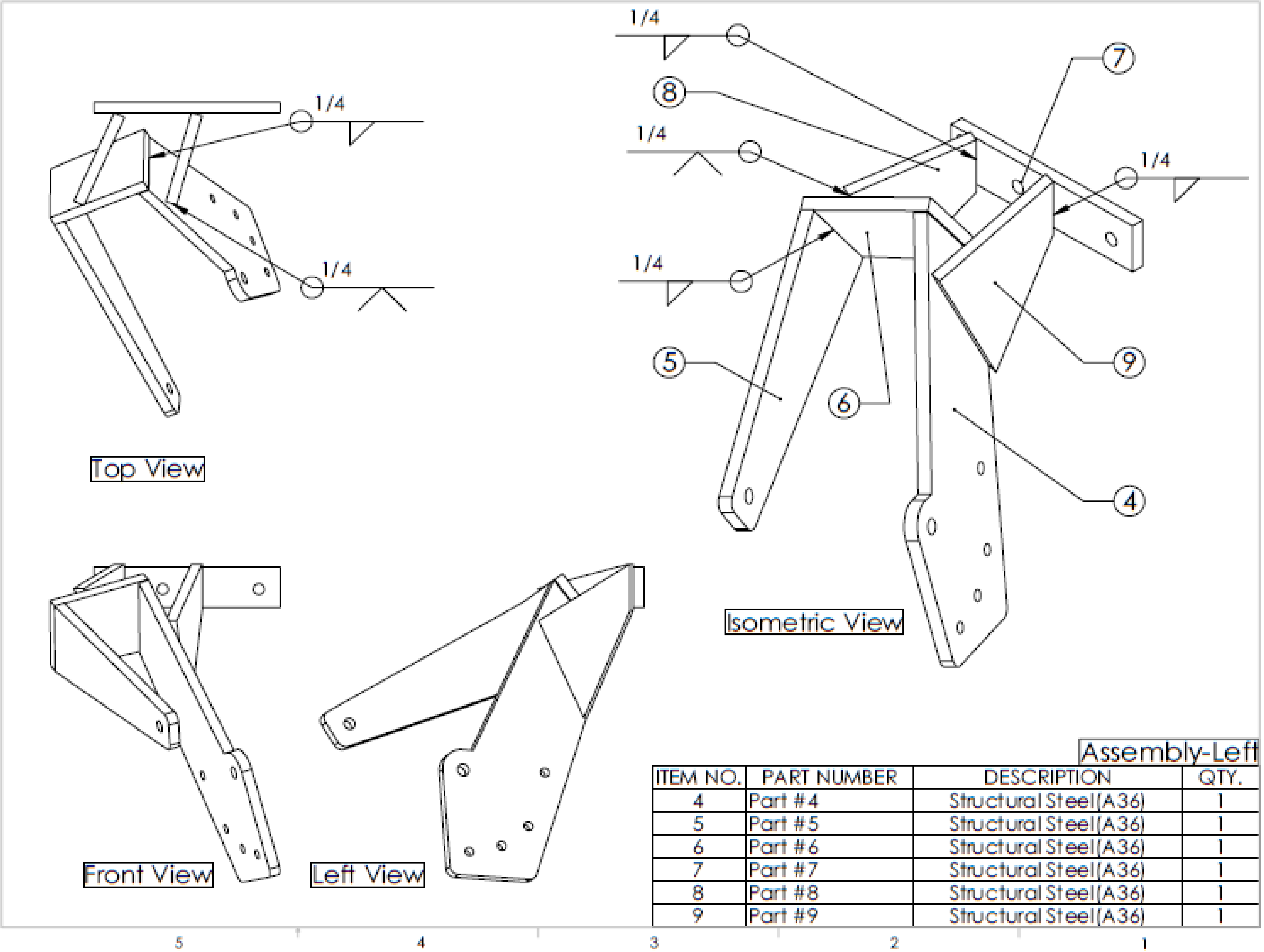

Assembly-Left

ITEM NO.	PART NUMBER	DESCRIPTION	QTY.
4	Part #4	Structural Steel(A36)	1
5	Part #5	Structural Steel(A36)	1
6	Part #6	Structural Steel(A36)	1
7	Part #7	Structural Steel(A36)	1
8	Part #8	Structural Steel(A36)	1
9	Part #9	Structural Steel(A36)	1

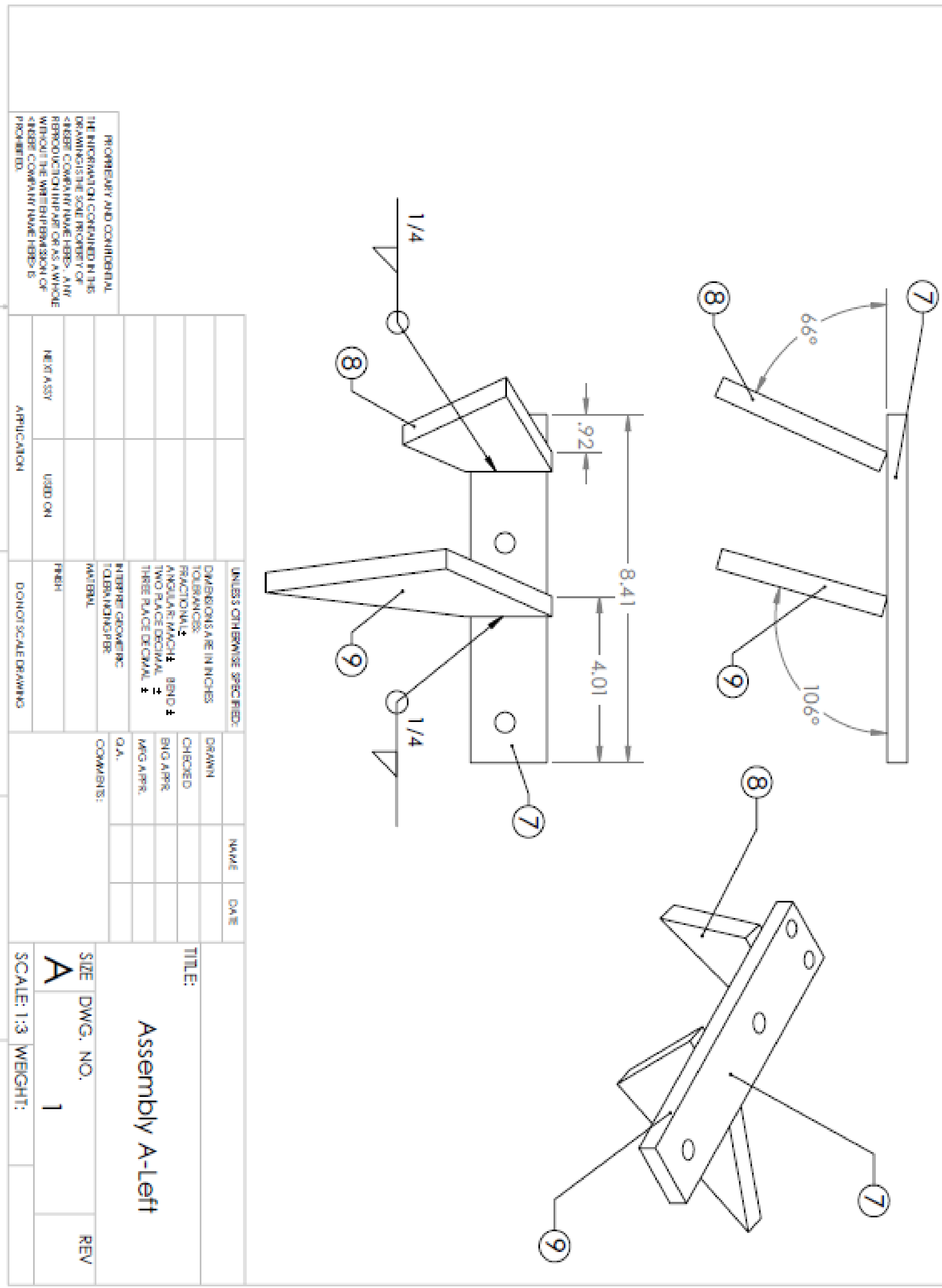

Assembly A-Left
TITLE:
SIZE
A
DWG. NO.
1
REV
SCALE: 1:3
WEIGHT:
UNLESS OTHERWISE SPECIFIED:
DIMENSIONS ARE IN INCHES
DRAWN
CHECKED
ENG APPR.
MFG APPR.
Q.A.
COMMENTS:
NAME
DATE
MATERIAL
FINISH
NEXT ASSY
USED ON
APPLICATION
DO NOT SCALE DRAWING
PROPRIETARY AND CONFIDENTIAL
8.41
4.01
.92
66°
106°
1/4

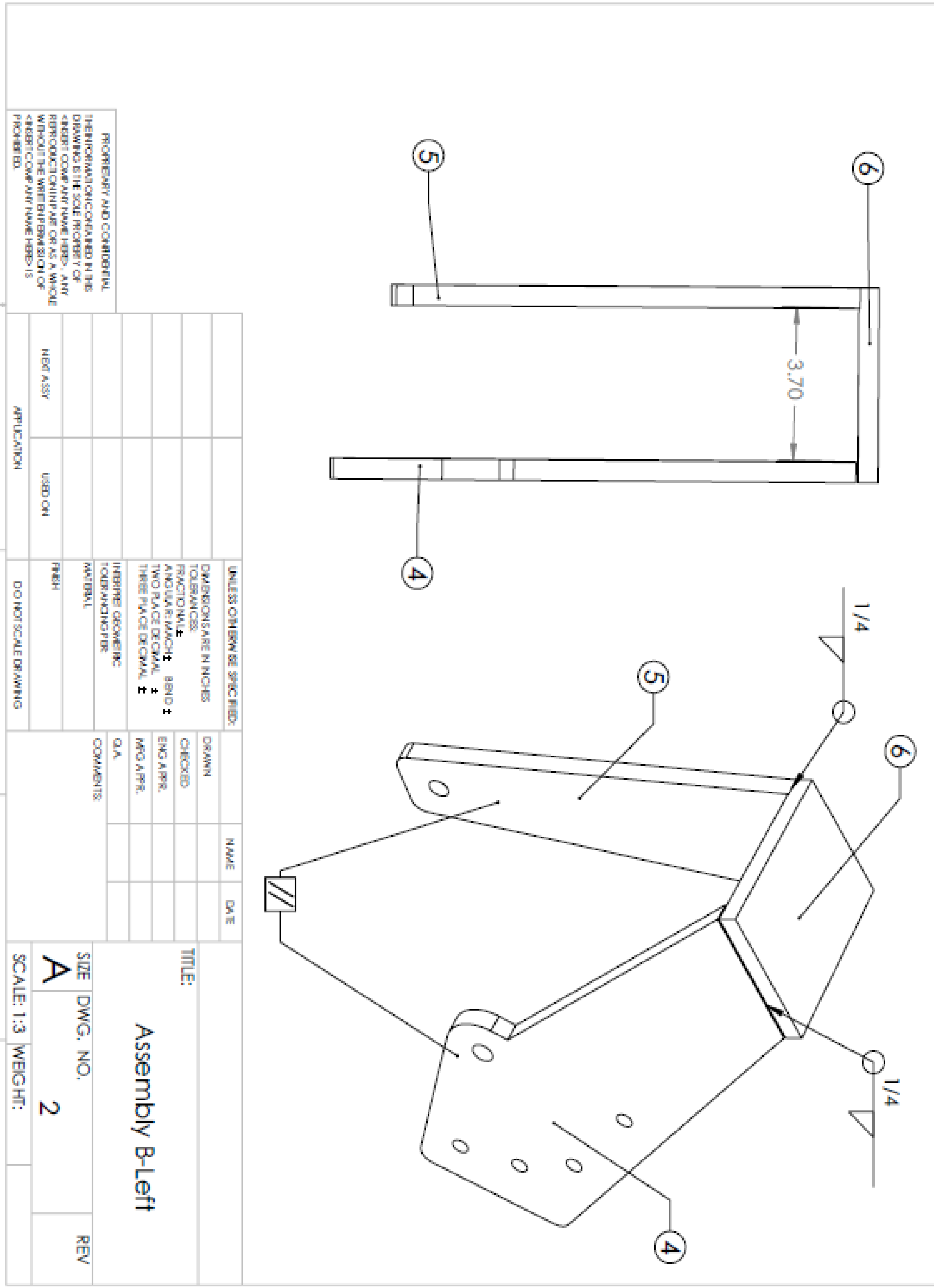
Assembly B-Left
TITLE:
SIZE
A
DWG. NO.
2
REV
SCALE: 1:3
WEIGHT:
3.70
1/4
1/4
4
5
6
UNLESS OTHERWISE SPECIFIED:
DIMENSIONS ARE IN INCHES
TOLERANCES:
FRACTIONAL ±
ANGULAR: MACH ± BEND ±
TWO PLACE DECIMAL ±
THREE PLACE DECIMAL ±
INTERPRET GEOMETRIC TOLERANCING PER:
MATERIAL
FINISH
DO NOT SCALE DRAWING
NAME
DATE
DRAWN
CHECKED
ENG APPR.
MFG APPR.
Q.A.
COMMENTS:
NEXT ASSY
USED ON
APPLICATION
PROPRIETARY AND CONFIDENTIAL

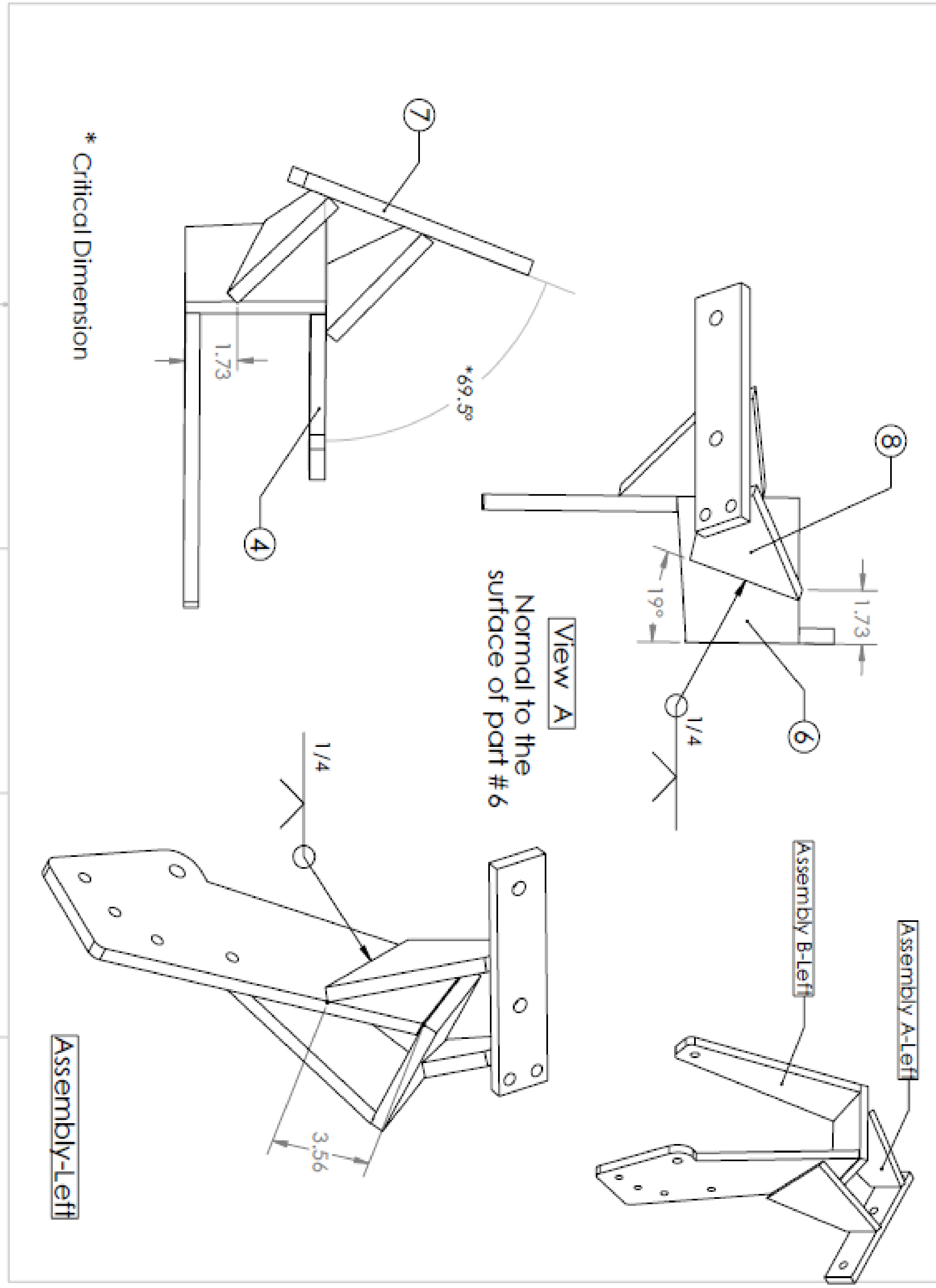
* Critical Dimension
7
4
1.73
*69.5°
8
6
1.73
19°
1/4
View A
Normal to the surface of part #6
1/4
3.56
Assembly-Left
Assembly B-Left
Assembly A-Left
5
4
3
2
1

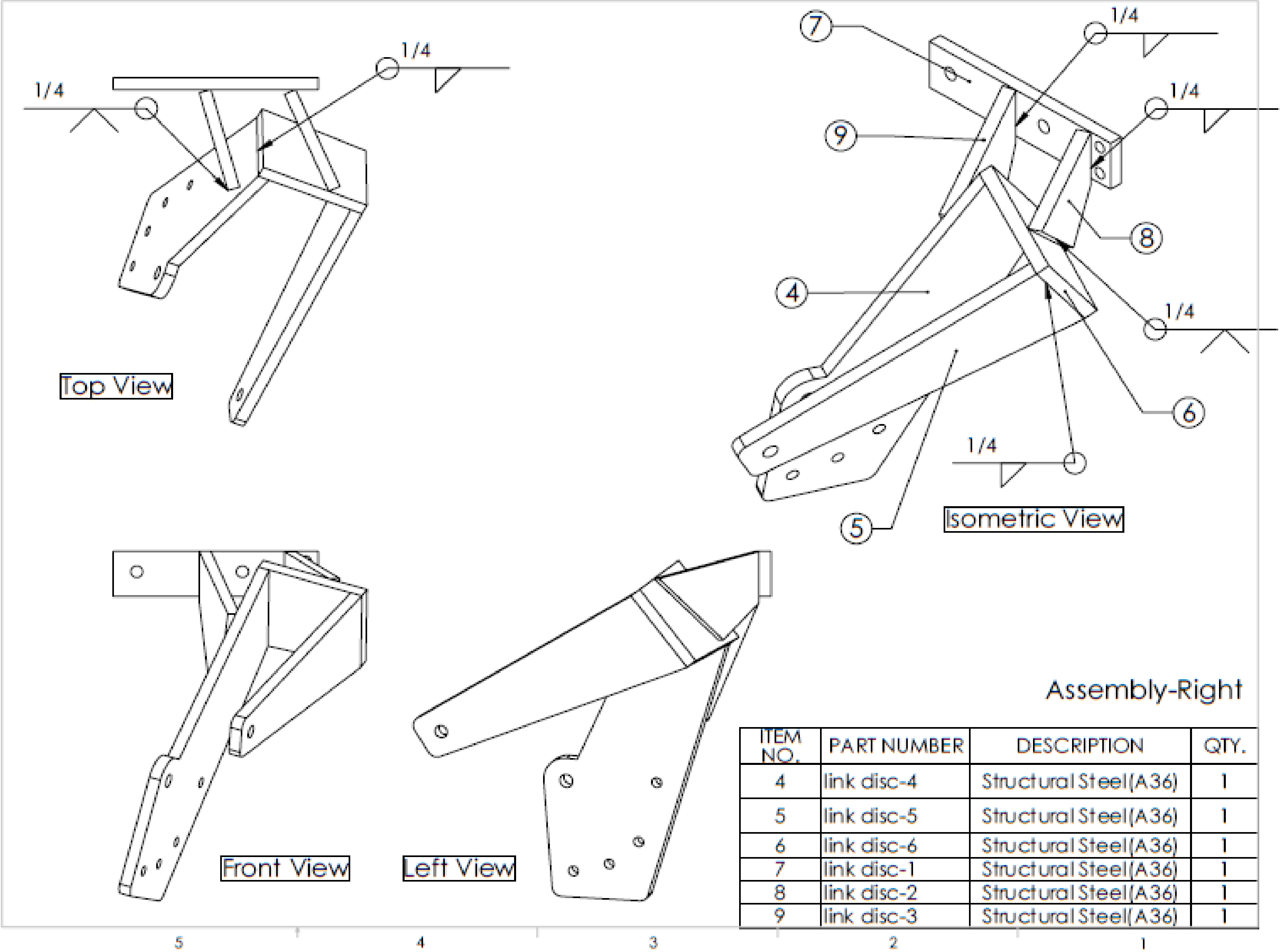

Assembly-Right

ITEM NO.	PART NUMBER	DESCRIPTION	QTY.
4	link disc-4	Structural Steel(A36)	1
5	link disc-5	Structural Steel(A36)	1
6	link disc-6	Structural Steel(A36)	1
7	link disc-1	Structural Steel(A36)	1
8	link disc-2	Structural Steel(A36)	1
9	link disc-3	Structural Steel(A36)	1

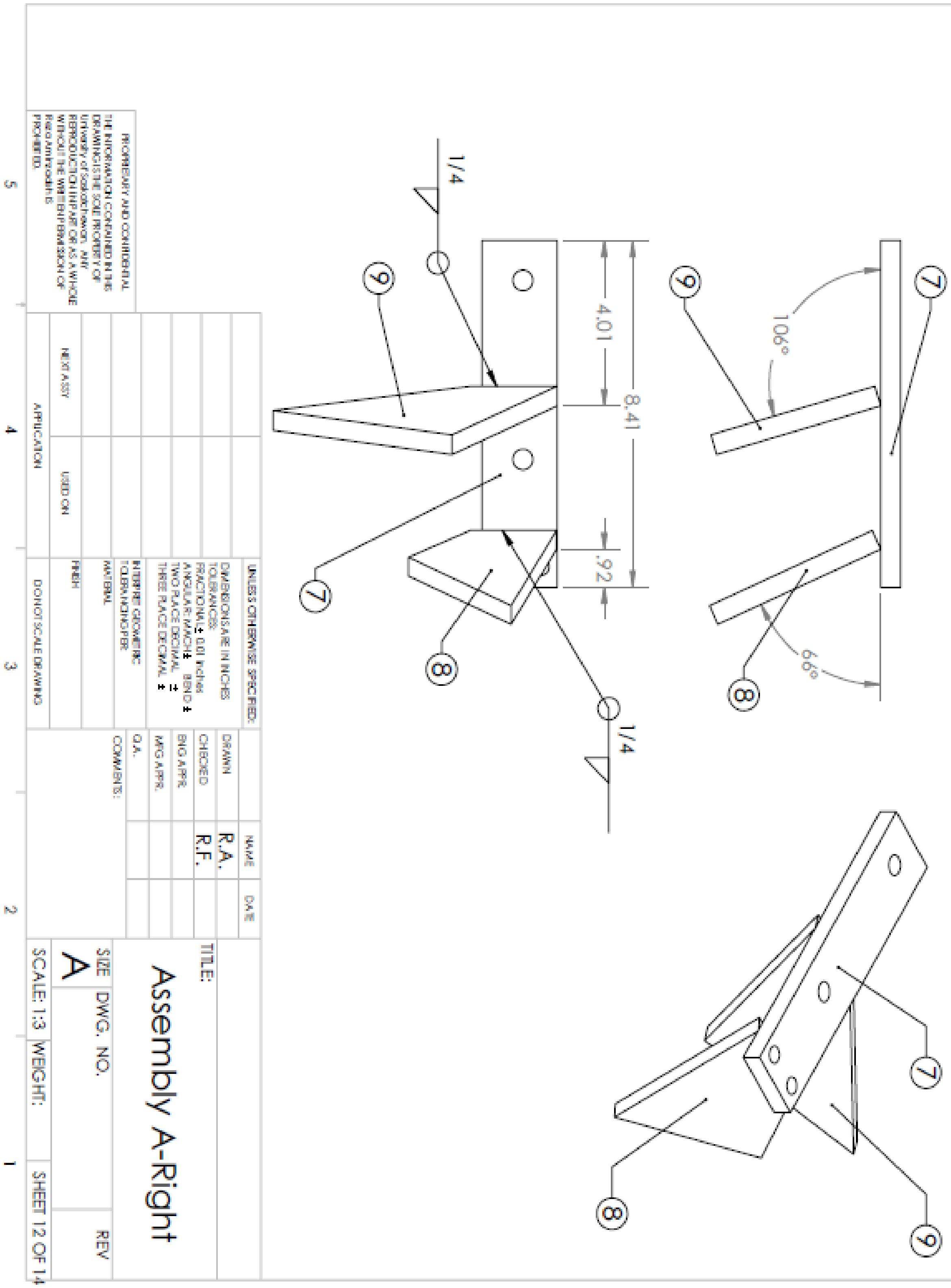

TITLE:
Assembly A-Right
SIZE
A
DWG. NO.
REV
SCALE: 1:3
WEIGHT:
SHEET 12 OF 14
NAME
DATE
DRAWN
R.A.
CHECKED
R.F.
ENG APPR.
MFG APPR.
Q.A.
COMMENTS:
UNLESS OTHERWISE SPECIFIED:
DIMENSIONS ARE IN INCHES
TOLERANCES:
FRACTIONAL ± 0.01 inches
ANGULAR: MACH ± BEND ±
TWO PLACE DECIMAL ±
THREE PLACE DECIMAL ±
INTERPRET GEOMETRIC
TOLERANCING PER:
MATERIAL
FINISH
NEXT ASSY
USED ON
APPLICATION
DO NOT SCALE DRAWING
PROPRIETARY AND CONFIDENTIAL
4.01
8.41
.92
1/4
106°
66°
7
8
9
1
2
3
4
5

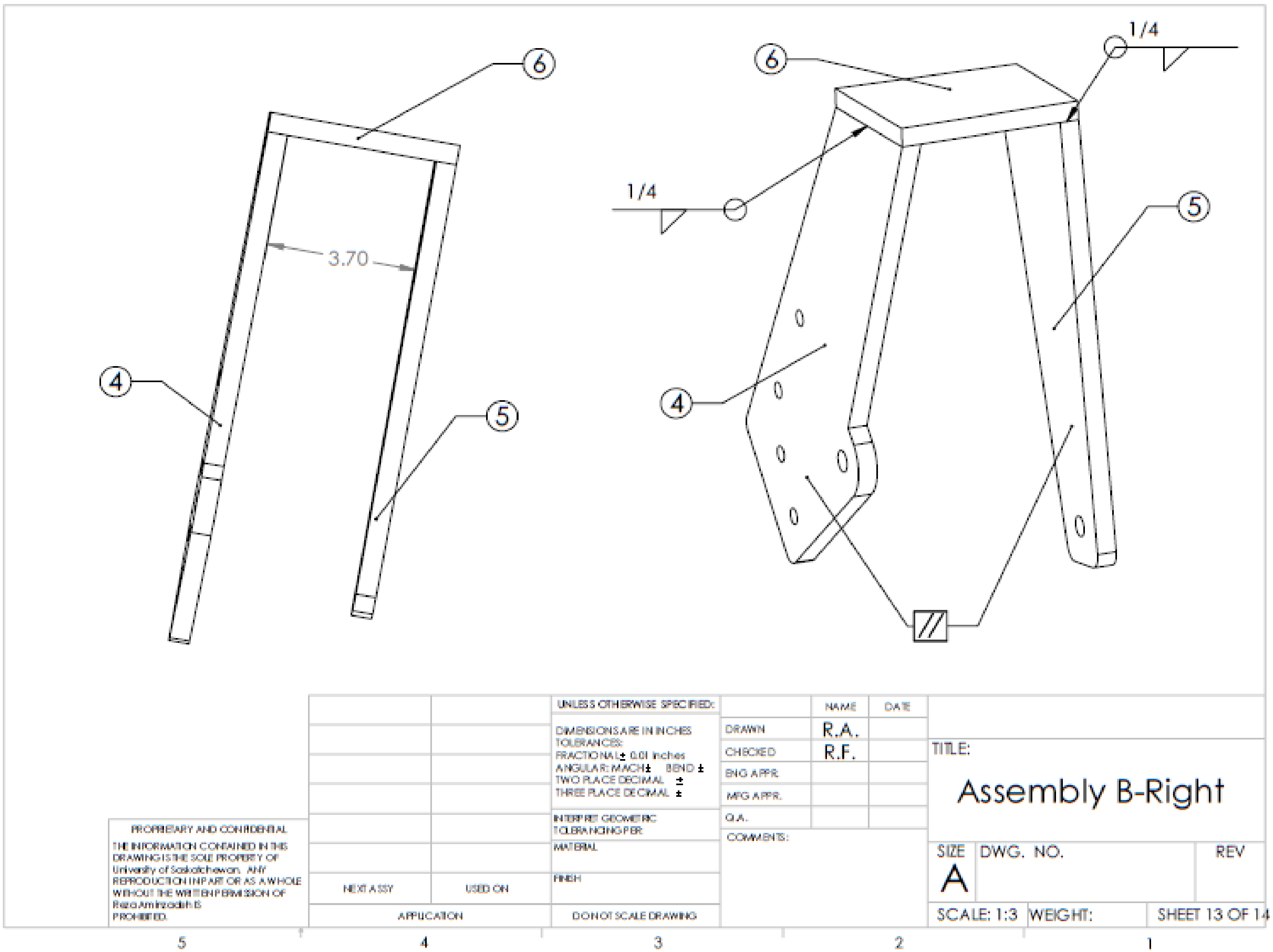
6
3.70
4
5
1/4
6
1/4
5
4
//
UNLESS OTHERWISE SPECIFIED:
DIMENSIONS ARE IN INCHES
TOLERANCES:
FRACTIONAL ± 0.01 inches
ANGULAR: MACH ± BEND ±
TWO PLACE DECIMAL ±
THREE PLACE DECIMAL ±
INTERPRET GEOMETRIC TOLERANCING PER:
MATERIAL
FINISH
DO NOT SCALE DRAWING
NEXT ASSY
USED ON
APPLICATION
NAME
DATE
DRAWN R.A.
CHECKED R.F.
ENG APPR.
MFG APPR.
Q.A.
COMMENTS:
TITLE:
Assembly B-Right
SIZE A
DWG. NO.
REV
SCALE: 1:3
WEIGHT:
SHEET 13 OF 14
PROPRIETARY AND CONFIDENTIAL
THE INFORMATION CONTAINED IN THIS DRAWING IS THE SOLE PROPERTY OF University of Saskatchewan. ANY REPRODUCTION IN PART OR AS A WHOLE WITHOUT THE WRITTEN PERMISSION OF Reza Aminzadeh IS PROHIBITED.
5
4
3
2
1

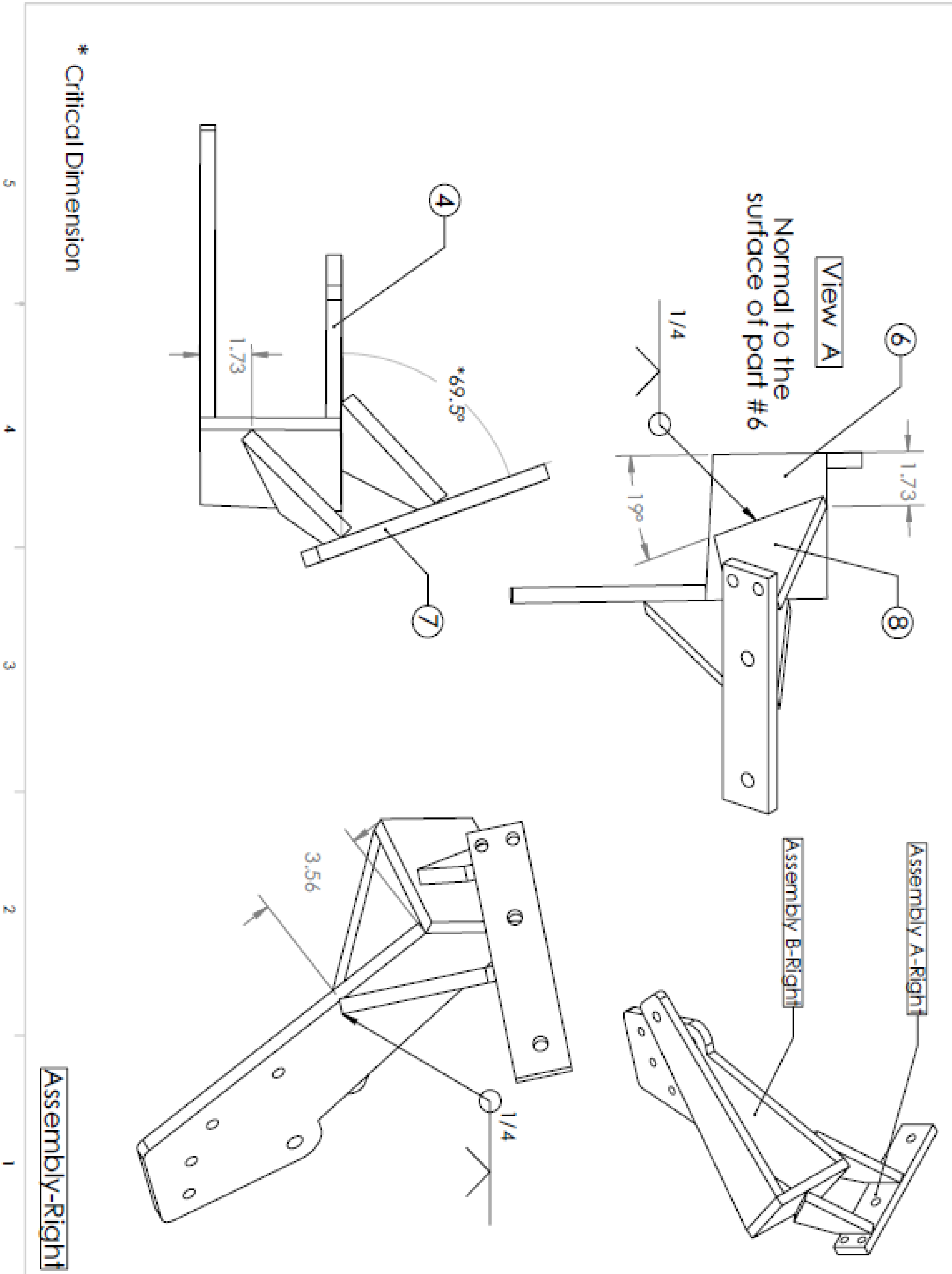
View A
Normal to the surface of part #6
1/4
1.73
19°
*69.5°
1.73
3.56
1/4
4
6
7
8
Assembly A-Right
Assembly B-Right
Assembly-Right
* Critical Dimension

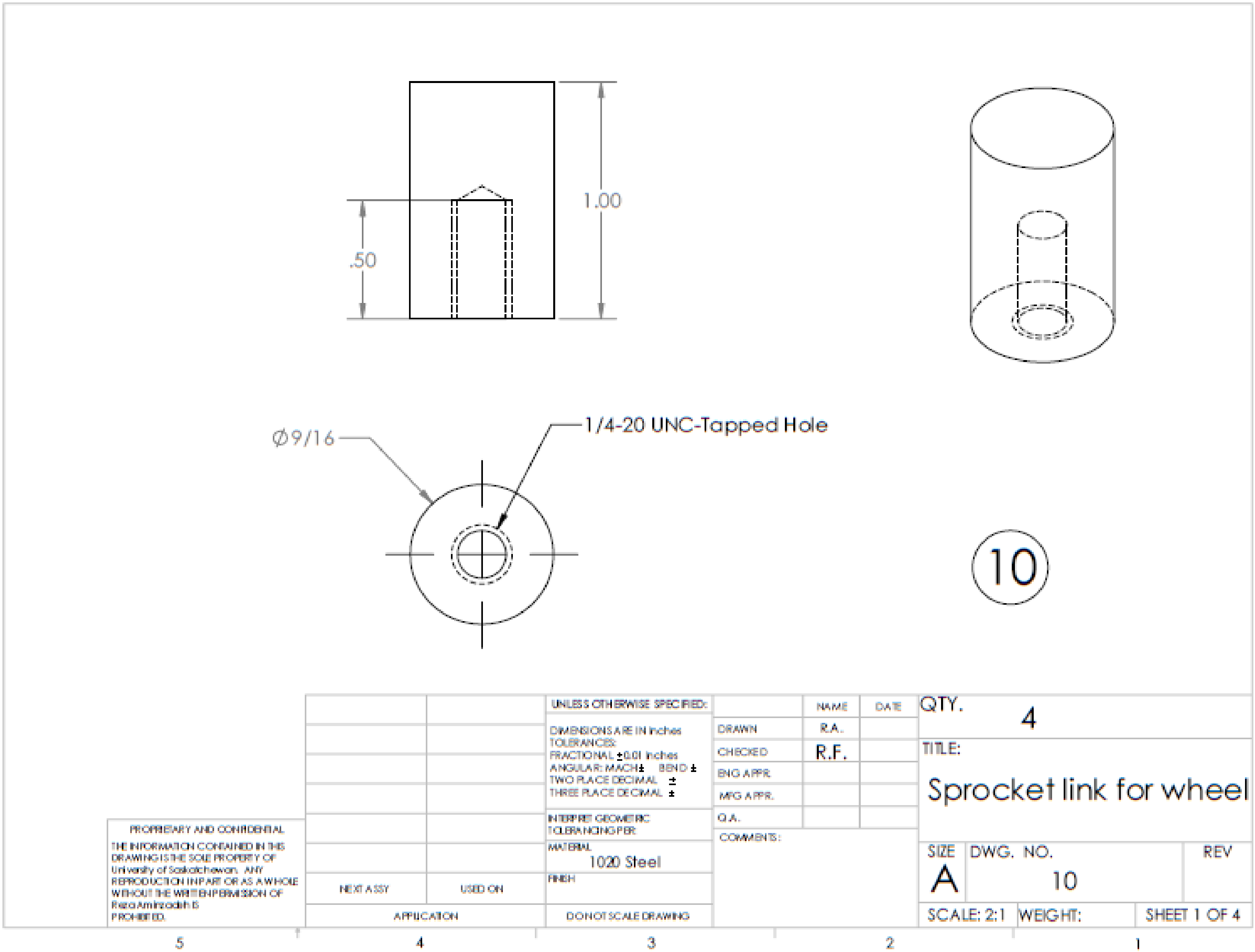
1.00
.50
Ø9/16
1/4-20 UNC-Tapped Hole
10
UNLESS OTHERWISE SPECIFIED:
DIMENSIONS ARE IN inches
TOLERANCES:
FRACTIONAL ±0.01 inches
ANGULAR: MACH± BEND ±
TWO PLACE DECIMAL ±
THREE PLACE DECIMAL ±
INTERPRET GEOMETRIC TOLERANCING PER:
MATERIAL
1020 Steel
FINISH
DO NOT SCALE DRAWING
NAME
DATE
DRAWN
R.A.
CHECKED
R.F.
ENG APPR.
MFG APPR.
Q.A.
COMMENTS:
QTY.
4
TITLE:
Sprocket link for wheel
SIZE
A
DWG. NO.
10
REV
SCALE: 2:1
WEIGHT:
SHEET 1 OF 4
NEXT ASSY
USED ON
APPLICATION
PROPRIETARY AND CONFIDENTIAL
THE INFORMATION CONTAINED IN THIS DRAWING IS THE SOLE PROPERTY OF University of Saskatchewan. ANY REPRODUCTION IN PART OR AS A WHOLE WITHOUT THE WRITTEN PERMISSION OF Reza Aminzadeh IS PROHIBITED.
5
4
3
2
1

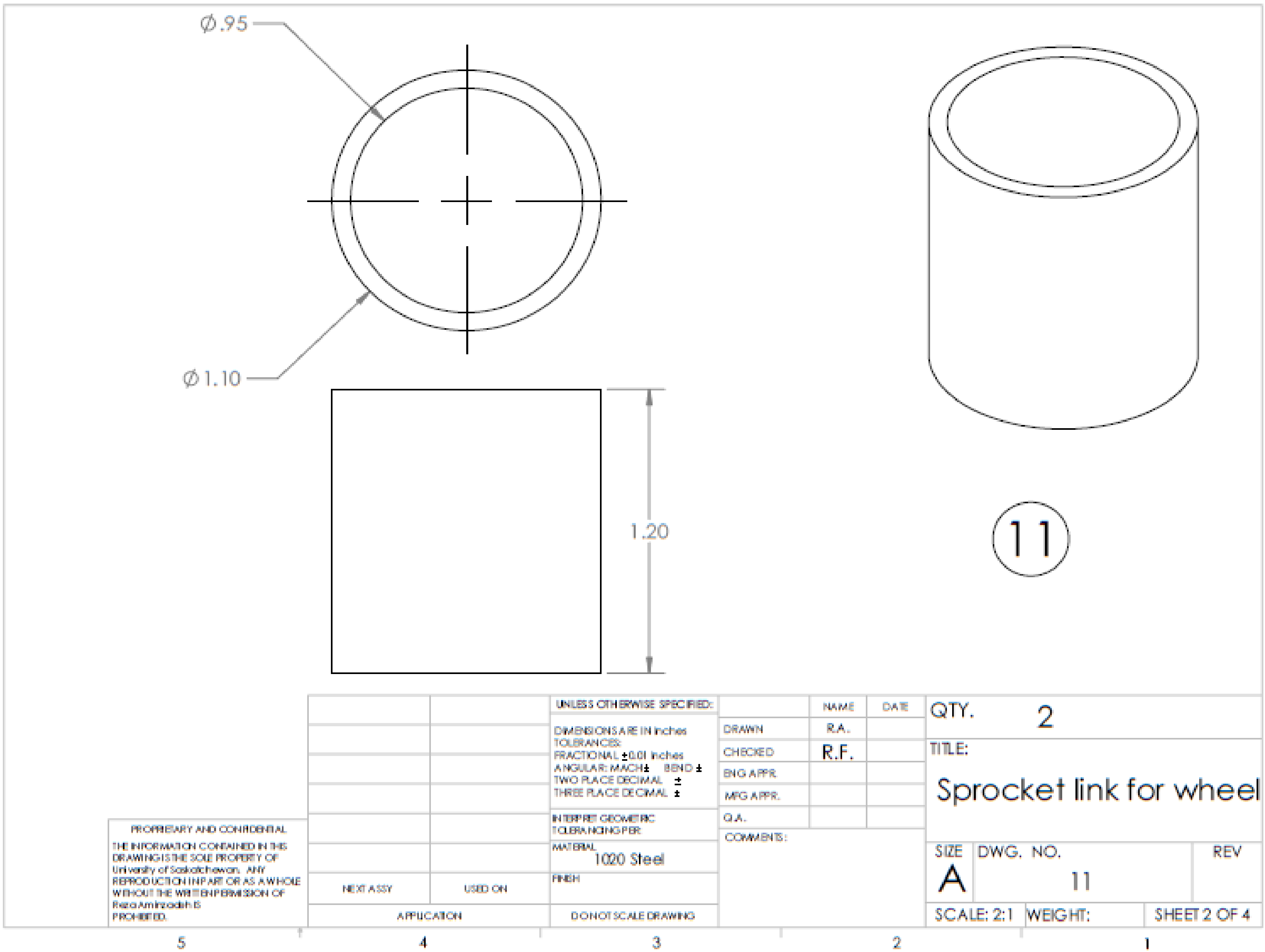
Ø.95
Ø1.10
1.20
11
UNLESS OTHERWISE SPECIFIED:
DIMENSIONS ARE IN inches
TOLERANCES:
FRACTIONAL ±0.01 inches
ANGULAR: MACH ± BEND ±
TWO PLACE DECIMAL ±
THREE PLACE DECIMAL ±
INTERPRET GEOMETRIC TOLERANCING PER:
MATERIAL
1020 Steel
FINISH
DO NOT SCALE DRAWING
NEXT ASSY
USED ON
APPLICATION
PROPRIETARY AND CONFIDENTIAL
THE INFORMATION CONTAINED IN THIS DRAWING IS THE SOLE PROPERTY OF University of Saskatchewan. ANY REPRODUCTION IN PART OR AS A WHOLE WITHOUT THE WRITTEN PERMISSION OF Reza Aminzadeh IS PROHIBITED.
NAME
DATE
DRAWN
R.A.
CHECKED
R.F.
ENG APPR.
MFG APPR.
Q.A.
COMMENTS:
QTY.
2
TITLE:
Sprocket link for wheel
SIZE
A
DWG. NO.
11
REV
SCALE: 2:1
WEIGHT:
SHEET 2 OF 4
5
4
3
2
1

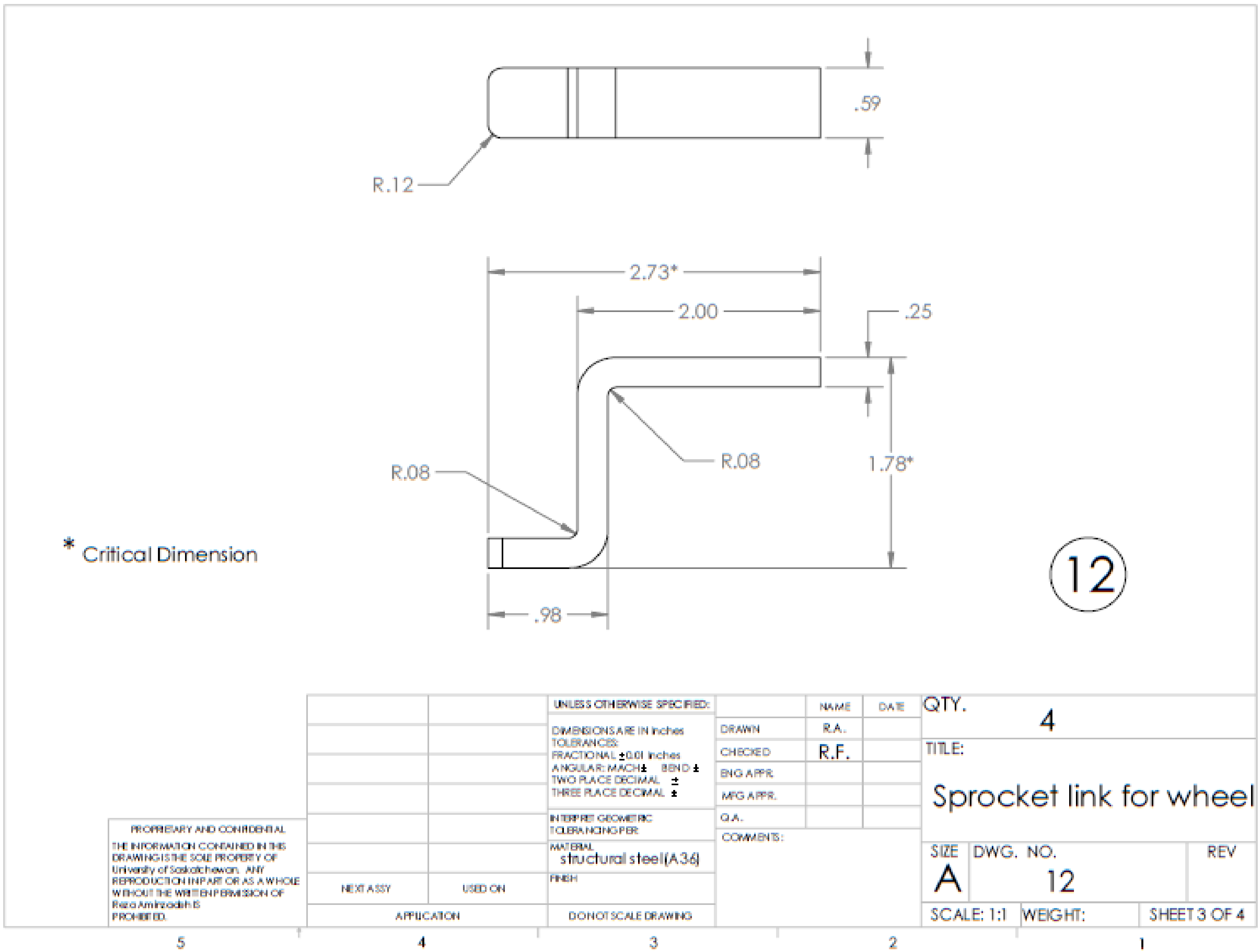
.59
R.12
2.73*
2.00
.25
R.08
R.08
1.78*
.98
* Critical Dimension
12
UNLESS OTHERWISE SPECIFIED:
DIMENSIONS ARE IN inches
TOLERANCES:
FRACTIONAL ±0.01 inches
ANGULAR: MACH± BEND ±
TWO PLACE DECIMAL ±
THREE PLACE DECIMAL ±
INTERPRET GEOMETRIC TOLERANCING PER:
MATERIAL
structural steel(A36)
FINISH
DO NOT SCALE DRAWING
NEXT ASSY
USED ON
APPLICATION
NAME
DATE
DRAWN
R.A.
CHECKED
R.F.
ENG APPR.
MFG APPR.
Q.A.
COMMENTS:
QTY.
4
TITLE:
Sprocket link for wheel
SIZE
A
DWG. NO.
12
REV
SCALE: 1:1
WEIGHT:
SHEET 3 OF 4
PROPRIETARY AND CONFIDENTIAL
THE INFORMATION CONTAINED IN THIS DRAWING IS THE SOLE PROPERTY OF University of Saskatchewan. ANY REPRODUCTION IN PART OR AS A WHOLE WITHOUT THE WRITTEN PERMISSION OF Reza Amirzadeh IS PROHIBITED.
5
4
3
2
1

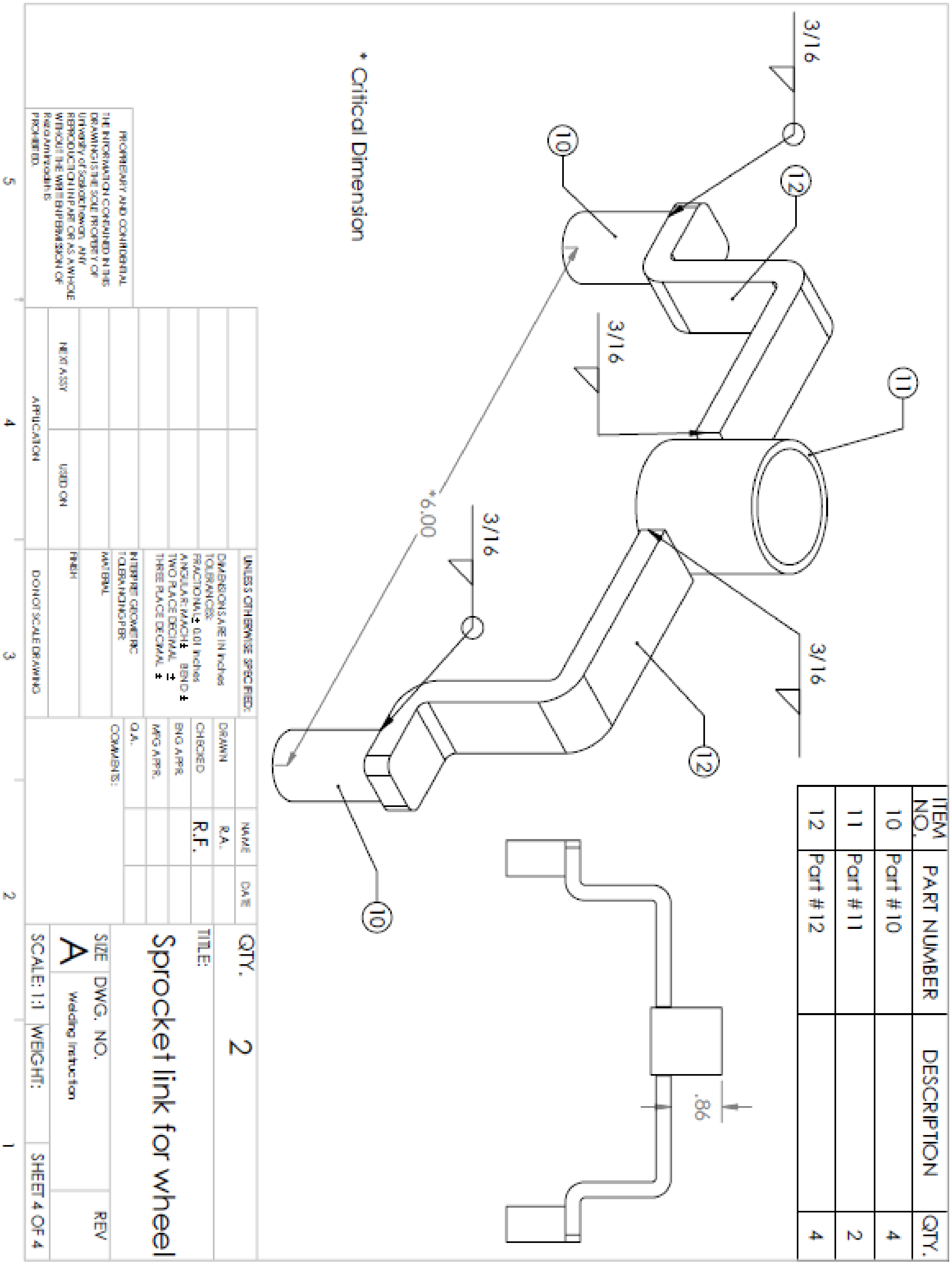

3/16
3/16
3/16
3/16
10
12
11
12
10
* Critical Dimension
*6.00
.86
ITEM NO. | PART NUMBER | DESCRIPTION | QTY.
10 | Part # 10 | | 4
11 | Part # 11 | | 2
12 | Part # 12 | | 4
PROPRIETARY AND CONFIDENTIAL
UNLESS OTHERWISE SPECIFIED:
DIMENSIONS ARE IN inches
TOLERANCES:
FRACTIONAL ± 0.01 inches
ANGULAR: MACH ± BEND ±
TWO PLACE DECIMAL ±
THREE PLACE DECIMAL ±
INTERPRET GEOMETRIC TOLERANCING PER:
MATERIAL
FINISH
NEXT ASSY
USED ON
APPLICATION
DO NOT SCALE DRAWING
NAME
DATE
DRAWN R.A.
CHECKED R.F.
ENG APPR.
MFG APPR.
Q.A.
COMMENTS:
QTY. 2
TITLE:
Sprocket link for wheel
SIZE A
DWG. NO.
Welding Instruction
REV
SCALE: 1:1
WEIGHT:
SHEET 4 OF 4

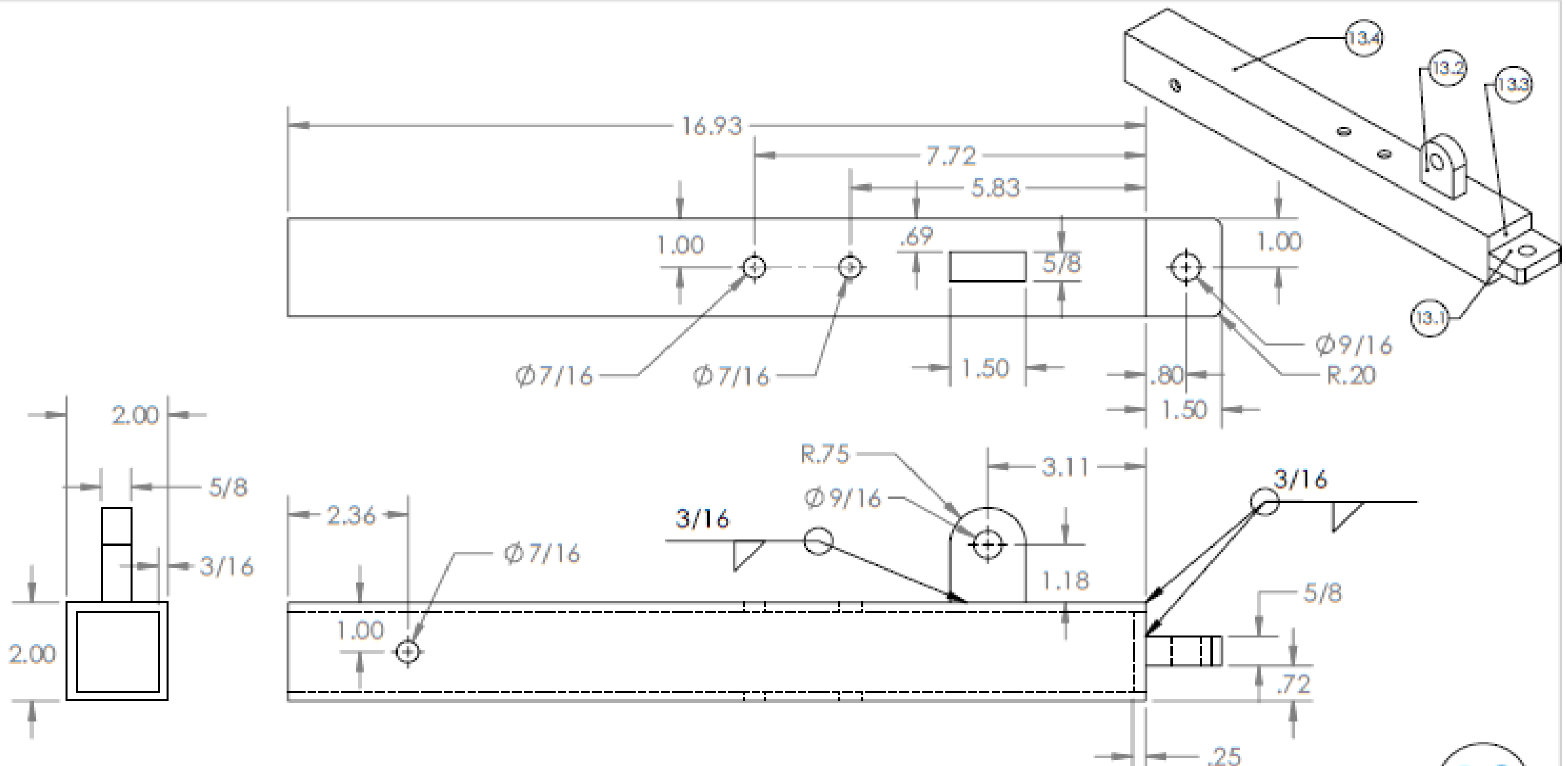

part #	name	material	QTY.
13.1	bolt plate	A36	1
13.2	Hinge	A36	1
13.3	1/4 inch plate	A36	1
13.4	HSS 2X2	A36	1

NEXT ASSY | USED ON
APPLICATION

UNLESS OTHERWISE SPECIFIED:
DIMENSIONS ARE IN inches
TOLERANCES:
FRACTIONAL ±0.01 inches
ANGULAR: MACH ± BEND ±
TWO PLACE DECIMAL ±
THREE PLACE DECIMAL ±
INTERPRET GEOMETRIC TOLERANCING PER:
MATERIAL
Structural steel(A36)
FINISH
DO NOT SCALE DRAWING

	NAME	DATE
DRAWN	R.A.	
CHECKED	R.F.	
ENG APPR.		
MFG APPR.		
Q.A.		

COMMENTS:

QTY. 1
TITLE:
lower connection bar-Left
SIZE A | DWG. NO. 13 | REV
SCALE: 1:3 | WEIGHT: | SHEET 1 OF 2

5 4 3 2 1

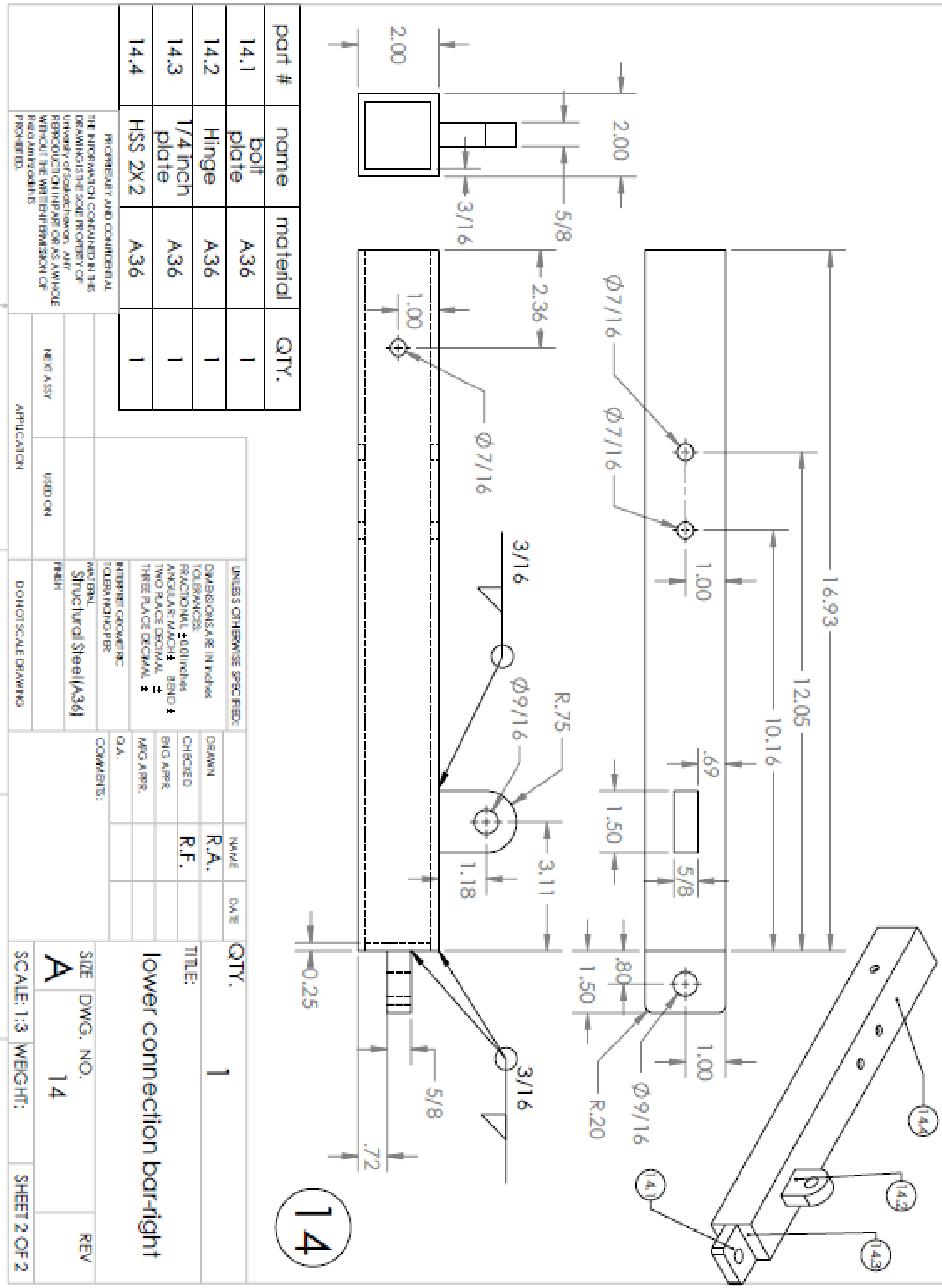
part # | name | material | QTY.
14.1 | bolt plate | A36 | 1
14.2 | Hinge | A36 | 1
14.3 | 1/4 inch plate | A36 | 1
14.4 | HSS 2X2 | A36 | 1
UNLESS OTHERWISE SPECIFIED:
DIMENSIONS ARE IN inches
MATERIAL Structural Steel(A36)
DO NOT SCALE DRAWING
DRAWN R.A.
CHECKED R.F.
QTY. 1
TITLE: lower connection bar-right
SIZE A
DWG. NO. 14
REV
SCALE: 1:3
WEIGHT:
SHEET 2 OF 2
14

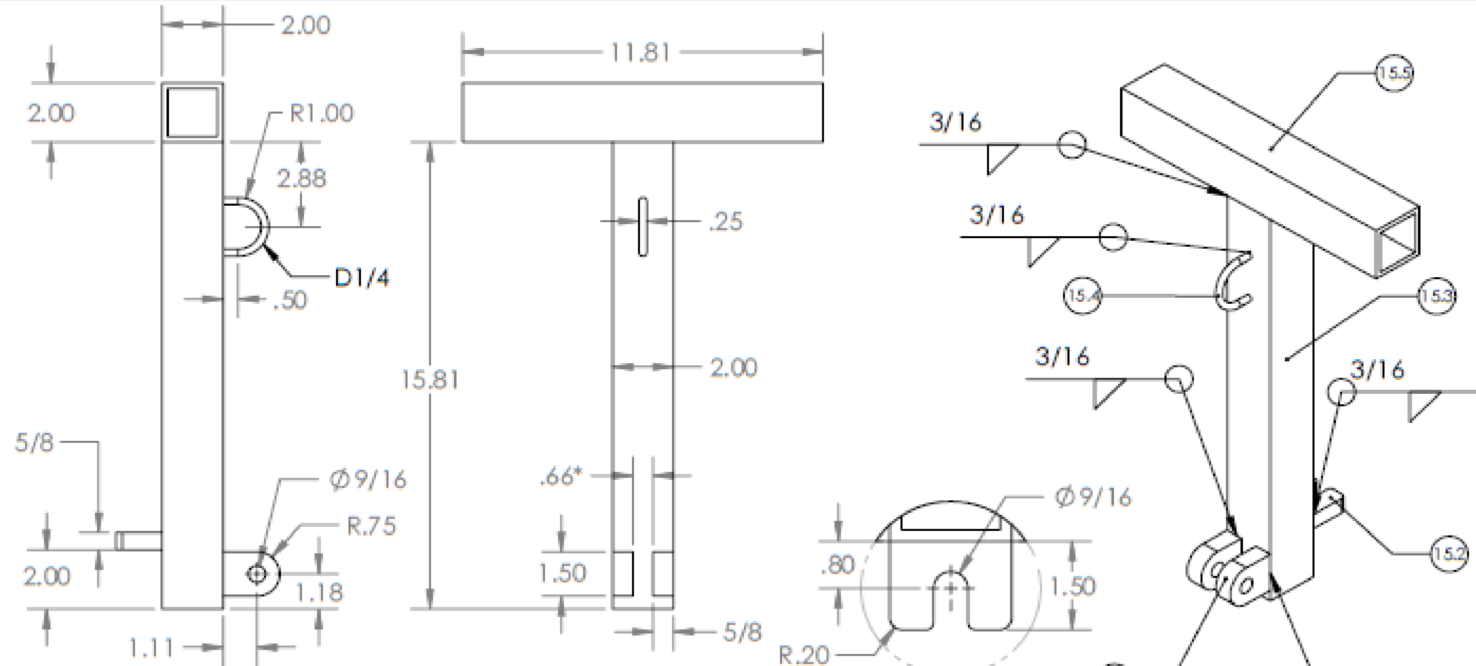

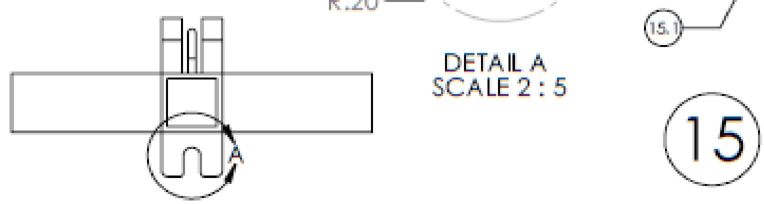

Part #	name	material	QTY.
15.1	Hinge	A36	2
15.2	Bolt plate	A36	1
15.3	HSS 2X2 Vertical	A36	1
15.4	U shape Hook	structural steel	1
15.5	HSS 2X2 Horizontal	A36	1

* Critical Dimension

NEXT ASSY | USED ON
APPLICATION

UNLESS OTHERWISE SPECIFIED:
DIMENSIONS ARE IN inches
TOLERANCES:
FRACTIONAL ±0.01 inches
ANGULAR: MACH ± BEND ±
TWO PLACE DECIMAL ±
THREE PLACE DECIMAL ±

INTERPRET GEOMETRIC TOLERANCING PER:
MATERIAL
Structural steel(A36)
FINISH
DO NOT SCALE DRAWING

	NAME	DATE
DRAWN	R.A.	
CHECKED	R.F.	
ENG APPR.		
MFG APPR.		
Q.A.		

COMMENTS:

QTY. 1

TITLE:
row connection bar

SIZE A | DWG. NO. 15 | REV
SCALE: 1:5 | WEIGHT: | SHEET 1 OF 1

5 4 3 2 1

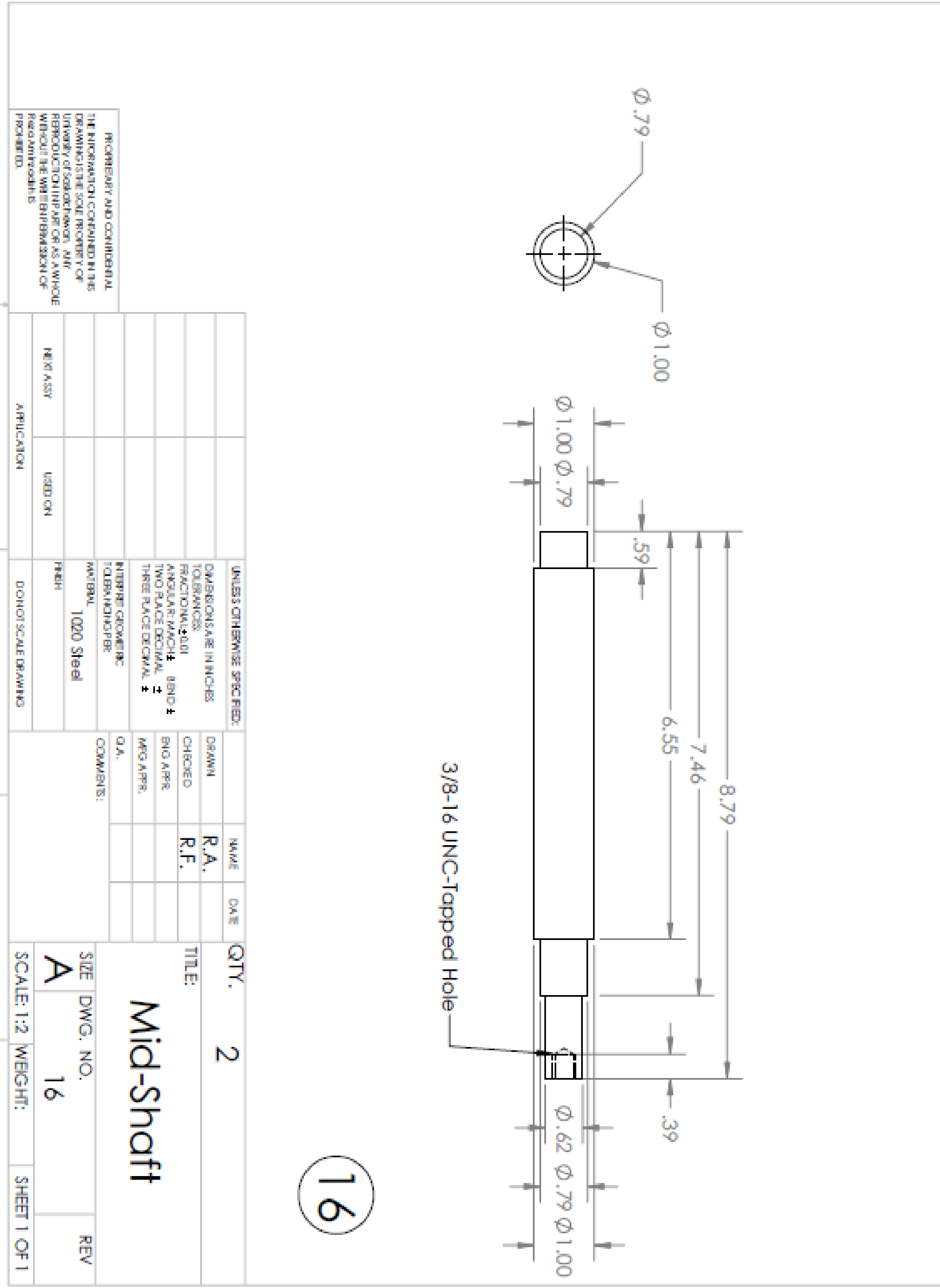
Ø.79
Ø1.00
Ø1.00 Ø.79
.59
6.55
7.46
8.79
.39
Ø.62 Ø.79 Ø1.00
3/8-16 UNC-Tapped Hole
16
QTY. 2
TITLE:
Mid-Shaft
SIZE A
DWG. NO. 16
REV
SCALE: 1:2
WEIGHT:
SHEET 1 OF 1
NAME
DATE
DRAWN R.A.
CHECKED R.F.
ENG APPR.
MFG APPR.
Q.A.
COMMENTS:
UNLESS OTHERWISE SPECIFIED:
DIMENSIONS ARE IN INCHES
TOLERANCES:
FRACTIONAL ± 0.01
ANGULAR: MACH ± BEND ±
TWO PLACE DECIMAL ±
THREE PLACE DECIMAL ±
INTERPRET GEOMETRIC TOLERANCING PER:
MATERIAL
1020 Steel
FINISH
DO NOT SCALE DRAWING
NEXT ASSY
USED ON
APPLICATION
PROPRIETARY AND CONFIDENTIAL
THE INFORMATION CONTAINED IN THIS DRAWING IS THE SOLE PROPERTY OF University of Saskatchewan. ANY REPRODUCTION IN PART OR AS A WHOLE WITHOUT THE WRITTEN PERMISSION OF Reza Amirsadeghi is PROHIBITED.
1
2
3
4
5

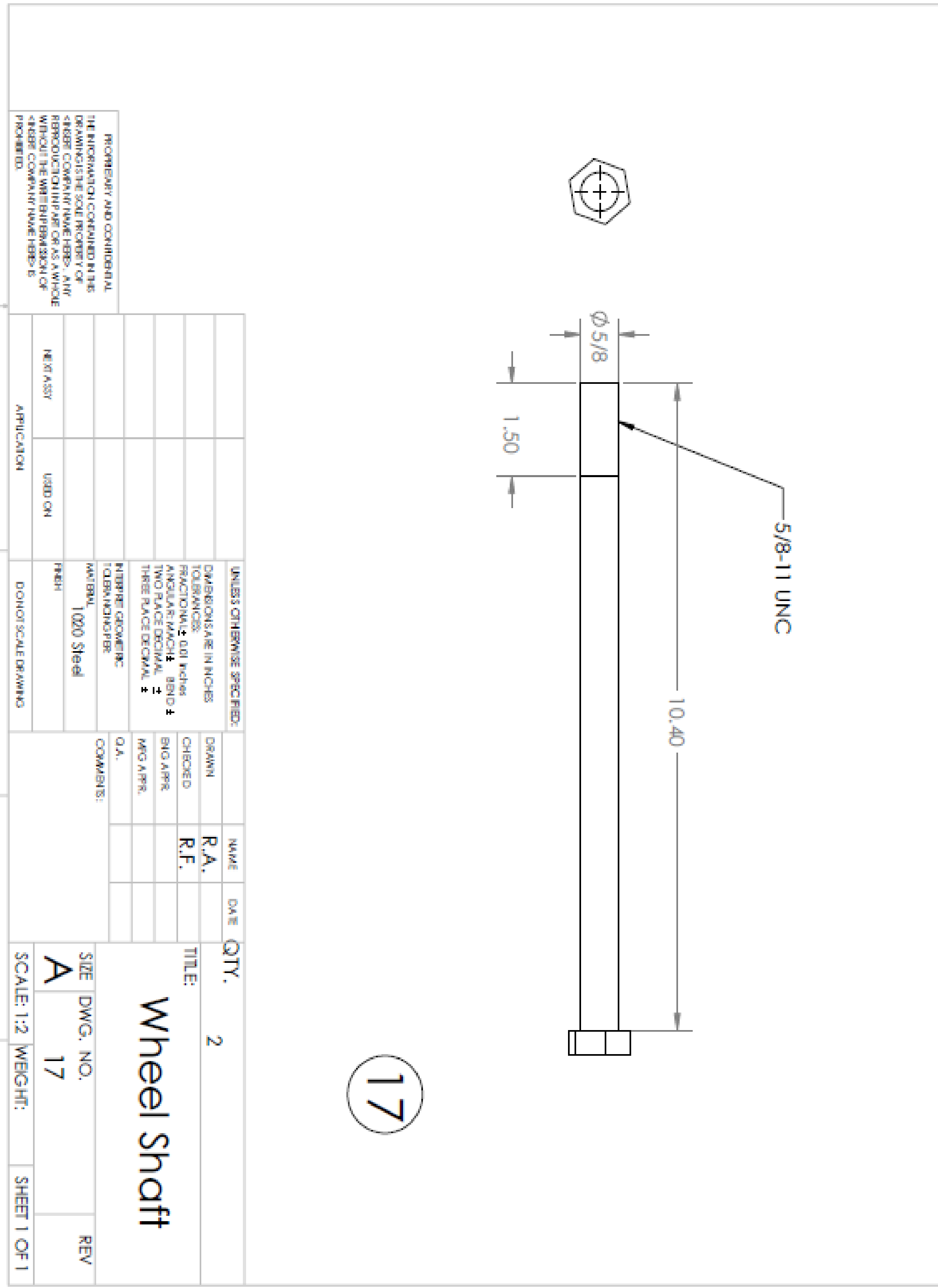
Ø5/8
1.50
5/8-11 UNC
10.40
17
PROPRIETARY AND CONFIDENTIAL
THE INFORMATION CONTAINED IN THIS DRAWING IS THE SOLE PROPERTY OF <INSERT COMPANY NAME HERE>. ANY REPRODUCTION IN PART OR AS A WHOLE WITHOUT THE WRITTEN PERMISSION OF <INSERT COMPANY NAME HERE> IS PROHIBITED.
NEXT ASSY
USED ON
APPLICATION
UNLESS OTHERWISE SPECIFIED:
DIMENSIONS ARE IN INCHES
TOLERANCES:
FRACTIONAL ± 0.01 inches
ANGULAR: MACH ± BEND ±
TWO PLACE DECIMAL ±
THREE PLACE DECIMAL ±
INTERPRET GEOMETRIC TOLERANCING PER:
MATERIAL
1020 Steel
FINISH
DO NOT SCALE DRAWING
NAME
DATE
DRAWN R.A.
CHECKED R.F.
ENG APPR.
MFG APPR.
Q.A.
COMMENTS:
QTY. 2
TITLE:
Wheel Shaft
SIZE A
DWG. NO. 17
REV
SCALE: 1:2
WEIGHT:
SHEET 1 OF 1
5
4
3
2
1

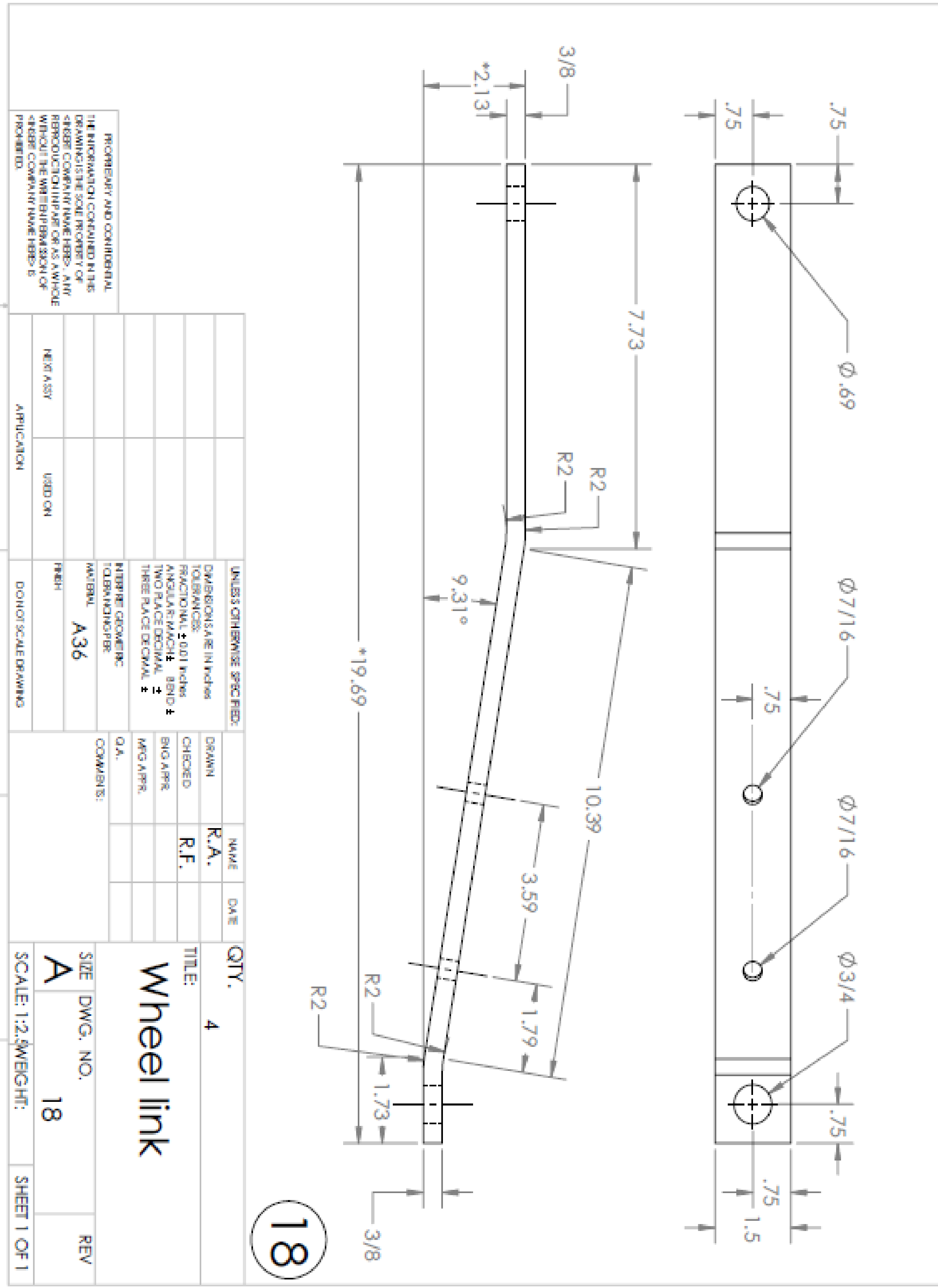
.75
.75
Ø.69
3/8
*2.13
7.73
R2
R2
9.31°
*19.69
Ø7/16
.75
Ø7/16
10.39
3.59
1.79
Ø3/4
R2
R2
1.73
.75
.75
1.5
3/8
18
QTY.
4
TITLE:
Wheel link
SIZE
A
DWG. NO.
18
REV
SCALE: 1:2.5
WEIGHT:
SHEET 1 OF 1
NAME
DATE
DRAWN
R.A.
CHECKED
R.F.
ENG APPR.
MFG APPR.
Q.A.
COMMENTS:
UNLESS OTHERWISE SPECIFIED:
MATERIAL
A36
FINISH
DO NOT SCALE DRAWING
NEXT ASSY
USED ON
APPLICATION
PROPRIETARY AND CONFIDENTIAL
5
4
3
2
1

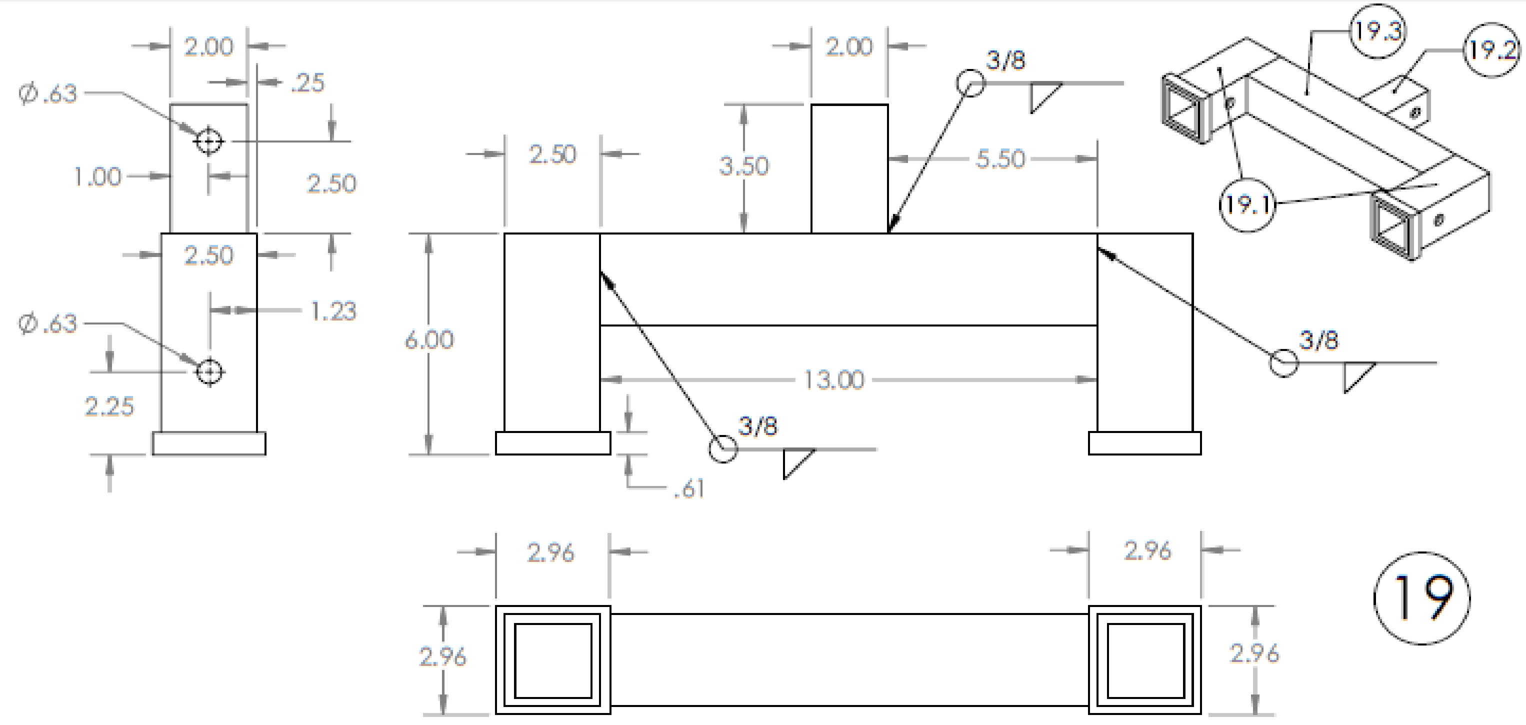

Part #	name	Material	QTY.	Description
19.1	HSS 2 1/2X 2 1/2 X1/4	A36	2	Already Provided
19.2	HSS 2 X 2 X 1/4	A36	1	Not Provided
19.3	HSS 2 1/2X 2 1/2 X1/4	A36	1	Not Provided

PROPRIETARY AND CONFIDENTIAL
THE INFORMATION CONTAINED IN THIS DRAWING IS THE SOLE PROPERTY OF <INSERT COMPANY NAME HERE>. ANY REPRODUCTION IN PART OR AS A WHOLE WITHOUT THE WRITTEN PERMISSION OF <INSERT COMPANY NAME HERE> IS PROHIBITED.

NEXT ASSY | USED ON
APPLICATION

UNLESS OTHERWISE SPECIFIED:
DIMENSIONS ARE IN INCHES
TOLERANCES:
FRACTIONAL ±0.01 Inches
ANGULAR: MACH ± BEND ±
TWO PLACE DECIMAL ±
THREE PLACE DECIMAL ±
INTERPRET GEOMETRIC TOLERANCING PER:
MATERIAL
A36
FINISH
DO NOT SCALE DRAWING

	NAME	DATE
DRAWN	R.A.	
CHECKED	R.F.	
ENG APPR.		
MFG APPR.		
Q.A.		
COMMENTS:		

TITLE:
Connection Link-Double

SIZE A | DWG. NO. 19 | REV
SCALE: 1:4 | WEIGHT: | SHEET 1 OF 1

5 4 3 2 1

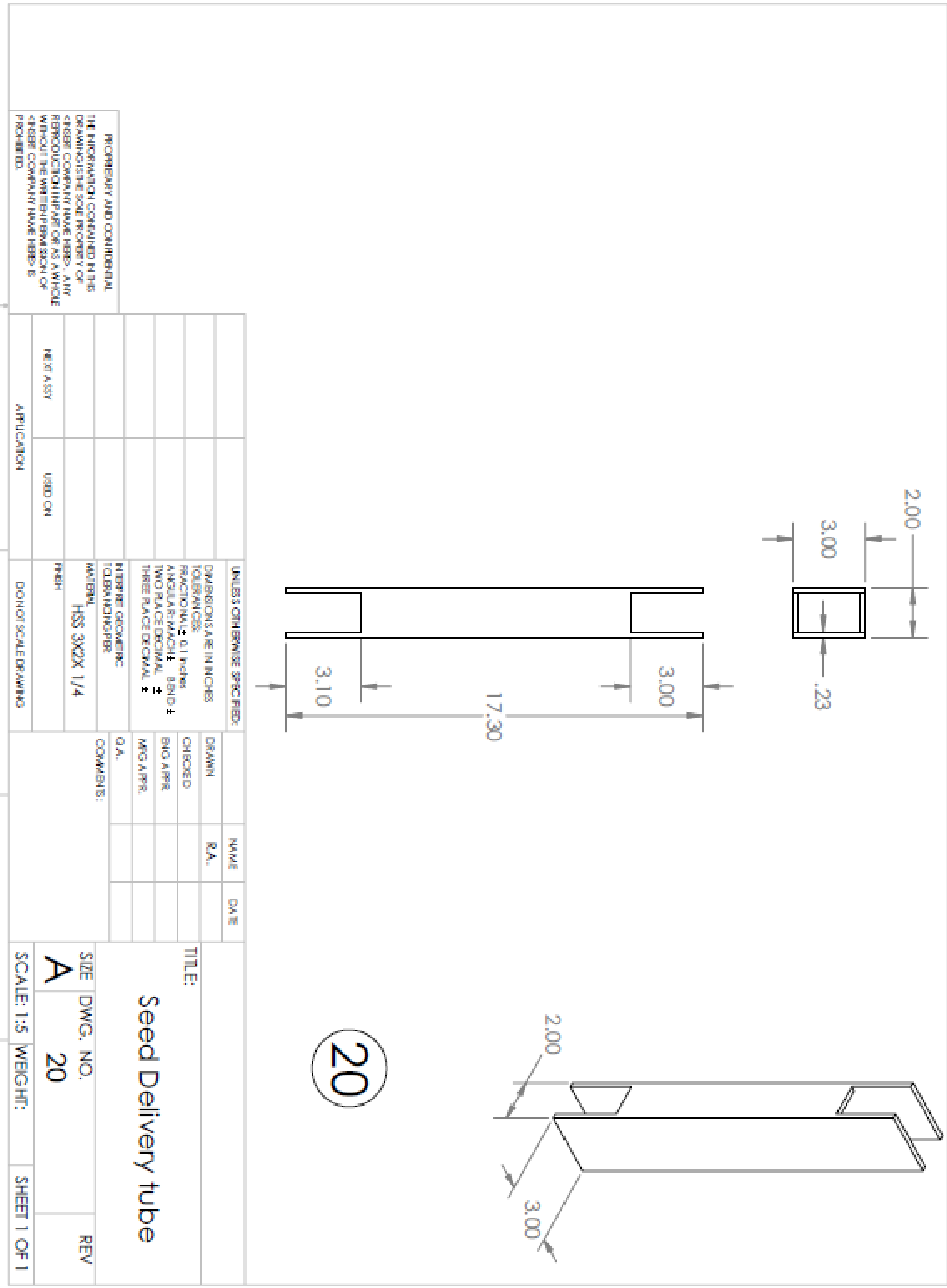
2.00
3.00
.23
3.10
17.30
3.00
2.00
3.00
20
UNLESS OTHERWISE SPECIFIED:
NAME
DATE
DRAWN
R.A.
CHECKED
ENG APPR.
MFG APPR.
Q.A.
COMMENTS:
MATERIAL
HSS 3X2X 1/4
FINISH
NEXT ASSY
USED ON
APPLICATION
DO NOT SCALE DRAWING
TITLE:
Seed Delivery tube
SIZE
A
DWG. NO.
20
REV
SCALE: 1:5
WEIGHT:
SHEET 1 OF 1

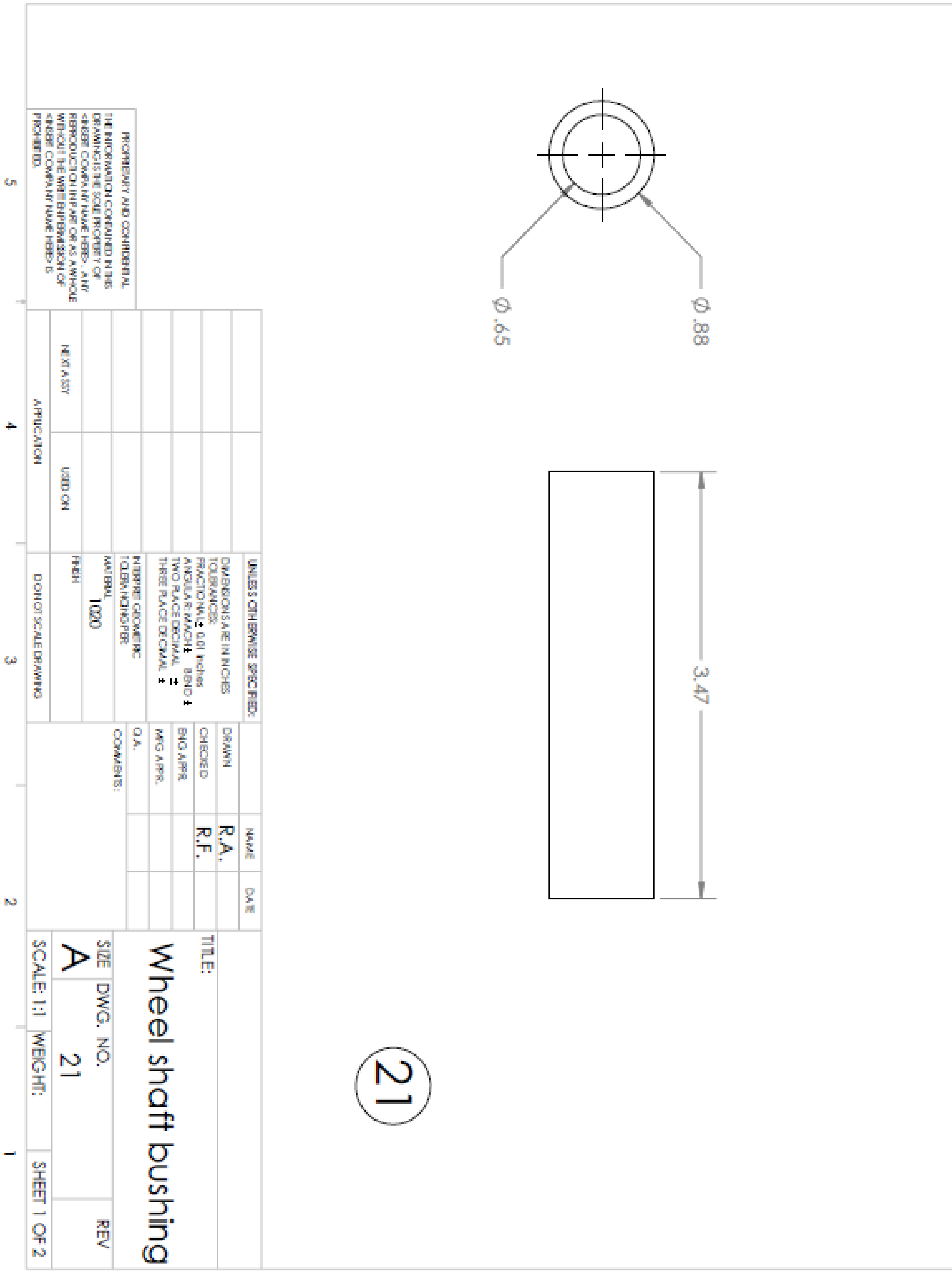

Ø.88
Ø.65
3.47
21
UNLESS OTHERWISE SPECIFIED:
DIMENSIONS ARE IN INCHES
MATERIAL
1020
FINISH
DO NOT SCALE DRAWING
NEXT ASSY
USED ON
APPLICATION
NAME
DATE
DRAWN
R.A.
CHECKED
R.F.
ENG APPR.
MFG APPR.
Q.A.
COMMENTS:
TITLE:
Wheel shaft bushing
SIZE
A
DWG. NO.
21
REV
SCALE: 1:1
WEIGHT:
SHEET 1 OF 2

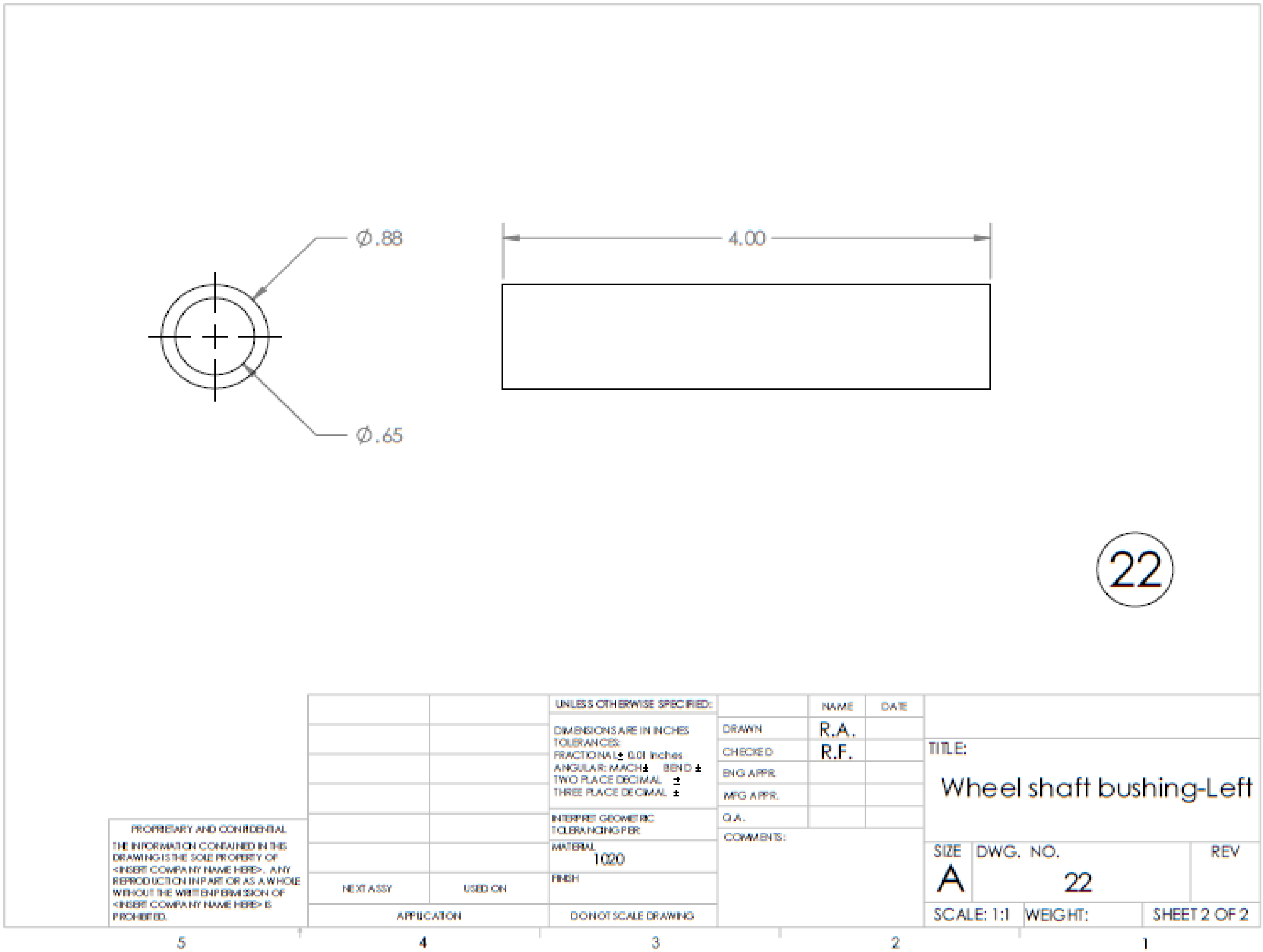
Ø.88
Ø.65
4.00
22
UNLESS OTHERWISE SPECIFIED:
DIMENSIONS ARE IN INCHES
TOLERANCES:
FRACTIONAL± 0.01 inches
ANGULAR: MACH± BEND ±
TWO PLACE DECIMAL ±
THREE PLACE DECIMAL ±
INTERPRET GEOMETRIC TOLERANCING PER:
MATERIAL
1020
FINISH
DO NOT SCALE DRAWING
NEXT ASSY
USED ON
APPLICATION
NAME
DATE
DRAWN
R.A.
CHECKED
R.F.
ENG APPR.
MFG APPR.
Q.A.
COMMENTS:
TITLE:
Wheel shaft bushing-Left
SIZE
A
DWG. NO.
22
REV
SCALE: 1:1
WEIGHT:
SHEET 2 OF 2
PROPRIETARY AND CONFIDENTIAL
THE INFORMATION CONTAINED IN THIS DRAWING IS THE SOLE PROPERTY OF <INSERT COMPANY NAME HERE>. ANY REPRODUCTION IN PART OR AS A WHOLE WITHOUT THE WRITTEN PERMISSION OF <INSERT COMPANY NAME HERE> IS PROHIBITED.
5
4
3
2
1